Novel structures of PII signal transduction proteins from oxygenic phototropic organisms

Dissertation

der Mathematisch-Naturwissenschaftlichen Fakultät

der Eberhard Karls Universität Tübingen

zur Erlangung des Grades eines

Doktors der Naturwissenschaften

(Dr. rer. nat.)

Vorgelegt von

Vasuki Ranjani Chellamuthu

aus Assam, Indien

Tübingen

2013

Tag der mündlichen Prüfung: 18.02.2014

Dekan:	Prof. Dr. Wolfgang Rosenstiel
1. Berichterstatter:	Prof. Dr. Karl Forchhammer
2. Berichterstatter:	Prof. Dr. Andrei Lupas

Table of contents

1. Abstract

PII proteins constitute one of the most widely distributed families of signal transduction proteins, whose representatives are present in archaea, bacteria and plants. They play a pivotal role to control the nitrogen, carbon and energy status of the cell in response to the central metabolites ATP, ADP and 2-oxoglutarate (2-OG). These signals from central metabolites are integrated by PII proteins and transmitted to the regulatory targets (protein modifying enzymes, metabolic enzymes, transporters and transcription factors). In oxygenic phototrophic organisms, from cyanobacteria to higher plants, the controlling enzyme of arginine synthesis, *N*-acetyl-L-glutamate kinase (NAGK) is a major PII target, whose activity responds to the cellular metabolites via PII signalling. In this work, novel crystal structures of PII signal transduction proteins from oxygenic phototrophs (*Synechococcus elongatus* and *Chlamydomonas reinhardtii*) in the presence of signalling metabolites and in complex with NAGK are reported. These structures give deeper insights into PII-mediated mechanism and regulation which are in accordance with the obtained biochemical data. The novel role of glutamine as a signalling molecule in *C. reinhardtii* is elucidated for the first time, which highlights the nitrogen regulation at a different level. Further, the interpretation of these structures together with the comparison of aminoacid sequences sheds light on the evolutionary adaptation of PII signal transduction from cyanobacteria to plastids.

2. Zusammenfassung

PII-Signaltransduktionsproteine fungieren als Relaisstationen bei der Verarbeitung von Signalen der zellulären Metaboliten ATP, ADP und 2-Oxoglutarat (2-OG). Abhängig vom Bindungsstatus dieser Effektormoleküle nehmen PII-Proteine verschiedene Konformationen ein. Diese konformativen Zustände entscheiden über die Interaktion mit den Zielproteinen, zu denen proteinmodifizierende Enzyme, Transkriptionsfaktoren, Stoffwechselenzyme und Transportproteine gehören. Ein Zielprotein ist N-Acetyl-L-Glutamatkinase (NAGK), das im Argininsyntheseweg eine regulatorische Rolle spielt. Biochemische und Strukturanalysen an PII und NAGK aus *Synechococcus elongatus* PCC 7942 zeigten eine in zwei Stufen verlaufende Komplexbildung. Zunächst wird ein Ionenpaar zwischen R233 von NAGK und E85 von PII gebildet, wodurch der ausgedehnte T-Loop eine gewinkelte Konformation einnimmt. Im zweiten Schritt erfolgt die Insertion des T-Loops in den NAGK-Torus. Die Komplexbildung wird durch die Bindung von 2-OG unterbunden, welche zu einer T-Loop- Faltung führt, die eine stabile Interaktion mit NAGK nicht mehr zulässt. Die Bindung von 2-OG an PII erfolgt dabei in einem Spalt zwischen den Untereinheiten über Kontakte zu den konservierten Resten K58 und Q39, zusätzlich gibt es Wechselwirkungen mit der Hauptkette im Bereich der T- und B-Loops. Die negativ-kooperative Bindung von 2-OG an ein PII-Trimer gibt einen Einblick in den Verlauf der Signalwege zwischen den Untereinheiten in *S. elongatus*. Ferner wurde die Rolle von Glutamin als Signalmolekül für die PII-NAGK-Komplexbildung in *Chlamydomonas reinhardti*i untersucht. Der Komplex bildet sich nur in der Gegenwart von Glutamin. Eine Strukturanalyse fand die Glutamin-Bindestelle am einzigartig langen C-Terminus von *Cr* PII. Eine C-terminal verkürzte Form von *Cr* PII bindet auch bei Anwesenheit von Glutamin nicht an *Cr* NAGK. Dies unterstreicht die Bedeutung der Konformation des *Cr* PII C-Terminus, der das gebundene Glutamin in seiner Lage fixiert. Im Komplex sitzt ein PII-Trimer auf einem NAGK-Torus. In den Komplexen von *S. elongatus* und *Arabidopsis thaliana* jedoch bedecken zwei PII-Trimere den NAGK-Torus wie in einem Sandwich. Die Stöchiometrie der PII-NAGK-Komplexe in Lösung wurde durch Multiwinkel-Lichtstreuung bestimmt. Die Ergebnisse sind im Einklang mit den Kristallstrukturen. Darüber hinaus zeigte ein bioinformatischer Ansatz zur PII-NAGK-Koevolution den von der Natur ausgeübten selektiven Druck, die Stickstoff-Regulierungsfunktion von Cyanobakterien bis hin zu Plastiden zu konservieren. Diese Studien zeigen, wie bedeutend das PII-Protein und seine Konservierung während der Evolution für die Wahrnehmung des und das Eingehen auf den Kohlenstoff-, Stickstoff- und Energiestatus der Zelle sind.

3. Summary

The PII signal transduction proteins act as a biological central processing unit by integrating the signals from various cellular metabolites such as ATP, ADP and 2-oxoglutarate (2-OG). Depending on the binding status of the effector molecules, PII proteins can adopt different conformational states. These conformational states control the interaction with regulatory targets such as protein modifying enzymes, metabolic enzymes, transporters and transcription factors. One of the targets of PII proteins is *N*-acetyl-L-glutamate kinase (NAGK), which is a controlling enzyme in the arginine synthesis pathway. Biochemical and structural studies reveal a two-step complex formation of PII-NAGK from *Synechococcus elongatus* PCC 7942. The first step involves the formation of an ion-pair between R233 from NAGK and E85 from PII which enables the extended T-loop to undergo a kinked conformation. The second step involves the insertion of the T-loop from PII trimer into the NAGK toroid. The complex formation is disrupted by the addition of 2-OG, which coordinates the T-loop into a specific folded state that is incapable to bind NAGK. The binding of 2-OG to PII occurs at the intersubunit cleft by establishing a contact with the conserved residues K58 and Q39 along with the backbone interactions from T and B-loop. The binding of 2-OG in a negative-cooperative fashion to PII trimer sheds light on the intersubunit signalling in *S. elongatus*. Further, the role of glutamine as a signalling molecule in the PII-NAGK complex formation in *Chlamydomonas reinhardtii* was investigated. Complex formation between these proteins requires the presence of glutamine. Structural studies revealed the binding site of glutamine on the unique extended C-terminus of *Cr* PII. A C-terminally truncated form of *Cr* PII was unable to form a complex with *Cr* NAGK even in the presence of glutamine. This highlights the essential conformation adopted by the *Cr* PII C-terminus which acts like a plug to hold the effector molecule glutamine. The complex consists of one PII trimer bound to the NAGK toroid unlike the complexes from *S. elongatus* and *Arabidopsis thaliana* which consist of two PII trimers sandwiching the NAGK toroid. The state of PII-NAGK oligomerization in solution was analysed through Multi-Angle Light Scattering detection, which was consistent with the crystal structure of the complex. In addition, a bioinformatics approach on the PII-NAGK coevolution highlighted nature's selective pressure to conserve the nitrogen regulation function from cyanobacteria to plastids. In conclusion, these studies highlight the importance of PII and its evolutionary conservation to sense and respond to the carbon, nitrogen and energy status of the cell.

4. Introduction

4.1 Origin of oxygenic phototrophs

Life on earth dates back to 3.8 billion years ago, as predicted from the existing evidences (Mojzsis *et al*, 1996; Hayes, 1996). The production of oxygen (O_2) by photosynthesis is the most dominant global process essential for the sustainability of life on earth. This mechanism is an ancient process which has evolved via complex pathways (Blankenship, 2002; Björn and Govindjee, 2009). Before the origin of the oxygenic photosynthesis process, the atmospheric oxygen levels were insignificantly low. The evolution of oxygenic phototrophs is thought to have originated from cyanobacterial ancestors and these events changed the face of earth (Rye and Holland, 1998). The accumulation of O_2 in the atmosphere was driven by the innovation of a photosynthetic apparatus capable of utilizing water as an electron donor, which is oxidized to O_2. Concomitantly with the fixation of atmospheric CO_2, the water-splitting activity of cyanobacteria transformed the earth's atmosphere suitable for the progression of complex life forms.

Chlorophyll-based photosynthesis can be found in bacterial and eukaryotic domains (Blankenship, 2010). The bacterial domains include six different phyla of photosynthetically active species: cyanobacteria, proteobacteria (purple bacteria), green sulfur bacteria, firmicutes (helicobacteria), filamentous anoxygenic phototrophs and acidobacteria (Raymond, 2008). A vast number of research articles support the notion that eukaryotic photosynthesis originated from the endosymbiosis of cyanobacteria which resulted in the formation of chloroplasts (Schimper, 1883; William *et al*, 2012; McFadden 2001; Nowack *et al*, 2008). The key players in fixing the atmospheric CO_2 are the oxygenic phototrophs which include plants, algae and cyanobacteria. These organisms aided the production of 18 times more energy (ATP) through aerobic mechanism thereby pumping enough energy to drive the emergence of complex evolutionary processes. Despite microorganisms, oxygenic phototrophs also in particular play a crucial role to govern the biogeochemical cycle in the biotic and abiotic layers of the earth. A vast majority of our planet is covered with water and algae, which include the Chlorophyta (green algae), Euglenophyta, Dinoflagellata, Chrysophyta (golden algae), Phaeophyta (brown alage), Rhodophyta (red algae) and Diatoms are considered to play a disproportionately major role to preserve the biological pump in the water bodies.

4.2 Importance of the oxygenic phototroph: *Chlamydomonas reinhardtii*

Cyanobacteria were the first organisms to carry out oxygenic photosynthesis. During evolution, as a result of endosymbiosis some cyanobacteria gave rise to chloroplasts, while others continued to evolve as independent organisms. The lineage of green algae, *Chlamydomonas reinhardtii* (~10 µM in size) diverged from land plants over one billion years ago. *C. reinhardtii* are single celled chlorophytes with the photosynthetic apparatus residing in the chloroplast and are able to swim with two flagella. They are distributed worldwide and majorly used as model organism in biology especially due to their short generation time. Further, these algae have gained increased attention with the release of several genomic resources to public domain that includes the complete nuclear, chloroplast and mitochondrial genome (Merchant *et al*, 2007; Grossman *et al*, 2003). As a model organism they are used for studying chloroplast based photosynthesis, structure and assembly of cilia which was inherited from the common ancestor of plant and animal kingdom but lost in land plants. *C. reinhardtii* is of great interest in the biopharmaceutical industry especially for the synthesis of astaxanthin which is a potent anti-oxidant and as an animal feed additive to bestow coloration (León *et al*, 2007). These organisms have also been genetically modified to increase the production of elemental hydrogen. Hydrogen is a desirable fuel without any greenhouse effects and has a high enthalpy value. This biofuel can be discharged by microalgae via reduction of protons to hydrogen by the hydrogenases catalysed reaction, thus *Chlamydomonas* are considered as the most suitable organisms in the biofuel field (Hemschemeier 2008; Work *et al*, 2010; Pinto *et al*, 2013). Recently, these microalgae are being used to study various aspects of evolutionary biology and ecology (De Visser *et al*, 1996; Collins and Bell, 2004). The physiological response of algae and plant communities to increasing CO_2 has been studied to estimate the effect on global warming. Further, to understand the maintenance of sex and adaptation to the changing environmental conditions, *Chlamydomonas* species are a major subject of research target (Colegrave, 2002). Functional proteomics approach has also been employed on these organisms to discover novel components of the circadian system (Mittag *et al*, 2005). In addition, there has been recent focus on *Chlamydomonas* in the field of bio-remediation for the removal of heavy metals and for excess nitrate consumption from waste water (Vílchez *et al*, 2001; Wei *et al*, 2011). Interestingly, unlike the angiosperms, *Chlamydomonas* has an ability to grow in darkness exclusively in the presence of carbon source (Harris, 2009). This makes it an ideal model to study the eukaryotic photosynthesis system.

4.3 Electron transport and carbon metabolism

The metabolism of *Chlamydomonas* is quite complex, which makes it difficult to comprehend the metabolic pathways. In the chloroplast of *Chlamydomonas*, NADPH and ATP are regenerated by the light reaction of photosynthesis and consumed in the Calvin cycle (carbon fixation pathway). The atmospheric CO_2 is captured into the Calvin cycle and the algae finally fix CO_2 with the help of light energy, which is driven by series of reactions. The carbon reserve is metabolized to yield ATP and reducing power. The carbon metabolism is linked to key cellular processes such as cell motility, division, partitioning, carbon uptake, circadian rhythm and nutritional stress. The energy derived from photosynthesis and electron transfer is a probable means of understanding the regulation and mechanisms of the pathways involved in cellular processes.

Electron transport

The 'linear electron flow' symbolizes the electron flow from Photosystem II (PSII) through cytochrome b_6f (a membrane bound protein) to Photosystem I (PSI). Two molecules of water are oxidized into one molecule of O_2 in the PSII. The four electrons generated are transferred to the electron transport chain to finally reduce two molecules of $NADP^+$. This process is mediated in the stroma by ferredoxin (Fd) and ferredoxin $NADP^+$ reductase (FNR) and at the thylakoid membrane through PSI, PSII, plastoquinones, cytochrome b_6f complex and plastocyanin. The electron transfer generates a proton gradient that drives the ATP synthase to produce ATP from ADP and Pi. In the case of *C. reinhardtii*, its chloroplast possesses a fully functional electron transport chain even in the absence of light (Johnson and Alric, 2013).

Carbon metabolism

C. reinhardtii has one chloroplast and multiple mitochondria that are tightly packed together. A malate shunt operates to transfer the reductants from one organelle to the other (Johnson and Alric, 2013). The metabolism of *Chlamydomonas* mainly relies on reduced carbon sources, from the endogenous starch accumulated during the presence of light or from exogenous compounds like acetate (Harris, 2009). Higher plants have duplicated the glycolytic and the oxidative pentose-phosphate pathways in the chloroplast and cytosol (Joyard *et al*, 2010; Plaxton, 1996). However, in *C. reinhardtii* the glycolytic pathway is not duplicated but it is compartmentalized. The 'upper half' of glycolysis (glucose to glyceraldehyde-3-phosphate [G3P]) is localized in the chloroplast whereas the 'lower half' (3-

phosphoglycerate [3-PGA] to pyruvate) occurs exclusively in the cytosol (Ball, 1998). During unfavourable conditions, the exogenously acquired acetate is fed to glyoxylate cycle via gluconeogenesis or into the TCA cycle to sustain respiration and ATP production. Acetate is converted into acetyl coenzyme A (acetyl-CoA), which is directed into the TCA cycle and results in the production of 2-oxoglutarate (2-OG). The GS/GOGAT pathway requires the carbon skeleton in the form of 2-OG for ammonium assimilation. Furthermore, 2-OG acts as a metabolic signal to coordinate the regulation of C and N metabolism.

4.4 Nitrogen assimilation

The primary sources of nitrogen are ammonium and nitrate for most of the organisms. The energy cost for the ammonium assimilation is lower than that of nitrate assimilation. Many organisms favour ammonium uptake, however the abundance of nitrate makes its utilization much preferred at times. *Chlamydomonas* have evolved to harbour requisite genes to ensure efficient nitrogen assimilation.

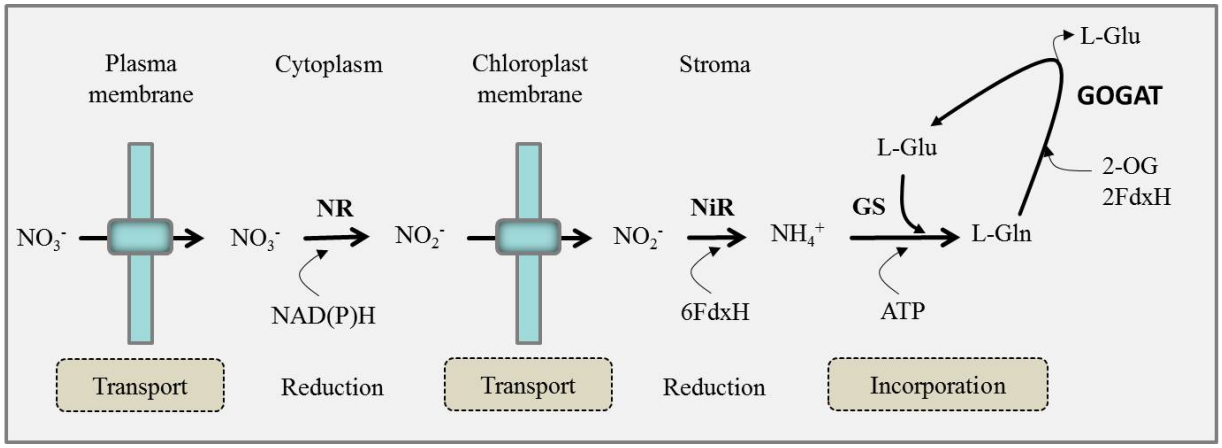

Figure 1. Nitrogen assimilation in Viridiplantae. The process of reduction of ammonium in the chloroplast and synthesis of glutamate through the GS/GOGAT cycle involves two transport and two reduction steps (adapted and modified from Fernandez and Galvan, 2008).
NO_3^-: Nitrate, NR: nitrate reductase, NO_2^-: Nitrite, NiR: Nitrite reductase, FdxH: [2Fe-2S]-type ferredoxin, NH_4^+: ammonium, GS: glutamine synthetase, L-Gln: L-glutamine, 2-OG: 2-oxoglutarate, GOGAT: glutamine-2-oxoglutarate-amido transferase, L-Glu: L-glutamate.

In photosynthetic eukaryotes the nitrate assimilation process involves two transport and two reduction steps to form ammonium in the chloroplast (Fig. 1). The ammonium incorporation into the carbon skeletons takes place through the glutamine synthetase/glutamate synthase (GS/GOGAT) cycle. The transport step consists of the entry of nitrate into the cell and nitrite into the chloroplast (Fernandez and Galvan, 2008). The first reduction step in the cytosol

involves the conversion of nitrate to nitrite with the assistance of the enzyme nitrate reductase (NR). The enzyme, nitrite reductase (NiR), catalyses the reduction of nitrite to ammonium in the chloroplast. The GS/GOGAT pathway results in conversion of one molecule of ammonium and 2-OG (with consumption of $2e^-$) to one molecule of glutamate from the hydrolysis of one ATP molecule (Fig. 1). The nitrate, nitrite and ammonium assimilation of *Chlamydomonas* needs to be further investigated in detail. The advent of genomic data for *Chlamydomonas* has helped to understand a few regulatory networks involved in nitrogen assimilation. However, yet more data needs to be examined to study the regulatory and metabolic circuits.

4.5 Regulation of nitrogen assimilation and glutamine synthesis

The *Chlamydomonas* cells when grown in the presence of light and ammonium, failed to utilize nitrate and nitrite due to the strong inhibition of ammonium (Florencio and Vega, 1983). This antagonistic effect of ammonium is as a result of inhibition of the permease which is responsible for the transport of nitrate. Such situations with excess of ammonium are toxic to the organism and cause repression and deactivation of GS. To counteract such conditions, ammonium is incorporated into the GS/GOGAT cycle. At low ammonium concentration, the GS/GOGAT is essential for glutamate synthesis and for the regulation of the glutamine pool.

Glutamine synthesis and role in metabolism

GS (Glutamine synthetase) is the prime enzyme needed for the introduction of nitrogen into the cellular metabolism. It occurs in all kingdoms of life and is involved in ammonium assimilation and glutamine synthesis. The enzyme GS catalyses the formation of glutamine from ammonia and glutamate in the presence of ATP and Mg. GS can be composed of 8, 10, or 12 identical subunits forming two rings directly facing each other (Eisenberg *et al*, 2000; Stryer *et al*, 2007; Krajewski *et al*, 2008). The widely distributed form of GS in prokaryotes is GSI, encoded by the *glnA* gene (Merrick and Edwards, 1995). This class is absent in the eukaryotic kingdom. GSI is a homo-dodecameric enzyme forming a double hexameric ring structure. The class II (GSII) enzymes consist of a decamer (Krajewski *et al*, 2008) that are found in eukaryotes and also in bacteria belonging to Rhizobiaceae, Frankiaceae, and Streptomycetaceae families. Plants have multiple copies of GSII isozymes; one of the isozymes is translocated into the chloroplast. The Class III enzyme (GSIII) has only been

found in *Bacteroides fragilis* and in *Butyrivibrio fibrisolvens* (Hill *et al*, 1989; Goodman and Woods, 1993). It is a double-ringed dodecamer of identical subunits and larger than the other enzymes GSI and GSII. In the case of *C. reinhardtii*, two isoforms of GS have been identified which have similar properties to plant GS enzymes. At the molecular genetics level, the accumulation of GS transcripts in green algae have been reported in response to the influence of ammonium, nitrate and light (Chen and Silflow, 1996). Molecular evolution studies of GSII suggest the non-endosymbiotic gene transfer of GSII from gammaproteobacteria (Eubacteria) to the Chloroplastida (Ghoshroy *et al*, 2010). This suggests the occurrence of multiple isoenzymes of GS in the chloroplastida due to acquisition through horizontal gene transfer process.

Organisms have evolved sophisticated mechanisms to monitor the nitrogen status of the cell and during the course of evolution a vast number of bacteria have utilized glutamine as an important signalling molecule (Forchhammer, 2007). An increasing number of mechanisms are known to control nitrogen regulation of archaea, bacteria and plants. One of the common regulatory features found across these kingdoms is the PII signal transduction protein. PII is tightly coupled to glutamine signalling in a variety of bacteria (Stadtman, 2001; Adler *et al*, 1975).

4.6 PII signal transduction proteins and their evolution

PII proteins are the most widely distributed signal transduction proteins in nature. They play a vital role in the C/N metabolism in bacteria, archaea and are also found in the plastids of plants. Depending on the carbon, nitrogen and energy status of the cell, PII proteins integrate the signals from effector molecules like ATP, ADP and 2-OG (Ninfa and Atkinson, 2000; Ninfa and Jiang, 2005; Leigh and Dodsworth, 2007; Forchhammer, 2008) resulting in allosteric and covalent modifications followed by conformational changes. These conformational changes dictate the binding of PII proteins to their regulatory targets. The targets constitute a wide range of metabolic enzymes, transport proteins, transcription factors and protein modifying enzymes (Fig. 2).

Based on the genes encoding the PII proteins they are classified into three groups as *glnK*, *glnB*, *nifI* (Arcondeguy *et al*, 2001; Forchhammer 2008). The GlnK protein is widely distributed in prokaryotes and is invariably linked to the ammonium transport protein AmtB

(Conroy *et al*, 2007; Gruswitz *et al*, 2007; Yildiz *et al*, 2007). The *glnK* and *amtB* genes most likely arose in archaea and were subsequently transferred between the lineage of archaea and bacteria (Sant'Anna *et al*, 2009; Huergo *et al*, 2012). It is speculated that the recent PII proteins could have originated from the ancient GlnK-AmtB complex involved in ammonium uptake. Gene duplication events could have resulted in the origin of the other PII paralogues GlnB and NifI. These paralogues are involved in nitrogen fixation mechanisms, gene expression and in the regulation of GS (Huergo *et al*, 2012; Leigh and Dodsworth, 2007). Some organisms have been found to harbour one, two and even three paralogues (*Microcoleus chthonoplastes and Rhodospirillum rubrum*) of PII proteins.

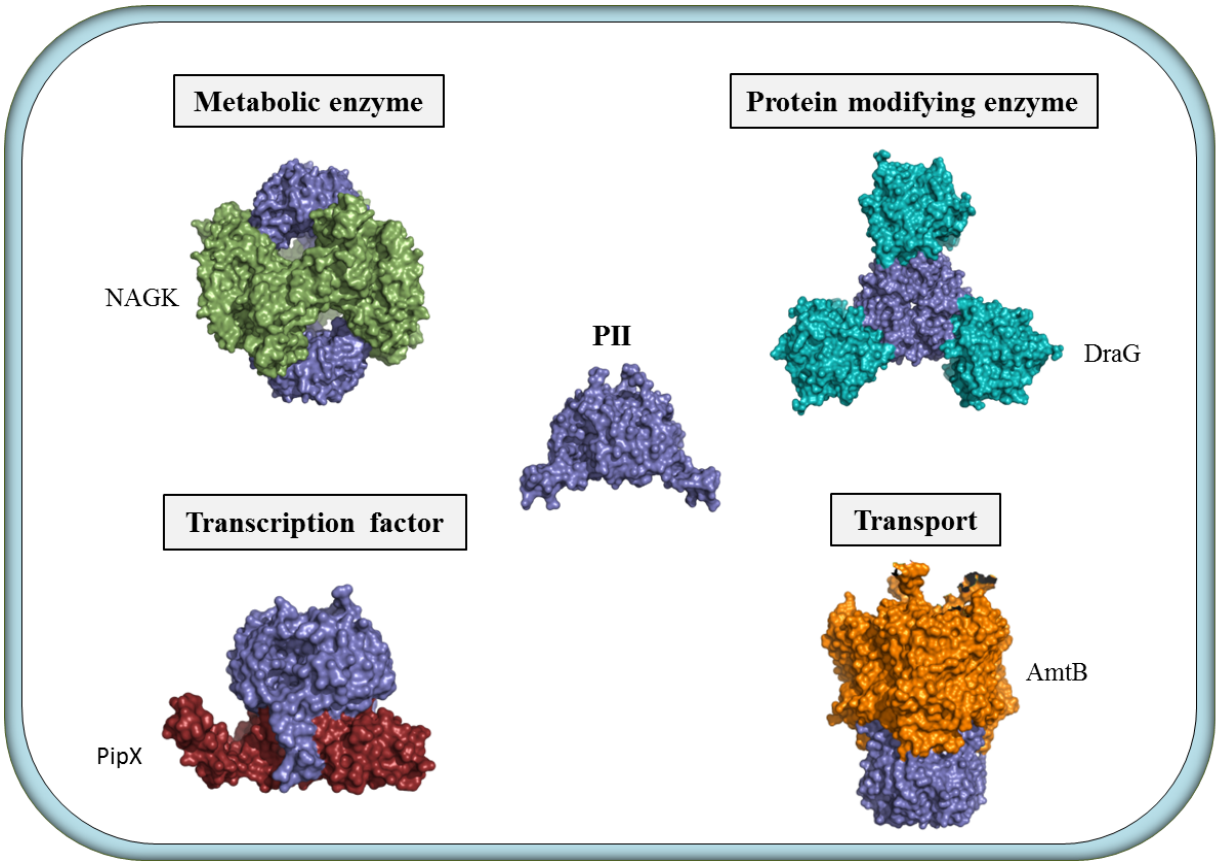

Figure 2. Schematic diagram of the PII protein hub (all known protein structures) representing the regulatory targets which include members from metabolic enzymes (NAGK-green), transcription factors (PipX-maroon), protein modifying enzymes (DraG-cyan) and transport proteins (AmtB-orange). [PII-NAGK, PDB: 2V5H, *Synechococcus elongatus* PCC 7942], [PII-PipX, PDB: 2XG8, *Synechococcus elongatus* PCC 7942], [GlnZ-DraG, PDB: 3O5T, *Azospirillum brasilense*], [PII-AmtB, PDB: 2NUU, *Escherichia coli*]. (Conroy *et al*, 2007; Llácer *et al*, 2007, 2010; Rajendran *et al*, 2011).

Two signature patterns of PII have been defined in the PROSITE (PS00496 and PS00638). The first pattern consist of the following conserved stretch of residues (Y-[KR]-G-[AS]-[AE]-Y) with a uridylylation site at Y51 and the second is derived from an invariant locus in the C-terminal part (Fig. 3A) of the PII protein ([ST]-x(3)-G-[DY]-G-[KR]-[IV]-[FW]-[LIVM]-

x(2)-[LIVM]). The C-terminal signature is more redundant than the first signature pattern (Sant'Anna *et al*, 2009). Bioinformatics analysis revealed a new out-group of PII proteins; PII-NG, which were predominantly present in proteobacteria and lacked the two signature patterns. These PII proteins were localized downstream and linked to the heavy metal transporter genes corresponding to *czcCBA* operon that encode for proton-cation antiporter of Cd^{2+}, Co^{2+} and Zn^{2+} (Sant'Anna *et al*, 2009). Hence, these PII-NG proteins seem to be associated with toxic heavy metal resistance conferring proteins.

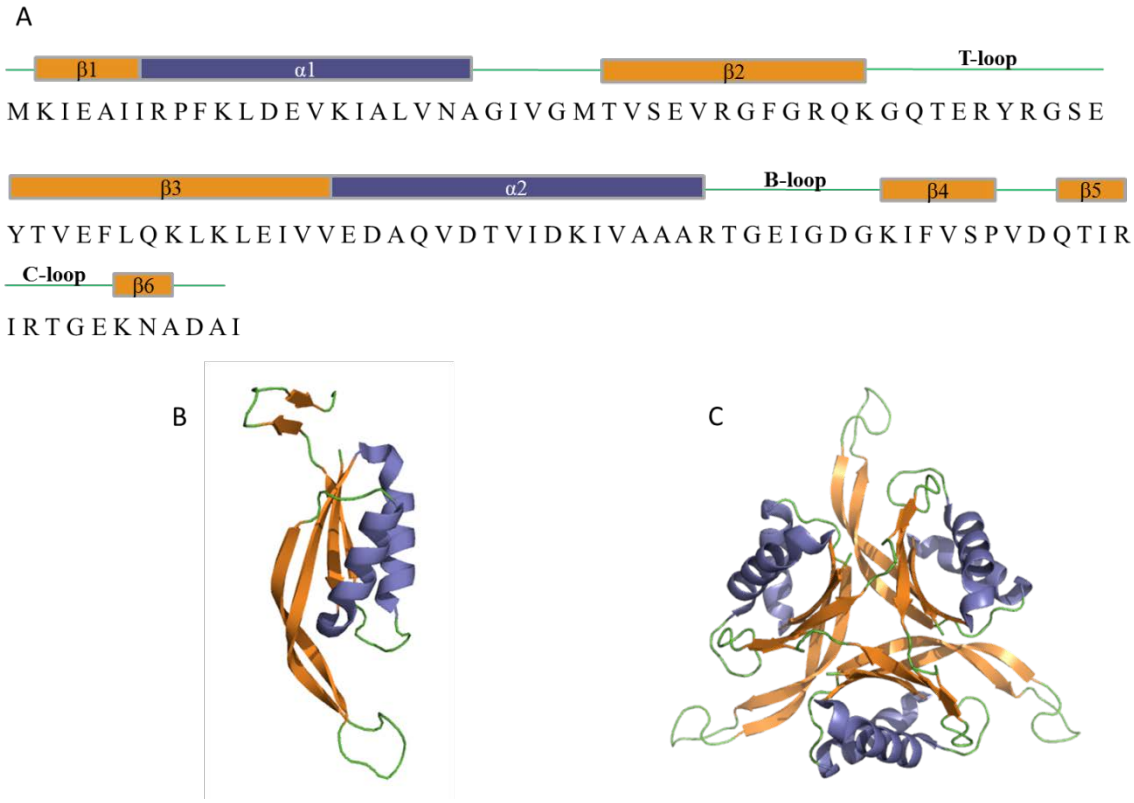

Figure 3. A) Representation of the secondary structural elements in the PII sequence from *S. elongatus* PCC 7942 B) Structure of PII monomer from *S. elongatus* highlighting the secondary structure: helix(slate), sheet(orange) and loop(green). C) Top view of the PII protein structure (PDB: 1QY7, Xu *et al*, 2003).

PII proteins are homotrimers of approx. 12 kDa/monomer with a highly conserved 3D structure across diverse group of organisms (Sant'Anna *et al*, 2009; Huergo *et al*, 2012). They are composed of a double ferredoxin-like fold (βαβ-βαβ) with three eminent loops (T-loop, B-loop and C-loop) emerging from the flattened barrel like structure (Fig. 4). The T-loops undergo covalent modification, conformational changes and mediate the interaction with targeted receptors (Truan *et al*, 2010; Litz *et al*, 2011; Radchenko and Merrick 2011; Zeth *et al*, 2012). The two other prominent loops (B and C) occupy the intersubunit cleft emerging face to face from the adjacent monomers. The cleft forms the binding site for the

effector molecules like ATP-Mg, ADP and 2-OG (Zeth *et al*, 2012). In *S. elongatus*, in the presence of excess 2-OG, the binding pockets are capable of accommodating up to three molecules of ATP-Mg-2-OG for a PII trimer. The crystal structures of PII protein from *Arabidopsis thaliana* bound to citrate and malonate; and *S. elongatus* bound to citrate have also been determined (Mizuno *et al*, 2007; Zeth *et al*, 2012).

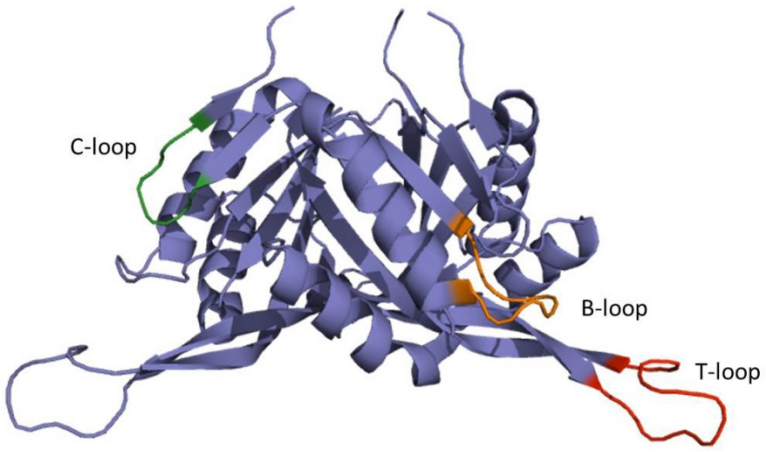

Figure 4. A) PII protein from the cyanobacteria *Synechococcus elongatus* PCC 7942 (PDB: 1QY7, Xu *et al*, 2003) with the loops highlighted as T-loop: red, B-loop: orange and C-loop: green.

The signal integration of PII protein involves a reversible covalent modification at the apex of the T loop region. This is not conserved in all organisms and different types of modifications ranging from phosphorylation, adenylylation to uridylylation have been observed so far. The PII protein in proteobacteria has been shown to undergo uridylylation/deuridylylation and the actinobacteria to undergo adenylylation/deadenylylation at the Y51 residue (Atkinson *et al*, 1994; Jonsson and Nordlund, 2007). The cyanobacterial PII proteins have been found to exhibit phosphorylation/dephosphorylation at the S49 residue (Forchhammer and de Marsac 1994; Forchhammer and de Marsac 1995). These modifications govern the conformation and fine tuning of the loops, especially the T-loop and determine the interaction with the target receptors.

4.6.1 PII signalling network in *E. coli*

The canonical PII protein in *E. coli* is GlnB that controls the expression of the nitrogen-regulated genes (Shapiro, 1969; Jiang and Ninfa, 1999, 2009; Jiang *et al*, 2012). GlnB regulates the reversible adenylylation of the glutamine synthetase (GS) in response to the cellular metabolite glutamine (nitrogen signal) and 2-OG (carbon signal). Covalent

adenylylation of GS and the regulation of the structural gene *glnA* encoding the protein GS helps in maintaining the balance between the ammonium and carbon assimilation (Fig. 5). During nitrogen limiting conditions, GlnB undergoes reversible uridylylation at Y51 (T-loop region) which is catalysed by the signal transducing uridylyltransferse/uridylyl-removing enzyme [(UTase/UR)-product of *glnD*] (Jaggi *et al*, 1996; Jiang *et al*, 1998a). In the presence of excess glutamine, the uridylyl removing activity of the uridylyltransferase is activated resulting in the deuridylylated form of GlnB. The receptor for GlnB is the enzyme glutamine synthetase adenylyltransfersae (ATase) which binds to the modified/unmodified form of GlnB. The binding of ATase to the deuridylylated form of GlnB results in the adenylylation of GS. Whereas, the complex formation between modified form of GlnB and ATase results in the deadenylylation and thereby activation of GS (Jiang *et al*, 1998c). GlnB also controls the expression of nitrogen regulated genes through binding to another receptor NRII (NtrB) histidine kinase of the two-component NRI/NRII regulatory system (Ninfa and Magasanik, 1986; Jiang *et al*, 1997; Jiang *et al*, 1998b). The unmodified GlnB causes dephosphorylation of NRII and thereby inactivates the transcriptional activator NRI (NtrC) (Jiang and Ninfa; 1999; Weiss *et al*, 1991). The binding of ATP to NRII promotes the reversible transfer of γ-phosphate from ATP to a histidine residue of NRII which is then reversibly transferred to the aspartic residue of NRI (Weiss and Magasanik, 1988). The uridylylated form of PII is unable to form a complex with NRII resulting in the activation of NRI by phosphorylation and hence activating the nitrogen regulatory genes (Atkinson *et al*, 1994). The binding of the effector molecule 2-oxoglutarate modulates the ability of GlnB to bind ATase and NRII under nitrogen limiting conditions (Ninfa and Atkinson, 2000).

In addition to *glnB*, *E. coli* cells harbour another gene encoding the protein PII known as GlnK which was noticed in nitrogen deprived cells (Atkinson *et al*, 2002). In prokaryotes, the *glnK* genes have been shown to be transcriptionally linked (Thomas *et al*, 2000; Javelle and Merrick, 2005) to the membrane-bound ammonium transport protein (AmtB). This linkage has been found in most of the eubacteria and archaea showing a high degree of conservation. In *E. coli*, the GlnK-AmtB system is coupled to the intracellular nitrogen regulation (Ntr) system to maintain the ammonium status in the cell (Javelle and Merrick, 2005; Coutts *et al*, 2002; Javelle *et al*, 2004). The uridylylation of GlnK dictates the binding to AmtB based on the intracellular increase in glutamine caused by ammonium excess. The crystal structure of the first PII bound receptor consisting of a GlnK-AmtB complex has been solved for *E. coli* (Conroy *et al*, 2007; Gruswitz *et al*, 2007). The GlnK is found to be structurally very similar

to the GlnB protein (Xu *et al*, 1998; Xu *et al*, 2001). The GlnK-AmtB forms a threefold symmetric complex with the GlnK trimer associated to the cytoplasmic side of the AmtB. The *E. coli* AmtB consists of the characteristic 11 transmembrane helices with N_{out} and C_{in} topology. It forms a homotrimer with a central pore involved in the conductance of ammonia. GlnK interacts with AmtB through the extended T-loop that inserts into the cytoplasmic pore of the AmtB thereby blocking the ammonia flux into the cell. The T-loop adopts an unusually different conformation consisting of two-stranded short antiparallel β-sheets which are separated by a β-turn (Conroy *et al*, 2007). The formation and dissociation of the complex has been found to be sensitive to the effector molecule 2-OG in the presence of ATP-Mg (Durand and Merrick, 2006; Wolfe *et al*, 2007). The occurrence of GlnK suggests the pivotal role played during the ammonium flux inside the cell and the genetic linkage of *glnK* and *amtB* genes suggests the evolutionary significance and conservation of ancestral PII proteins.

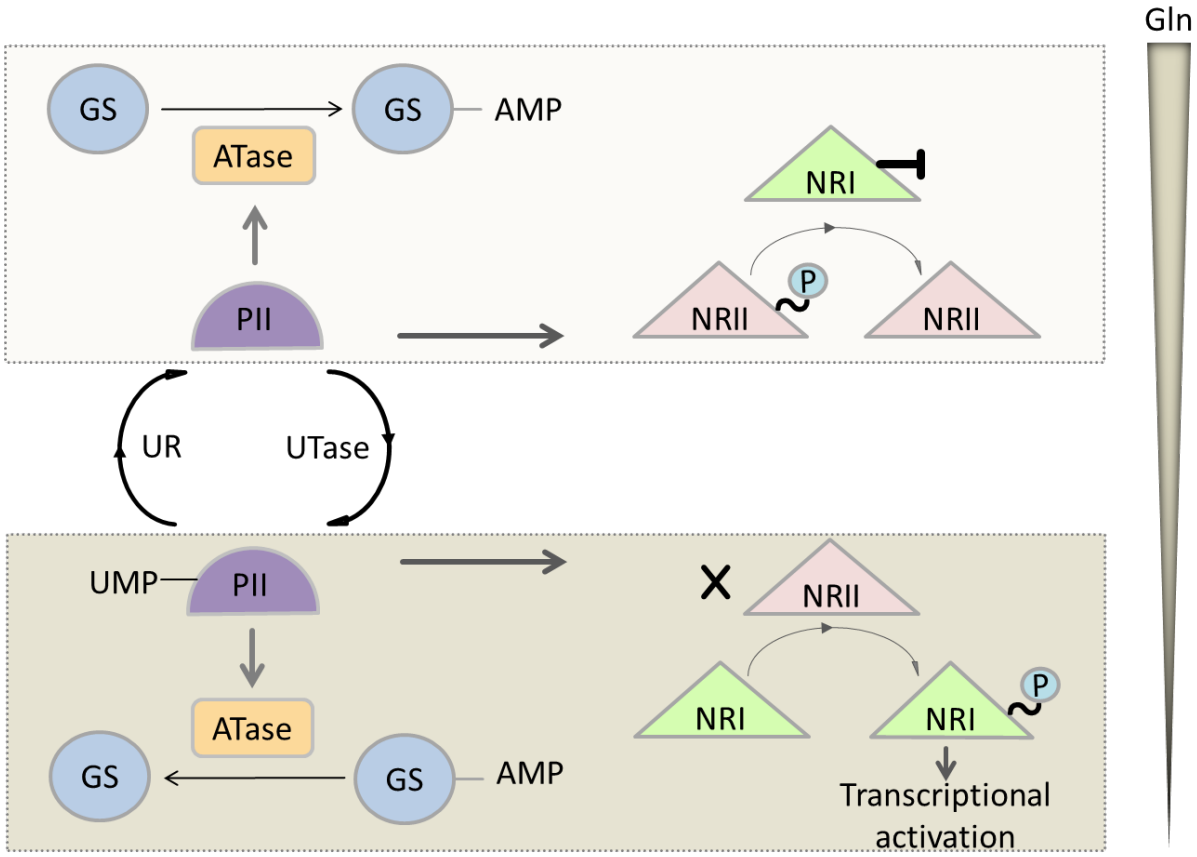

Figure 5. Regulation of GS and the Ntr regulon.
During nitrogen (glutamine) excess condition the PII protein mediates the adenylylation of GS through the enzyme ATase. In the unmodified state, PII also causes the dephosphorylation of the NRII and thereby inactivates the NRI. Nitrogen (glutamine) limitation conditions result in uridylylation of PII which results in deadenylylation of GS and hence its activation. The uridylylated form of PII inhibits the complex formation with NRII and this promotes the phosphorylation of NRI. The NRI in the phosphorylated form is capable to activate the genes involved in nitrogen regulation.
GS: glutamine synthetase, ATase: glutamine synthetase adenylyltransfersae, UTase: uridylyltransferse, UR: uridylyl-removing enzyme, NRI and NRII: nitrogen regulator I and II.

4.6.2 PII signalling in cyanobacteria

The signal perception and receptor interaction for PII proteins has been mainly studied in the unicellular cyanobacteria *Synechococcus elongatus* PCC 7942 and *Synechocystis* PCC 6803. The structures of PII protein from both the organisms have been resolved to be highly identical (Xu *et al*, 2003). The binding pocket for ATP/ADP occurs in the intersubunit crevice through interaction with the residues of T-loop, B-loop and the adjoining C-loop from the neighbouring subunit. The ATP binding site can compete for the binding of ADP and the divalent cation Ca^{2+} was found to antagonize the effect of ATP-2OG (Maheswaran *et al*, 2004).

A. Phosphorylation/dephosphorylation of PII proteins

Besides binding to the effector molecules ATP, ADP and 2-OG, the PII proteins act as a highly sensitive signal receiver/transducer protein. In *S. elongatus* and *Synechocystis* PCC 6803, the covalent modification event of phosphorylation occurs in the S49 residue at the tip of the T-loop (Forchhammer and de Marsac, 1995; Kloft and Forchhammer, 2005). However, it has been reported that the cyanobacteria *Prochlorococcus* and *Anabaena* PCC 7120 are devoid of this covalent modification (Palinska *et al*, 2002; Zhang *et al*, 2007). Surprisingly, this *Anabaena* strain seems rather to undergo nitration at the Y51 residue, which corresponds to the same position in proteobacteria being subjected to uridylylation (Zhang *et al*, 2007). Increasing nitrogen starvation coupled with increasing inorganic C-supply has been found to be proportional to the amount of PII proteins undergoing phosphorylation. The phosphorylation can take place at three sites in the apex of each T-loop of a trimeric PII protein. With the introduction of nitrate into the medium the occurrence of intermediate phosphorylation states ($P^0_{II,}$ P^1_{II}, P^2_{II}, and P^3_{II}) of PII protein was observed (Forchhammer and de Marsac, 1994; Forchhammer, 2010).

Attempts to decipher the kinase responsible for PII phosphorylation through knockout studies have been a failure so far leaving the speculation for a possible kinase to be cryptic. In PII proteins, the binding of 2-OG to the first two sites has been shown to have a lower dissociation constant and the third site needs millimolar concentrations of 2-OG to occupy the binding pocket. Hence, the kinase is likely activated in the presence of ATP and high concentrations of 2-OG (Forchhammer and de Marsac, 1995). In contrast, the PII phosphatase

PphA (responsible for removing the phosphate) has been identified in *Synechocystis* PCC 6803 (Irmler and Forchhammer, 2001; Ruppert *et al*, 2002). The phosphatase belongs to PP2C family and is found to be strongly inhibited in the presence of ATP-$Mg^{2+}$and 2-OG. Recently, the crystal structure of PP2Cs from bacterial and plant origin has been solved which implicates the important role of three Mg^{2+}/Mn^{2+} ions in catalysis (Schlicker *et al*, 2008; Melcher *et al*, 2009; Su *et al*, 2011). The tPphA from *Thermosynechococcus elongatus* has been well studied among the known PP2C family members and it sheds light on the importance of a flap domain that controls the access to catalytic centre and also highlights the importance of metal coordination to the catalytic site (Schlicker *et al*, 2008; Su *et al*, 2011; Su and Forchhammer, 2012; Su and Forchhammer, 2013).

B. Receptor interaction in PII proteins

To identify the interacting partners of PII proteins, two main strategies were employed. The first strategy was performed in *S. elongatus*, which involved the determination of the phenotype caused by PII-deficient mutants. The second strategy consisted of yeast two-hybrid screening with *glnB* genes from *S. elongatus* or *Synechocystis* PCC 6803 as the bait (Burillo *et al*, 2004; Heinrich *et al*, 2004; Osanai *et al*, 2005b). This strategy resulted in finding *N*-acetyl-L-glutamate kinase (NAGK), which catalyses the prominent step in arginine biosynthesis, PipX: a cofactor of the transcription factor NtcA; and a membrane protein PamA of unknown physiological function.

PII-NAGK complex formation

PII proteins have evolved to regulate the ornithine pathway which leads to the synthesis of arginine and polyamine (Fig. 6). The second step in the synthesis of arginine; *N*-acetyl-L-glutamate (NAG) to *N*-acetyl-L-glutamyl 5-phosphate (NAG-P) is coordinated by the enzyme *N*-acetyl-L-glutamate kinase (NAGK, encoded by *argB* gene). In the presence of excess arginine, NAGK is feed-back inhibited by arginine and unmodified PII protein plays a vital role to relieve this inhibition (Heinrich *et al*, 2004; Maheswaran *et al*, 2004). The catalytic efficiency of NAGK is remarkably enhanced with the binding of PII which results in approx. 4-fold increase in the V_{max} values and considerable decrease in the K_m value (Maheswaran *et al*, 2004; Beez *et al*, 2009). Further, the binding of PII favours the release of arginine and increases the affinity for NAG. The formation of PII-NAGK complex is strongly influenced

by the effector loaded state of the PII protein. The binding of ADP leads to immediate dissociation of the complex and similar effects have been noted with the addition of ATP-Mg and 2-OG (Maheswaran *et al*, 2004).

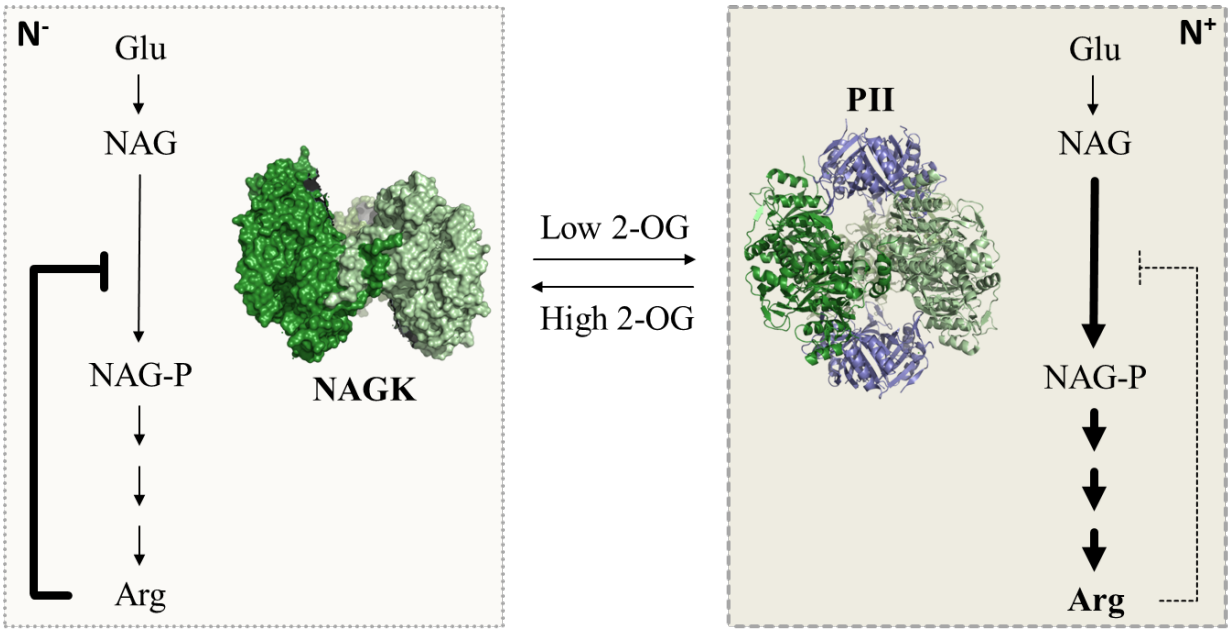

Figure 6. Arginine biosynthesis and storage mechanism in cyanobacteria.
During the conditions of nitrogen limitation (high 2-OG and high ADP) NAGK has very low activity and is susceptible to feedback inhibition by its pathway product arginine. However, during nitrogen excess conditions (low 2-OG and low ADP) PII protein forms a stable complex with NAGK and helps in the conversion of the substrate NAG to NAG-P. The arginine synthesized is stored as cyanophycin for later use.
Glu: glutamate, NAG: *N*-acetyl-L-glutamate, NAGK: *N*-acetyl-L-glutamate kinase, NAG-P: *N*-acetyl-L-glutamyl 5-phosphate, Arg: arginine, 2-OG: 2-oxoglutarate. (PDB: 2V5H, Llácer *et al*, 2007).

Structure and function of the PII-NAGK complex

The crystal structure of the bacterium, *S. elongatus* has been solved at 2.75 Å (Llácer *et al*, 2007). The complex reveals two trimers of PII sandwiching the NAGK toroid ring (trimer of dimers). NAGK forms a $\alpha_3\beta_8\alpha_4$ fold which can be divided into N and C domain. The N domain of NAGK contains a mobile kinked α-helix (N-helix) which by interlacing with another N-helix forms the toroid. The binding site of NAG and ATP are confined in the N and C-domain respectively and the arginine occupies the space near the intersection of the N-helix. The three fold symmetry axis of PII-NAGK is arranged such that upon encounter, one PII subunit makes a contact with one subunit of NAGK. A salt bridge formed in the B-loop of free PII between the residues R47 and E85 is broken and a new ion-pair between E85 and R233 from NAGK aids in the formation of the complex. Further, the B-loop residues and the distal end of the kinked T-loop together establish a firm interaction with the NAGK. The

contact also involves the hydrophobic residues F11 and T83 of PII; and I229, I253 and A257 of NAGK. The residues R45 and S49 (involved in phosphorylation) in the T-loop and E85 in the B-loop of PII play a vital role in complex formation and are highly conserved in the photosynthetic organisms. Similarly, the conserved residues E194, R233, R254, Q258 and A257 (located in the hydrophobic interface) in NAGK play an essential role during the formation of complex. The occurrence of these residues is considered as a signature of the PII-NAGK signalling system. The binding of PII body to the C-terminus of the NAGK causes for widening of the rings thereby resulting in lower affinity for holding the arginine in its inhibitory pocket (Llácer *et al*, 2008). About 14.3% of the exposed surface of PII and 5.8% of the exposed surface of the NAGK is buried in the complex.

PII-PipX interaction

The yeast two-hybrid screening with *glnB* genes as bait resulted in the identification of PipX (PII interaction protein X) as well which had no homology to known proteins (Espinosa *et al*, 2006). PipX is a protein of 89 aminoacids and is found exclusively in cyanobacteria. In order to understand the mechanism of PipX further, it was used as bait for the yeast two-hybrid screening which resulted in the recruitment of NtcA (transcription factor) as an interaction partner. NtcA (Crp family) is involved in the nitrogen regulated gene expression, where it binds and activates the promoter of genes such as: *glnA* (glutamine synthetase), nir-operon (nitrate/nitrite reductase) and *ntcA* gene itself (Wei *et al*, 1993; Luque *et al*, 1994; Vega-Palas *et al*, 1992). NtcA occurs as homodimer of approx. 50 kDa and in the active state forms a complex with PipX in the presence of high 2-oxoglutarate concentration. The PipX-NtcA complex binds to DNA but PipX does not alter the affinity of NtcA towards its binding site (Espinosa *et al*, 2007). The structures of the PII-PipX and PipX-NtcA complexes have been solved for the cyanobacteria, *S. elongatus* (Llácer *et al*, 2010). The PipX structure consists of a tudor like domain which mediates most of the interaction with PII and NtcA. In the PII-PipX complex, one PII trimer sequesters three PipX molecules preventing the PipX activation of NtcA. Nitrogen starvation (2-OG excess) condition leads to loading of 2-OG molecules to PII that result in an extended T-loop conformation leading to the dissociation of PII from PipX. Under this condition, PipX favours complex formation with the transcription factor NtcA. The PipX-NtcA complex is composed of a dimer of NtcA and two monomers of PipX. This complex has been postulated to be involved in the recruitment of the RNA polymerase for transcription initiation.

PamA-PII interaction: still a mystery unsolved

PamA [PII associated membrane protein A, encoded by *sll0985*], a transmembrane protein was identified as the potential target for PII through the yeast two-hybrid screening process (Osanai *et al*, 2005b). PamA consists of 260 aminoacids and was predicted to contain seven-membrane spanning segments and a Blast analysis resulted in sequence similarity to a protein family elucidated as a mechanosensitive ion channel. Biochemical analyses confirmed the interaction of PII and PamA and the inhibitory role exerted by ATP and 2-OG. Further, the deletion mutant of PamA resulted in the down regulation of the transcripts (*nblA, nrtABCD* and *ureG*) involved in nitrogen metabolism and the sigma factor SigE. A SigE mutant of *Synechocystis* showed decrease in the levels of genes involved in glycolysis, oxidative pentose phosphate pathway and glycogen metabolism (Osanai *et al*, 2005a). These results shed light on the role of SigE in the transcriptional activation of sugar catabolic pathway. In addition, phylogenetic studies revealed that the C-terminus of PamA was composed of a three membrane spanning region consisting of the MscS family domain (Osanai and Tanaka, 2007). MscS is responsible for relieving the hypo-osmotic shock in bacteria by the release of turgor pressure.

4.6.3 PII signalling in plants

PII proteins in plants have been majorly studied in *A. thaliana*, *Oryza sativa* and *Ricinus communis*. They are found to be nuclear encoded and localize in the chloroplast of plants (Hsieh *et al*, 1998; Smith *et al*, 2003; Sugiyama *et al*, 2004). Until now, there has been no covalent modification in the T-loop reported for plants. A well-studied interaction partner of plant PII protein is NAGK. The crystal structure of PII-NAGK complex from *Arabidopsis* has been solved (Mizuno *et al*, 2007). The complex structure is highly similar to the *S. elongatus* structure with an exception of the presence of additional ligands that include ADP, NAG and arginine resolved in NAGK and ATP-Mg bound to PII. Similar to *S. elongatus*, the corresponding residues in *A. thaliana* which include the T-loop residue R56 and S60 and B-loop residue E96 are highly conserved and are involved in the complex formation between PII and NAGK (Mizuno *et al*, 2007). The residue W22 replaces the residue F11 found in the *S. elongatus* PII protein which has been implicated to play an important role in complex formation. Despite high degree of similarity between the complex structures, there are some substantial functional differences between the PII and NAGK from *A. thaliana* in comparison

to cyanobacteria. The PII from *Arabidopsis* is highly dynamic and activates NAGK with an increase in the V_{max} of up to ~30% (Chen *et al*, 2006). In the coupled assay, free *At* NAGK displays elevated activity than *Se* NAGK with a 100-fold overall higher catalytic efficiency. In plants neither ADP, 2-OG nor ATP at lower concentrations are effective in disrupting the complex (Beez *et al*, 2009). This could be because of the high affinity of ATP for plant PII proteins leading to impairment of the sensing and binding of ADP (Mizuno *et al*, 2007; Beez *et al*, 2009). However, the *Arabidopsis* PII alone has been shown to respond to ATP, ADP, 2-OG and lower amounts of oxaloacetate (Smith *et al*, 2003).

The plant and the cyanobacterial PII and NAGK proteins have been found to complement each other when these proteins were swapped between the organisms (Beez *et al*, 2009). Collectively, it can be concluded that the PII-NAGK interaction is a primitively conserved mechanism which has been altered from prokaryotes to eukaryotic phototrophs for the control of nitrogen regulation during the evolution. Apart from the regulatory role of PII-NAGK complex, recent finding show the involvement of PII in the NO_2^- uptake by the *A. thaliana* chloroplast (Ferrario-Méry *et al*, 2008). A knockout of PII resulted in the significant increase in NO_2^- toxicity. Such a phenomenon was already observed in cyanobacteria where PII proteins phenotypically regulate an ABC type NO_2^-/NO_3^- transporter (Lee *et al*, 1998; Kloft and Forchhammer, 2005). In plants, the molecular mechanism of NO_2^- uptake is unknown raising the possibility for existence of a NO_2^- channel or NO_2^- transporter.

Recently a family of 'biotin-binding proteins' was found to interact with PII proteins from *A. thaliana* leaf extracts, one of the most important being Acetyl-CoA carboxylase (ACCase), an enzyme involved in initiating the synthesis of fatty acids in plastids (Feria Bourrellier *et al*, 2010). The activity of ACCase was antagonised by PII and it was possible to relieve this inhibition by addition of the metabolites 2-OG, pyruvate or lower amounts of oxaloacetate. Understanding the mechanism of ACCase activity through PII regulation would be helpful to increase the oil content in seeds. Further, a transcription factor WRINKLED1 (inducer of glycolytic and fatty acid biosynthetic genes) was found to directly control the *At* GLB1 gene (encoding PII protein) expression during early seed maturation (Baud *et al*, 2010). Altogether, these results have indicated a new role of PII in the fine tuning of fatty acid production in seeds. Preliminary research work has been done in seed maturation and it's yet unclear whether PII has a role in other developmental stages of plants and this needs to be further investigated.

4.6.4 PII proteins in *Chlamydomonas reinhardtii*

PII proteins (encoded by *CrGLB1* gene) from *Chlamydomonas reinhardtii* localize in the chloroplast. Unlike red algae, where the *glnB* gene is chloroplast encoded, PII from Viridiplantate (green plants) are coded in the nucleus. The *Chlamydomonas* PII (17.5 kDa) has an exceptionally long N and C-terminus in comparison to bacterial homologues. The N-terminus includes a signal peptide (1-46 aminoacids) and the C-terminus ends unusually with four positively charged residues (KKKK). A protein BLAST search with the C-terminus resulted in a hypothetical protein (XP_002956980.1) with 123 aminoacids from *Volvox carteri f. nagariensis* consisting of highly similar C-terminus ending with a stretch of positive residues (RRKR).

The *CrGLB1* gene expression is found to be meagrely altered in different cell types and growth conditions (Ermilova and Forchhammer, 2013); however dark-light shift and nitrogen starvation have some influence in the increase of transcript level. The position Y51 that corresponds to the uridylylation site of proteobacteria is substituted with a phenylalanine residue. This indicates no possibility of uridylylation in *C. reinhardtii*. The S49 position in cyanobacteria which corresponds to the phosphorylation site is substituted with threonine and is not phosphorylated like plant PII proteins (Ermilova *et al*, 2013). Hence, the mature *Cr* PII doesn't seem to undergo covalent modifications.

PII has been shown to be involved in NO_2^- uptake in *S. elongatus* PCC 7942 and *A. thaliana* (Ferrario-Méry *et al*, 2008; Lee *et al*, 1998; Kloft and Forchhammer, 2005). Nitrite, a metabolite of the nitrate assimilation is produced in the cytosol and needs to be transferred immediately into the chloroplast to avoid NO_2^- toxicity. Two different mechanisms have been proposed for the nitrite diffusion in the illuminated chloroplast (Anderson and Done 1978; Brunswick and Cresswell, 1988). The first mechanism suggests the free diffusion of nitrite due to a sink effect or through an active transport coupled through a photochemical signal cascade. Under low nitrate supply, the knockout of a nitrite transporter (NAR1) in *C. reinhardtii* chloroplast caused nitrogen deficiency (Rexach *et al*, 2000). It needs to be further investigated if the PII from *Chlamydomonas* is also involved in nitrogen regulation mechanism through interaction with the nitrite transporters.

5. Research objective

PII proteins have evolved to adapt themselves to coordinate the central metabolism with nitrogen assimilation in different organisms. These proteins undergo allosteric and covalent modifications in order to bind diverse interaction partners and control their regulation. They act as a hub protein to coordinate multiple pathways and thereby increasing the complexity for interpretation. The presence of multiple PII paralogues in some organism suggests their role to interact with multiple targets. As PII proteins are involved in sensing the nitrogen, carbon and the energy status of the cells, it is highly interesting to study these control mechanisms and pathways in different organisms.

The major player of these interactions is the T-loop which adapts different conformations in response to sensing distinct effector molecules. One of the key targets for the PII proteins is NAGK and the structure of PII-NAGK complexes have been solved for *S. elongatus* and *A. thaliana*. However, the sequence of steps leading to the complex formation has been unclear so far. This research work attempts to investigate the mechanism underlying the complex formation through structural and biochemical studies. Further, the T-loop senses the metabolite 2-OG through the coordination with ATP-Mg which aids in the disruption of the PII-NAGK complex. The affinity for 2-OG binding to PII from *S. elongatus* and the structural basis that mediates these interaction have been examined in this work. Though the recent research work in the PII field has been focused majorly on bacteria and plants, there is not much information on the characterization of PII from the green algae, *C. reinhardtii*. The current work interrogates the role and importance of glutamine as a signalling molecule of PII proteins. The influence of glutamine in the complex formation process of PII-NAGK has been explored through structural studies in this work. Further, bioinformatics analyses have been performed to understand the co-evolution of PII-NAGK and to interpret their functional and structural conservation. Through exploring the possible functions and mechanisms of PII proteins from *C. reinhardtii*, it would be possible to bridge the gap in the understanding of PII protein evolution from cyanobacteria to plastids.

6. Publication 1

A novel signal transduction protein P(II) variant from *Synechococcus elongatus* PCC 7942 indicates a two-step process for NAGK-P(II) complex formation.
Fokina O, Chellamuthu VR, Zeth K, Forchhammer K
J Mol Biol: 399(3), 410-421, 2010.
Page 28

7. Publication 2

Mechanism of 2-oxoglutarate signaling by the *Synechococcus elongatus* PII signal transduction protein.
Fokina O, Chellamuthu VR, Forchhammer K, Zeth K
Proc Natl Acad Sci: 107(46), 19760-19765, 2010.
Page 40

8. Publication 3

From cyanobacteria to plants: conservation of PII functions during plastid evolution.
Chellamuthu VR, Alva V, Forchhammer K
Planta: 237(2), 451-462, 2013.
Page 51

doi:10.1016/j.jmb.2010.04.018 J. Mol. Biol. (2010) 399, 410–421

JMB

Available online at www.sciencedirect.com

ScienceDirect

ELSEVIER

A Novel Signal Transduction Protein P_{II} Variant from *Synechococcus elongatus* PCC 7942 Indicates a Two-Step Process for NAGK–P_{II} Complex Formation

Oleksandra Fokina[1], Vasuki-Ranjani Chellamuthu[2], Kornelius Zeth[2] and Karl Forchhammer[1]*

[1]*Interfakultäres Institut für Mikrobiologie und Infektionsmedizin der Eberhard-Karls-Universität Tübingen, Auf der Morgenstelle 28, 72076 Tübingen, Germany*

[2]*Max Planck Institute for Developmental Biology, Department of Protein Evolution, Spemannstrasse 35, 72076 Tübingen, Germany*

Received 15 December 2009; received in revised form 17 March 2010; accepted 13 April 2010
Available online
24 April 2010

P_{II} signal transduction proteins are highly conserved in bacteria, archaea and plants and have key functions in coordination of central metabolism by integrating signals from the carbon, nitrogen and energy status of the cell. In the cyanobacterium *Synechococcus elongatus* PCC 7942, P_{II} binds ATP and 2-oxoglutarate (2-OG) in a synergistic manner, with the ATP binding sites also accepting ADP. Depending on its effector molecule binding status, P_{II} (from this cyanobacterium and other oxygenic phototrophs) complexes and regulates the arginine-controlled enzyme of the cyclic ornithine pathway, *N*-acetyl-L-glutamate kinase (NAGK), to control arginine biosynthesis. To gain deeper insights into the process of P_{II} binding to NAGK, we searched for P_{II} variants with altered binding characteristics and found P_{II} variants I86N and I86T to be able to bind to an NAGK variant (R233A) that was previously shown to be unable to bind wild-type P_{II} protein. Analysis of interactions between these P_{II} variants and wild-type NAGK as well as with the NAGK R233A variant suggested that the P_{II} I86N variant was a superactive NAGK binder. To reveal the structural basis of this property, we solved the crystal structure of the P_{II} I86N variant at atomic resolution. The large T-loop, which prevails in most receptor interactions of P_{II} proteins, is present in a tightly bended conformation that mimics the T-loop of *S. elongatus* P_{II} after having latched onto NAGK. Moreover, both P_{II} I86 variants display a specific defect in 2-OG binding, implying a role of residue I86 in 2-OG binding. We propose a two-step model for the mechanism of P_{II}–NAGK complex formation: in an initiating step, a contact between R233 of NAGK and E85 of P_{II} initiates the bending of the extended T-loop of P_{II}, followed by a second step, where a bended T-loop deeply inserts into the NAGK clefts to form the tight complex.

Keywords: 2-oxoglutarate; nitrogen regulation; *Synechococcus*; metabolic signalling; arginine

Edited by I. B. Holland

Introduction

P_{II} proteins belong to a large protein family present in bacteria, plants and archaea, where they play pivotal roles as sensors and signal transducers in processes connected to nitrogen assimilation.[1–4] Generally, P_{II} proteins are signal integrators that bind the key metabolites ATP, ADP and 2-oxoglutarate (2-OG) and in many cases are subjected to reversible covalent modification in response to the carbon/nitrogen status of the cell.[3,5] Depending on the signal input state, P_{II} proteins bind and regulate the activity of key metabolic and regulatory enzymes, transcription factors or transport proteins.[1–3]

P_{II} proteins are homotrimers of 12- to 13-kDa subunits with a highly conserved three-dimensional structure. From the body of the trimer, which is almost hemispheric, three large T-loops, one per subunit, protrude into the solvent. The T-loops are

*Corresponding author. E-mail address: karl.forchhammer@uni-tuebingen.de.

Abbreviations used: 2-OG, 2-oxoglutarate; NAGK, *N*-acetyl-L-glutamate kinase; SPR, surface plasmon resonance; ITC, isothermal titration calorimetry; FC, flow cell; RU, resonance units; NAG, *N*-acetyl-L-glutamate.

able to adopt multiple conformations and are the key to the versatile protein–protein interactions of P_{II} proteins.[3] Further to the T-loop, each subunit has two smaller loops: the B- and C-loop from opposing subunits face each other in the intersubunit clefts, where they are engaged in adenyl nucleotide binding.[6–8] The trimeric P_{II} protein thus contains three ATP/ADP binding sites, each one in the cleft between neighbouring subunits. In the presence of ATP, up to three 2-OG molecules can bind per trimer; however, the binding site for 2-OG is not clear hitherto.[1,6,9] For a P_{II} paralogue from *Methanococcus jannaschii*, GlnK1, one 2-OG molecule was shown to bind from outside to the distal side of the T-loop in the presence of Mg-ATP.[10] This finding is, however, in conflict with earlier data, which showed by deletion mutagenesis that this part of the T-loop is dispensable for 2-OG binding, at least for the P_{II} protein of *Escherichia coli*.[11] Recent studies suggest that, in *E. coli*, 2-OG controls the conformation of the T-loop after P_{II} binding to its receptor.[12] The binding of ATP and 2-OG are synergistic toward each other, meaning that the binding of ATP favours the binding of 2-OG and *vice versa*. However, the sites for ATP exhibit negative cooperativity toward the other ATP binding sites and the same holds true for the 2-OG binding sites. This feature of anti-cooperatively communicating metabolite binding sites allows P_{II} to sense these metabolites in a wide range of concentrations.[5,13]

In the cyanobacterium *Synechococcus elongatus* PCC 7942, P_{II} plays essential roles in control of nitrogen utilization.[8] Under nitrogen-poor conditions, P_{II} is phosphorylated at the T-loop residue S49 (P_{II}-P),[8] whereas under nitrogen-sufficient conditions, P_{II}-P is dephosphorylated.[14] Phosphorylation and dephosphorylation of P_{II} had been shown *in vitro* to depend on the 2-OG levels, with high 2-OG stimulating P_{II} phosphorylation and low 2-OG levels favouring the dephosphorylation of P_{II}-P. The known regulatory targets of P_{II} in *S. elongatus* involve regulation of gene expression controlled by transcription factor NtcA through binding to an NtcA-activating factor PipX[15] and control of arginine biosynthesis by activating *N*-acetyl-L-glutamate kinase (NAGK).[16–18] NAGK converts *N*-acetyl-L-glutamate (NAG) to *N*-acetyl-glutamyl phosphate, and its activity is regulated through feedback inhibition by arginine.[19] P_{II} exerts control over NAGK in the following manner: nonphosphorylated P_{II} protein, at low 2-OG concentrations, binds to NAGK. Complex formation not only increases enzymatic activity by affecting the K_m and V_{max} of the catalyzed reaction, but also relieves NAGK from arginine feedback inhibition by approximately 10-fold.[17] The P_{II}–NAGK complex consists of two P_{II} trimers sandwiching one NAGK hexamer (trimer of dimers) with their threefold axes aligned.[20] Two surfaces of each P_{II} subunit are involved in the contact with NAGK: at the body of the P_{II} protein, residues F11 and F13 at the β1–α1 junction of P_{II} make hydrophobic NAGK interactions; residue E85 of the B-loop of P_{II} forms a salt bridge with R233 of NAGK; and B-loop residue T83 is engaged in hydrophobic interactions. In the complexed state, the T-loop of P_{II} adopts a unique bended shape and inserts into the interdomain cavity of NAGK, making contact with the NAGK N domain, with R45 and E50 being engaged in an ion pair network and S49 in tight hydrogen-bond interactions with NAGK. This compact T-loop conformation requires that an intramolecular salt bridge between R47 and E85, which stabilizes an extended T-loop conformation of free P_{II} protein, is broken, so that the salt bridge between B-loop R45 and NAGK R233 can be formed. Almost the same structure as for the *S. elongatus* proteins was revealed for the P_{II}–NAGK complex from *Arabidopsis thaliana*,[21] and the mode of interaction has apparently been conserved throughout the evolution of eukaryotic phototrophs, highlighted by the fact that the cyanobacterial and plant proteins are able to functionally interact *in vitro* with each other.[22]

The current study was carried out to gain deeper insights into the molecular events leading to P_{II} interaction with NAGK. A random mutagenesis approach yielded novel P_{II} variants (I86N and I86T) that display unique features of NAGK and effector molecule binding. To explain these features, the structure of the I86N variant was solved, shedding new light on the process of how the P_{II} NAGK complex forms.

Results

Identification of a P_{II} variant with altered NAGK interaction

To investigate the process of interaction between *S. elongatus* P_{II} and its receptor NAGK, we created a randomly mutated *glnB* library (encoding P_{II}) cloned in a bacterial two-hybrid vector. In the course of this study, a P_{II} variant (carrying an E85-to-D substitution) was identified as being unable to interact with NAGK (not shown). Since the resulting variant has retained the negative charge required for a critical ion pair interaction with R233 in NAGK, the loss of interaction indicated a sophisticated role of the P_{II}-E85–NAGK-R233 interface for complex formation. To reveal this issue, a bacterial two-hybrid screening was performed using the *glnB* random mutant library against an *argB* bait that encodes an NAGK variant with an R233A substitution. This NAGK variant shows no interaction *in vitro* with P_{II} protein of wild-type sequence (wt P_{II}),[20] in yeast two-hybrid analysis interaction,[20] or in the actual bacterial two-hybrid assay (not shown). Screening this library for P_{II} variants capable of interacting with NAGK R233A yielded out of seven clones two types of complementing P_{II} variants, both containing substitutions at position 86 (I86T or I86N P_{II}). To analyze the interaction between NAGK R233A with the I86 P_{II} variants, the interaction of these proteins was measured by surface plasmon resonance (SPR) spectroscopy (Fig. 1a–c). Wild-type

P_{II} protein showed almost no interaction with immobilized NAGK R233A, either in the absence or in the presence of 100 μM ATP (Fig. 1a), confirming the previous results.[20] Strikingly, the two I86 P_{II} variants were able to form complexes with NAGK R233A, but only in the presence of nucleotides. ATP stimulated complex formation in a concentration-dependent manner (Fig. 1b and c). For the I86N variant, 1 μM ATP resulted in clearly detectable NAGK binding (Fig. 1b). Formation of the complex between the P_{II} variant I86T and NAGK R233A required higher ATP concentrations; the association occurred considerably slower than that of the I86N variant and the complex dissociated almost immediately at the end of analyte injection in the ATP-free running buffer (Fig. 1c). Furthermore, the influence of the two P_{II} variants on the enzymatic activity of the NAGK R233A variant was determined.[22] Arginine inhibition of NAGK activity was determined in the absence of P_{II} (IC_{50} for arginine, 14 μM) and with wt, I86N or I86T P_{II} proteins (Fig. 1d). The wt P_{II} protein and the I86T variant both slightly relieved R233A NAGK from arginine inhibition by increasing the IC_{50} for arginine to 40 or 32 μM, respectively. By contrast, the I86N P_{II} protein was much more efficient in relieving NAGK R233A from arginine inhibition by increasing the IC_{50} for arginine to 197 μM. This is in agreement with the result from the SPR analysis, which revealed efficient binding of I86N P_{II} to the R233A NAGK variant. Interestingly, wt P_{II} showed a weak effect on NAGK R233A in the enzyme assay but no interaction in bacterial two-hybrid screening or almost no binding by SPR analysis. This indicates that the arginine inhibition assay of NAGK is very sensitive and detects even very weak interactions, resulting in slightly enhanced NAGK activity. That the P_{II} I86T variant is not more efficient than wt P_{II} in protecting NAGK R233A from arginine inhibition may be attributed to the instability of the complex (as revealed by SPR analysis, see above) or could be a direct effect of this mutation, affecting the ability to relieve NAGK from arginine feedback inhibition (compare below).

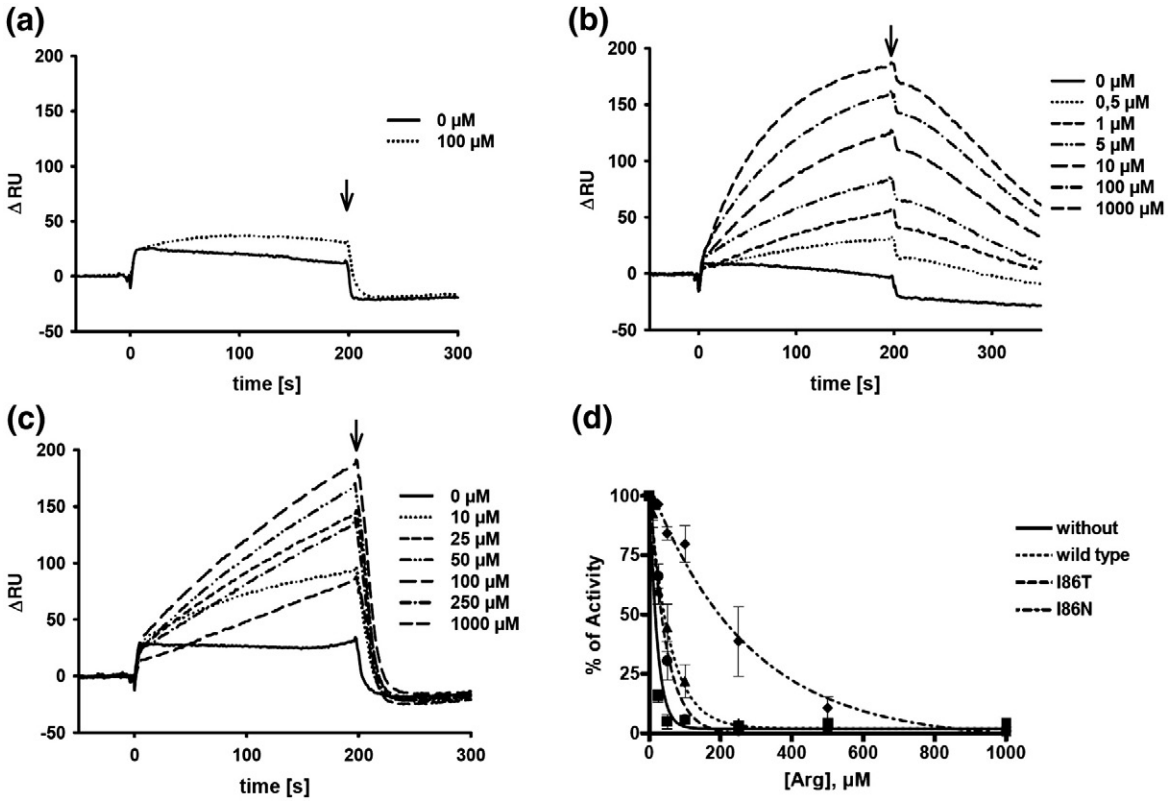

Fig. 1. Interaction of R233A NAGK with recombinant P_{II} proteins. (a)–(c), R233A NAGK was bound to FC2 of a Ni^{2+}-loaded NTA sensor chip (see Materials and Methods) and FC1 was used as background control. The response difference (ΔRU) between FC1 and FC2 is shown. An arrow indicates the end of the injection phase. (a) Binding of 100 nM wt P_{II} in the presence of 0 and 100 μM ATP, as indicated. (b) Influence of ATP on the complex formation of I86N P_{II} (100 nM) and R233A NAGK; ATP was used at a concentration of 0, 0, 5, 1, 5, 10, 100 and 1000 μM, as indicated. (c) Binding of I86T in the presence of ATP at a concentration of 0, 10, 25, 50, 100, 250 and 1000 μM, as indicated. (d) Inhibition of R233A NAGK activity by arginine in the absence and in the presence of P_{II}. Coupled NAGK assays were performed in the presence of 50 mM NAG and 10 mM ATP, together with increasing concentrations of arginine, as indicated, in the absence of P_{II} (squares) and in the presence of wt P_{II} (triangles), I86N (rhombus) or I86T (circles). The percentage of NAGK activity, using reaction velocity without analyte as 100%, was plotted against the respective analyte concentration (standard deviations from different measurements for each data point are indicated by error bars) and the data points were fitted to a hyperbolic curve.

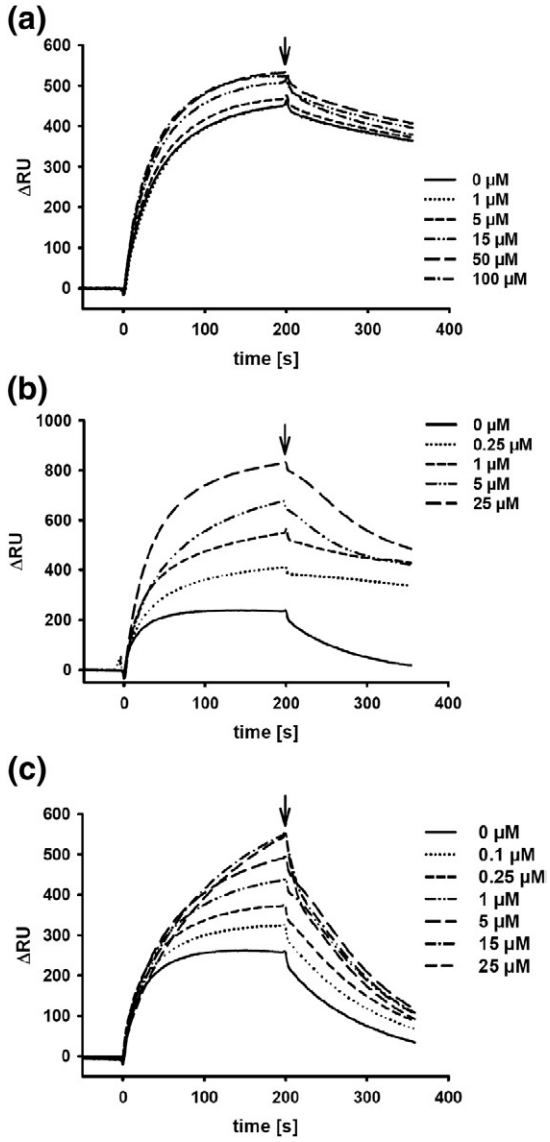

Fig. 2. SPR analysis of the effect of ATP on complex formation between wt NAGK and wt, I86N or I86T P_{II} proteins. SPR spectroscopy was performed as described in Materials and Methods. The response difference (ΔRU) between FC1 and FC2 is shown. An arrow indicates the end of the injection phase. (a) Binding of 100 nM wt P_{II} in the presence of 0, 1, 5, 15, 50 and 100 µM ATP, as indicated. (b) Influence of ATP on the complex formation of I86N P_{II} (100 nM) and wt NAGK; ATP was used at a concentration of 0, 0, 25, 1, 5 and 25 µM, as indicated. (c) Binding of I86T in the presence of ATP at a concentration of 0, 0,1, 0,25, 1, 5, 15 and 25 µM, as indicated.

Interaction of wt NAGK with P_{II} variants I86N and I86T

Next, the interaction of the P_{II} variants I86N and I86T with wild-type NAGK was analyzed to find out how the substitution of I86 in P_{II} affects its NAGK-binding properties. Complex formation was first assayed by SPR spectroscopy. Without effectors, both variants bound significantly weaker to NAGK compared to wt P_{II} and the complex appeared to be less stable, as revealed by the dissociation of the complex after the end of analyte injection (Fig. 2a–c, continuous lines; end of inject indicated by the arrow). However, binding to NAGK was significantly improved in the presence of adenyl nucleotides. The I86N variant responded to submicromolar concentrations of ATP. In the presence of 25 µM ATP, four times more binding was observed than without ATP, whereas wt P_{II} protein is only slightly affected by ATP (Fig. 2a).

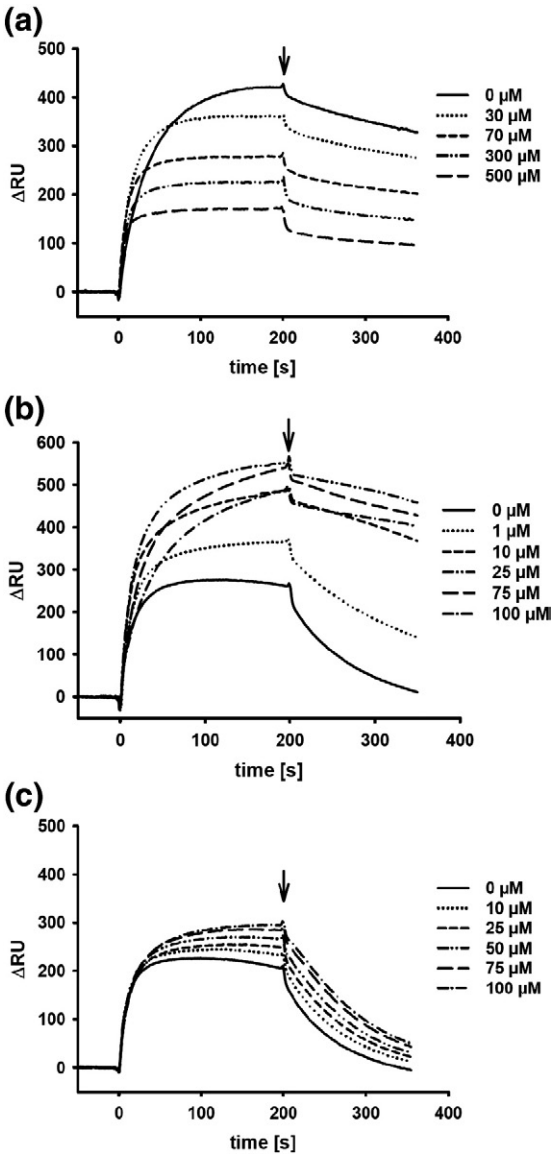

Fig. 3. SPR analysis of the effect of ADP on complex formation between wt NAGK and wt, I86N or I86T P_{II} proteins. SPR spectroscopy was performed as described in Materials and Methods. The response difference (ΔRU) between FC1 and FC2 is shown. An arrow indicates the end of the injection phase. (a) Binding of 100 nM wt P_{II} in the presence of 0, 30, 70, 300 and 500 µM ADP, as indicated. (b) Influence of ADP on the complex formation of I86N P_{II} and wt NAGK; ADP was used at a concentration of 0, 1, 10, 25, 75 and 100 µM, as indicated. (c) binding of I86T in the presence of ADP at a concentration of 0, 10, 25, 50, 75 and 100 µM, as indicated.

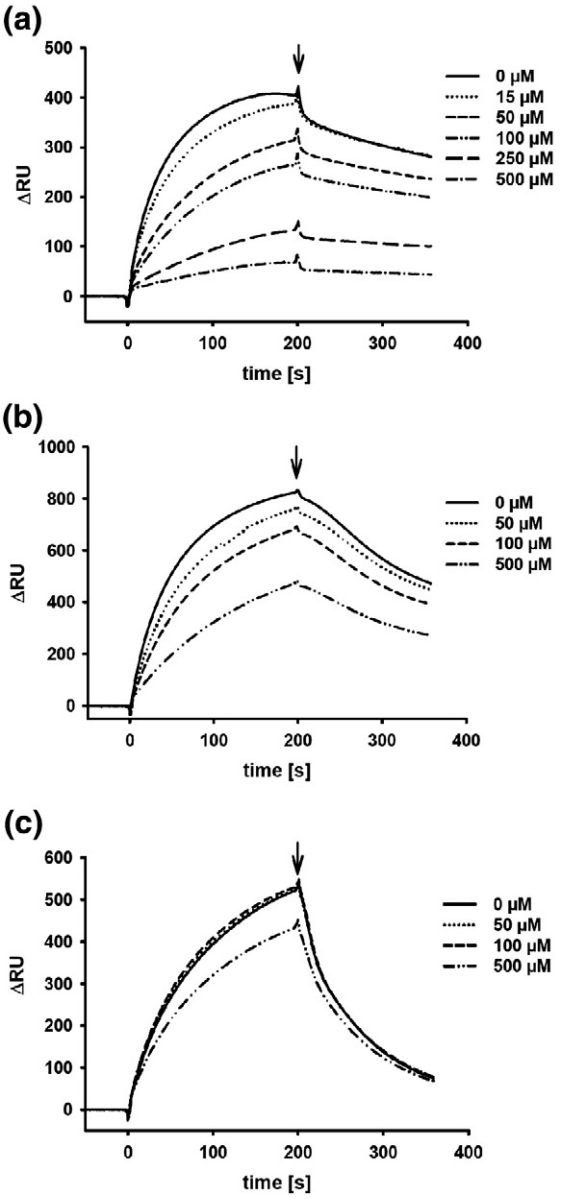

Fig. 4. SPR analysis of the effect of 2-OG on complex formation between wt NAGK and wt, I86N or I86T P_{II} proteins in the presence of 1 mM ATP. SPR spectroscopy was performed as described in Materials and Methods. The response difference (ΔRU) between FC1 and FC2 is shown. An arrow indicates the end of the injection phase. (a) Binding of 100 nM wt P_{II} in the presence of 1 mM ATP and 2-OG at a concentration of 0, 15, 50, 100, 250 and 500 μM, as indicated. (b) Influence of 2-OG on the complex formation of I86N P_{II} and wt NAGK in the presence of 1 mM ATP; 2-OG was used at a concentration of 0, 50, 100 and 500 μM, as indicated. (c) Influence of 2-OG on the complex formation of I86T P_{II} and wt NAGK in the presence of 1 mM ATP; 2-OG was added at a concentration of 0, 50, 100 and 500 μM, as indicated.

Compared to wt P_{II} protein in the presence of saturating ATP, the I86N variant bound even better to the NAGK surface and the complex was apparently stable (compare Fig. 2a and b), indicating that the I86N variant is a superactive NAGK binder. Concerning the P_{II} variant I86T, ATP also enhanced complex formation; however, the complex was unstable, as indicated by the rapid dissociation following the injection phase (Fig. 2c).

As demonstrated previously,[17] ADP negatively affects wt P_{II}–NAGK interaction (Fig. 3a). Apparently, ADP does not completely abolish P_{II}–NAGK interaction, but rather increases the dissociation constant, as deduced from the decreasing levels of P_{II} binding to the NAGK surface with increasing ADP concentrations. In striking contrast to wt P_{II}, ADP enhanced and stabilized the binding of both P_{II} I86 variants to NAGK (Fig. 3b and c). Addition of 1 μM ADP noticeably increased the binding of P_{II} variant I86N to NAGK, and a maximum was reached in the presence of 25 μM ADP, with higher ADP concentrations slightly reducing complex formation again. This P_{II} variant remained stably bound on the NAGK surface during the dissociation phase (Fig. 3b, right to the arrow) and in contrast to wt P_{II} could not be dissociated by injection of 1 mM of ADP (data not shown). In the case of the I86T variant, ADP only weakly stimulated NAGK interaction (Fig. 3c).

2-OG is known to be a major effector molecule involved in P_{II} signal transduction.[17] As shown in Fig. 4a, micromolar amounts of 2-OG in the presence of 1 mM ATP diminished wt P_{II}–NAGK interaction, and in the presence of 500 μM 2-OG, complex formation between wt P_{II} and NAGK was almost completely inhibited. Interestingly, addition of 2-OG to the I86N variant had only a small effect on complex formation, since significant binding was observed even in the presence of 500 μM 2-OG and 1 mM ATP (Fig. 4b). Even more strikingly, the I86T variant was almost completely insensitive toward 2-OG (Fig. 4c).

The interaction of I86 P_{II} variants with wt NAGK was further investigated by using the coupled NAGK enzyme assay (see above). As shown in Fig. 5a, the I86N P_{II} variant was as efficient as wt P_{II} in relieving NAGK from arginine inhibition (IC_{50} values of approximately 460 μM for wt P_{II} and 630 μM for P_{II} I86N). On the other hand, the I86T variant showed a much weaker effect on NAGK arginine inhibition (IC_{50}, 75 μM). In the absence of P_{II}, NAGK had an IC_{50} of 18 μM for arginine, as reported previously. These results correspond to SPR measurements shown above, where wt P_{II} and the I86N variant formed a stable complex with wt NAGK in the presence of ATP (ATP was also present in the coupled assay at 10 mM concentration). By contrast, the I86T variant dissociates rapidly from NAGK, leading to the conclusion that the stability of the P_{II}–NAGK complex could be important for relieving the enzyme from arginine inhibition.

The next step was to test the inhibitory effects of 2-OG on NAGK activation by P_{II} variants I86N and I86T via the coupled assay. Therefore, 2-OG was titrated to P_{II}–NAGK in a buffer containing 50 μM arginine. This amount of arginine is highly inhibitory for free NAGK, but only slightly inhibitory for the P_{II}–NAGK complex.[22] In the control experiment, NAGK activity in the presence of wt P_{II} was inhibited by the addition of 2-OG in a concentration-dependent

manner with an IC_{50} of 116 μM, as reported previously.[22] With both P_{II} variants, 2-OG was not effective in antagonizing the P_{II}-mediated protection of NAGK from arginine inhibition even at high concentrations (Fig. 5b). This result confirmed data from SPR experiments, which showed that P_{II} variants I86N or I86T are insensitive toward 2-OG.

Binding of effector molecules to P_{II} and its I86N and I86T variants

The experiments shown above indicated that the P_{II} variants I86N and I86T responded to the effector molecules ATP, ADP and 2-OG quite differently from wt P_{II}. Therefore, the effector-binding properties of these P_{II} variants were determined by isothermal titration calorimetry (ITC). Previously, the ligand-binding properties of *S. elongatus* P_{II} have not been determined by this method. Therefore, the ITC characteristics of wt P_{II} protein will be presented first in some detail. The measurements were performed with different ligand/protein concentrations to determine the conditions under which the best fitting to the binding model could be achieved. Subsequently, the experiments were repeated to confirm the result. As shown in Fig. 6a, wt P_{II} protein exhibits high affinity toward ATP. Optimal fitting of the raw data was obtained using a three sequential binding sites model (Fig. 6a, lower part). This analysis revealed a low dissociation constant for the first binding site ($K_d1 = 4$ μM) and increased K_d for binding sites 2 and 3 ($K_d2 = 12.5$ μM, $K_d3 = 47.4$ μM) as shown in Table 1, indicative of negative cooperativity between the binding sites, similar to values reported previously using equilibrium dialysis or ultrafiltration techniques.[13] Direct binding of ADP to *S. elongatus* P_{II} has so far never been reported. Here we show that ADP binds almost as efficiently as ATP (Fig. 6b), with similar anti-cooperativity among the three sites ($K_d1 = 10.6$ μM, $K_d2 = 19.3$ μM, $K_d3 = 133.4$ μM). Apparently, for each site, ATP binding is preferred over ADP. The binding isotherm for 2-OG was measured in the presence of 1 mM ATP (Fig. 6c). According to the model, assuming three sequential binding sites, the first two sites are occupied at low 2-OG concentrations ($K_d1 = 5.1$ μM, $K_d2 = 11.1$ μM), whereas occupation of the third site requires approximately 10-fold higher concentration of 2-OG ($K_d3 = 106.7$ μM). Interestingly, the dissociation constant of site 3 corresponds quite well to the IC_{50} of 2-OG for antagonizing the P_{II}-mediated protection of NAGK from arginine inhibition (116 μM, see above) or with the 2-OG concentration that is required to inhibit NAGK binding (as determined by SPR analysis; Fig. 4a). This suggests that for inhibiting the binding of P_{II} to NAGK, all three 2-OG sites have to be occupied.

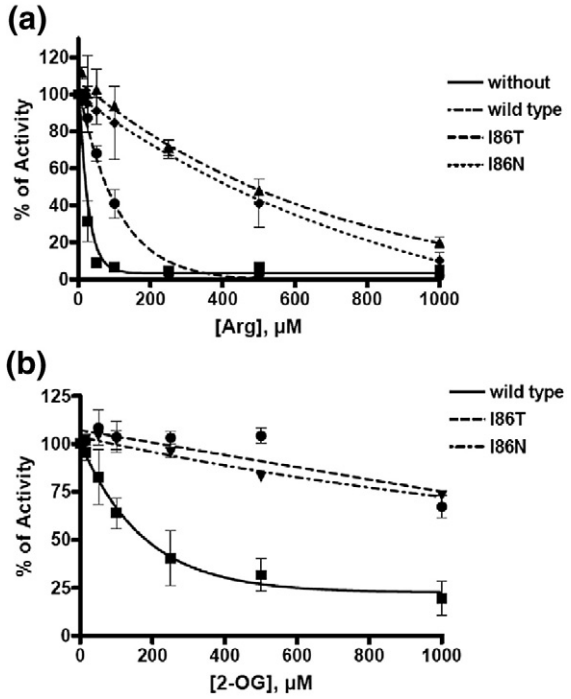

Fig. 5. Arginine inhibition of NAGK and influence of 2-OG in the presence of recombinant P_{II} proteins. Coupled NAGK assays were performed as described in Materials and Methods in the presence of 10 mM ATP. The percentage of NAGK activity, using reaction velocity without analyte as 100%, was plotted against the respective analyte concentration (standard deviations from different measurements for each data point are indicated by error bars) and the data points were fitted to a hyperbolic curve. (a) Inhibition of wt NAGK activity by increasing concentrations of arginine, as indicated, in the absence of P_{II} (squares) and in the presence of wt P_{II} (triangles), I86N (rhombus) or I86T (circles). (b) Effect of 2-OG on the activation of NAGK by P_{II} in the presence of arginine. Assays were performed in the presence 50 μM arginine and increasind 2-OG concentrations, as indicated, with wt P_{II} (squares), I86N (triangles) and I86T (circles).

The P_{II} variant I86N has completely lost the anti-cooperativity of the ATP binding sites: all three sites were occupied independently with a K_d of approximately 9.6 μM. The raw data could not be fitted properly using a three sequential binding sites model; therefore, a one-site binding model was used for these measurements. This model allowed us to determine three independent binding sites for a I86N trimer (Table 1). The I86T variant also showed lack of anti-cooperativity of the ATP binding sites. The affinity toward ADP in both variants was weaker than for wt P_{II}. For both P_{II} variants, addition of 2-OG in the presence of 1 mM ATP did not yield any calorimetric signals. This result agrees with data shown above, which demonstrate that these P_{II} variants are insensitive toward 2-OG (Fig. 4 and 5b), implying that I86 of the B-loop may take part in 2-OG binding.

Structure of the P_{II} I86N variant

The observation that P_{II} variant I86N, in particular, is able to bind to the NAGK variant R233A, whereas the wt P_{II} protein was unable to interact, clearly shows that the P_{II} E85–NAGK R233 interaction is not required for the I86N variant. This led us

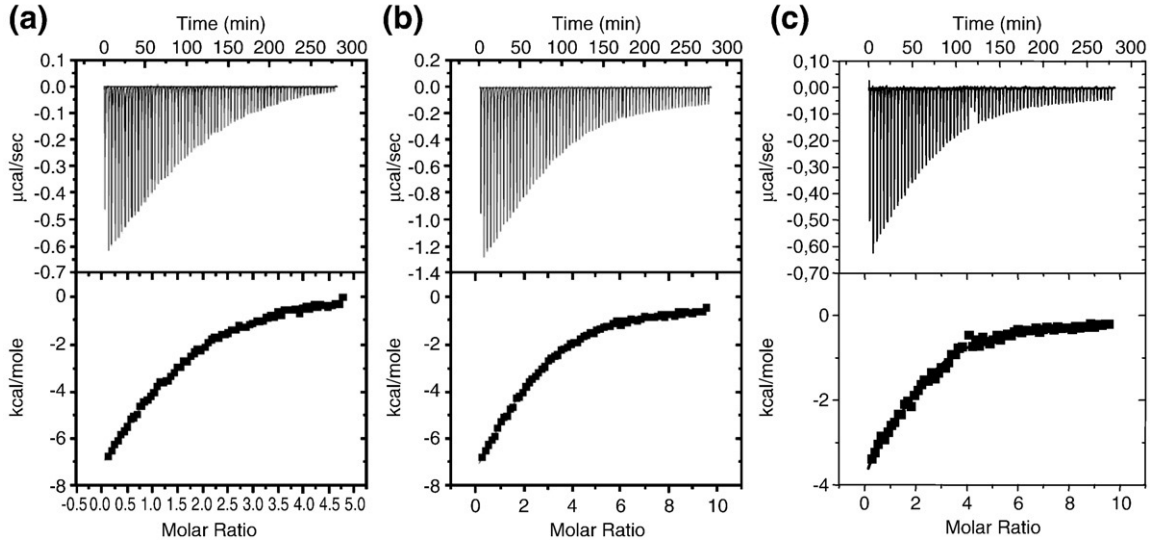

Fig. 6. ITC of ligand binding to wt P_{II} protein. The upper panels show the raw data in the form of the heat effect during the titration of 33 µM wt P_{II} solution (trimer concentration) with ligands. The lower panels show the binding isotherm and the best-fit curve according to the three sequential binding sites model. (a) ATP binding (titration from 2.1 to 146.8 µM). (b) ADP binding (4.2–293.7 µM). (c) 2-OG binding (4.2–293.7 µM) in the presence of 1 mM ATP.

to hypothesize that this variant may adopt a conformation that facilitates interaction with NAGK to make it independent of the NAGK R233 contact. To resolve this issue, the structure of the P_{II} I86N variant in the presence of ATP was solved by X-ray crystallography. Protein crystals diffracted to a resolution of 1.2 Å with one monomer of the protein in the asymmetric unit (see also Table 2). The structure was solved by molecular replacement using the structure of nonliganded *S. elongatus* P_{II} [Protein Data Bank (PDB) entry 1Q7Y] as the search model. As shown in Fig. 7, the backbone of the I86N variant is almost identical to that of the wt P_{II} structure[7] (r.m.s.d. of 1.9 Å for 100 aligned residues). In contrast to the nonliganded *S. elongatus* P_{II} protein (Fig. 7b), the T-loop adopts a compact conformation, which is very similar to that of the wt P_{II} protein in complex with NAGK[20] (Fig. 7a). The I86N substitution results in a newly formed hydrogen bond between the amido nitrogen of N86 and the backbone oxygen of T43, contracting the anterior part of the T-loop toward the body of P_{II} (Fig. 7c). This compact conformation is further stabilized by a salt bridge between E44 and K58. The same stabilizing salt bridge is observed in the compact T-loop of NAGK-bound P_{II} (Fig. 7a). Moreover, residues R45 and E50 at the tip of the T-loop are connected by another salt bridge in the I86N variant and E50 forms an additional H-bond with T43. The same interaction has been observed in NAGK-complexed P_{II}, where these surface-exposed residues organize an ion pair network with NAGK, which appears to be a major determinant for this interaction.[20] In the I86N variant, the hydroxyl group of S49 is surface-exposed to perfectly match the corresponding contact surface of NAGK. Overall, the structure of the I86N variant appears as a perfect mimic of wt P_{II} structure in complex with NAGK.

Mg-ATP is bound to the canonical ATP binding site of P_{II} proteins, which lies in the intersubunit clef between neighbouring subunits.[6,23] Accordingly, key contact residues for Mg-ATP binding are G27, T29, R101 and R103 from one subunit and G37, G87, G89 and K90 from the opposing subunit. The C-terminus of the I86N variant forms a short α-helix, which folds back toward the ATP binding pocket (Fig. 7a). This structure is reminiscent of the C-terminal end of *A. thaliana* P_{II}.[21] In the I86N P_{II} variant, this segment is well ordered until the C-terminal end of the native *S. elongatus* P_{II} sequence (amino acid 112). The additional 10 amino acids from the C-terminal fused Streptag II peptide are not ordered and therefore not visible, indicating that

Table 1. Dissociation constants of ATP, ADP and 2-OG binding to recombinant P_{II} proteins

	K_d1 (µM)	K_d2 (µM)	K_d3 (µM)	*N* (no. of sites in one-site model)
ATP				
wt	4.0±0.1	12.5±0.9	47.4±21.9	—
I86N		9.6±1.3		3.0±0.1
I86T		14.3±0.5		3.51±0.62
ADP				
wt	10.6±3.2	19.3±2.3	133.4±5.2	—
I86N	165.3±59.0	59.5±49.3	66.2±38.5	—
I86T	41.4±11.5	53.7±13.1	149.9±13.6	—
2-OG (+1 mM ATP)				
wt	5.1±4.0	11.1±1.8	106.7±14.8	—
I86N	n	n	n	—
I86T	n	n	n	—

n, not detectable.

Values for wt P_{II} correspond to the mean±SEM of three experiments for I86N and to the mean±SEM of two experiments for I86T.

The raw data for I86N- and I86T-ATP binding was fitted using a one-site binding model for a P_{II} trimer.

Table 2. Data collection and refinement statistics

	P_{II} I86N variant
Data collection	
Space group	$P2_13$
Cell dimensions	
a, *b*, *c* (Å)	80.68, 80.68, 80.68
α, β, γ (°)	90
Resolution (Å)	1.2 (1.27–1.2)
R_{sym} or R_{merge}	0.1 (0.64)
$I/\sigma I$	17 (2.3)
Completeness (%)	99.9 (99.7)
Redundancy	13.3 (10.3)
Refinement	
Resolution (Å)	36–1.2
No. of reflections	52,061
R_{work}/R_{free}	0.12/0.14
No. of atoms (all)	
Protein	919
Ligand/ion (ATP/Mg^{2+}/Cl)	31/1/1
Water	174
B-factors	
Protein	9.7
Ligand/ion (ATP/Mg^{2+}/Cl)	8.4/8.9/8.4
Water	31
r.m.s.d.	
Bond lengths (Å)	0.03
Bond angles (°)	2.7

Values in parentheses are for the highest-resolution shell.

this C-terminal extension is highly flexible and does not interfere with the P_{II} structure, in accord with the full functionality of the C-terminal Strep-tagged P_{II} protein compared to the untagged version with respect to effector molecule binding and NAGK interaction.[13,20]

Discussion

The structure of the novel P_{II} I86N variant together with its binding properties to NAGK offers a mechanistic explanation for the process of complex formation between P_{II} and NAGK and explains the role of the P_{II} 85E–NAGK 233R interface. In the complex of wt P_{II} and NAGK, there are two surfaces of interaction: a smaller exterior interface (303 A^2) is formed by the peripheral part of the NAGK C domain and the β1–α1 junction (F11–E15) and B-loop residues T83 and E85 of P_{II}, the latter forming a salt bridge with R233 of NAGK. The larger surface (393 A^2) involves the T-loop hairpin that is deeply buried within the NAGK interdomain cleft.[20] There is a drastic difference between this compact T-loop conformation and that of the nonliganded free P_{II}, where the T-loop exhibits an extended conformation. The extended T-loop of *S. elongatus* P_{II} may be a

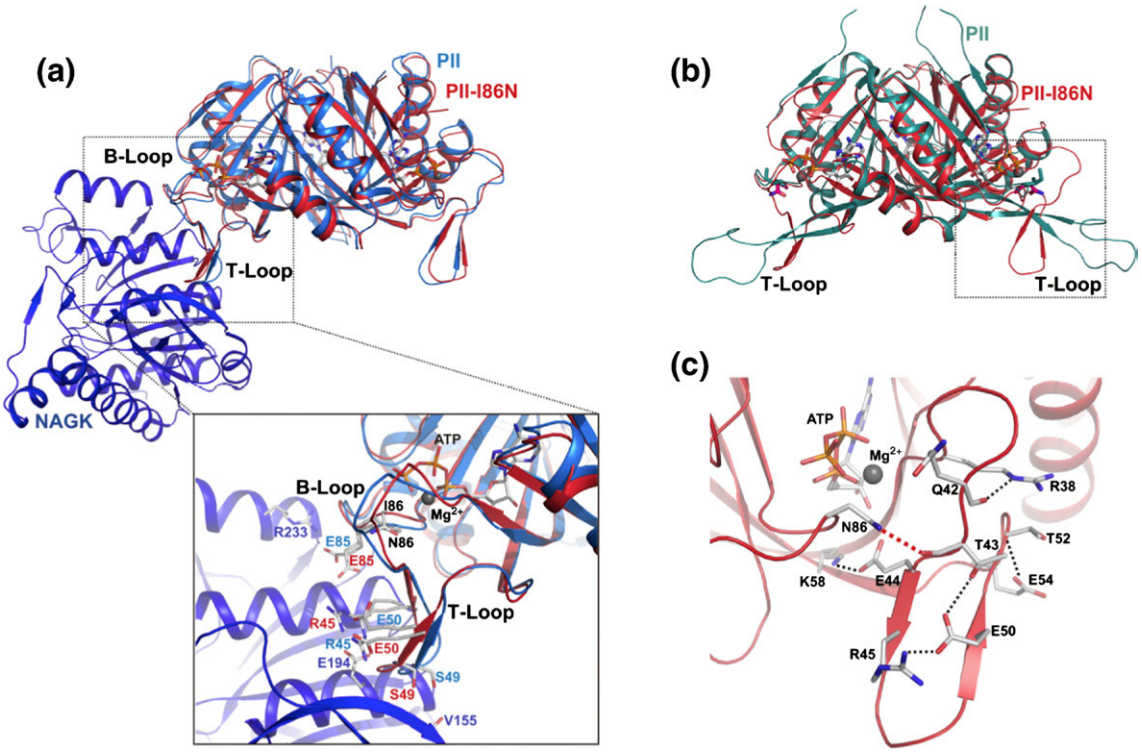

Fig. 7. The structure of the P_{II} I86N variant mimics the structure of *S. elongatus* P_{II} in complex with NAGK. Proteins are shown as strings and ribbons. ATP, residue side and main chains are shown as sticks and Mg^{2+} ions as spheres. (a) Superimposed structure of *S. elongatus* P_{II} in complex with NAGK coloured blue (PDB ID 2V5H) and the P_{II} variant I86N coloured red. The magnification below shows B- and T-loop residues important for NAGK interaction. Note the similar arrangement of residues R45, S49 and E50. (b) Superimposed structure of nonliganded *S. elongatus* P_{II} in green (PDB ID 1QY7) and the I86N variant (red). (c) T-loop of the I86N variant (red). Red broken lines show the hydrogen bond of the amido nitrogen of N86 with the backbone oxygen of T43; broken lines show the hydrogen bonds between E50 and T43 and, additionally, salt bridges R45–E50 and E44–K58, which stabilize the bent conformation.

specificity of cyanobacterial P_{II} proteins, since the R47–E85 pair, which apparently stabilizes this conformation, is only present in cyanobacterial P_{II} proteins. In agreement, from the numerous P_{II} structures that are available today, only the *S. elongatus* P_{II} structure exhibits this type of extended T-loop.[3,23] Obviously, in the process of NAGK–P_{II} complex formation, the R47–E85 bridge must be broken and the T-loop must undergo a large conformational rearrangement to adopt the compact bended structure. Based on the results of this study, we propose a two-step mechanism of P_{II} interaction with NAGK, giving the B-loop a key role in initiating this process. According to this model, in the first step, NAGK approaches P_{II} and the NAGK residue R233 triggers the break of the P_{II} R47–E85 bridge by presenting a more suitable partner for E85. In the second step, the extended T-loop collapses into the NAGK interdomain cleft, generating the large surface for P_{II} binding to NAGK and stabilizing the complex. As shown in this study, the salt bridge R233-NAGK–E85-P_{II} is not essential for binding *per se*, since the NAGK R233A variant is able to bind P_{II} variants I86N and I86T. According to the two-step model, wt P_{II} is not able to bind to NAGK R233A because the initiating step cannot take place. For the same reason, P_{II} variant E85A would be unable to bind wt NAGK. The P_{II} variant E85D may be impaired in performing the initiating step because the aspartate side chain could be too short to interact with R233 of NAGK. Binding of the P_{II} variant I86N to NAGK R233A is explained in light of the new structure. It binds to NAGK without the need of the initiating P_{II} E85–NAGK R233 interaction, because due to the I86N substitution, this P_{II} variant exhibits a conformation that *a priori* fits into NAGK. In this variant, the T-loop is fixed in a conformation that mimics that of the P_{II} T-loop in the NAGK complex. The interaction of the I86T variant with NAGK is weaker than that of the I86N variant. The location of the hydroxyl group of the T86 residue in this variant may be less favourable for hydrogen-bonding the backbone oxygen of T43 than the corresponding amide group of N86, resulting in a T-loop conformation that less perfectly fits into the NAGK binding pocket and may be less capable of relieving NAGK from arginine inhibition.

Whether a two-step binding process as proposed here for the NAGK–P_{II} interaction is a general mechanism occurring in P_{II} receptor interactions remains to be elucidated. Considering the wide variety of P_{II} interactions with different receptor proteins, there may be different processes of complex formation. However, in any case, the flexibility of the T-loop is predestined for highly sophisticated interactions involving multistage binding processes. A recent investigation of *E. coli* P_{II} interacting with its receptors NtrB and ATase implies that in *E. coli*, P_{II} binds its receptors in a first step independent of the effector molecule 2-OG. T-loop structural rearrangements, triggered by 2-OG binding, could occur in this case at a post-binding step, thereby modulating the regulation of receptors by 2-OG through P_{II}. Two distinct interaction surfaces were predicted for such a process, one that is insensitive toward 2-OG, and a second one that mediates the regulatory effects and responds to 2-OG.[12]

More than shedding light on the process of P_{II}–NAGK complex formation, the I86 variants reveal an unexpectedly important contribution of the I86 residue to effector molecule binding properties of P_{II}. First, the I86N variant has completely lost anti-cooperativity between the ATP binding sites, indicating a role for the B-loop in intersubunit signalling. Second, the failure to bind 2-OG is remarkable. Other P_{II} variants, which were reported previously to be unable to bind 2-OG, had in addition impaired ATP binding properties. This hampers the interpretation of the phenotype, since as a general rule for P_{II} proteins, 2-OG binding requires the previous binding of ATP.[1,13] Only upon ATP binding is the 2-OG binding site of P_{II} created; however, the position of the 2-OG binding site remains enigmatic so far. The I86 variants are the only P_{II} variants reported so far that have retained ATP binding, although modified, but are completely impaired in 2-OG binding. This suggests that this B-loop residue is probably directly involved in 2-OG binding, proposing a possible location of the 2-OG binding site near the B-loop and the binding site for ATP. This conclusion is supported by mutational studies of *E. coli* P_{II}, which revealed residue Q39 that lies at the base of the T-loop and opposing residue I86,[24] being involved in 2-OG binding.[11] A similar position for the 2-OG binding sites has already been proposed for the *Herbaspirillum seropedicae* GlnK protein (a member of the P_{II} family) based on sequence comparisons with other 2-OG binding proteins.[25] Alternatively (or in addition), the conformation of the T-loop adopted by the I86N variant could be incompatible with 2-OG binding. Since the same T-loop conformation is found in NAGK-bound P_{II}, which is able to respond to 2-OG, further conclusions could be made: 2-OG binding could unlock the bent T-loop conformation, ascribing the failure of the I86N variant to bind to 2-OG to the fact that the T-loop in this variant is fixed in the tightly bent conformation. Unlocking the bent T-loop would also provide a rationale for the antagonistic effect of 2-OG on P_{II}–NAGK binding. The location of the 2-OG binding site near the B-loop is in apparent contradiction with a recently reported structure of the P_{II} protein GlnK1 from the archaeon *M. jannaschii*. In the crystal structure soaked with 2-OG, the effector was found on the T-loop of GlnK1 with several hydrogen bonds between the keto-carboxyl group and main-chain NH of I52, V53 and D54.[10] Since a deletion of the corresponding residues in *E. coli* P_{II} did not affect 2-OG binding,[11] it is unlikely that this 2-OG-binding site of the archaeal P_{II} protein applies to bacterial P_{II} proteins. Furthermore, it is hardly conceivable how 2-OG could bind to such a site, once the complex with NAGK has formed, since in the complex the 2-OG site would be shielded by NAGK. However, a

binding site close to the B-loop would be accessible even in NAGK-complexed P_{II}. Resolution of the 2-OG binding site in bacterial P_{II} proteins is urgently needed to understand the regulatory function of this effector molecule in P_{II}-regulated processes.

Materials and Methods

Random mutagenesis of recombinant P_{II} protein and bacterial two-hybrid screen

Before mutagenesis, the *glnB* gene was cloned into the bacterial two-hybrid vector pBT (Stratagene) to generate pBT-*glnB* with the following oligonucleotides: glnB/pBTfor (5′-CGGAATTCCATGAAGAAGATTGAGGCGATTATT-3′), carrying an EcoRI restriction site, and glnB/pBTrev (5′-CGGGATCCCTGTTGTCGACGCTGACTTAGA-3′), carrying a BamHI restriction site. Random mutagenesis on pBT-*glnB* was performed with the GeneMorph II Random Mutagenesis Kit from Stratagene (La Jolla, CA) with the following oligonucleotides containing EcoRI and BamHI restriction sites: glnBRacefor (5′-CGGCCGCATCGAATTCCATGTAG-3′) and glnBRacerev (5′-TCGAGGATCCCTGTTGTCGACGTCGAC-3′), using 2.6 μg of pBT-*glnB* DNA as template. The randomly mutated PCR fragments were purified, restricted with EcoRI and BamHI and re-ligated into the pBT bait vector to produce the pBT-*glnB* random mutant library. For the *in vivo* assay of the P_{II}–NAGK interaction, the BacterioMatch II Two-Hybrid System Vector Kit from Stratagene was used. The *argB* gene from *S. elongatus*, coding for NAGK, was cloned into pTRG target vector (Stratagene) with the following primers: NAGK/pTRGfor (5′-CGGGATCCATGTCTAGCGAGTTTATCGAAGC-3′), carrying a BamHI restriction site, and NAGK/pTRGrev (5′-CCGCTCGAGTCACGGATCGCTCATTGCCAG-3′), carrying an XhoI restriction site, with *S. elongatus* chromosomal DNA as template. To screen for P_{II} variants that lost the ability to interact with NAGK, the pBT-*glnB* random mutant library was transformed into *E. coli* strain 200190 BacterioMatch II Screening Reporter Competent Cells (Stratagene) carrying pTRG-*argB*. The transformants were replica-plated on nonselective Cm/Tet Luria–Bertani (LB) plates and Cm/Tet/3-AT (3-amino-1,2,4-troazole) plates that only allow growth of cells, in which hybrid P_{II}–NAGK interaction occurs. Clones that failed to grow in the presence of the selective agent 3-AT were further investigated. To exclude *glnB* variants that produced instable or truncated versions of P_{II}, we grew the clones of interest in liquid LB-Cm/Tet and analyzed the integrity of P_{II} by immunoblot analysis using P_{II}-specific antibodies.[16] From clones that contained full-size P_{II} fusion protein, the mutant pBT-*glnB* plasmids were checked again by bacterial two-hybrid assay for loss of NAGK interaction; interaction-negative clones were isolated and the *glnB* gene was sequenced from both sides with primers glnB/pBTfor and glnB/pBTrev.

Overexpression and purification of recombinant P_{II} and NAGK

The mutant *glnB* genes were amplified from the respective mutant pBT-*glnB* plasmids by PCR using the following primers: glnBStrep-for (5′-GCAATTGGTCTCAAATGAAGAAGATTGAGGCGATTATTC-3′) and glnBStrep-rev (5′-GATCATGGTCTCAGCGCTGATTGCGTCGGCGTTTTTCTC-3′). The PCR products containing mutant *glnB* genes were cloned into the Strep-tag fusion vector pASK-IBA3 (IBA, Göttingen, Germany) as described previously.[16] Overexpression of mutant *glnB* in *E. coli* RB9060[26] and purification of recombinant P_{II} proteins with a C-terminal fused Strep-tag II peptide was performed according to Heinrich *et al.*[16]

The His_6-tagged recombinant wt NAGK from *S. elongatus* was overexpressed in *E. coli* strain BL21(DE3)[27] and purified as reported previously.[17]

The *argB* gene carrying a R233A mutation was cloned into expression vector pET15b with pUAGC569-*argB* plasmid as DNA template according to the protocol described previously.[17]

SPR detection

SPR experiments were performed with a BIAcore X biosensor system (Biacore AB, Uppsala, Sweden) as described previously at 25 °C in HBS-Mg buffer [10 mM Hepes, 150 mM NaCl, 1 mM $MgCl_2$, 0.005% Nonidet P-40 (pH 7.5)] at a flow rate of 15 μl/min.[17] The purified His_6-NAGK was immobilized on the Ni^+-loaded NTA sensor chip to flow cell 2 (FC2) in a volume of 50 μl at a concentration of 30 nM (hexamer) to receive a binding signal of approximately 3000 resonance units (RU), which corresponds to a surface concentration change of 3 ng/mm^2. To analyze the effect of ATP, ADP or the combined effect of 2-OG and ATP on binding of P_{II} variants to the His_6-NAGK surface compared to wt P_{II}, we incubated the analyte (100 nM), diluted in HBS-Mg buffer, with each of the effector molecules on ice for 5 min and injected (50 μl) it to both FC1 and FC2 on the sensor chip. The specific binding of P_{II} to NAGK was recorded as the response signal difference FC2 − FC1. P_{II} was removed from the His_6-NAGK surface by injecting 25 μl of 1 mM ADP. For novel reload of proteins on the NTA sensor chip, 25 μl of 0.4 M EDTA (ethylenediaminetetraacetic acid) (pH 7.5) was injected to remove His_6-NAGK and Ni^+. Subsequently, the chip could be loaded again with 5 mM $NiSO_4$ solution and His_6-NAGK as described above.

Isothermal titration calorimetry

ITC experiments were performed on a VP-ITC microcalorimeter (MicroCal, LCC) in 10 mM Hepes–NaOH, 50 mM KCl, 50 mM NaCl, and 1 mM $MgCl_2$ (pH 7.4) at 20 °C. For determination of ATP, ADP and 2-OG binding isotherms for wt P_{II} protein, 33 μM protein solution (trimer concentration) was titrated with 1 mM ATP, 2 mM ADP or 2 mM 2-OG (in the presence of 1 mM ATP), respectively. The ligand (3 μl) was injected 70 times into the 1.4285 ml cell with stirring at 350 rpm.

For determination of ATP, ADP and 2-OG binding isotherms for I86T and I86N P_{II} variants, 17 μM protein solution was titrated with 1 mM ATP, 1.5 mM ADP or 2 mM 2-OG (in the presence of 1 mM ATP), respectively. The ligand (5 μl) was injected 35 times. The binding isotherms were calculated from received data and fitted to a three-site binding model or one-site binding model with the MicroCal ORIGIN software (Northampton, MA) as indicated.

Coupled NAGK activity assay

The activity of NAGK was assayed by coupling NAG phosphorylation via pyruvate kinase and lactate

dehydrogenase to the oxidation of NADH. The assay was performed as described previously; the reaction buffer consisted of 50 mM imidazole (pH 7.5), 50 mM KCl, 20 mM $MgCl_2$, 0.4 mM NADH, 1 mM phosphoenolpyruvate, 10 mM ATP, 0.5 mM DTT, 11 U lactate dehydrogenase, 15 U pyruvate kinase and 50 mM NAGK.[22] The reaction was started by the addition of 3 μg NAGK. When needed, 1.2 μg P_{II} was added to the reaction mixture before beginning the assay. Phosphorylation of one molecule of NAG leads to oxidation of one molecule of NADH, followed by the linear decrease of absorbance at 340 nm.[28] The reaction was recorded in a volume of 1 ml over a period of 10 min with a SPECORD 200 photometer (Analytik Jena) at 340 nm. The reaction velocity was calculated from the slope of the resulting time curve as change in absorbance per time with 1 U of NAGK (ε_{340} = 6178 L mol^{-1} cm^{-1}) catalyzing the conversion of 1 mmol NAG per minute.

Crystallization of I86N P_{II} variant

Crystallization was performed with the sitting-drop technique by mixing 400 nl of the protein solution with equal amounts of the reservoir solution using the honeybee robot (Genomic Solutions Ltd). Drops were incubated at 20 °C and pictures were recorded by the RockImager system (Formulatrix, Waltham, MA). The protein buffer was composed of 10 mM Tris (pH 7.4), 0.5 mM EDTA, 100 mM NaCl, 1% glycerol, 2 mM ATP-Mg; crystals appeared after 7 days in a precipitant condition containing 0.1 M Mes (pH 6.5) and 25% PEG (polyethylene glycol) 1000. Crystals were mounted directly in cryoloops and flash-frozen in liquid nitrogen. Diffraction data were collected at the Swiss Light Source (SLS, Villigen, Switzerland). Diffraction images were recorded on a MarCCD camera 225 (Marreserarch, Norderstedt, Germany) and images were processed using the XDS/XSCALE software.[29] The structure was solved by molecular replacement using the program Molrep.[30] Rebuilding of the structure and structure refinement was performed using the programs Coot and Refmac.[31,32] The quality of the structure was analyzed by the Procheck program.[33] Figures were generated using PyMOL†.

PDB accession numbers

Coordinates and structure factors for the P_{II} I86N variant have been deposited in the PDB with accession number 2xbp.

Acknowledgements

We thank Dr. Gregor Meiss and Verena Schuenemann for their help in performing the ITC measurements. Ulrike Ruppert and Christina Herrmann are gratefully acknowledged for excellent technical assistance. We thank the Fonds der Chemischen Industrie for generous allocation of the BIAcore equipment and the Landesstiftung Baden-Württemberg program SI-BW for supporting the ITC equipment. This work was also supported by a grant from the DFG (Fo 194/4).

† http://www.pymol.org/

References

1. Ninfa, A. J. & Jiang, P. (2005). P_{II} signal transduction proteins: sensors of alpha-ketoglutarate that regulate nitrogen metabolism. *Curr. Opin. Microbiol.* **8**, 168–173.
2. Leigh, J. A. & Dodsworth, J. A. (2007). Nitrogen regulation in bacteria and archaea. *Annu. Rev. Microbiol.* **61**, 349–377.
3. Forchhammer, K. (2008). P(II) signal transducers: novel functional and structural insights. *Trends Microbiol.* **16**, 65–72.
4. Sant'Anna, F. H., Trentini, D. B., de Souto Weber, S., Cecagno, R., da Silva, S. C. & Schrank, I. S. (2009). The P_{II} superfamily revised: a novel group and evolutionary insights. *J. Mol. Evol.* **68**, 322–336.
5. Jiang, P. & Ninfa, A. J. (2007). *Escherichia coli* P_{II} signal transduction protein controlling nitrogen assimilation acts as a sensor of adenylate energy charge in vitro. *Biochemistry*, **46**, 12979–12996.
6. Xu, Y., Cheah, E., Carr, P. D., van Heeswijk, W. C., Westerhoff, H. V., Vasudevan, S. G. & Ollis, D. L. (1998). GlnK, a P_{II}-homologue: structure reveals ATP binding site and indicates how the T-loops may be involved in molecular recognition. *J. Mol. Biol.* **282**, 149–165.
7. Xu, Y., Carr, P. D., Clancy, P., Garcia-Dominguez, M., Forchhammer, K., Florencio, F. *et al.* (2003). The structures of the P_{II} proteins from the cyanobacteria *Synechococcus* sp. PCC 7942 and *Synechocystis* sp. PCC 6803. *Acta Crystallogr., Sect. D: Biol. Crystallogr.* **59**, 2183–2190.
8. Forchhammer, K. (2004). Global carbon/nitrogen control by P_{II} signal transduction in cyanobacteria: from signals to targets. *FEMS Microbiol. Rev.* **28**, 319–333.
9. Sakai, H., Wang, H., Takemoto-Hori, C., Kaminishi, T., Yamaguchi, H., Kamewari, Y. *et al.* (2005). Crystal structures of the signal transducing protein GlnK from *Thermus thermophilus* HB8. *J. Struct. Biol.* **149**, 99–110.
10. Yidiz, Ö., Kalthoff, C., Raunser, S. & Kühlbrandt, W. (2007). Structure of GlnK1 with bound effectors indicates regulatory mechanism for ammonia uptake. *EMBO J.* **26**, 589–599.
11. Jiang, P., Zucker, P., Atkinson, M. R., Kamberov, E. S., Tirasophon, W., Chandran, P. *et al.* (1997). Structure/function analysis of the P_{II} signal transduction protein of *Escherichia coli*: genetic separation of interactions with protein receptors. *J. Bacteriol.* **179**, 4343–4353.
12. Jiang, P. & Ninfa, A. J. (2009). alpha-Ketoglutarate controls the ability of the *Escherichia coli* P_{II} signal transduction protein to regulate the activities of NRII (NtrB) but does not control the binding of P_{II} to NRII. *Biochemistry*, **48**, 11514–11521.
13. Forchhammer, K. & Hedler, A. (1997). Phosphoprotein P_{II} from cyanobacteria—analysis of functional conservation with the P_{II} signal-transduction protein from *Escherichia coli*. *Eur. J. Biochem.* **244**, 869–875.
14. Kloft, N., Rasch, G. & Forchhammer, K. (2005). Protein phosphatase PphA from *Synechocystis* sp. PCC 6803: the physiological framework of P_{II}-P dephosphorylation. *Microbiology*, **151**, 1275–1283.
15. Espinosa, J., Forchhammer, K., Burillo, S. & Contreras, A. (2006). Interaction network in cyanobacterial nitrogen regulation: PipX, a protein that interacts in

a 2-oxoglutarate dependent manner with P_{II} and NtcA. *Mol. Microbiol.* **61**, 457–469.
16. Heinrich, A., Maheswaran, M., Ruppert, U. & Forchhammer, K. (2004). The *Synechococcus elongatus* P signal transduction protein controls arginine synthesis by complex formation with *N*-acetyl-L-glutamate kinase. *Mol. Microbiol.* **52**, 1303–1314.
17. Maheswaran, M., Urbanke, C. & Forchhammer, K. (2004). Complex formation and catalytic activation by the P_{II} signaling protein of *N*-acetyl-L-glutamate kinase from *Synechococcus elongatus* strain PCC 7942. *J. Biol. Chem.* **279**, 55202–55210.
18. Burillo, S., Luque, I., Fuentes, I. & Contreras, A. (2004). Interactions between the nitrogen signal transduction protein P_{II} and *N*-acetyl glutamate kinase in organisms that perform oxygenic photosynthesis. *J. Bacteriol.* **186**, 3346–3354.
19. Llacer, J. L., Fita, I. & Rubio, V. (2008). Arginine and nitrogen storage. *Curr. Opin. Struct. Biol.* **18**, 673–681.
20. Llacer, J. L., Contreras, A., Forchhammer, K., Marco-Marin, C., Gil-Ortiz, F., Maldonado, R. *et al.* (2007). The crystal structure of the complex of P_{II} and acetylglutamate kinase reveals how P_{II} controls the storage of nitrogen as arginine. *Proc. Natl. Acad. Sci. USA*, **104**, 17644–17649.
21. Mizuno, Y., Moorhead, G. B. & Ng, K. K. (2007). Structural basis for the regulation of *N*-acetylglutamate kinase by P_{II} in *Arabidopsis thaliana*. *J. Biol. Chem.* **282**, 35733–35740.
22. Beez, S., Fokina, O., Herrmann, C. & Forchhammer, K. (2009). *N*-Acetyl-L-glutamate kinase (NAGK) from oxygenic phototrophs: P(II) signal transduction across domains of life reveals novel insights in NAGK control. *J. Mol. Biol.* **389**, 748–758.
23. Nichols, C. E., Sainsbury, S., Berrow, N. S., Alderton, D., Saunders, N. J., Stammers, D. K. & Owens, R. J. (2006). Structure of the P_{II} signal transduction protein of *Neisseria meningitidis* at 1.85 Å resolution. *Acta Crystallogr., Sect. F: Struct. Biol. Cryst. Commun.* **62**, 494–497.
24. Carr, P. D., Cheah, E., Suffolk, P. M., Vasudevan, S. G., Dixon, N. E. & Ollis, D. L. (1996). X-ray structure of the signal transduction protein from *Escherichia coli* at 1.9 A. *Acta Crystallogr., Sect. D: Biol. Crystallogr.* **52**, 93–104.
25. Benelli, E. M., Buck, M., Polikarpov, I., de Souza, E. M., Cruz, L. M. & Pedrosa, F. O. (2002). *Herbaspirillum seropedicae* signal transduction protein P_{II} is structurally similar to the enteric GlnK. *Eur. J. Biochem.* **269**, 3296–3303.
26. Bueno, R., Pahel, G. & Magasanik, B. (1985). Role of *glnB* and *glnD* gene products in regulation of the glnALG operon of *Escherichia coli*. *J. Bacteriol.* **164**, 816–822.
27. Studier, F. W., Rosenberg, A. H., Dunn, J. J. & Dubendorff, J. W. (1990). Use of T7 RNA polymerase to direct expression of cloned genes. *Methods Enzymol.* **185**, 60–89.
28. Jiang, P. & Ninfa, A. J. (1999). Regulation of autophosphorylation of *Escherichia coli* nitrogen regulator II by the P_{II} signal transduction protein. *J. Bacteriol.* **181**, 1906–1911.
29. Kabsch, W. (2010). XDS. *Acta Crystallogr., Sect. D: Biol. Crystallogr.* **66**, 125–132.
30. Vagin, A. & Teplyakov, A. (1997). MOLREP: an automated program for molecular replacement. *J. Appl. Crystallogr.* **30**, 1022–1025.
31. Emsley, P. & Cowtan, K. (2004). Coot: model-building tools for molecular graphics. *Acta Crystallogr., Sect. D: Biol. Crystallogr.* **60**, 2126–2132.
32. Murshudov, G. N., Vagin, A. A. & Dodson, E. J. (1997). Refinement of macromolecular structures by the maximum-likelihood method. *Acta Crystallogr., Sect. D: Biol. Crystallogr.* **53**, 240–255.
33. Laskowski, R. A., Macarthur, M. W., Moss, D. S. & Thornton, J. M. (1993). Procheck—a program to check the stereochemical quality of protein structures. *J. Appl. Crystallogr.* **26**, 283–291.

Mechanism of 2-oxoglutarate signaling by the *Synechococcus elongatus* P_{II} signal transduction protein

Oleksandra Fokina[a], Vasuki-Ranjani Chellamuthu[b], Karl Forchhammer[a,1], and Kornelius Zeth[b,1]

[a]Interfakultäres Institut für Mikrobiologie und Infektionsmedizin der Eberhard-Karls-Universität Tübingen, Auf der Morgenstelle 28, 72076 Tübingen, Germany; and [b]Department of Protein Evolution, Max Planck Institute for Developmental Biology, Spemannstrasse 35, 72076 Tübingen, Germany

Edited by David L. Bain, University of Colorado Denver, Denver, CO, and accepted by the Editorial Board September 14, 2010 (received for review June 3, 2010)

P_{II} proteins control key processes of nitrogen metabolism in bacteria, archaea, and plants in response to the central metabolites ATP, ADP, and 2-oxoglutarate (2-OG), signaling cellular energy and carbon and nitrogen abundance. This metabolic information is integrated by P_{II} and transmitted to regulatory targets (key enzymes, transporters, and transcription factors), modulating their activity. In oxygenic phototrophs, the controlling enzyme of arginine synthesis, *N*-acetyl-glutamate kinase (NAGK), is a major P_{II} target, whose activity responds to 2-OG via P_{II}. Here we show structures of the *Synechococcus elongatus* P_{II} protein in complex with ATP, Mg^{2+}, and 2-OG, which clarify how 2-OG affects P_{II}–NAGK interaction. P_{II} trimers with all three sites fully occupied were obtained as well as structures with one or two 2-OG molecules per P_{II} trimer. These structures identify the site of 2-OG located in the vicinity between the subunit clefts and the base of the T loop. The 2-OG is bound to a Mg^{2+} ion, which is coordinated by three phosphates of ATP, and by ionic interactions with the highly conserved residues K58 and Q39 together with B- and T-loop backbone interactions. These interactions impose a unique T-loop conformation that affects the interactions with the P_{II} target. Structures of P_{II} trimers with one or two bound 2-OG molecules reveal the basis for anticooperative 2-OG binding and shed light on the intersubunit signaling mechanism by which P_{II} senses effectors in a wide range of concentrations.

metabolic signaling | nitrogen regulation | cyanobacteria | chloroplasts

The P_{II} proteins constitute one of the largest and most widely distributed family of signal transduction proteins present in archaea, bacteria, and plants. They control key processes of nitrogen metabolism in response to central metabolites ATP, ADP, and 2-oxoglutarate (2-OG), signaling cellular energy and carbon and nitrogen abundance (1–4). These effectors bind to P_{II} in an interdependent manner (see below), thereby transmitting metabolic information into structural states of this sensor protein (3, 5). Furthermore, P_{II} proteins may be posttranslationally modified (1, 6). Depending on the signal input states, P_{II} proteins bind and thereby regulate the activity of key metabolic and regulatory enzymes, transcription factors, or transport proteins (1–3). In cyanobacteria and plants, the controlling enzyme of arginine biosynthesis, *N*-acetyl-L-glutamate kinase (NAGK), is a major P_{II} target (7–9). Moreover, P_{II} affects gene expression in cyanobacteria through binding to the transcriptional coactivator of NtcA, PipX (10). In plants, acetyl-CoA carboxylase was recently shown to be regulated by P_{II}, providing an additional link between carbon and nitrogen regulation (11). Although these P_{II} targets share no common structural element, interaction with P_{II} is inhibited by 2-OG.

P_{II} proteins are homotrimers of 12- to 13-kDa subunits, built of a double ferredoxin-like fold-containing core (βαβ-βαβ), with a characteristic and highly conserved 3D structure, as revealed from numerous crystal structures (3, 12). The trimeric P_{II} architecture resembles a flattened barrel with long and flexible T loops extending outward, from the flat side (see Fig. 1 and Fig. S1). These T loops can adopt multiple conformations and mediate the versatile protein–protein interactions (3). Each subunit further comprises two small loops (B and C loop) in the intersubunit clefts, facing each other from opposing subunits and taking part in a unique mode of ATP-ADP binding (13–15). ADP and ATP compete here for the same site. In the presence of Mg-ATP, up to three 2-OG molecules can bind per trimer (1) with ADP antagonizing 2-OG binding (16). Notably, *Arabidopsis thaliana* P_{II} is an exception, because it binds 2-OG also in the presence of ADP (5, 17). Another feature characteristic for many P_{II} proteins is also intriguing: The three ATP-binding sites and the three 2-OG–binding sites each exhibit negative cooperativity. Anticooperativity implies strong conformational coupling between the subunits, and this feature probably allows P_{II} to sense a wide range of metabolite concentrations (5, 16, 18, 19). In contrast to the ATP-ADP–binding site, the 2-OG–binding site is controversial (3). From the crystal structure of a P_{II} paralogue from *Methanococcus jannaschii*, GlnK1, one 2-OG molecule was shown to bind from outside to the distal side of the T loop in the presence of Mg-ATP (20). By contrast, a recently published structure of a P_{II} homologue form *Azospirillum brasiliense* in complex with Mg-ATP and 2-OG revealed the 2-OG–binding site close to the base of the T loop and near the ATP-binding site (21). However, neither of these two structures was proved by biochemical studies nor could they explain the anticooperative binding of 2-OG.

The structures of complexes of P_{II} with its regulatory target NAGK from *Synechococcus elongatus* and *A. thaliana* are highly similar (22, 23), and the mode of interaction and regulation is apparently conserved in cyanobacteria and plants (24). The P_{II}–NAGK complex involves one hexameric (trimer of dimers) NAGK toroid sandwiched between two P_{II} trimers with the threefold axis aligned (23). Each P_{II} subunit engages two contact surfaces in NAGK binding: A smaller surface involves the B loop and a larger is formed by the T loop, which adopts a tightly bent conformation that fits into the interdomain crevice of NAGK. Binding of P_{II} enhances the catalytic activity of NAGK and alleviates feedback inhibition by arginine. To bind NAGK, free P_{II} has to contract its extended T loop. Recently, a two-step process of P_{II}–NAGK binding was proposed on the basis of the properties of a newly identified *S. elongatus* P_{II} variant (I86N), which mimics the P_{II} conformation in the NAGK-bound state (18): First, a salt bridge between P_{II}-E85 and NAGK-R233 forms,

Author contributions: K.F. and K.Z. designed research; O.F. and V.-R.C. performed research; O.F., K.F., and K.Z. analyzed data; and O.F., K.F., and K.Z. wrote the paper.

The authors declare no conflict of interest.

This article is a PNAS Direct Submission. D.L.B. is a guest editor invited by the Editorial Board.

Freely available online through the PNAS open access option.

Data deposition: The crystallography, atomic coordinates, and structure factors have been deposited in the Protein Data Bank, www.pdb.org (PDB ID codes 2XUL and 2XUN).

[1]To whom correspondence may be addressed. E-mail: karl.forchhammer@uni-tuebingen.de or kornelius.zeth@tuebingen.mpg.de.

This article contains supporting information online at www.pnas.org/lookup/suppl/doi:10.1073/pnas.1007653107/-/DCSupplemental.

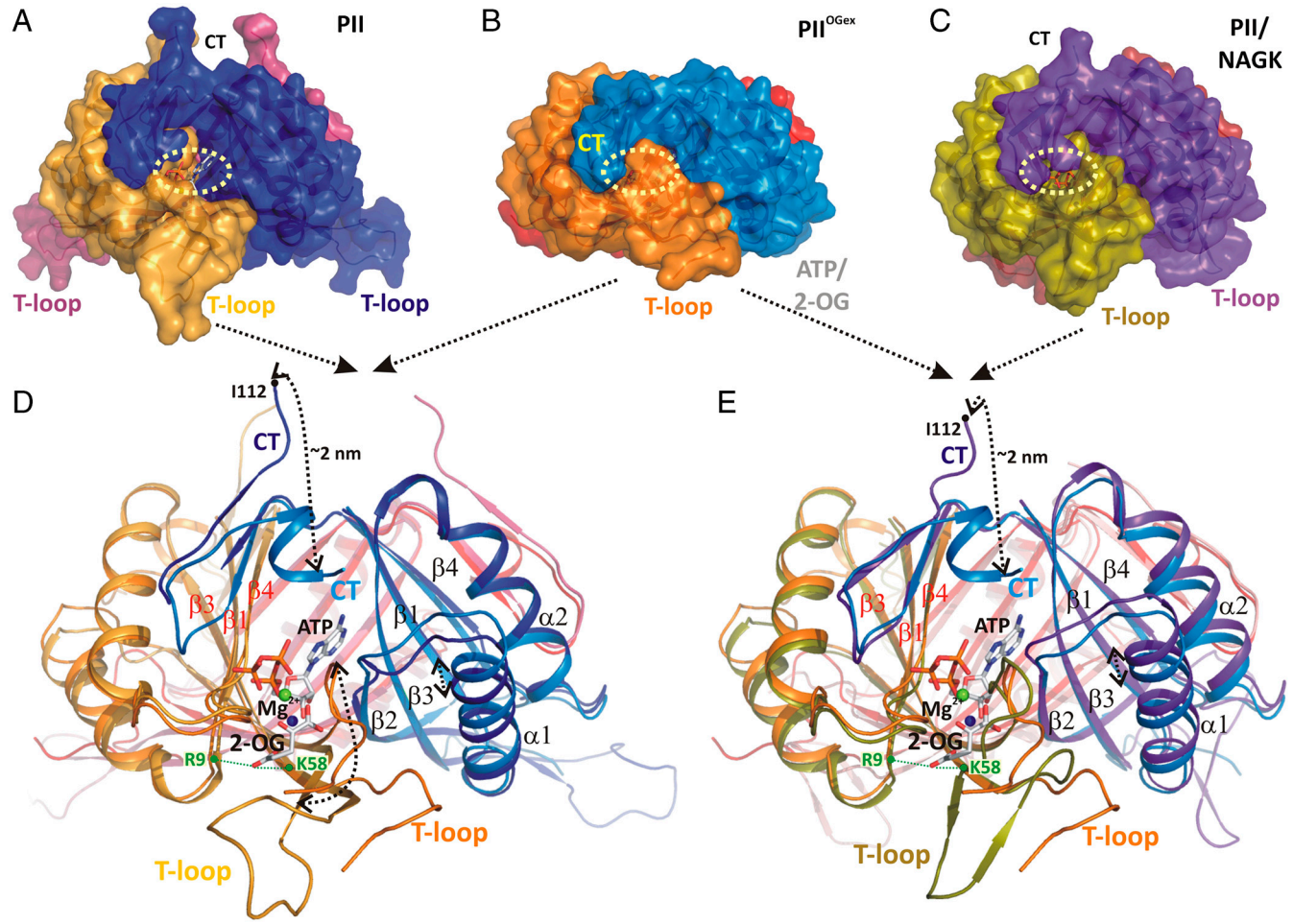

Fig. 1. Structural basis of P_{II} regulation by 2-oxoglutarate. (*A*–*C*) Side views of different *S. elongatus* P_{II} structures in surface representation. The location of the ATP-binding site is indicated by a yellow dashed circle; the red boxes highlight the structure part discussed detailed in *D*. (*A*) Ligand-free P_{II} modeled together with ATP (placed according to the superimposed P_{II}^{OGex} structure). The subunits are color coded in dark blue, light orange, and warm pink. The extended C termini and T loops of the proteins chains are marked CT and T-loop, respectively. (*B*) P_{II}/ATP/2-OG (P_{II}^{OGex}) complex structure; subunits color coded in orange, marine blue, and red. The structure adopts a compact conformation because of the back folding of the C terminus (CT) onto the core domain structure and the T loop observed in a partially disordered conformation. (*C*) Structure of P_{II} in the P_{II}–NAGK complex (PDB ID code: 2V5H) modeled together with ATP. Subunits are color coded in magenta, deep olive, and salmon. (*D*) Superposition of the ligand-free P_{II} and P_{II}^{OGex} structure as ribbon models in the color codes derived from *A* and *B*. Secondary structure elements are marked with β1–β5 and α1–α2 and ATP and 2-OG are shown in stick representation, whereas the Mg ion is marked in green. The sites of two mutations, R9L and K58M, introduced to prove the binding mode of 2-OG are marked with green dots. Remarkable conformational transitions are marked with dashed lines: movement of the C terminus, a shift of helix 1, and displacement of the T-loop base by 2-OG while the tip becomes disordered. (*E*) Superposition of P_{II}^{OGex} and P_{II}–NAGK structures as ribbon models in the color codes derived from *B* and *C*. Structural details are indicated as in *D*.

triggering the extended T loop to fold into the tightly bent conformation that fits into NAGK.

Detailed structural information together with the well-studied biochemical features and highly sensitive complex formation assays render the P_{II}–NAGK system ideal to study the transduction of metabolic signals into protein action. Until now, it was unclear how the 2-OG signal, perceived by P_{II}, results in inhibition of P_{II}–NAGK complex formation. To answer this question, we solved structures of P_{II} with ATP, Mg^{2+}, and 2-OG, revealing the mechanism by which the 2-OG signal is perceived by P_{II} and controls receptor interactions.

Results

Structure of P_{II} in Complex with ATP and 2-OG. Crystals of recombinant P_{II} protein from *S. elongatus* were obtained in the presence of excess 2-OG/Mg-ATP (P_{II}^{OGex}) and at substoichiometric amounts of 2-OG ($P_{II}^{OG1–3}$) (Table S1). All structures were solved by molecular replacement using the free *S. elongatus* P_{II} as a model [Protein Data Bank (PDB) ID code 1QY7]. The P_{II}^{OGex} crystal diffracting to 2.2 Å contains two identical trimers in the asymmetric unit (with an rmsd of 0.2 $Å^2$ for all C atoms superposed). Each trimer contains three Mg^{2+}, ATP, and 2-OG molecules. In Fig. 1, this structure is compared to the structures of ligand-free P_{II} (14) and P_{II} in complex with NAGK (23). In the ligand-free structure, the T loop, and the C terminus adopt highly extended conformations away from the ATP-binding site (see Fig. 1 *A* and *D*). Here, P_{II} offers an open binding cavity volume of approximately 1,000 $Å^3$ for the ligands. Upon ATP and 2-OG binding, a significant conformational change in the T loop and the C terminus occurs: The C-terminal β-sheet of the free form moves toward the ATP-binding site by up to 20 Å (for the terminal residue I112) to change into a small helix (see Fig. 1*D*). The T loop contracts and the tip (from residues 44–50) becomes disordered. Part of the flexible T loop moves toward the ATP-binding site to form a kink-like structure (residues 36–41), thereby forming the scaffold for proper ATP and 2-OG assembly. As a result, the ATP/2-OG–binding cavity is completely enclosed by this unique T-loop conformation and the movement of the C terminus (see Fig. 1*B*, yellow

circle). In the P_{II} structure complexed with NAGK, the T loop is clamped in a different conformation (see Fig. 1 *C* and *E*). Here, access to the ligand-binding cavity is slightly reduced compared to the ATP-free form because of a bend in the T-loop conformation, thereby reducing the cavity volume to about 600 $Å^3$.

The 2-OG–binding site of P_{II} is formed by an ATP-chelated Mg^{2+} ion and residues from one side of the intersubunit cleft (Fig. 2). The ATP molecule bound in the intersubunit cleft is ligated mainly by arginine residues (R38 from monomer A; R101 and R103 from monomer B) together with K90 from monomer A and a small number of hydrogen bonds. ATP fixed by these residues forms the scaffold for Mg^{2+}-mediated binding of 2-OG. The Mg^{2+} ion has an almost perfect hexagonal coordination sphere of oxygen atoms, three of which are contributed by oxo groups of the α-, β-, and γ-phosphate of ATP. Two additional ligating atoms are accounted for by the O2 and O5 of 2-OG. The last coordination position is contributed by the OE1 atom of residue Q39. Notably, the 2-OG–binding sphere mainly comprises residues from the T loop. Backbone atoms from residues Q39, K40, and G41 (all contacting O1 or O2 of 2-OG) together with the Q39 side-chain ligate the O5 atom and form one area of interactions. A second interaction region is composed of the backbone nitrogen of G87 (forming a second H bridge to O5) and a strong salt bridge of K58 toward the O3 and O4 atoms (distance of 2.7 Å). Furthermore, residue R9 approaches the O4 to 3.5 Å. All these residues with the exception of K40 are highly conserved in P_{II} proteins (4) (Fig. S1).

To validate that 2-OG in the crystal occupies the true binding site, P_{II} variants were constructed, in which residues K58 and R9, whose side chains according to the P_{II}^{OGex} structure specifically interact with 2-OG, were replaced by similar-sized uncharged residues (K58M and R9L). Binding of 2-OG in the presence of Mg-ATP was determined by isothermal calorimetry (ITC). Indeed, the P_{II} K58M variant was completely unable to bind 2-OG, although ATP could still be bound, showing that the loss of 2-OG binding is a specific effect of the K58 replacement. In further agreement with the structural prediction, the P_{II} R9L variant was strongly impaired in 2-OG binding (Table 1). Moreover, both P_{II} variants were impaired in NAGK binding, confirming that K58 is indeed pivotal for folding the T loop in the tightly bent structure. The R9 side chain is near the contact surface to NAGK and appears to stabilize the B-loop–T-loop interface (23) (Fig. S2).

Structural Basis of Sequential/Anticooperative 2-OG Binding. Crystallization of P_{II} protein in the presence of low 2-OG amounts

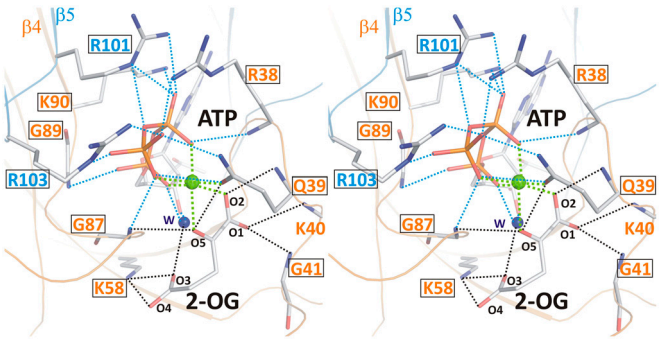

Fig. 2. Stereo image of the 2-OG–binding site. Residues involved in binding of 2-OG (atoms are marked with small numbers) and the hydrophilic portion of ATP are numbered according to the sequence. Cofactors as well as side- and main-chain atoms are marked in stick representation; Mg^{2+} is marked as a green sphere. Colors of residue numbers (orange and blue) correspond to those of the respective subunits. Residues conserved in standard alignments are boxed. Dashed blue lines represent bonds between residues and ATP and black lines indicate bonds for the ligation of 2-OG, whereas green lines mark the hexagonal coordination of the Mg^{2+} ion.

Table 1. Effector molecule binding to P_{II} variants R9L and K58M

	K_d1, μM	K_d2, μM	K_d3, μM
2-OG (+1 mM ATP)			
R9L	441 ± 40	123 ± 7	509 ± 116
K58M	ND	ND	ND
(WT)	(5.1 ± 4.0)	(11.1 ± 1.8)	(106.7 ± 14.8)
ATP			
R9L	NM	NM	NM
K58M	10 ± 5	262 ± 136	31 ± 15
(WT)	(4.0 ± 0.1)	(12.5 ± 0.9)	(47.4 ± 21.9)

Values correspond to the mean of two independent experiments ±SEM. The raw data were fitted by using a three-site binding model for a P_{II} trimer. For comparison, the original data for WT P_{II} protein are given in parentheses. ND, not detectable; NM, not measured.

yielded P_{II} structures with differing 2-OG content. The structure resolved at a resolution of 1.95 Å contains three P_{II} trimers in the asymmetric unit; one trimer contained three ATP, one Mg^{2+}, and one 2-OG (P_{II}^{OG1}), the second three ATP, two Mg^{2+}, and two 2-OG (P_{II}^{OG2}), and the third three each ATP, Mg^{2+}, and 2-OG (P_{II}^{OG3}) (Fig. 3 and Fig. S3). Additional details of structural parameters are given in *SI Text* (Tables S1 and S2). Binding of 2-OG does not significantly render the *B*-factor distribution of the three monomers significantly, unless the mobile elements (C terminus and T loop) contributing to binding are involved (Fig. S4). A superimposition of the three structurally similar trimers (Fig. 3 *A* and *B*) reveals the structure identity of the S1 site, which is occupied by 2-OG in all three P_{II}^{OG1-3} trimers, and the divergence in the S2 and S3 sites, respectively (Fig. 3*B*). The ligands are bound in S1 identical in topology to the mode described for the P_{II}^{OGex} structure (Figs. 2 and 3*B*). The P_{II}^{OG1} structure reveals that binding of the first 2-OG molecule to P_{II} (S1 site) generates unequal ligand-binding sites in the adjacent monomers, and, remarkably, sites not occupied by 2-OG also lack the Mg^{2+} ion. The conformational differences in the nonoccupied binding sites provide a structure-based explanation for the anticooperativity observed in biochemical experiments: After occupation of the first site, the K_d for the second site increases slightly, but after occupation of the second site, the K_d for the third site increases strongly (about 20-fold higher than the K_d for the first site; see Table 1). In P_{II}^{OG1}, the ATP molecule attached to the S2 site exhibits a significantly altered conformation of the phosphate moiety (Fig. 3 *B–D*); furthermore, the T-loop basis is displaced and the C terminus is ordered similar to the S1 site (Fig. 3 *C* and *D*). The S2 site in P_{II}^{OG1} resembles the S3 site of the P_{II}^{OG2} structure, which, according to the sequential 2-OG–binding mode, corresponds to the lowest affinity site (for detailed comparison of the binding sites, see Fig. S3). The S3 site of P_{II}^{OG2} exhibits further changes, visible most significantly in the T loop, the C terminus, and a small distortion in the β4-strand. Together these changes can lead to the strongly altered affinity of 2-OG toward the stereochemically differing S2 and S3 sites.

Effect of 2-OG on the Dissociation of the P_{II}–NAGK Complex. The structure of the P_{II} Mg-ATP/2OG complex suggests that 2-OG prevents interaction of P_{II} with NAGK by hindrance of the T loop folding into the tightly bent conformation needed for NAGK binding: The NAGK-bound P_{II} structure involves a salt bridge between K58 and E44 (18, 23), but because K58 is an important ligand for 2-OG, formation of this salt bridge is prevented. Furthermore, binding of 2-OG introduces a significant bend in the backbone of residues 38–43 (Fig. 1*E*) and together with the side chain of residue 42 induces a new T-loop conformation, which is incompatible with NAGK binding. When the P_{II}–NAGK complex has already been formed, is 2-OG still able to bind to P_{II} and antagonize the P_{II}–NAGK complex? Because this issue has not yet been investigated, the dissociation of the P_{II}–NAGK complex by 2-OG was studied. First, complex dissociation was directly

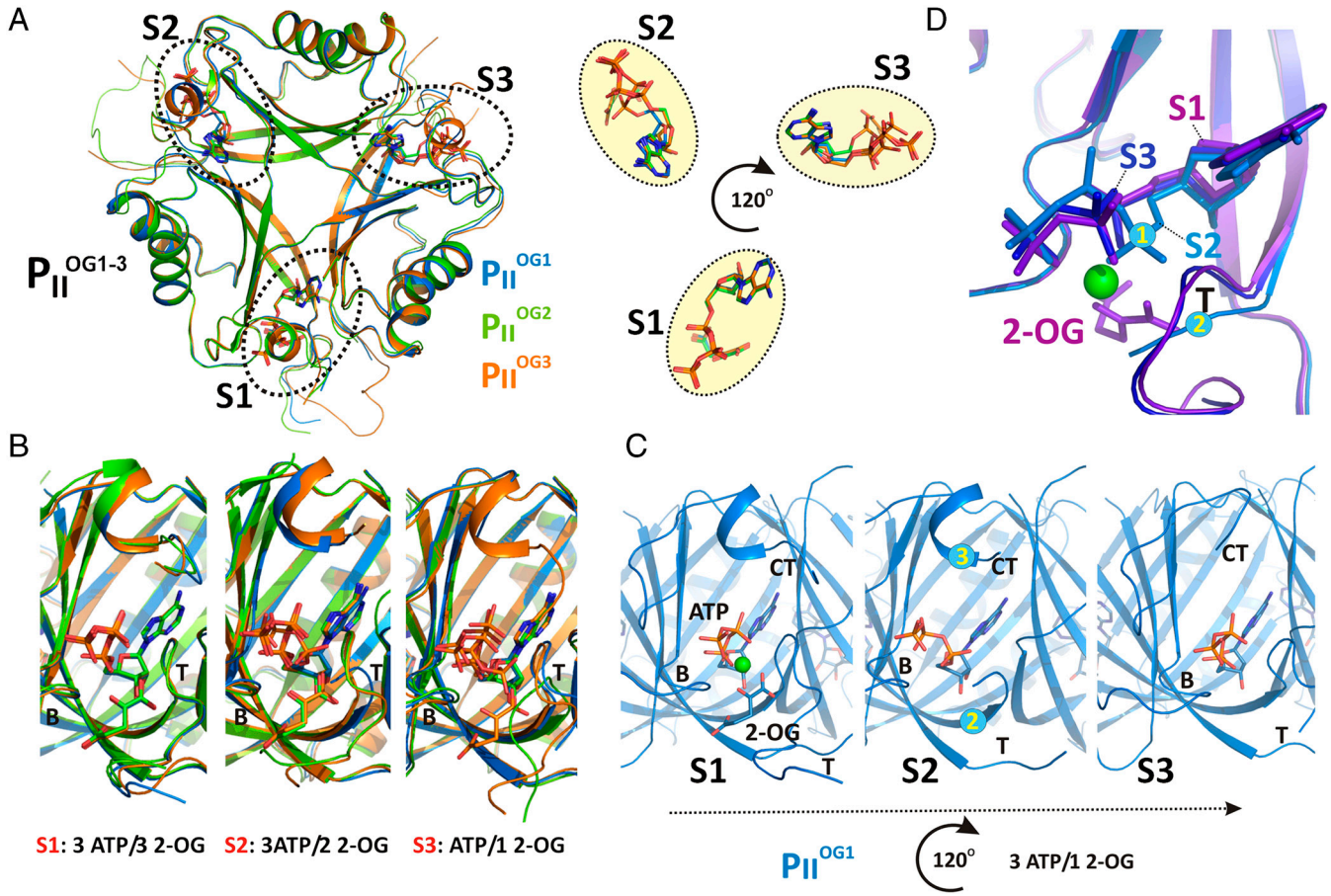

Fig. 3. Anticooperativity of 2-OG–binding sites. (*A*) Top view of the P_{II}^{OG} structure as a ribbon plot and superposition of the P_{II}^{OG1} (in blue), P_{II}^{OG2} (in green), and P_{II}^{OG3} (in orange) structures. The three ATP/2-OG–binding sites are marked by dashed circles and numbered (S1, S2, and S3). The picture on the right represents the cofactors bound in the individual sites (highlighted in yellow) with three ATP and 2-OG molecules in S1, three ATP and two 2-OG molecules in S2, and three ATP and one 2-OG molecules located in S3, respectively. The clockwise consecutive 120° binding into S1 → S2 → S3 sites is shown by an arrow. (*B*) Zoom in (side view) of the three binding sites after superposition of the molecules. The content of the individual binding sites is marked below the picture. T and B loops are marked with T and B, respectively, for clarity. (*C*) Binding sites S1, S2, and S3 of the P_{II}^{OG1} structure. In the S1 site, ATP, 2-OG, and Mg^{2+} (green sphere) are bound, whereas S2 and S3 contain only ATP and no Mg^{2+}. Significant changes in the C terminus and the T loop in site S2 are marked with numbered circles. (*D*) Superposition of effector molecules bound to sites S1, S2, and S3 in the P_{II}^{OG1} structure. The ATP molecule observed in the S2 site is significantly distorted relative to that in S1 and S3.

recorded by surface plasmon resonance (SPR) spectroscopy (Fig. 4*A*). The P_{II}–NAGK complex was formed on the sensor chip, and, subsequently, 2-OG was injected (Fig. 4*A*, arrow) to dissociate the complex. No dissociation was observed in the presence of Mg-ATP alone; with 0.5 mM 2-OG, the complex decayed slowly with a rate of 1.8×10^{-3} s^{-1}. With 1 mM 2-OG the decay rate increased to 9.0×10^{-3} s^{-1} and at 3 mM 2-OG to 28.6×10^{-3} s^{-1}. By comparison, association of the complex was inhibited by much lower 2-OG concentrations, with an IC_{50} of approximately 130 μM (18). In the second assay, the catalytic activity of NAGK/P_{II} in the presence of 50 μM arginine as an indicator of the degree of complex formation (24) was assayed (Fig. 4*B*). When 2-OG was added after formation of the P_{II}–NAGK complex, the inhibitory 2-OG concentration had an IC_{50} of 0.9 mM. By contrast, addition of 2-OG to P_{II} prior to the addition of NAGK inhibited the activity with an IC_{50} for 2-OG of approximately 120 μM (Fig. 4*B*, *Inset*) (18). Thus, 2-OG is able to dissociate the P_{II}–NAGK complex; however, one order of magnitude higher 2-OG concentrations are required to achieve dissociation compared to those required to inhibit association.

Discussion

The structures presented here explain the known features of P_{II}-mediated 2-OG signaling: A Mg^{2+} ion, chelated by the phosphates of ATP, ligates carboxylate oxygens of 2-OG, and, therefore, Mg-ATP binding is the prerequisite for 2-OG binding to P_{II}. Binding of 2-OG to *A. thaliana* P_{II} in the presence of Mg-

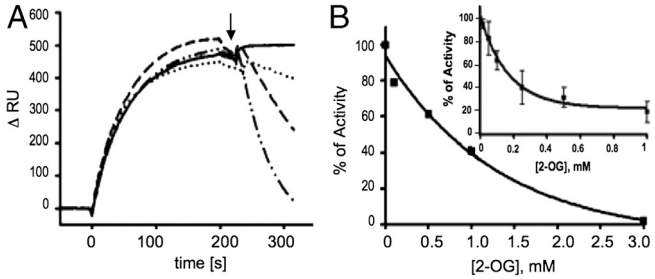

Fig. 4. The 2-OG effect on P_{II}–NAGK complex dissociation. (*A*) SPR analysis of 2-OG-induced dissociation of NAGK–P_{II} complex in the presence of 1 mM ATP. The response difference (ΔRU) between flow cells FC2 and FC1 (control) is shown. After binding of 100 nM P_{II} to NAGK in FC2, a mixture of 1 mM ATP, 1 mM $MgCl_2$, and 2-oxoglutarate [at a concentration of 0 (solid line), 0.5 (dotted line), 1 (dashed line), and 3 mM (dot-dashed line), as indicated] was injected at the point indicated by an arrow. (*B*) The effect of 2-OG on NAGK activity in the presence of 50 μM arginine. Increasing 2-OG concentrations were added to reaction mixtures after the formation of the P_{II}–NAGK complex, and NAGK activity was determined as detailed in *Materials and Methods*. (*Inset*) Effect of 2-OG on NAGK activity in the presence of P_{II}, when 2-OG was preincubated with P_{II}.

ADP could involve additional residues, possibly from its prolonged C-terminal segment, which contacts the effector molecule-binding site (22). The fact that all residues revealed here to be involved in 2-OG binding are highly conserved among P_{II} proteins (see also Fig. S1) strongly suggests that the reported mode of 2-OG binding could apply to all P_{II} proteins. The only contradiction is the previously reported structure of the P_{II} family member GlnK1 from *M. jannaschii*, where 2-OG bound from outside to the apex of a bent T loop (20). Because no biochemical evidence to support this binding mode was provided, it remains to be clarified whether this 2-OG binding mode is a peculiarity of the archaeal P_{II} protein or whether this mode of binding resulted from special crystallization conditions. In contrast, a recently described structure of the P_{II} homologue GlnZ from the proteobacterium *A. brasiliense* in complex with Mg-ATP and 2-OG revealed a mode of 2-OG binding, which is highly similar to the 2-OG binding described here, in particular the involvement of the Mg^{2+} ion and the highly conserved key residues Q39 and K58 (21). This one and our P_{II} structures perfectly agree with the properties of *S. elongatus* P_{II} variants bearing mutations in residues R9 and K58 described in this work and with the previously described I86N variant, displaying a closed 2-OG–binding site (18). Furthermore, they agree with previously reported properties of other P_{II} mutant variants. For instance, a Q39 mutation was shown to strongly impair 2-OG binding, whereas a deletion of the apical T-loop residues did not prevent 2-OG binding to *Escherichia coli* P_{II} (25). Furthermore, a K58 substitution abolished 2-OG signaling in *Rhodospirillum rubrum* P_{II} (26). Moreover, the actual structure reveals how precisely the carboxylate oxygens of 2-OG are probed by Mg^{2+} coordination and by interactions with protein backbone and side-chain atoms, explaining the high selectivity of P_{II} proteins for 2-OG (1, 16, 19). All together, these evidences strongly imply that the mode of 2-OG binding described here can be generalized for P_{II} proteins.

It has been shown that 2-OG controls P_{II} target interactions that involve the T loop, with X-ray structural information available for the *S. elongatus* and *A. thaliana* P_{II}–NAGK complex (22, 23), the *S. elongatus* P_{II}–PipX complex (27), and the *E. coli* GlnK–AmtB complex (28, 29). The mechanism of 2-OG-mediated P_{II}-target control was clarified here with the cognate P_{II}–NAGK complex. When P_{II} binds 2-OG, the base of the T loop (R38-G41) wraps around this metabolite, thereby adopting a unique retracted conformation. Furthermore, residues K58 and R9, which are involved in folding the T loop into the tightly bent conformation that fits into the NAGK crevice, perform ionic and H-bond interactions with the 2-OG γ-carboxylate oxygens, preventing formation of this fold. The IC_{50} for 2-OG to inhibit P_{II}–NAGK association (120–130 μM, depending on the method) matches the dissociation constant of the third, low-affinity 2-OG–binding site (approximately 110 μM). This correlation implies that all three sites in P_{II} have to be occupied by 2-OG in order to inhibit NAGK binding. Consequently, P_{II} partially loaded with 2-OG should be able to bind NAGK, whereby 2-OG should be displaced from P_{II}. The driving force squeezing out 2-OG could be provided by the encounter complex between P_{II} and NAGK, which, according to a recent analysis, could be formed by an ionic interaction of the B-loop residue E85 of P_{II} with R233 of NAGK (18).

The present study also revealed how 2-OG dissociates the P_{II}–NAGK complex. As shown in Fig. 1*C*, 2-OG can access its binding site from the P_{II} periphery, which is not shielded by NAGK in the complex. However, approximately 10-fold higher concentrations of 2-OG are required to dissociate the P_{II}–NAGK complex than to inhibit its association. The difference could be explained by the 2-OG–binding site being closed in the P_{II}–NAGK complex by the tightly bent T loop. The 2-OG should unlock this compact conformation to gain access to its binding site, and this process probably requires much higher concentrations than binding to the open sites, which are accessible when P_{II} is not attached to NAGK.

The structure of the second cyanobacterial P_{II} target complex, P_{II}–PipX, has been determined recently (27). It reveals three PipX molecules bound on the flat bottom surface of the P_{II} body (orientation of Fig. 1), trapped between vertically extended T loops whose tip residues grasp the PipX monomers. Notably, this extended T-loop conformation is incompatible with the T-loop fold imposed by Mg-ATP-2-OG binding (see structure overlay in Fig. S5). Binding of 2-OG to the P_{II}–PipX complex will retract the extended T loop, releasing the bound PipX molecules, which explains the biochemical data, showing that binding of PipX to P_{II} is antagonized by Mg-ATP/2-OG (10). A similar antagonistic mechanism of Mg-ATP/2-OG can be assumed for the complex of the P_{II} family member GlnK with the ammonium transport channel AmtB, as deduced from the complex structure of the *E. coli* proteins (28, 29). In complex with AmtB, the T loop is in a vertically extended structure, resembling the T loop of *S. elongatus* P_{II} in complex with PipX. In the AmtB complex, GlnK residue Q39 interacts with K58 and ADP is bound to the adenylate-binding pocket (28, 29). Given that the binding mode of Mg-ATP/2-OG to GlnK is identical as outlined above, the resulting T-loop conformation will be incompatible with formation of the GlnK–AmtB complex (21). Studies with other *E. coli* P_{II} receptors such as NtrB imply that 2-OG does not always inhibit complex formation, but it may affect receptor activity at a postbinding step (16). In this case, it is conceivable that receptor binding occurs apart from the T loop (like the B-loop interaction of P_{II} with NAGK) and the conformational changes of the T loop imposed by 2-OG binding to P_{II} are transduced into conformational changes in the receptor, thereby altering its activity.

P_{II} proteins are highly sophisticated devices for measuring the concentration of central metabolites ATP, ADP, and 2-OG in an interdependent manner. This study reveals the mechanisms underlying this process. Binding of one, two, or three 2-OG molecules generates, via intersubunit communication, distinct structural states of P_{II}. Intermolecular signaling is based on the highly conserved trimeric architecture of the P_{II} proteins. The β2-strands, which directly connect the three binding sites, could play an important role. Binding of 2-OG to one site affects the two neighboring sites asymmetrically, generating the anticooperativity that allows metabolite sensing in a wide concentration range. Moreover, the free site in clockwise orientation displays a characteristic T-loop structure. P_{II} receptors perceive the signal via intimate T-loop interactions, which affect binding or influence the receptor at a postbinding stage (16, 18). This mode of signal transduction by P_{II} is unique, and the complexity of interactions explains the remarkably high conservation of P_{II} proteins.

Materials and Methods

Full protocols are available in *SI Materials and Methods*.

Overexpression and Purification of Recombinant P_{II} and NAGK. The R9L and K58M variants were created with artificial *glnB* genes carrying the respective mutations and cloned into the Strep-tag fusion vector pASK-IBA3 (IBA) after restriction with BsaI as described previously (7). Overexpression of wild-type and mutant *S. elongatus glnB* in *E. coli* RB9060 (30) and purification of recombinant P_{II} proteins with a C-terminal-fused Strep-tag II peptide were performed according to Heinrich et al. (7). His_6-tagged recombinant NAGK from *S. elongatus* was overexpressed in *E. coli* strain BL21(DE3) (31) and purified as reported previously (8).

SPR Detection. SPR experiments were performed by using a BIAcore X biosensor system (GE Healthcare) at 25 °C in Hepes-buffered saline-Mg buffer as described previously (8). In order to analyze the effect of 2-OG on the dissociation of the P_{II}–NAGK complex, 100 nM P_{II} was first bound to immobilized His_6–NAGK in flow cell 2 (FC2) (ascending curves). Subsequently, 50 μL buffer containing 1 mM ATP and different concentrations of 2-OG was injected (start of injection indicated by the arrow). Binding and dissociation

of P_{II} to NAGK was recorded as the response signal difference (ΔRU) of FC2-FC1; FC1, reference cell without His_6–NAGK.

ITC. ITC experiments were performed on a VP-ITC microcalorimeter (MicroCal, LCC) in ITC buffer containing 10 mM Hepes-NaOH, pH 7.4, 50 mM KCl, 50 mM NaCl, and 1 mM $MgCl_2$ at 20 °C as described previously (18). For determination of ATP- and 2-OG–binding isotherms for P_{II} variants R9L and K58M, solutions with different protein concentration were titrated with 1 mM ATP or 4 mM 2-OG (in the presence of 1 mM ATP). The binding isotherms were calculated from received data and fitted to a three-site binding model using the MicroCal ORIGIN software (Northampton) as indicated.

Coupled NAGK Activity Assay. Activity of NAGK was assayed by a coupled assay (32) with modifications as described previously (24), in the buffer consisting of 50 mM imidazole, pH 7.5, 50 mM KCl, 20 mM $MgCl_2$, 0.4 mM NADH, 1 mM phosphoenolpyruvate, 10 mM ATP, 0.5 mM DTT, 11 U lactate dehydrogenase, 15 U pyruvate kinase, 50 μM arginine, 1.2 μg P_{II}, and 3 μg NAGK. The mixture was preincubated for 3 min to allow P_{II}–NAGK complex formation. Then the reaction was started by the addition of 50 mM NAG and 2-OG (to determine the effect of increasing 2-OG concentrations on disruption of P_{II}–NAGK complex in the presence of NAGK-inhibiting concentrations of arginine). Then, 20 s after addition of substrate, the change in absorbance at 340 nm was recorded for 10 min. Linear kinetics were observed over that period of time.

Crystallization of Recombinant *S. elongatus* P_{II} Protein. Crystallization was performed with the sitting-drop technique by mixing 400 nL of the protein solution with equal amounts of the reservoir solution by using the honeybee robot (Genomic Solutions Ltd). Drops were incubated at 20 °C, and pictures were recorded by the RockImager system (Formulatrix). The crystallization buffer was composed of 10 mM Tris (pH 7.4), 0.5 mM EDTA, 100 mM NaCl, 1% glycerol, and 2 mM ATP-Mg, and also 2 mM 2-OG was added; crystals appeared in a precipitant condition containing PEG 4000. Glycerol was used as the cryoprotectant, and the crystals were flash-frozen in liquid nitrogen. Diffraction data were collected at the Swiss Light Source. Diffraction images were recorded on a MarCCD camera 225 (Marresearch), and images were processed by using the XDS/XSCALE software (33). The structure was solved by molecular replacement using the program Molrep (34). Rebuilding of the structure and structure refinement was performed by using the programs Coot and Refmac (35, 36). The quality of the structure was analyzed by the Procheck program (37). Figures were generated by using PyMOL (www.pymol.org).

ACKNOWLEDGMENTS. We thank Gary Sawers for critically reading the manuscript. The help of Reinhard Albrecht in crystallization of P_{II} proteins and Christina Herrmann for technical assistance is gratefully acknowledged. This work was strongly supported by the Max Planck Society and the PXII Beamline personnel and grants from the Deutsche Forschungsgemeinschaft (Fo195).

1. Ninfa AJ, Jiang P (2005) P_{II} signal transduction proteins: Sensors of alpha-ketoglutarate that regulate nitrogen metabolism. *Curr Opin Microbiol* 8:168–173.
2. Leigh JA, Dodsworth JA (2007) Nitrogen regulation in bacteria and archaea. *Annu Rev Microbiol* 61:349–377.
3. Forchhammer K (2008) P(II) signal transducers: Novel functional and structural insights. *Trends Microbiol* 16:65–72.
4. Sant'Anna FH, et al. (2009) The P_{II} superfamily revised: A novel group and evolutionary insights. *J Mol Evol* 68:322–336.
5. Jiang P, Ninfa AJ (2007) *Escherichia coli* P_{II} signal transduction protein controlling nitrogen assimilation acts as a sensor of adenylate energy charge in vitro. *Biochemistry* 46:12979–12996.
6. Forchhammer K (2004) Global carbon/nitrogen control by P_{II} signal transduction in cyanobacteria: From signals to targets. *FEMS Microbiol Rev* 28:319–333.
7. Heinrich A, Maheswaran M, Ruppert U, Forchhammer K (2004) The *Synechococcus elongatus* P_{II} signal transduction protein controls arginine synthesis by complex formation with *N*-acetyl-L-glutamate kinase. *Mol Microbiol* 52:1303–1314.
8. Maheswaran M, Urbanke C, Forchhammer K (2004) Complex formation and catalytic activation by the P_{II} signaling protein of *N*-acetyl-L-glutamate kinase from *Synechococcus elongatus* strain PCC 7942. *J Biol Chem* 279:55202–55210.
9. Burillo S, Luque I, Fuentes I, Contreras A (2004) Interactions between the nitrogen signal transduction protein P_{II} and *N*-acetyl glutamate kinase in organisms that perform oxygenic photosynthesis. *J Bacteriol* 186:3346–3354.
10. Espinosa J, Forchhammer K, Burillo S, Contreras A (2006) Interaction network in cyanobacterial nitrogen regulation: PipX, a protein that interacts in a 2-oxoglutarate dependent manner with P_{II} and NtcA. *Mol Microbiol* 61:457–469.
11. Feria Bourrellier AB, et al. (2010) Chloroplast acetyl-CoA carboxylase activity is 2-oxoglutarate-regulated by interaction of P_{II} with the biotin carboxyl carrier subunit. *Proc Natl Acad Sci USA* 107:502–507.
12. Helfmann S, Lu W, Litz C, Andrade SL (2010) Cooperative binding of MgATP and MgADP in the trimeric P_{II} protein GlnK2 from *Archaeoglobus fulgidus*. *J Mol Biol* 402:165–177.
13. Xu Y, et al. (1998) GlnK, a P_{II}-homologue: Structure reveals ATP binding site and indicates how the T-loops may be involved in molecular recognition. *J Mol Biol* 282:149–165.
14. Xu Y, et al. (2003) The structures of the P_{II} proteins from the cyanobacteria *Synechococcus* sp. PCC 7942 and *Synechocystis* sp. PCC 6803. *Acta Crystallogr, Sect D: Biol Crystallogr* 59:2183–2190.
15. Sakai H, et al. (2005) Crystal structures of the signal transducing protein GlnK from *Thermus thermophilus* HB8. *J Struct Biol* 149:99–110.
16. Jiang P, Ninfa AJ (2009) Alpha-ketoglutarate controls the ability of the *Escherichia coli* P_{II} signal transduction protein to regulate the activities of NRII (NtrB) but does not control the binding of P_{II} to NRII. *Biochemistry* 48:11514–11521.
17. Smith CS, Weljie AM, Moorhead GB (2003) Molecular properties of the putative nitrogen sensor P_{II} from *Arabidopsis thaliana*. *Plant J* 33:353–360.
18. Fokina O, Chellamuthu VR, Zeth K, Forchhammer K (2010) A novel signal transduction protein P(II) variant from *Synechococcus elongatus* PCC 7942 indicates a two-step process for NAGK-P(II) complex formation. *J Mol Biol* 399:410–421.
19. Forchhammer K, Hedler A (1997) Phosphoprotein P_{II} from cyanobacteria—analysis of functional conservation with the P_{II} signal-transduction protein from *Escherichia coli*. *Eur J Biochem* 244:869–875.
20. Yidiz Ö, Kalthoff C, Raunser S, Kühlbrandt W (2007) Structure of GlnK1 with bound effectors indicates regulatory mechanism for ammonia uptake. *EMBO J* 26:589–599.
21. Truan D, et al. (2010) A new P_{II} protein structure identifies the 2-oxoglutarate binding site. *J Mol Biol* 400:531–539.
22. Mizuno Y, Moorhead GB, Ng KK (2007) Structural basis for the regulation of *N*-acetylglutamate kinase by P_{II} in *Arabidopsis thaliana*. *J Biol Chem* 282:35733–35740.
23. Llacer JL, et al. (2007) The crystal structure of the complex of P_{II} and acetylglutamate kinase reveals how P_{II} controls the storage of nitrogen as arginine. *Proc Natl Acad Sci USA* 104:17644–17649.
24. Beez S, Fokina O, Herrmann C, Forchhammer K (2009) *N*-acetyl-L-glutamate kinase (NAGK) from oxygenic phototrophs: P_{II} signal transduction across domains of life reveals novel insights in NAGK control. *J Mol Biol* 389:748–758.
25. Jiang P, et al. (1997) Structure/function analysis of the P_{II} signal transduction protein of *Escherichia coli*: Genetic separation of interactions with protein receptors. *J Bacteriol* 179:4342–4353.
26. Jonsson A, Nordlund S (2007) In vitro studies of the uridylylation of the three P_{II} protein paralogs from *Rhodospirillum rubrum*: The transferase activity of *R. rubrum* GlnD is regulated by alpha-ketoglutarate and divalent cations but not by glutamine. *J Bacteriol* 189:3471–3478.
27. Llacer JL, et al. (2010) Structural basis for the regulation of NtcA-dependent transcription by proteins PipX and PII. *Proc Natl Acad Sci USA* 107:15397–15402.
28. Conroy MJ, et al. (2007) The crystal structure of the *Escherichia coli* AmtB-GlnK complex reveals how GlnK regulates the ammonia channel. *Proc Natl Acad Sci USA* 104:1213–1218.
29. Gruswitz F, O'Connell J, 3rd, Stroud RM (2007) Inhibitory complex of the transmembrane ammonia channel, AmtB, and the cytosolic regulatory protein, GlnK, at 1.96 A. *Proc Natl Acad Sci USA* 104:42–47.
30. Bueno R, Pahel G, Magasanik B (1985) Role of glnB and glnD gene products in regulation of the glnALG operon of Escherichia coli. *J Bacteriol* 164:816–822.
31. Studier FW, Rosenberg AH, Dunn JJ, Dubendorff JW (1990) Use of T7 RNA polymerase to direct expression of cloned genes. *Methods Enzymol* 185:60–89.
32. Jiang P, Ninfa AJ (1999) Regulation of autophosphorylation of Escherichia coli nitrogen regulator II by the P_{II} signal transduction protein. *J Bacteriol* 181:1906–1911.
33. Kabsch W (2010) XDS. *Acta Crystallogr, Sect D: Biol Crystallogr* 66:125–132.
34. Vagin A, Teplyakov A (1997) MOLREP: An automated program for molecular replacement. *J Appl Crystallogr* 30:1022–1025.
35. Murshudov GN, Vagin AA, Dodson EJ (1997) Refinement of macromolecular structures by the maximum-likelihood method. *Acta Crystallogr, Sect D: Biol Crystallogr* 53:240–255.
36. Emsley P, Cowtan K (2004) Coot: Model-building tools for molecular graphics. *Acta Crystallogr, Sect D: Biol Crystallogr* 60:2126–2132.
37. Laskowski RA, Macarthur MW, Moss DS, Thornton JM (1993) Procheck—a program to check the stereochemical quality of protein structures. *J Appl Crystallogr* 26:283–291.

Supporting Information

Fokina et al. 10.1073/pnas.1007653107

SI Materials and Methods

Overexpression and Purification of Recombinant P_{II} and *N*-Acetyl-Glutamate Kinase (NAGK). The R9L and K58M variants were created with artificial *glnB* genes carrying the respective mutations and cloned into the Strep-tag fusion vector pASK-IBA3 (IBA) after restriction with BsaI as described previously (1). Overexpression of wild-type and mutant *Synechococcus elongatus glnB* in *Escherichia coli* RB9060 (2) and purification of recombinant P_{II} proteins with a C-terminal fused Strep-tag II peptide was performed according to Heinrich et al. (1). His_6-tagged recombinant NAGK from *S. elongatus* was overexpressed in *E. coli* strain BL21(DE3) (3) and purified as reported previously (4).

Surface Plasmon Resonance Detection (SPR). SPR experiments were performed using a BIAcore X biosensor system (Biacore AB) at 25 °C in Hepes-buffered saline (HBS)-Mg buffer containing 10 mM Hepes, 150 mM NaCl, 1 mM $MgCl_2$, and 0.005% Nonidet P-40, pH 7.5 at a flow rate of 15 μL/min as described previously (4). The purified His_6–NAGK was immobilized on the Ni^+-loaded nitrilotriacetate (NTA) sensor chip to flow cell 2 (FC2) in a volume of 50 μL at a concentration of 30 nM (hexamer) to receive a binding signal of approximately 3,000 resonance units (RU), which corresponds to a surface concentration change of 3 ng/mm^2.

In order to analyze the effect of 2-oxoglutarate (2-OG) on the dissociation of WT P_{II}–NAGK complex, 100 nM P_{II} was bound to the His_6–NAGK and then the analyte containing 1 mM ATP and different concentrations of 2-OG diluted in HBS-Mg buffer (50 μL) was injected to both FC1 and FC2 on the sensor chip. The specific binding of P_{II} to NAGK and dissociation was recorded as the response signal difference FC2-FC1.

P_{II} was removed from the His_6–NAGK surface by injecting 25 μL of 1 mM ADP. For novel reload of proteins on the NTA sensor chip, 25 μL of 0.4 M EDTA pH 7.5 was injected to remove His_6–NAGK and Ni^+. Subsequently, the chip could be loaded again with 5 mM Ni_2SO_4 solution and His_6–NAGK as described above.

Isothermal Titration Calorimetry (ITC). ITC experiments were performed on a VP-ITC microcalorimeter (MicroCal, LCC) in buffer containing 10 mM Hepes-NaOH, pH 7.4, 50 mM KCl, 50 mM NaCl, and 1 mM $MgCl_2$ at 20 °C. For determination of ATP- and 2-OG–binding isotherms for P_{II} variants R9L and K58M, different amounts of protein solution (16, 25, or 33 μM trimer concentration) were titrated with 1 mM ATP or 4 mM 2-OG (in the presence of 1 mM ATP). For one measurement 5 μL ligand was injected 35 times in 1.4285 mL cell with stirring at 350 rpm. The binding isotherms were calculated from received data and fitted to a three-site binding model using the MicroCal ORIGIN software (Northampton) as indicated.

Coupled NAGK Activity Assay. Activity of NAGK was determined by coupling NAG phosphorylation via pyruvate kinase and lactate dehydrogenase to the oxidation of NADH. The assay was performed as described previously, the reaction buffer consisting of 50 mM imidazole, pH 7.5, 50 mM KCl, 20 mM $MgCl_2$, 0.4 mM NADH, 1 mM phosphoenolpyruvate, 10 mM ATP, 0.5 mM DTT, 11 U lactate dehydrogenase, 15 U pyruvate kinase, 50 μM arginine, 1.2 μg P_{II}, and 3 μg NAGK (5). The mixture was preincubated for 3 min to allow P_{II}–NAGK complex formation. Then, the reaction was started by the addition of 50 mM NAG and 2-OG (to determine the effect of increasing 2-OG concentrations on disruption of P_{II}–NAGK complex in the presence of NAGK-inhibiting concentrations of arginine). Then 20 s after addition of substrate, the change in absorbance at 340 nm was recorded for 10 min. Linear kinetics were observed over the period of time. Phosphorylation of one molecule of NAG leads to oxidation of one molecule of NADH, which is followed by the linear decrease of absorbance at 340 nm. The reaction was recorded in a SPECORD 200 photometer (Analytik Jena). The reaction velocity was calculated from the slope of the resulting time curve as change in absorbance per time with one unit of NAGK ($e_{\tilde{34}} = 6{,}178\ \mathrm{L\,mol^{-1}\,cm^{-1}}$) catalyzing the conversion of 1 mmol NAG per min.

Crystallization of Recombinant *S. elongatus* P_{II} Protein. Crystallization was performed with the sitting-drop technique by mixing 400 nL of the protein solution with equal amounts of the reservoir solution using the honeybee robot (Genomic Solutions Ltd.). Drops were incubated at 20 °C and pictures were recorded by the RockImager system (Formulatrix). The crystallization buffer was composed of 10 mM Tris (pH 7.4), 0.5 mM EDTA, 100 mM NaCl, 1% glycerol, and 2 mM ATP-Mg, and also 2 mM 2-OG was added; crystals appeared in a precipitant condition containing PEG 4000. Glycerol was used as the cryoprotectant and the crystals were flash-frozen in liquid nitrogen. Diffraction data were collected at the Swiss Light Source. Diffraction images were recorded on a MarCCD camera 225 (Marresearch) and images were processed using the XDS/XSCALE software (6). The structure was solved by molecular replacement using the program Molrep (7). Rebuilding of the structure and structure refinement was performed using the programs Coot and Refmac (8, 9). The quality of the structure was analyzed by the Procheck program (10). Figures were generated using PyMOL (www.pymol.org).

For crystallization of $P_{II}{}^{OG1-3}$ structures, 2-OG-containing P_{II} protein was used. Crystals appeared after 30 d in a precipitant condition containing sodium acetate trihydrate 0.1 M, pH 5, PEG 4000, and 2-methyl-2,4-pentanediol.

1. Heinrich A, Maheswaran M, Ruppert U, Forchhammer K (2004) The *Synechococcus elongatus* P_{II} signal transduction protein controls arginine synthesis by complex formation with *N*-acetyl-L-glutamate kinase. *Mol Microbiol* 52:1303–1314.
2. Bueno R, Pahel G, Magasanik B (1985) Role of glnB and glnD gene products in regulation of the glnALG operon of Escherichia coli. *J Bacteriol* 164:816–822.
3. Studier FW, Rosenberg AH, Dunn JJ, Dubendorff JW (1990) Use of T7 RNA polymerase to direct expression of cloned genes. *Methods Enzymol* 185:60–89.
4. Maheswaran M, Urbanke C, Forchhammer K (2004) Complex formation and catalytic activation by the P_{II} signaling protein of *N*-acetyl-L-glutamate kinase from *Synechococcus elongatus* strain PCC 7942. *J Biol Chem* 279:55202–55210.
5. Beez S, Fokina O, Herrmann C, Forchhammer K (2009) *N*-acetyl-L-glutamate kinase (NAGK) from oxygenic phototrophs: P_{II} signal transduction across domains of life reveals novel insights in NAGK control. *J Mol Biol* 389:748–758.
6. Kabsch W (2010) XDS. *Acta Crystallogr, Sect D: Biol Crystallogr* 66:125–132.
7. Vagin A, Teplyakov A (1997) MOLREP: An automated program for molecular replacement. *J Appl Crystallogr* 30:1022–1025.
8. Murshudov GN, Vagin AA, Dodson EJ (1997) Refinement of macromolecular structures by the maximum-likelihood method. *Acta Crystallogr, Sect D: Biol Crystallogr* 53:240–255.
9. Emsley P, Cowtan K (2004) Coot: Model-building tools for molecular graphics. *Acta Crystallogr, Sect D: Biol Crystallogr* 60:2126–2132.
10. Laskowski RA, Macarthur MW, Moss DS, Thornton JM (1993) Procheck—a program to check the stereochemical quality of protein structures. *J Appl Crystallogr* 26:283–291.

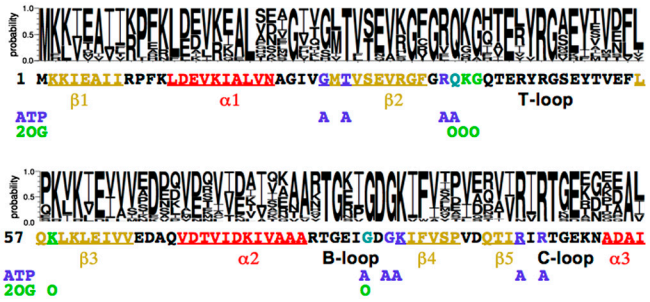

Fig. S1. Primary and secondary structure of the *S. elongatus* P_{II} protein with representation of sequence conservation and indication of amino acids, involved in ATP and 2-OG binding. Below the amino acid sequence of the *S. elongatus* P_{II} protein (middle line), the secondary structure elements and T, B, and C loops are indicated; α-helices and β-strands are underlined and colored in red or in brown, respectively. The position of amino acids involved in ATP binding (blue), 2-OG binding (green), or both (cyan) are highlighted with A or O (the coloring of these amino acids overrides the coloring of secondary structure elements). On top, the amino acid sequence conservation is represented as a sequence logo, derived from multiple sequence alignment of 14 different P_{II} proteins from the major prokaryotic lineages. The sequence logo was created with the program WebLogo 3.0. (http://weblogo.threeplusone.com/). The frequency of an amino acid in the multiple alignment is represented by the height of the letter. Multiple sequence alignment was carried out with the program ClustalW (http://www.ebi.ac.uk/Tools/clustalw2/) using the following P_{II} sequences (Gene Bank accession numbers in parentheses): *S. elongatus* (YP_171902.1); *Nostoc* sp. strain 7120 (BAB74018.1); *Prochlorococcus marinus* MIT 9301 (YP_001091877.1); *Thiobacillus denitrificans* ATCC25259 (AAZ96761.1); *E. coli* GlnB (AAB28779.1); *E. coli* GlnK (CAQ30923.1); *Azospirillum brasiliense* GlnB (AAK01659.1); *A. brasiliense* GlnK (ADK11050.1); *A. brasiliense* GlnZ (AAG10012.1); *Bacillus subtilis* GlnK (AAA17400.1); *Lactococcus lactis* subsp. cremoris MG1363 (AAX82491.1); *Streptomyces coelicolor* A3 (NP_733668.1); *Methanococcus maripaludis* GlnB (CAF29622.1); *Methanocaldococcus jannaschii* DSM 2661 GlnB (AAB98041.1).

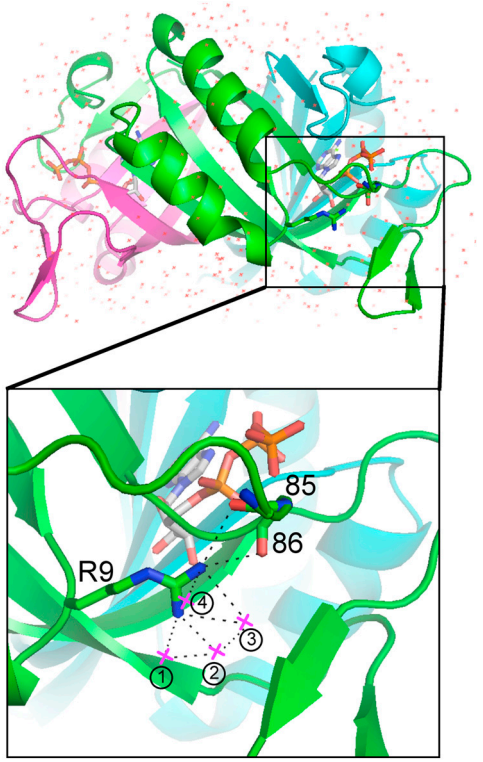

Fig. S2. Role of R9 residue in stabilizing the active site of P_{II} in the NAGK-binding conformation. Ribbon presentation of the structure of the P_{II} I86N variant (mimicking the NAGK-binding conformation) with unbound water molecules. ATP and relevant side- or main-chain residues are shown in sticks; black broken lines indicate contacts between R9 and main-chain oxygens of B-loop residues or water molecules that are designated 1, 2, 3, and 4. One of these water molecules (2) makes contact with T-loop backbone oxygen of R45 (2.80 Å), water 3 with the carboxyl group of E85 (2.83 Å), and water 4 also with E85 (2.66 Å) and the hydroxyl group of T83 (2.84 Å).

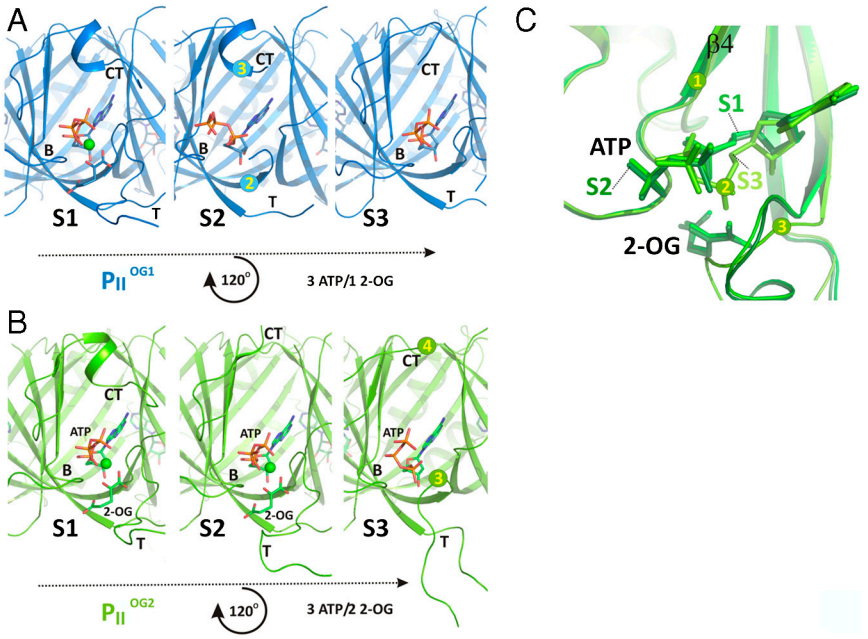

Fig. S3. Comparison of effector molecule-binding sites between P_{II}^{OG1} and P_{II}^{OG2}. (*A*) Ribbon representation figure identical to Fig. 3*C* (this paper) for comparison. (*B*) Ribbon representation of the P_{II}^{OG2} structure with a view into the three ligand-binding sites (S1, S2, and S3). Cofactors as well as the B loop, T loop, and C terminus are marked and the composition of the complex is marked below the structure figure. Significant structural changes between the three monomers are marked in S3 with encircled numbers (3, T loop; 4, C terminus). (*C*) Superposition of the three monomers of P_{II}^{OG2} and zoom into the ligand-binding pocket with the ligands of one monomer color coded in different greens. Significant changes are visible in the ATP conformation (marked with 2), in the T-loop conformation (marked with 3), and in strand β4 with residues contributing to ATP and 2-OG complexation located close to the binding site (marked with 1).

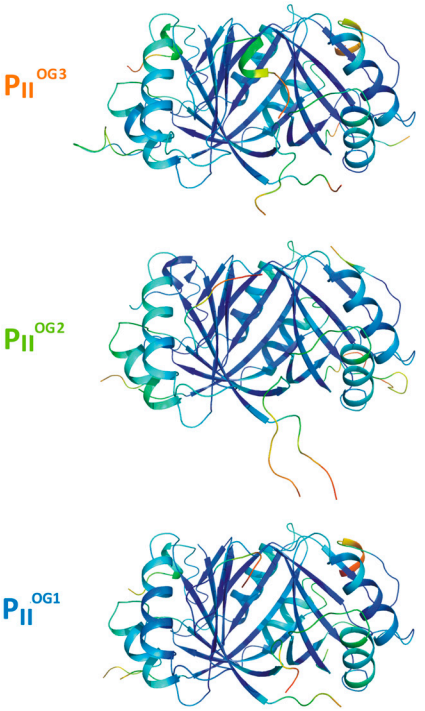

Fig. S4. Representation of the *B* factors in structures P_{II}^{OG1}–P_{II}^{OG3} with blue color indicating lowest *B* factors and red color highest temperature factors. The structures indicate that binding of the 2-OG ligand does not induce major changes in the protein flexibility and thereby the *B* factors.

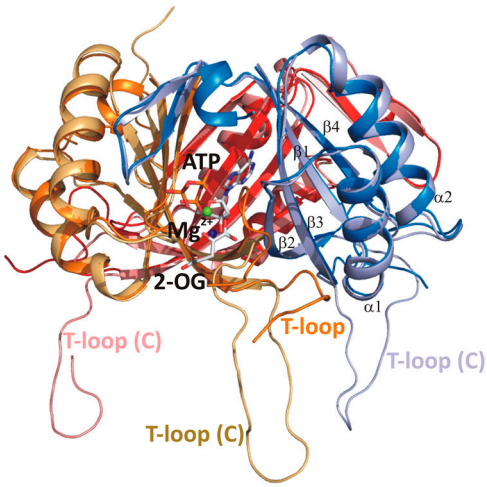

Fig. S5. Superposition of the P_{II}^{OGex} structure with the structure of P_{II} in complex with PipX [Protein Data Bank (PDB) ID code 2XG8] as ribbon models. The color code for the P_{II}^{OGex} structure is derived from Fig 1*B*, and that for P_{II} from the P_{II}–PipX complex is adapted. Secondary structure elements are marked. ATP and 2-OG are shown in stick representation whereas the Mg^{2+} ion is marked in green. The T loop from the P_{II}–PipX complex structure, labeled as "T loop (C)", displays a vertically extended conformation, which retracts upon 2-OG binding.

Table S1. Data collection and refinement statistics

	P_{II}^{OGex}	$P_{II}^{OG1–3}$
Data collection		
Space group	$P2_12_12_1$	$P22_12_1$
Cell dimensions		
a, *b*, *c*, Å	71.87, 87.99, 116.34	72.33, 102.37, 135.77
α, β, γ, °	90	90
Resolution, Å	29 – 2.2 (2.33-2.2)	48 – 1.95 (2.06-1.95)
R_{sym} or R_{merge}	0.12 (0.78)	0.12 (0.85)
$I/\sigma I$	13.3 (2.6)	12.2 (1.8)
Completeness, %	99.6 (98.1)	98.1 (94.1)
Redundancy	7.2 (7.1)	7.1 (6.9)
Refinement		
Resolution, Å	29 – 2.2 (2.25-2.2)	48 – 1.95 (2-1.95)
No. reflections	36239 (2522)	69753 (3672)
R_{work}/R_{free}	0.18/0.22 (0.22/0.29)	0.17/0.22 (0.22/0.29)
No. atoms (all)	5433	8101
Protein (chains/residues)	6/646	9/965
Ligands (ATP/αKG/CIT/Mg^{2+})	6/6/-/6	9/7/-/7
Water	248	318
B factors		
Protein	22	24.6
Ligand/ion (ATP/αKG/CIT/Mg^{2+})	22.4/31.1/-/29.6	22.5/27.6/-/23.4
Water	59	59.4
rmsd		
Bond lengths, Å	0.029	0.025
Bond angles, °	2.1	2.2
Ramachandran statistics		
No. of residues in favored region (%)	605 (97.4)	912 (97.7)
No. of residues in allowed region (%)	16 (2.6)	21 (2.3)
No. of residues in outlier region (%)	0	0
PDB ID code	2XOH	2XOJ

Values in parentheses are for the highest-resolution shell.

Table S2. Molecular interface analysis of the subunits in the P_{II}^{OG1-3} structure (values are given in $Å^2$)

	A	B	C
P_{II}^{OG1}			
A		1,200	1,180
B	1,200		1,070
C	1,180	1,070	
P_{II}^{OG2}			
A		1,210	1,190
B	1,210		1,090
C	1,190	1,090	
P_{II}^{OG3}			
A		1,260	1,250
B	1,260		1,160
C	1,250	1,160	

Planta (2013) 237:451–462
DOI 10.1007/s00425-012-1801-0

REVIEW

From cyanobacteria to plants: conservation of PII functions during plastid evolution

Vasuki Ranjani Chellamuthu · Vikram Alva · Karl Forchhammer

Received: 3 August 2012 / Accepted: 26 October 2012 / Published online: 29 November 2012

Abstract This article reviews the current state-of-the-art concerning the functions of the signal processing protein PII in cyanobacteria and plants, with a special focus on evolutionary aspects. We start out with a general introduction to PII proteins, their distribution, and their evolution. We also discuss PII-like proteins and domains, in particular, the similarity between ATP-phosphoribosyltransferase (ATP-PRT) and its PII-like domain and the complex between *N*-acetyl-L-glutamate kinase (NAGK) and its PII activator protein from oxygenic phototrophs. The structural basis of the function of PII as an ATP/ADP/2-oxoglutarate signal processor is described for *Synechococcus elongatus* PII. In both cyanobacteria and plants, a major target of PII regulation is NAGK, which catalyzes the committed step of arginine biosynthesis. The common principles of NAGK regulation by PII are outlined. Based on the observation that PII proteins from cyanobacteria and plants can functionally replace each other, the hypothesis that PII-dependent NAGK control was under selective pressure during the evolution of plastids of Chloroplastida and Rhodophyta is tested by bioinformatics approaches. It is noteworthy that two lineages of heterokont algae, diatoms and brown algae, also possess NAGK, albeit lacking PII; their NAGK however appears to have descended from an alphaproteobacterium and not from a cyanobacterium as in plants. We end this article by coming to the conclusion that during the evolution of plastids, PII lost its function in coordinating gene expression through the PipX-NtcA network but preserved its role in nitrogen (arginine) storage metabolism, and subsequently took over the fine-tuned regulation of carbon (fatty acid) storage metabolism, which is important in certain developmental stages of plants.

Keywords Chloroplast · CLANS · NAGK · Oxygenic phototroph · PII signaling · *Synechococcus elongatus*

Abbreviations

ATP-PRT	ATP-phosphoribosyltransferase
NAGK	*N*-acetyl-L-glutamate kinase
2-OG	2-Oxoglutarate

Introduction to PII signal processors: general properties and evolution of canonical PII proteins

PII proteins constitute a superfamily of the most widely distributed signaling proteins in nature, represented in all domains of life (Sant'Anna et al. 2009; Huergo et al. 2012). Members of this superfamily are present in almost all taxonomic groups of bacteria and are ubiquitous in nitrogen-fixing methanogens of the archaeal kingdom; however, in eukaryotes they are only found in oxygenic phototrophs (Arcondéguy et al. 2001; Forchhammer 2008). In all cases studied so far, PII proteins are involved in the control of anabolic nitrogen metabolism. They detect the metabolite

A contribution to the Special Issue on Evolution and Biogenesis of Chloroplasts and Mitochondria.

V. R. Chellamuthu · V. Alva
Department of Protein Evolution, Max Planck Institute for Developmental Biology, Spemannstrasse 35, 72076 Tübingen, Germany
e-mail: vasuki-ranjani.chellamuthu@tuebingen.mpg.de

V. R. Chellamuthu · K. Forchhammer (✉)
Interfakultäres Institut für Mikrobiologie und Infektionsmedzin der Eberhard-Karls-Universität Tübingen, Auf der Morgenstelle 28, 72076 Tübingen, Germany
e-mail: karl.forchhammer@uni-tuebingen.de

state of the cell by interdependent binding of ATP and 2-oxoglutarate (2-OG) or ADP in a highly conserved manner, and thereby regulate the activity of transcription factors or key metabolic enzymes (Fokina et al. 2010a, b; Truan et al. 2010; Litz et al. 2011; Radchenko and Merrick 2011; Zeth et al. 2012). Interestingly, these PII-regulated target proteins are distinct in different phylogenetic groups of organisms.

Based on the widespread occurrence of the PII superfamily member GlnK in diverse prokaryotes and its conserved genetic coupling with the ammonium transport protein AmtB, it has been hypothesized that modern trimeric PII proteins may have arisen from an ancient trimeric PII protein that originated early in the evolution of prokaryotes in conjunction with the trimeric ammonium transporters to control ammonium uptake in response to the metabolite state of the cells (Thomas et al. 2000; Sant'Anna et al. 2009). Other PII paralogues, GlnB and NifI, may have evolved subsequently from this primordial GlnK protein by gene duplication and functional diversification. These paralogues are implicated in the regulation of nitrogen-dependent gene expression, in the activity regulation of glutamine synthetase, and in the control of nitrogen fixation through a stupendous variety of mechanisms (Huergo et al. 2012; Leigh and Dodsworth 2007; Luque and Forchhammer 2007; Masepohl and Forchhammer 2007).

In cyanobacteria, PII proteins are present in all known species. While most cyanobacteria harbor one PII protein, some strains encode a second or even a third paralogue (Laichoubi et al. 2011). In contrast to many bacteria, where PII proteins (mainly of the GlnB subfamily) are involved in regulation of glutamine synthetase at various levels (Ninfa and Atkinson 2000; Leigh and Dodsworth 2007), cyanobacterial PII proteins have evolved to regulate the ornithine pathway, which leads to arginine and polyamine synthesis, and to the modulation of nitrogen-dependent transcription. In eukaryotes, PII homologues have only been identified in Chloroplastida (green algae and land plants), where they are nuclear-encoded, and in Rhodophyta, where they are coded by the plastid genome (Uhrig et al. 2009). In both these groups, PII is localized in the chloroplast (Hsieh et al. 1998; Ermilova et al. 2012) and appears to control the key step in arginine synthesis, as in cyanobacteria.

PII-like proteins: witnesses of a widely distributed signal processing mode

In the phylogenetic analysis carried out by Sant'Anna et al. (2009), a novel group of PII-like proteins, termed PII-new group (PII-NG), was identified and included in the PII superfamily based on sequence similarity. These sequences however lack the two PROSITE signatures characteristic of PII proteins (http://prosite.expasy.org). One of these PROSITE patterns (PS00496; Nitrogen regulatory protein P-II, uridylation site 46–51) is not highly conserved even among canonical bacterial PII proteins; it is located in the flexible T-loop region and is subjected to covalent modifications. The second PROSITE signature (PS00638; [ST]-x(3)-G-[DY]-G-[KR]-[IV]-[FW]-[LIVM]-x(2)-[LIVM]) is part of the nucleotide binding site (Xu et al. 1998) and is intimately involved in signal perception by PII proteins. Therefore, especially the lack of this latter site indicates that these proteins cannot fulfill canonical PII functions as previously described. Intriguingly, however, the PII-NG encoding genes are localized next to heavy metal efflux pumps and thus might be involved in the regulation of these transporters. The architectural principle of PII proteins seems to be apparently even more widely distributed. It is seen in proteins that do not share appreciable sequence conservation with canonical PII, but have structures that are highly similar to the PII core architecture, except for the loops, which seem to be characteristic for the canonical PII protein. These proteins form a widespread superfamily of trimeric proteins with potential regulatory roles and occur in almost all known organisms (Kinch and Grishin 2002; Arnesano et al. 2003; Saikatendu et al. 2006). While in most cases their function is unknown, in some cases they are known to be involved in diverse functions such as copper tolerance (Arnesano et al. 2003) or anchoring acetylcholinesterase in mammalian neurons (Perrier et al. 2000). Whether these proteins are evolutionary related to PII proteins or not remains to be clarified. A protein domain that exhibits a structure highly similar to PII has been found in the enzyme ATP-phosphoribosyltransferase (ATP-PRT) from *Mycobacterium tuberculosis* (Cho et al. 2003) and *Escherichia coli* (Lohkamp et al. 2004). ATP-PRT is the first enzyme of the histidine pathway and is allosterically inhibited by AMP and histidine. The C-terminal PII-like domain comprises the binding site for the allosteric inhibitor histidine. The structure of the PII-like domain of ATP-PRT has striking similarities with the PII in complex with the key enzyme of arginine synthesis, *N*-acetyl-L-glutamate kinase (see structure comparison in Fig. 1). Note that the orientation of the PII-like domain is upside down compared to *Synechococcus elongatus* PII bound to NAGK. This similarity is highly intriguing and indicates that the PII-like domain is possibly a relic of an ancestral PII-like protein found in ATP-PRT. At present, the PII-like domain functions as a sensory device for ATP-PRT, using the architectural principle of PII proteins as signal processing units. Regulation of amino acid biosynthesis reactions (glutamine, arginine, and histidine) thus emerges as a common basis of the function of PII and PII-like proteins.

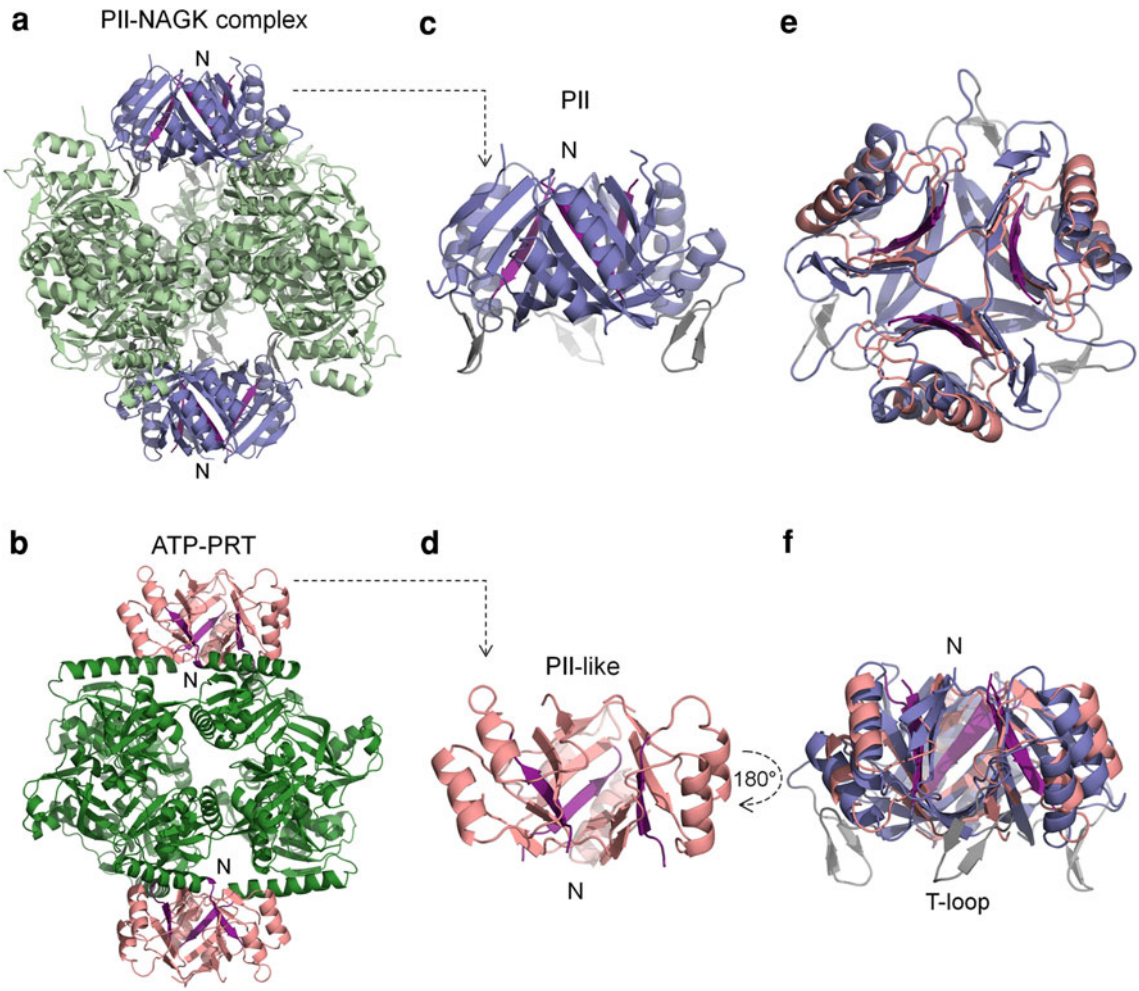

Fig. 1 Comparison of the structures of ATP-phosphoribosyltransferase and PII-NAGK complex. **a** The complex of PII (*slate*) and the hexameric *N*-acetyl-L-glutamate-kinase (*light green*) from *S. elongatus* (PDB ID: 2V5H) are shown. **b** In the structure of ATP-PRT (PDB ID: 1Q1K) from *E. coli*, the enzymatic domain is colored in *green* and the C-terminal, PII-like domain in *salmon*. **c**, **d** Enlarged views of the PII and PII-like domain are shown in the same orientation as in panels (**a**) and (**b**). The N-terminal β-strands are colored in *magenta*. **e**, **f** The structural superimposition of the PII and PII-like domain, in top and side view, is depicted. The large T-loops of PII, which are absent in the PII-like domain, are colored in *gray*. This figure was generated using PyMOL (www.pymol.org)

The PII architecture: from structure to function

PII proteins have a common architecture: a typical bacterial PII protein consists of three identical subunits of 112 amino acids, which fold into a β1–α1–β2–[T-loop]–β3–α2–β4–β5 structure. The three subunits assemble with the β-sheets in the center, forming an intertwined triangular core of three extended β2-sheets that pair with the neighboring β2′- and β2″-sheets (Fig. 1e). The C-terminal β5-sheet swaps to the β4-strand of the neighboring subunit to form part of the active site (Cheah et al. 1994; Leigh and Dodsworth 2007; Forchhammer 2008). The periphery is made up of six (three times two) α-helices and nine (three times three) loop regions, which connect the secondary structural elements, to form a barrel-like structure with three lateral clefts between the subunits. For the function of PII proteins, the three signal transducing T-loops (one per subunit) are of particular importance, since they transmit information on the ligand-binding state of PII into conformational change and mediate many (but not all) of the PII-receptor interactions. The T-loop is a large solvent-exposed and flexible loop that extends between the β2- and β3-strand and protrudes from the bottom of the intersubunit cleft. The three clefts arrange the binding sites for the effector molecules. About 20 structures of PII proteins (Huergo et al. 2012) in complex with ATP or ADP have been deposited in the PDB, including PII from cyanobacteria and *Arabidopsis*. Comparison of these structures reveals a highly conserved adenyl nucleotide binding mode (Xu et al. 1998; Zeth et al. 2012) with ATP and ADP competing for the same site. The nucleotide is bound essentially through positively charged residues and

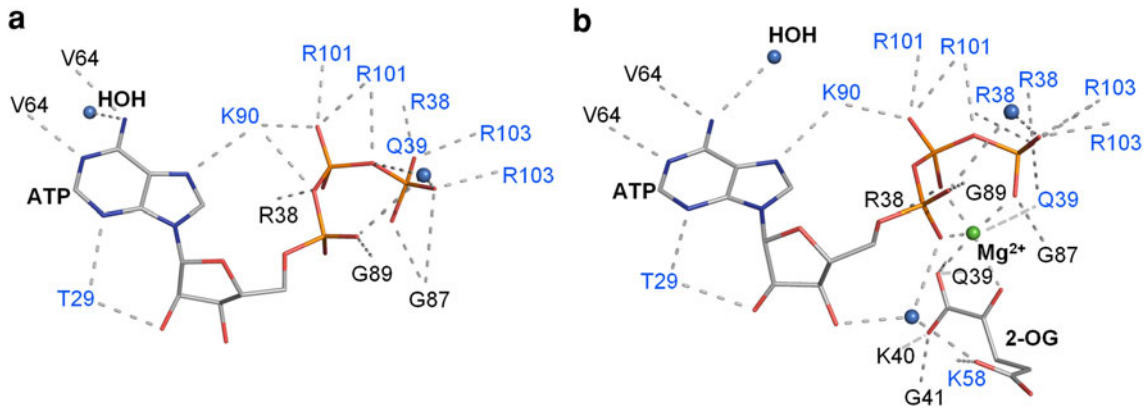

Fig. 2 Comparison of all residues and water molecules that form polar contacts with ATP alone and ATP ligated to 2-OG in PII protein from *S. elongatus* (PDB ID: 2XZW). Amino acids forming contacts with the side-chains are indicated in *blue* letter code, amino acids forming backbone interactions are indicated in *black*. **a** Polar contacts formed by ATP when bound to PII protein, **b** ATP undergoes minor changes in conformation to establish polar contacts with residues to enable the 2-OG molecule to ligate in the presence of ATP and Mg^{2+}

hydrogen bonding contacts contributed from two opposing subunits of the cleft (Fig. 2a): from one subunit, Arg38 and Gln39 residues (belonging to the basal part of the T-loop) contact the γ-phosphate of ATP, whereas Lys90 and Gly89 contact the β- and α-phosphate; from the opposite subunit, two Arg residues (101 and 103) of the C-loop contact γ- and β-phosphates, whereas Thr29 and Val64 coordinate the adenosine moiety. The mode of 2-oxoglutarate binding to PII has been clarified recently by solving the crystal structures of PII proteins with Mg-ATP and 2-OG from the archaeon *Archaeoglobus fulgidus* (Maier et al. 2011), the proteobacterium *Azospirillum brasiliense* (Truan et al. 2010), and the cyanobacterium *S. elongatus* (Fokina et al. 2010a). In the latter case, a snapshot of the sequential anticooperative binding of 2-OG to the three sites could be obtained. In all cases, a Mg^{2+} ion bound by the β- and γ-phosphate of ATP plays an essential role by coordinating the 1-carboxy- and carbonyl-oxygens of 2-OG (Fig. 2b). Furthermore, a universally conserved Lys58 residue forms a salt bridge with the 5-carboxy-group of 2-OG. The basal part of the T-loop wraps around the 2-OG molecule mainly through backbone interactions of Gln39, Lys40, and Gly41. This results in a unique conformation of the T-loop, thereby affecting the T-loop-mediated protein interactions. From the plant kingdom, only the structure of *Arabidopsis thaliana* PII has been resolved to date. Overall, its structure corresponds to the archetypical PII architecture described above. However, *A. thaliana* PII contains N- and C-terminal extensions of 13 and 15 amino acids length, respectively. These extensions are also found in all other plant PII proteins analyzed so far, including green algae, with an exception of chloroplast-encoded PII of red algae (Uhrig et al. 2009; Ermilova et al. 2012). In the *A. thaliana* structure, the N-terminal extension is organized opposite to the T-loop, whereas the C-terminal extension folds back towards the effector binding site and in the ATP-free structure, it occupies part of the ATP binding site (Mizuno et al. 2007). It was suggested that these additional sequence elements could mediate plant-specific functions. The effector molecule binding properties of *A. thaliana* PII are quite similar to those of cyanobacterial PII proteins (Forchhammer and Hedler 1997; Smith et al. 2003; Fokina et al. 2010b): ATP and ADP compete for the same binding site and 2-OG binds in synergy with ATP. However, in case of PII from *S. elongatus*, ADP does not support the binding of 2-OG, and antagonizes 2-OG binding even in the presence of ATP (Fokina et al. 2011); in contrast ADP does support the binding of 2-OG to *A. thaliana* PII. Curiously however, 2-OG lowered the affinity of ADP for *A. thaliana* PII, indicating unfavorable ligand contacts. The unique C-terminal segment, which contacts the effector molecule binding site, might cause these differences. However, ligand-binding properties of other plant PII proteins should be analyzed before generalizing the properties of *A. thaliana* to all plants.

Modification of PII proteins

The *E. coli* GlnB protein was the first PII protein to be carefully studied. As in many other proteobacteria, *E. coli* PII proteins (GlnB and GlnK) are subject to covalent UMP-modification (uridylylation) at Tyr51, located at the apex of the T-loop (Adler et al. 1975; Atkinson et al. 1994). In fact, uridylylation was long regarded as the hallmark of PII signaling (Arcondeguy et al. 2000; Ninfa and Atkinson 2000). Uridylylation is brought about by the bifunctional enzyme GlnD (Uridylyltransferase/uridylyl-removase), whose activity is regulated by glutamine, with low glutamine levels favoring PII uridylylation and high glutamine

levels favoring PII deuridylylation. By these means, the PII protein becomes a highly sensitive transmitter of the cellular glutamine status (Jiang and Ninfa 2011). However, uridylylation is not a general trait of PII signaling. The PII protein in the cyanobacterium *S. elongatus* was shown to be phosphorylated at Ser49, a position adjacent to the uridylylation site of *E. coli* PII (Forchhammer and Tandeau de Marsac 1994). In vivo, the phosphorylation status of PII depends on the carbon/nitrogen supply of the cells: nitrogen-limiting conditions favor PII phosphorylation, excess nitrogen, preferably in the form of ammonia, causes PII dephosphorylation. With *S. elongatus* cell-free extracts, phosphorylation could be achieved in the presence of millimolar concentrations of 2-OG and ATP. The PII kinase is still unknown; however, the phosphatase of PII-P, PphA, could be identified in *Synechocystis* PCC 6803 (Irmler and Forchhammer 2001) and has since then been thoroughly studied (Ruppert et al. 2002; Kloft and Forchhammer 2005; Schlicker et al. 2008; Su et al. 2011; Su and Forchhammer 2011, 2012). PphA is a Ser/Thr phosphatase of the PP2C family and the crystal structure of the PphA homologue from the thermophilic cyanobacterium *Thermosynechococcus* has been solved (Schlicker et al. 2008). In addition to the binuclear metal center, a third metal, which is occasionally observed in bacterial PP2C homologues, was shown to be an essential part of the catalytic center (Su et al. 2011). Recognition of the phosphorylated PII protein involves a flap subdomain, which shields the catalytic center of PphA (Su and Forchhammer 2011). The formation of a precisely fitted substrate-enzyme complex is a prerequisite for dephosphorylation. The conformation of the T-loop plays a critical role in this process: only when PII is non-ligated with 2-OG, PphA is able to dephosphorylate PII. As long as PII-P resides in the Mg-ATP/2-OG ligated state, it is protected from dephosphorylation (Ruppert et al. 2002; Su and Forchhammer 2011), implying that the 2-OG induced conformation of the T-loop does not fit into the catalytic crevice of PphA. Ser49 phosphorylation seems not to be generally conserved in cyanobacteria. In *Prochlorococcus marinus*, an abundant marine prochlorophyte, the evidences indicate absence of PII phosphorylation (Palinska et al. 2002), in agreement with the lack of a PphA homologue gene (Cyanobase: http://genome.kazusa.or.jp/cyanobase). In filamentous cyanobacteria, the situation is less clear. No PII phosphorylation could be detected in *Nostoc punctiforme* extracts but the *N. punctiforme* PII protein could be phosphorylated in vitro by *S. elongatus* cell extracts (Hanson et al. 1998). Mass spectroscopic analysis of the PII protein from *Anabaena* extracts revealed Tyr51 to be subjected to nitration under diazotrophic conditions while no phosphorylation at Ser49 was detected (Zhang et al. 2007). Absence of PII phosphorylation in the *Nostocales* is, however, in contrast to the presence of a PphA homologue. Mutation of the PphA homologue gene resulted in altered PII functions in *Anabaena* (Laurent et al. 2004). In plants, potential PII phosphorylation was investigated in *A. thaliana.* Its PII protein has conserved the seryl-phosphorylation site, but no phosphorylation could be identified. Recently, the PII protein from *Chlamydomonas reinhardtii* was characterized. It has a potentially phosphorylatable threonyl residue at the corresponding position, but like in *Arabidopsis*, protein phosphorylation analysis revealed only non-phosphorylated PII protein (Ermilova et al. 2012). At a first glance, it seems odd that in spite of conservation of this site, phosphorylation of PII seems not to be conserved. However, conservation of this site could be due to its pivotal role in PII-NAGK interaction.

PII-mediated regulation of the arginine pathway in cyanobacteria and plants

Yeast-two hybrid screening for PII-interaction partners in cyanobacteria and plants using genomic DNA from *S. elongatus* and *A. thaliana* identified the enzyme *N*-acetyl-L-glutamate kinase (NAGK) as a novel PII receptor (Burillo et al. 2004; Heinrich et al. 2004; Sugiyama et al. 2004). In plants and cyanobacteria, NAGK catalyzes the committed step of arginine biosynthesis and in agreement, the enzyme is feedback-inhibited by arginine. In *S. elongatus* and *A. thaliana*, PII modulates the catalytic properties of NAGK. Initial experiments (Heinrich et al. 2004; Chen et al. 2006) yielded some inconsistent results due to the use of a non-optimized assay buffer, which impaired 2-OG effects and which lacked a reducing agent, necessary for high NAGK activities (Beez et al. 2009). When tested under optimized conditions, the following common properties between the proteins from *S. elongatus* and *A. thaliana* became evident (Beez et al. 2009): (1) PII activates the overall catalytic efficiency (k_{cat}/K_m) of NAGK, for *S. elongatus* 8-fold and for *A. thaliana* 1.5-fold. In the latter case, activation is mainly an effect on k_{cat}. (2) PII relieves NAGK from arginine feed-back inhibition. It also increases the half maximal inhibitory concentration of arginine (IC_{50}) from 20 to 200 μM for *S. elongatus*, and from 1 to 6 mM for *A. thaliana* NAGK. Arginine inhibits NAGK by increasing the K_m for the substrate NAG, an effect, which is counteracted by PII. (3) 2-OG antagonizes the protection of NAGK by PII from arginine inhibition.

The most prominent differences between NAGK of *S. elongatus* and *A. thaliana* are a much higher activity (almost 100-fold) of *A. thaliana* NAGK and a much higher IC_{50} towards arginine. In *A. thaliana*, ATP accelerated complex formation; however, ADP did not negatively affect this process (Beez et al. 2009). By contrast, in

S. elongatus, ADP lowered the affinity of the PII-NAGK complex formation (Fokina et al. 2011). Therefore, in *S. elongatus*, PII activation of NAGK activity not only depends on 2-OG but also on the ATP/ADP ratio (Fokina et al. 2011), whereas in *A. thaliana*, only 2-OG antagonizes NAGK activation by PII (Beez et al. 2009). A remarkable finding was the observation that the *A. thaliana* PII protein could completely replace *S. elongatus* PII in activating its NAGK. Conversely, *S. elongatus* PII protein could at least partially activate *A. thaliana* NAGK. This functional swapping between the cyanobacterial and higher plant PII-NAGK protein pair points out that the fine-tuned interactions between PII and NAGK are extremely conserved. The high degree of similarity was also revealed by the crystal structures of PII-NAGK complexes from *S. elongatus* (Llacer et al. 2007) and *A. thaliana* (Mizuno et al. 2007). The NAGK enzyme is a trimer of dimers (each subunit approximately 32 kDa), assembling into a hexameric toroid with two identical faces. On each side of the toroid one PII trimer attaches (see Fig. 1a) mainly by contacts from the T-loop and by a second interaction surface contributed by the body of the PII protein and B-loop residues (Llacer et al. 2007, 2008; Mizuno et al. 2007). To bind NAGK, the T-loop of PII has to adopt a tightly folded conformation (Llacer et al. 2007; Fokina et al. 2010b). In the 2-OG ligated state, the T-loop is not able to adopt this fold, explaining the antagonistic effect of 2-OG on PII-NAGK complex formation. The tightly folded T-loop inserts into the interdomain crevice of NAGK, a process in which hydrogen bonding interactions of T-loop residue Ser49 (the site of phosphorylation in *S. elongatus* PII) and an ion pair network organized by Arg45 play a critical role (Llacer et al. 2008). Phosphorylation of Ser49 impairs these interactions and thus prevents NAGK binding in *S. elongatus*. The pivotal PII residues for NAGK interaction, Arg45, Ser49, and Glu85, as well as the corresponding NAGK residues for these contacts, Glu194, Arg233, Arg254, Ala257, and Gln258, comprise sequence signatures for PII-NAGK interaction unique for most oxygenic phototrophic organisms. Lack of this signature in NAGK sequences from two red algae (*Gracilaria tenuistipitata* and *Cyanidioschyzon merolae*) correlates with the apparent absence of PII proteins in these organisms (Llacer et al. 2007). Figure 3 shows an alignment of the C-terminal part of NAGK sequences from oxygenic phototrophs and from various bacteria. Besides the above-mentioned signature sequences, a Cys–Cys pair located between signature residues Arg233 and Ala257 is almost unique for the oxygenic phototrophs. These residues do not directly take part in complex formation. However, it is tempting to speculate that this cysteine-pair could be the cause for the demand of reducing conditions in vitro for the NAGK enzyme activity in cyanobacteria/plants (Beez et al. 2009). Thus, it is likely that NAGK could be redox controlled in oxygenic phototrophs, a mechanism that would allow them to switch off the energy consuming arginine synthesis during light to dark transition.

Fig. 3 Multiple sequence alignment of the C-terminal region of NAGK. Representative NAGK sequences from cyanobacteria, green plants, red algae, proteobacteria, archaea, brown algae, and diatoms were aligned using T-Coffee (Di Tommaso et al. 2011) with default settings. Residues important for interactions with PII are highlighted in *salmon*. The highly conserved adjacent cysteine residues seen in NAGK sequences of oxygenic phototrophs are shown in *yellow* with an exception of a proteobacteria *Desulfovibrio vulgaris*

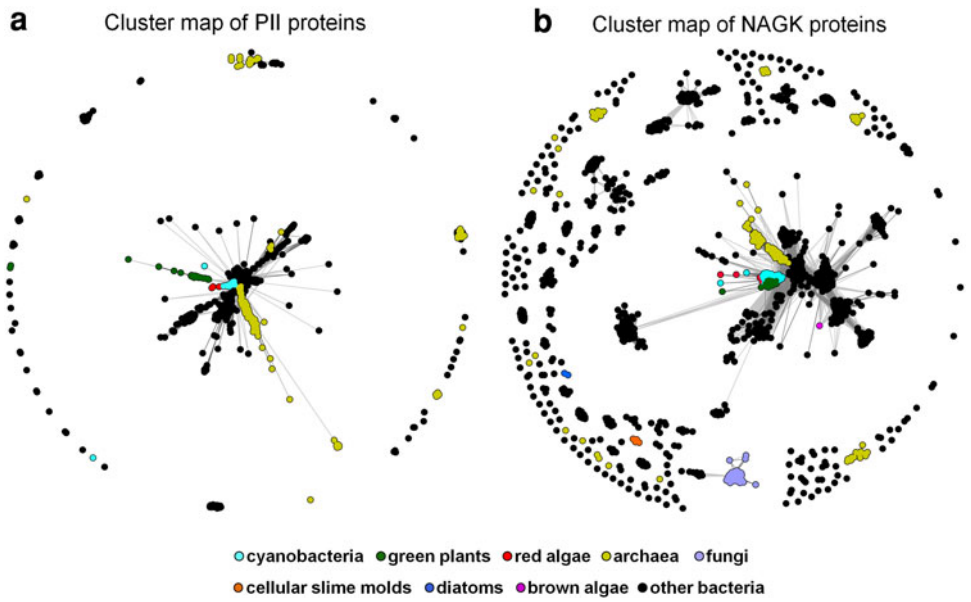

Fig. 4 Cluster map of PII and NAGK proteins. To gather PII and NAGK sequences for cluster analysis, the non-redundant protein sequence database at the NCBI, filtered to a maximum sequence identity of 90 % (nr90), was searched by seeding BLAST (Altschul et al. 1997) with the PII (gi 3885943) and NAGK (gi 332646151) sequences from *S. elongatus* PCC 6301. All sequence matches with an *E*-value of less than 1E−10 were pooled together. In the next step, the obtained PII and NAGK sequences were clustered separately in CLANS (Frickey and Lupas 2004) based on their all-against-all pairwise similarities as measured by BLAST *P*-values. In the cluster map, dots represent sequences and line coloring reflects BLAST *P*-values; the brighter a line, the lower the *P*-value. Sequences are colored as follows: cyanobacteria—*cyan*, green plants (Viridiplantae)—*green*, red algae—*red*, archaea—*yellow*, fungi—*light violet*, cellular slime molds—*orange*, diatoms—*blue*, brown algae—*magenta*, and other bacteria—*black*. **a** 1744 PII sequences obtained using BLAST were clustered at a *P*-value cut-off of 1E-33. At this stringent cut-off, while highly similar sequences remain connected to each other and form central clusters, less similar sequences drift to the periphery of the map. PII sequences from green plants and red algae make their best matches to cyanobacteria, whereas sequences from cyanobacteria are closer to other bacteria. **b** 1,583 NAGK sequences identified by BLAST are shown. Clustering was carried out at a *P*-value cut-off of 1E-83. NAGK sequences from cyanobacteria, green plants, and red algae form a tight cluster in the obtained cluster map

Conservation of PII-NAGK interaction during plastid evolution

The high degree of conservation in sequence, structure, and function between *S. elongatus* and *A. thaliana* PII-NAGK complexes implies a strong selective pressure for maintaining PII-regulated arginine biosynthesis in the evolution of plastids from an ancestral cyanobacterium. If this is indeed the case, the phylogeny of PII and NAGK sequences should be similar to each other, and should also reflect the evolution of plants. Hitherto studies have only focused on the phylogenetic analysis of the PII superfamily and they have not been conclusive on whether plant PII proteins are of cyanobacterial origin or not (Osanai and Tanaka 2007; Uhrig et al. 2009; Sant'Anna et al. 2009). Since PII proteins are short and highly similar in sequence, reliable inference of their phylogeny is difficult. Also, to our knowledge, a comprehensive phylogenetic analysis of NAGK proteins has not been performed yet. Spurred by this, we decided to revisit the analysis of PII and NAGK proteins using cluster analysis and maximum likelihood-based phylogenetic reconstruction. In cluster analysis, sequences are treated as point masses in a virtual multi-dimensional space which attract or repel each other depending on the statistical significance of their pairwise sequence similarities. Sequences find their equilibrium position in the map not only by attraction to similar sequences but also by repulsion of different ones. Unlike phylogenetic methods, which have exponential computational complexity and only allow calculation of trees with a few thousand sequences at most, the computational complexity of cluster analyses only increases approximately quadratically with the number of sequences, making calculation of maps with several thousand sequences within a reasonable time possible. In fact, cluster maps become more accurate with an increasing number of sequences as the larger number of pairwise relationships average out the random error arising from simpler pairwise similarity-based comparisons.

In the map of PII proteins (Fig. 4a), the sequences from cyanobacteria (cyan) form a tight cluster that groups together with clusters of sequences from other bacteria (black), whereas sequences from plants (green) and red algae (red) build individual clusters only connected to

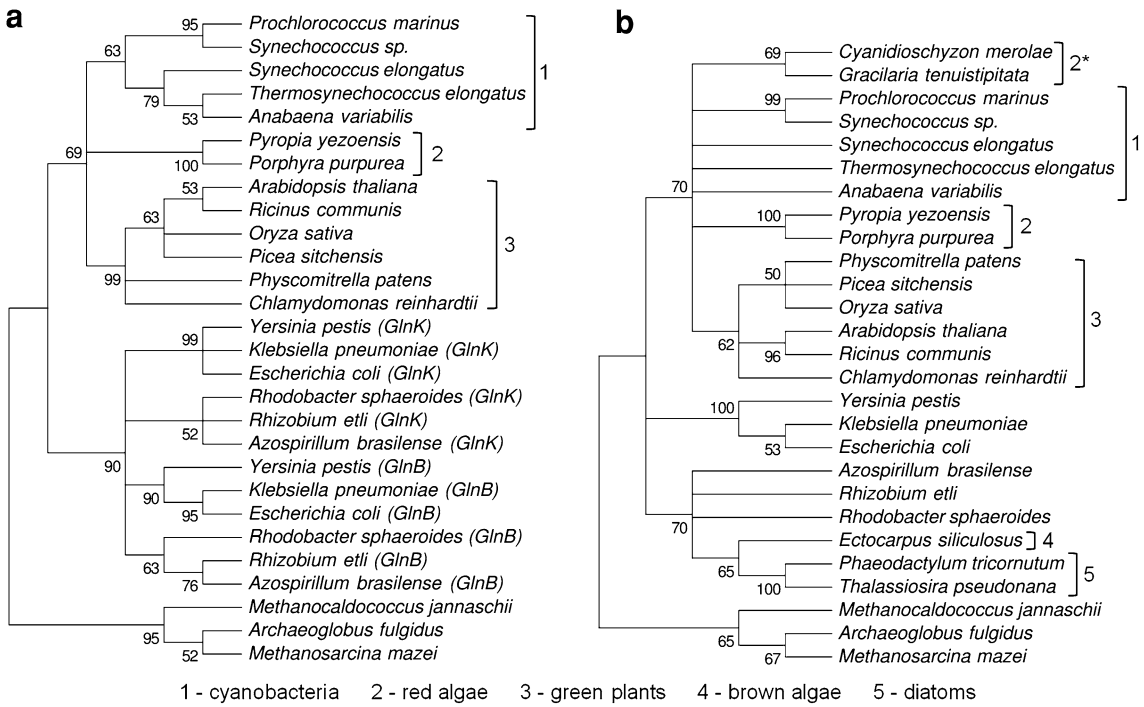

Fig. 5 Molecular phylogenetic analyses of PII and NAGK proteins. For the analysis, representative PII (GlnB), PII-like (GlnK), and NAGK proteins were selected from cyanobacteria, green plants, red algae, α-proteobacteria, γ-proteobacteria, archaea, brown algae, and diatoms. Multiple sequence alignments of PII and NAGK sequences were calculated using T-Coffee (Di Tommaso et al. 2011) with default parameters. Poorly aligned positions and highly divergent regions were removed using Gblocks (Talavera and Castresana 2007). The refined alignments were then used to infer phylogenetic trees in MEGA 5.0 (Tamura et al. 2011), employing the maximum likelihood (ML) method with the WAG model of substitutions and the discrete Gamma distribution model of evolutionary rate variation among sites. The bootstrap consensus trees inferred from 1,000 replicates are shown; branches corresponding to partitions reproduced in less than 50 % bootstrap replicates are collapsed. The phylogenetic tree of PII (**a**) contains 28 amino acid sequences and that of NAGK (**b**) consists of 27 sequences

cyanobacterial sequences (cyan). This suggests that PII proteins of plants and red algae are of cyanobacterial origin, which is in accordance with previous proposals (Osanai and Tanaka 2007; Sant'Anna et al. 2009; Uhrig et al. 2009). While the cyanobacterial cluster is in close proximity to the other bacterial clusters, the plant cluster is further removed from the cyanobacterial cluster. This indicates that PII proteins from cyanobacteria had limited freedom to evolve, but PIIs from plants were altered to adapt to new niches after being acquired from an ancient cyanobacterium. By contrast, in the NAGK map (Fig. 4b), the sequences from cyanobacteria, red algae, and Chloroplastida cluster together indicating an endosymbiotic origin of these proteins. NAGK from the two sequenced diatoms (blue), *Thalassiosira pseudonana* and *Phaeodactylum tricornutum*, cluster together with NAGK from alphaproteobacteria. It is possible that in the evolution of heterokonts, which include diatoms and brown algae, an argB gene (encoding NAGK) was acquired by horizontal gene transfer from an alphaproteobacterium while the original cyanobacterial/plastidal NAGK and PII genes were lost. To exclude that this grouping was an artifact of the cluster analysis, we inferred phylogeny of PII (Fig. 5a) and NAGK (Fig. 5b) sequences using maximum likelihood-based reconstruction. The resulting trees support the phylogenetic grouping exhibited by the cluster maps. Overall, the evolutionary trees of PII and NAGK sequences are in perfect agreement with the assumed evolution of cyanobacteria and of the plant kingdom (Deschamps and Moreira 2009). In support of co-evolution between PII and NAGK, the phylogenetic tree of NAGKs matches the tree of PII sequences, except for the two red algae *Gracilaria tenuistipitata* and *Cyanidioschyzon merolae* (denoted as 2* in Fig. 5b), which have lost PII during evolution. Their NAGKs are distantly related to the NAGKs from the other red algae. In these organisms, the loss of PII has released NAGK from the constraint to interact with PII and therefore, their NAGK sequences gained more freedom to evolve. Together, this analysis shows that control of arginine synthesis through PII-dependent signaling was kept under selective pressure in the evolution of plastids of Chloroplastida and most Rhodophyta.

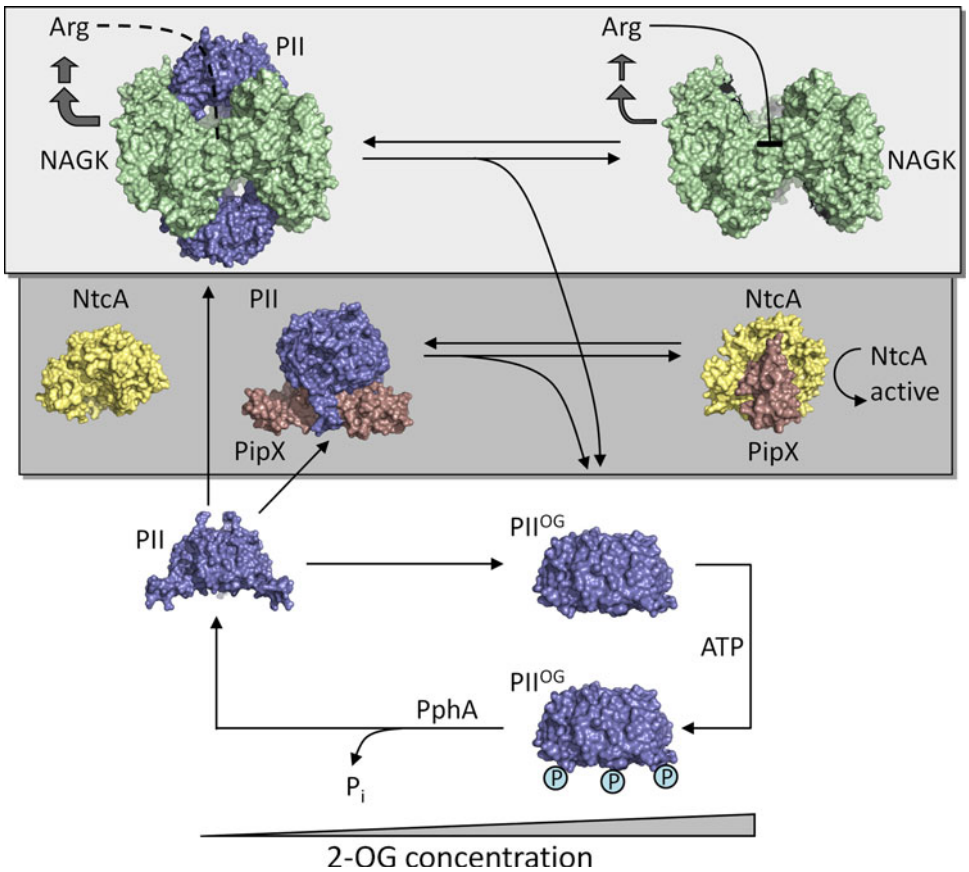

Fig. 6 Schematic representation of the 2-oxoglutarate (2-OG) dependent cycle of PII interactions in cyanobacteria under ATP-replete conditions. Under low 2-OG conditions (*left*), PII (*slate*) forms a complex with NAGK (*light green*), the key enzyme of the arginine pathway (*top*, *light gray* background), or with PipX (*brown*), the co-activator of transcription factor NtcA (*yellow*) (*middle part, dark gray* background). In complex with PII, NAGK is highly active and protected from tight arginine feedback-inhibition. The NtcA-factor is unable to bind PipX. At increasing 2-OG levels, the PII-complexes dissociate and release 2-OG-ligated PII, which becomes phosphorylated by PII kinase activity. Free NAGK has diminished activity and is tightly feedback-inhibited by arginine. PipX associates with NtcA and activates NtcA-dependent gene expression. When the 2-OG levels drop again, phosphorylated PII has to be dephosphorylated by PII phosphatase PphA before being able to form complexes with NAGK and PipX again. In the chloroplasts of plants, PII-NAGK interaction is conserved, whereas no homologues of PipX, NtcA, and PphA are found. Instead, PII interacts with ACCase (see text for details). PDB ID of structures: 2V5H (PII-NAGK complex), 2XGX (NtcA), 2XG8 (PII-PipX), 2XKO (NtcA-PipX), 1QY7 (free PII), and 2XUL (PII^{2OG}). This figure was generated using PyMOL

Further functions of PII signaling in oxygenic phototrophs

The complete network of interactions of PII with its binding partners in cyanobacteria (summarized in Fig. 6) has been reviewed previously (Osanai and Tanaka 2007; Forchhammer 2008, 2010). In brief, two major targets of PII regulation have been identified at the molecular level, the transcriptional co-activator PipX and NAGK. PipX, a small protein of approximately 90 amino acids, was shown to be required for full expression of NtcA-activated genes (Espinosa et al. 2006, 2007; Laichoubi et al. 2012). Binding of PipX to NtcA is favored by high 2-OG levels in vitro, whereas 2-OG in concert with Mg-ATP prevents binding of PipX to PII. The structures of PipX-NtcA and PipX-PII complexes have been solved (Llacer et al. 2010; Zhao et al. 2010). It is thought that PII binding of PipX tunes down NtcA-dependent gene expression (Espinosa et al. 2007). PipX homologues have been identified in all cyanobacterial genomes, but they are absent in eukaryotes, implying that modulation of gene expression by PII was lost during the endosymbiotic transition of the cyanobacterial ancestor into a chloroplast. A few cyanobacteria possess multiple PII paralogues, and in these cases, the organisms also contain multiple PipX paralogues. In the case of the marine cyanobacterium *Synechococcus* WH5701, it could be shown that only one of the two PII paralogues activates NAGK and binds to PipX protein; the function of the other PII paralogue is unknown (Laichoubi et al. 2011). A further target of PII was identified as PamA in the cyanobacterium *Synechocystis* PCC 6803. PamA is a potential transmembrane channel protein of the MscS family with unknown function.

Mutation of PamA affects the expression of a subset of nitrogen-regulated genes, among them is a sigma-factor required for the expression of sugar-catabolic genes (Osanai et al. 2005). Furthermore, circumstantial evidence suggests that PII is also involved in the control of nitrate/nitrite uptake in *S. elongatus* (Forchhammer 2010).

The above-mentioned PII receptors are absent in plants; however, a new PII receptor, the chloroplast acetyl-CoA carboxylase (ACCase), a key enzyme in fatty acid synthesis in plastids, was identified by pull-down experiments with *A. thaliana* extracts (Feria Bourrellier et al. 2010). ACCase activity was repressed by PII, but this repression was antagonized by 2-OG and oxaloacetate and to a lesser extent by pyruvate. So far this interaction has not been characterized in great detail and also it needs to be confirmed if this interaction can be generalized for all plants. Nevertheless, the regulation of ACCase by PII represents an intriguing link to carbon storage metabolism. Physiological analyses in *A. thaliana* support the function of PII in storage metabolism. The PII gene is upregulated in early seed maturation by the transcription factor WRINKLED1 (Baud et al. 2010), and in seeds of PII deficient mutants, a transient increase of fatty acid production and an alteration in fatty acid composition were observed. From these results, a regulatory role of PII in the fine-tuning of fatty acid biosynthesis and partitioning in seeds had been inferred (Baud et al. 2010). Furthermore, in *A. thaliana* PII mutants, nitrite uptake in chloroplast is enhanced (Ferrario-Mery et al. 2008), resembling the regulatory defect of nitrite/nitrate uptake in cyanobacterial PII mutants (Kloft and Forchhammer 2005). Altogether, the data indicate that during the evolution of plastids, PII lost its primary function of coordinating gene expression through interactions with PipX, but preserved its role in nitrogen (arginine) storage metabolism, and eventually took over fine-tuned regulation of carbon (fatty acid) storage metabolism. Currently, PII is known to play a role in early seed maturation, but it is unclear if it also has roles in other developmental stages of plants. Studies of phylogenetically more ancient plants and of unicellular green algae will be necessary to unravel the roles of PII in the metabolic pathways of Chloroplastida.

Acknowledgments We thank Andrei Lupas for helpful discussions. This study was supported by DFG grant Fo195/9 and by institutional funds from the Max Planck Society.

Conflict of interest The authors declare that they have no conflict of interest.

References

Adler SP, Purich D, Stadtman ER (1975) Cascade control of *Escherichia coli* glutamine synthetase. Properties of the PII regulatory protein and the uridylyltransferase-uridylyl-removing enzyme. J Biol Chem 250:6264–6272

Altschul SF, Madden TL, Schaffer AA, Zhang J, Zhang Z, Miller W, Lipman DJ (1997) Gapped BLAST and PSI-BLAST: a new generation of protein database search programs. Nucleic Acids Res 25:3389–3402

Arcondeguy T, Lawson D, Merrick M (2000) Two residues in the T-loop of GlnK determine NifL-dependent nitrogen control of nif gene expression. J Biol Chem 275:38452–38456

Arcondéguy T, Jack R, Merrick M (2001) P(II) signal transduction proteins, pivotal players in microbial nitrogen control. Microbiol Mol Biol Rev 65:80–105

Arnesano F, Banci L, Benvenuti M, Bertini I, Calderone V, Mangani S, Viezzoli MS (2003) The evolutionarily conserved trimeric structure of CutA1 proteins suggests a role in signal transduction. J Biol Chem 278:45999–46006

Atkinson MR, Kamberov ES, Weiss RL, Ninfa AJ (1994) Reversible uridylylation of the *Escherichia coli* PII signal transduction protein regulates its ability to stimulate the dephosphorylation of the transcription factor nitrogen regulator I (NRI or NtrC). J Biol Chem 269:28288–28293

Baud S, Feria Bourrellier AB, Azzopardi M, Berger A, Dechorgnat J, Daniel-Vedele F, Lepiniec L, Miquel M, Rochat C, Hodges M, Ferrario-Mery S (2010) PII is induced by WRINKLED1 and fine-tunes fatty acid composition in seeds of *Arabidopsis thaliana*. Plant J 64:291–303

Beez S, Fokina O, Herrmann C, Forchhammer K (2009) *N*-acetyl-L-glutamate kinase (NAGK) from oxygenic phototrophs: P(II) signal transduction across domains of life reveals novel insights in NAGK control. J Mol Biol 389:748–758

Burillo S, Luque I, Fuentes I, Contreras A (2004) Interactions between the nitrogen signal transduction protein PII and *N*-acetyl glutamate kinase in organisms that perform oxygenic photosynthesis. J Bacteriol 186:3346–3354

Cheah E, Carr PD, Suffolk PM, Vasudevan SG, Dixon NE, Ollis DL (1994) Structure of the *Escherichia coli* signal transducing protein PII. Structure 2:981–990

Chen YM, Ferrar TS, Lohmeier-Vogel EM, Morrice N, Mizuno Y, Berenger B, Ng KK, Muench DG, Moorhead GB (2006) The PII signal transduction protein of *Arabidopsis thaliana* forms an arginine-regulated complex with plastid *N*-acetyl glutamate kinase. J Biol Chem 281:5726–5733

Cho Y, Sharma V, Sacchettini JC (2003) Crystal structure of ATP phosphoribosyltransferase from *Mycobacterium tuberculosis*. J Biol Chem 278:8333–8339

Deschamps P, Moreira D (2009) Signal conflicts in the phylogeny of the primary photosynthetic eukaryotes. Mol Biol Evol 26:2745–2753

Di Tommaso P, Moretti S, Xenarios I, Orobitg M, Montanyola A, Chang JM, Taly JF, Notredame C (2011) T-Coffee: a web server for the multiple sequence alignment of protein and RNA sequences using structural information and homology extension. Nucleic Acids Res 39 (Web Server issue):W13–17

Ermilova E, Lapina T, Zalutskaya Z, Minaeva E, Fokina O, Forchhammer K (2012) PII Signal Transduction Protein in *Chlamydomonas reinhardtii*: localization and Expression Pattern. Protist. doi:10.1016/j.protis.2012.04.002

Espinosa J, Forchhammer K, Burillo S, Contreras A (2006) Interaction network in cyanobacterial nitrogen regulation: PipX, a protein that interacts in a 2-oxoglutarate dependent manner with PII and NtcA. Mol Microbiol 61:457–469

Espinosa J, Forchhammer K, Contreras A (2007) Role of the *Synechococcus* PCC 7942 nitrogen regulator protein PipX in NtcA-controlled processes. Microbiology 153:711–718

Feria Bourrellier AB, Valot B, Guillot A, Ambard-Bretteville F, Vidal J, Hodges M (2010) Chloroplast acetyl-CoA carboxylase activity

is 2-oxoglutarate-regulated by interaction of PII with the biotin carboxyl carrier subunit. Proc Natl Acad Sci USA 107:502–507
Ferrario-Mery S, Meyer C, Hodges M (2008) Chloroplast nitrite uptake is enhanced in *Arabidopsis* PII mutants. FEBS Lett 582:1061–1066
Fokina O, Chellamuthu VR, Forchhammer K, Zeth K (2010a) Mechanism of 2-oxoglutarate signaling by the *Synechococcus elongatus* PII signal transduction protein. Proc Natl Acad Sci USA 107:19760–19765
Fokina O, Chellamuthu VR, Zeth K, Forchhammer K (2010b) A novel signal transduction protein P(II) variant from *Synechococcus elongatus* PCC 7942 indicates a two-step process for NAGK-P(II) complex formation. J Mol Biol 399:410–421
Fokina O, Herrmann C, Forchhammer K (2011) Signal-transduction protein P(II) from *Synechococcus elongatus* PCC 7942 senses low adenylate energy charge in vitro. Biochem J 440:147–156
Forchhammer K (2008) P(II) signal transducers: novel functional and structural insights. Trends Microbiol 16:65–72
Forchhammer K (2010) The network of P(II) signalling protein interactions in unicellular cyanobacteria. Adv Exp Med Biol 675:71–90
Forchhammer K, Hedler A (1997) Phosphoprotein PII from cyanobacteria–analysis of functional conservation with the PII signal-transduction protein from *Escherichia coli*. Eur J Biochem 244:869–875
Forchhammer K, Tandeau de Marsac N (1994) The PII protein in the cyanobacterium *Synechococcus sp.* strain PCC 7942 is modified by serine phosphorylation and signals the cellular N-status. J Bacteriol 176:84–91
Frickey T, Lupas A (2004) CLANS: a Java application for visualizing protein families based on pairwise similarity. Bioinformatics 20:3702–3704
Hanson TE, Forchhammer K, Tandeau de Marsac N, Meeks JC (1998) Characterization of the glnB gene product of *Nostoc punctiforme* strain ATCC 29133: glnB or the PII protein may be essential. Microbiology 144:1537–1547
Heinrich A, Maheswaran M, Ruppert U, Forchhammer K (2004) The *Synechococcus elongatus* P signal transduction protein controls arginine synthesis by complex formation with *N*-acetyl-L-glutamate kinase. Mol Microbiol 52:1303–1314
Hsieh MH, Lam HM, van de Loo FJ, Coruzzi G (1998) A PII-like protein in *Arabidopsis*: putative role in nitrogen sensing. Proc Natl Acad Sci USA 95:13965–13970
Huergo LF, Chandra G, Merrick M (2012) PII signal transduction proteins: nitrogen regulation and beyond. FEMS Microbiol Rev. doi:10.1111/j.1574-6976.2012.00351.x
Irmler A, Forchhammer K (2001) A PP2C-type phosphatase dephosphorylates the PII signaling protein in the cyanobacterium *Synechocystis* PCC 6803. Proc Natl Acad Sci USA 98:12978–12983
Jiang P, Ninfa AJ (2011) A source of ultrasensitivity in the glutamine response of the bicyclic cascade system controlling glutamine synthetase adenylylation state and activity in *Escherichia coli*. Biochemistry 50:10929–10940
Kinch LN, Grishin NV (2002) Expanding the nitrogen regulatory protein superfamily: homology detection at below random sequence identity. Proteins 48:75–84
Kloft N, Forchhammer K (2005) Signal transduction protein PII phosphatase PphA is required for light-dependent control of nitrate utilization in *Synechocystis* sp. strain PCC 6803. J Bacteriol 187:6683–6690
Laichoubi KB, Beez S, Espinosa J, Forchhammer K, Contreras A (2011) The nitrogen interaction network in *Synechococcus* WH5701, a cyanobacterium with two PipX and two P(II)-like proteins. Microbiology 157:1220–1228
Laichoubi KB, Espinosa J, Castells MA, Contreras A (2012) Mutational analysis of the cyanobacterial nitrogen regulator PipX. PLoS ONE 7(4):e35845. doi:10.1371/journal.pone.0035845
Laurent S, Forchhammer K, Gonzalez L, Heulin T, Zhang CC, Bedu S (2004) Cell-type specific modification of PII is involved in the regulation of nitrogen metabolism in the cyanobacterium *Anabaena* PCC 7120. FEBS Lett 576:261–265
Leigh JA, Dodsworth JA (2007) Nitrogen regulation in bacteria and archaea. Annu Rev Microbiol 61:349–377
Litz C, Helfmann S, Gerhardt S, Andrade SL (2011) Structure of GlnK1, a signalling protein from *Archaeoglobus fulgidus*. Acta Crystallogr Sect F Struct Biol Cryst Commun 67:178–181
Llacer JL, Contreras A, Forchhammer K, Marco-Marin C, Gil-Ortiz F, Maldonado R, Fita I, Rubio V (2007) The crystal structure of the complex of PII and acetylglutamate kinase reveals how PII controls the storage of nitrogen as arginine. Proc Natl Acad Sci USA 104:17644–17649
Llacer JL, Fita I, Rubio V (2008) Arginine and nitrogen storage. Curr Opin Struct Biol 18:673–681
Llacer JL, Espinosa J, Castells MA, Contreras A, Forchhammer K, Rubio V (2010) Structural basis for the regulation of NtcA-dependent transcription by proteins PipX and PII. Proc Natl Acad Sci USA 107:15397–15402
Lohkamp B, McDermott G, Campbell SA, Coggins JR, Lapthorn AJ (2004) The structure of *Escherichia coli* ATP-phosphoribosyltransferase: identification of substrate binding sites and mode of AMP inhibition. J Mol Biol 336:131–144
Luque I, Forchhammer K (2007) Nitrogen assimilation and C/N balance sensing. In: Herrero A, Flores E (eds) The Cyanobacteria: Molecular Biology. Genomics and Evolution Caister Academic Press, Norfolk, pp 335–382
Maier S, Schleberger P, Lu W, Wacker T, Pfluger T, Litz C, Andrade SL (2011) Mechanism of disruption of the Amt-GlnK complex by P(II)-mediated sensing of 2-oxoglutarate. PLoS ONE 6:e26327. doi:10.1371/journal.pone.0026327
Masepohl B, Forchhammer K (2007) Regulatory cascades to express nitrogenase. In: Bothe H, Ferguson S, Newton WE (eds) Molecular biology, biochemistry and applied aspects of the nitrogen cycle. Elsevier B.V, Amsterdam, pp 131–145
Mizuno YB, Moorhead GB, Ng KK (2007) Crystal structure of *Arabidopsis* PII reveals novel structural elements unique to plants. Biochemistry 46:1477–1483
Ninfa AJ, Atkinson MR (2000) PII signal transduction proteins. Trends Microbiol 8:172–179
Osanai T, Tanaka K (2007) Keeping in touch with PII: PII-interacting proteins in unicellular cyanobacteria. Plant Cell Physiol 48:908–914
Osanai T, Kanesaki Y, Nakano T, Takahashi H, Asayama M, Shirai M, Kanehisa M, Suzuki I, Murata N, Tanaka K (2005) Positive regulation of sugar catabolic pathways in the cyanobacterium *Synechocystis sp.* PCC 6803 by the group 2 sigma factor sigE. J Biol Chem 280:30653–30659
Palinska KA, Laloui W, Bedu S, Loiseaux-de Goer S, Castets AM, Rippka R, Tandeau de Marsac N (2002) The signal transducer P(II) and bicarbonate acquisition in *Prochlorococcus marinus* PCC 9511, a marine cyanobacterium naturally deficient in nitrate and nitrite assimilation. Microbiology 148:2405–2412
Perrier AL, Cousin X, Boschetti N, Haas R, Chatel JM, Bon S, Roberts WL, Pickett SR, Massoulie J, Rosenberry TL, Krejci E (2000) Two distinct proteins are associated with tetrameric acetylcholinesterase on the cell surface. J Biol Chem 275:34260–34265
Radchenko M, Merrick M (2011) The role of effector molecules in signal transduction by PII proteins. Biochem Soc Trans 39:189–194

Ruppert U, Irmler A, Kloft N, Forchhammer K (2002) The novel protein phosphatase PphA from *Synechocystis* PCC 6803 controls dephosphorylation of the signalling protein PII. Mol Microbiol 44:855–864

Saikatendu KS, Zhang X, Kinch L, Leybourne M, Grishin NV, Zhang H (2006) Structure of a conserved hypothetical protein SA1388 from *S. aureus* reveals a capped hexameric toroid with two PII domain lids and a dinuclear metal center. BMC Struct Biol 6:1. doi:10.1186/1472-6807-6-27

Sant'Anna FH, Trentini DB, de Souto Weber S, Cecagno R, da Silva SC, Schrank IS (2009) The PII superfamily revised: a novel group and evolutionary insights. J Mol Evol 68:322–336

Schlicker C, Fokina O, Kloft N, Grune T, Becker S, Sheldrick GM, Forchhammer K (2008) Structural analysis of the PP2C phosphatase tPphA from *Thermosynechococcus elongatus*: a flexible flap subdomain controls access to the catalytic site. J Mol Biol 376:570–581

Smith CS, Weljie AM, Moorhead GB (2003) Molecular properties of the putative nitrogen sensor PII from *Arabidopsis thaliana*. Plant J 33:353–360

Su J, Forchhammer K (2011) Determinants for substrate specificity of the bacterial PP2C protein phosphatase tPphA from *Thermosynechococcus elongatus*. FEBS J. doi:10.1111/j.1742-4658.2011.08466.x

Su J, Forchhammer K (2012) The Role of Arg13 in Protein Phosphatase M tPphA from *Thermosynechococcus elongatus*. Enzyme Res 2012:272706. doi:10.1155/2012/272706

Su J, Schlicker C, Forchhammer K (2011) A third metal is required for catalytic activity of the signal-transducing protein phosphatase M tPphA. J Biol Chem 286:13481–13488

Sugiyama K, Hayakawa T, Kudo T, Ito T, Yamaya T (2004) Interaction of *N*-acetylglutamate kinase with a PII-like protein in rice. Plant Cell Physiol 45:1768–1778

Talavera G, Castresana J (2007) Improvement of phylogenies after removing divergent and ambiguously aligned blocks from protein sequence alignments. Syst Biol 56:564–577

Tamura K, Peterson D, Peterson N, Stecher G, Nei M, Kumar S (2011) MEGA5: molecular evolutionary genetics analysis using maximum likelihood, evolutionary distance, and maximum parsimony methods. Mol Biol Evol 28:2731–2739

Thomas G, Coutts G, Merrick M (2000) The *gln*K*amt*B operon. A conserved gene pair in prokaryotes. Trends Genet 16:11–14

Truan D, Huergo LF, Chubatsu LS, Merrick M, Li XD, Winkler FK (2010) A new P(II) protein structure identifies the 2-oxoglutarate binding site. J Mol Biol 400:531–539

Uhrig RG, Ng KK, Moorhead GB (2009) PII in higher plants: a modern role for an ancient protein. Trends Plant Sci 14:505–511

Xu Y, Cheah E, Carr PD, van Heeswijk WC, Westerhoff HV, Vasudevan SG, Ollis DL (1998) GlnK, a PII-homologue: structure reveals ATP binding site and indicates how the T-loops may be involved in molecular recognition. J Mol Biol 282:149–165

Zeth K, Fokina O, Forchhammer K (2012) An engineered PII protein variant that senses a novel ligand: atomic resolution structure of the complex with citrate. Acta Cryst D68:901–908

Zhang Y, Pu H, Wang Q, Cheng S, Zhao W, Zhao J (2007) PII is important in regulation of nitrogen metabolism but not required for heterocyst formation in the Cyanobacterium *Anabaena sp*. PCC 7120. J Biol Chem 282:33641–33648

Zhao MX, Jiang YL, Xu BY, Chen Y, Zhang CC, Zhou CZ (2010) Crystal structure of the cyanobacterial signal transduction protein PII in complex with PipX. J Mol Biol 402:552–559

9. Contribution of the candidate

Publication 1: A novel signal transduction protein P(II) variant from *Synechococcus elongatus* PCC 7942 indicates a two-step process for NAGK-P(II) complex formation.

The crystallization of PII I86N variant (PDB: 2XBP, 1.20 Å) from *Synechococcus elongatus* PCC 7942 in the presence of ligands ATP and Mg^{2+} was done by me. The protein was set up for sitting drop crystallization in the presence of ATP-Mg or ADP-Mg. I had screened, selected and frozen the crystals with various cryoprotectants. The data was collected at atomic resolution from the Swiss Light Source, Villigen, Switzerland. I had refined and solved the structure with the guidance of Prof. Kornelius Zeth. I contributed for the structural data analysis and interpretation. I also contributed in the writing and revising of the manuscript.

Publication 2: Mechanism of 2-oxoglutarate signaling by the *Synechococcus elongatus* PII signal transduction protein.

PII proteins in the presence of ATP-Mg and also with ATP-Mg plus 2-OG were prepared by me for crystallization trials. The drops were set up in the presence of low (PDB: 2XZW) and excess (PDB: 2XUL) amounts of 2-OG. The crystals were screened and frozen with glycerol as the cryoprotectant. The diffraction quality crystals were subjected to X-ray diffraction at the Swiss Light Source, Villigen, Switzerland. The data was collected and the structure was solved by me with the guidance of Prof. Kornelius Zeth. I was also involved in the structure analysis, writing and revision of manuscript.

Publication 3: From cyanobacteria to plants: conservation of PII functions during plastid evolution.

I contributed to writing, creating figures and manuscript preparation. I was involved in the PII-NAGK coevolution analysis from sequence to structural level through bioinformatics approach by employing phylogenetic tree construction and CLANS analysis. The paper was submitted by me and I took part in the revision of manuscript.

10. Additional Research

10.1 Cloning, expression and purification of proteins

Cloning of the *Cr* PII gene was performed as described in Ermilova *et al*, 2013. A C-terminal truncated *Cr* PII was designed to mimic the length of a bacterial PII protein by deletion of the terminal 12 aminoacids. This truncated version of *Cr* PII (Delta C *Cr* PII) was obtained by amplification of the *Cr* PII gene with the primer pair 5'-ATTGGTCTCAAATGGAACTGGAAAG-3' and 5'-GATGGTCTCAGCGCTCATTTTTTC CGCTTCCAGGCCGGTTTC-3'. In order to obtain the native *Cr* PII protein without any tag, a construct was designed for insertion into the pASK-IBA15 vector which encodes a enterokinase cleavage site between the N-terminal Strep-tag and the gene of interest. The *Cr* PII synthetic gene was amplified with the forward primer 5'-GCCACCCGCAGTTCGAAAAAGGCGCCGACGACGACGACAAGATGGAACTGGAAA GCATTCAGTGCG-3' and the reverse primer 5'-CCATTTTTCACTTCACAGGTCA-AGCTTAGTTAGATATCAGAGACCTTACTTTTTTTTCTTCATCATATCTTCC-3'. The amplified fragment was cloned into the Strep-tag fusion vector pASK-IBA15 using the Gibson cloning strategy (Gibson *et al*, 2009). Overexpression of the recombinant PII proteins was performed in *E. coli* RB9060 strain (Bueno *et al*, 1985), which is GlnB deficient in order to prevent any formation of heterotrimers. The protein was affinity purified on a Strep-Tactin column according to Heinrich *et al*, 2004. The N-terminal Strep-tag *Cr* PII protein was subjected to enterokinase treatment to derive the native protein after an additional affinity purification step.

The *Cr* NAGK synthetic gene with an optimized codon usage for the *E. coli* expression was synthesized by Geneart/Life Technologies, Germany. The DNA sequence was derived from the aminoacid sequence of the potential chloroplast-localized *Cr* NAGK; starting with the aminoacid 44 (MAAAT) based on the prediction from the program ChloroP (Emanuelsson *et al*, 1999) and homology deduction with the *A. thaliana* NAGK. The synthetic gene in pMA-T vector was digested with NdeI and EcoRI and cloned into the pET15b vector. Overexpression of the recombinant *Cr* NAGK protein was performed in *E. coli* BL21(DE3) and the protein with a N-terminal fused His_6-tag was affinity purified on a NiNTA column according to Maheswaran *et al*, 2004.

10.2 Enzymatic assay for NAGK activity

A coupled enzyme assay system was used to determine the NAGK activity in which the production of ADP was coupled to the oxidation of NADH by pyruvate kinase and lactate dehydrogenase as described previously (Jiang and Ninfa, 1999; Beez *et al*, 2009; Fokina *et al*, 2010a, b). The reaction mix consisted of 50 mM imidazole pH 7.5, 50 mM KCl, 20 mM $MgCl_2$, 0.4 mM NADH, 1 mM phosphoenolpyruvate, 10 mM ATP, 0.5 mM DTT, 11 U lactate dehydrogenase, 15 U pyruvate kinase and 50 mM NAG. When necessary, 2.4 µg of PII protein was added to the reaction mix and the reaction was started by the addition of 3 µg NAGK, unless indicated otherwise. The reaction was recorded over a period of 10 min with a SPECORD 200 photometer (Analytik Jena) at 340 nm. Phosphorylation of one molecule of NAG is proportional to the oxidation of one molecule of NADH, with an indication of linear decrease of absorbance at 340 nm. One unit of NAGK catalyses the conversion of 1 µmol of NAG min^{-1}, calculated with the molar absorption coefficient of NADH [ε_{340} = 6178 L mol^{-1} cm^{-1}]. Means of triplicate experimental determinations are shown with a Standard Deviation of less than 5%. The enzymatic parameters K_m, k_{cat}, Hill slope and IC_{50} were calculated from the velocity slopes using the GraphPad Prism-6.01 software program (GraphPad Software, USA).

10.2.1 Effect of NAG on *Cr* NAGK activity

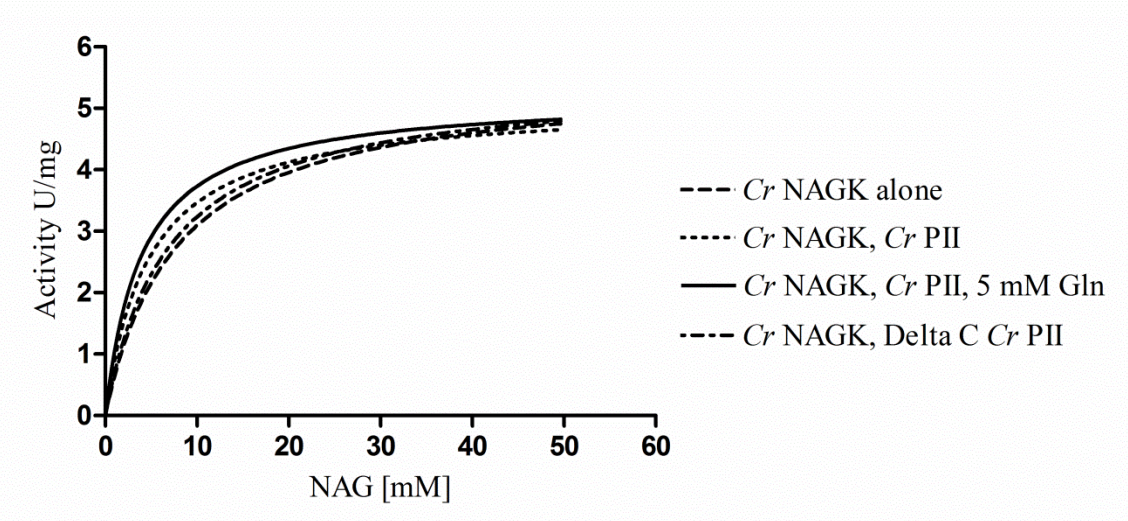

	V_{max} [mM s^{-1}]	K_m [mM]	k_{cat} [s^{-1}]
Cr NAGK alone	5.49	7.77±0.85	56.76
Cr NAGK, *Cr* PII	5.09	4.71±0.87	52.62
Cr NAGK, *Cr* PII, 5 mM Gln	5.20	3.94±0.44	53.76
Cr NAGK, Delta C *Cr* PII	5.45	6.87±1.17	56.36

Figure 7. Effect of increasing NAG on *Cr* NAGK activity.

For determination of kinetic parameters (V_{max}, K_m and k_{cat}), the coupled enzyme assay for *Cr* NAGK was performed by increasing the substrate (NAG) concentration from 2.5 to 50 mM (Fig. 7). Addition of *Cr* PII to *Cr* NAGK enhances the catalytic efficiency (lowers K_m for NAG); nevertheless, the activity of *Cr* NAGK is further enhanced in the presence of *Cr* PII and 5 mM Gln. The Michaelis-Menten constant (K_m) of *Cr* NAGK decreases from 7.77 mM to 3.94 mM with addition of *Cr* PII and glutamine implying the favourable direction of reaction. The enzymatic studies for *A. thaliana* revealed moderate activation of NAGK upon binding PII; however, the *S. elongatus* PII highly activated (increase in V_{max} and decrease in K_m values) its NAGK protein (Maheswaran *et al*, 2004; Chen *et al*, 2006). The C-terminal truncation of *Cr* PII (Delta C *Cr* PII) resulted in no further increase of *Cr* NAGK activity even in the presence of glutamine. Three individual measurements were performed and the data points were fitted to a hyperbolic curve.

10.2.2 Effect of arginine on *Cr* NAGK activity

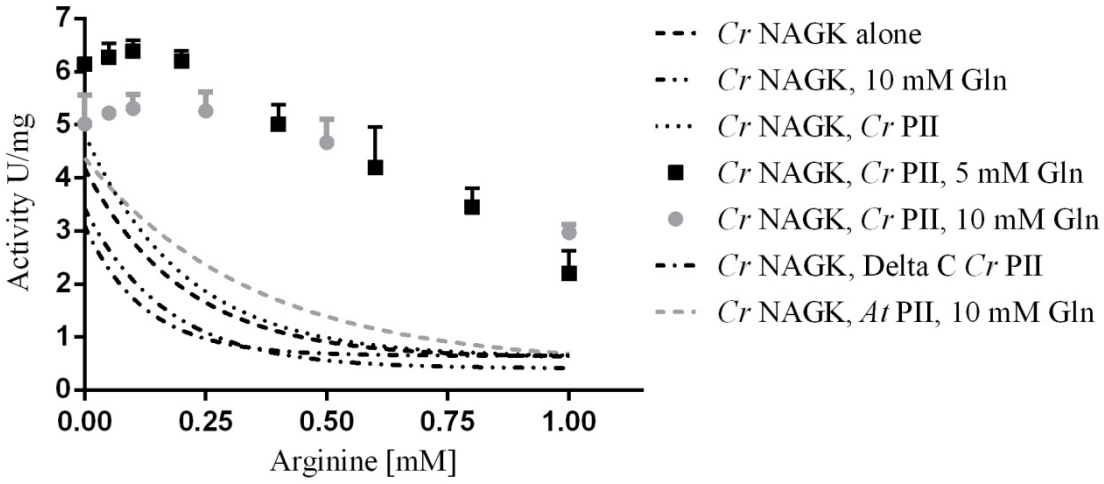

	Plateau	Arg IC_{50} [mM]
Cr NAGK alone	0.60	0.14
Cr NAGK, 10 mM Gln	0.40	0.11
Cr NAGK, *Cr* PII	0.62	0.14
Cr NAGK, *Cr* PII, 5 mM Gln	n.a.	n.a.
Cr NAGK, *Cr* PII, 10 mM Gln	n.a.	n.a.
Cr NAGK, Delta C *Cr* PII	0.64	0.08
Cr NAGK, *At* PII, 10 mM Gln	0.47	0.23

Figure 8. Effect of increasing arginine on *Cr* NAGK activity. [n.a.-not applicable]

PII relieves the feedback inhibition of arginine on NAGK (Mizuno *et al*, 2007; Forchhammer, 2008; Llácer *et al*, 2008). The arginine sensitivity of *Cr* NAGK was determined by increasing the concentration of arginine up to 1 mM in the enzymatic assay (Fig. 8). The half maximum

inhibitory concentration of arginine (Arg IC_{50}) to inhibit the *Cr* NAGK activity was found to be 140 µM. With the addition of up to 10 mM glutamine in the presence of *Cr* PII, the Arg IC_{50} gradually increased. In the absence of glutamine, *Cr* PII was unable to relieve the feedback inhibition of arginine on NAGK. The data points from triplicate experiments were fitted to a one phase exponential decay equation.

10.2.3 Maximal arginine inhibition on *Cr* NAGK

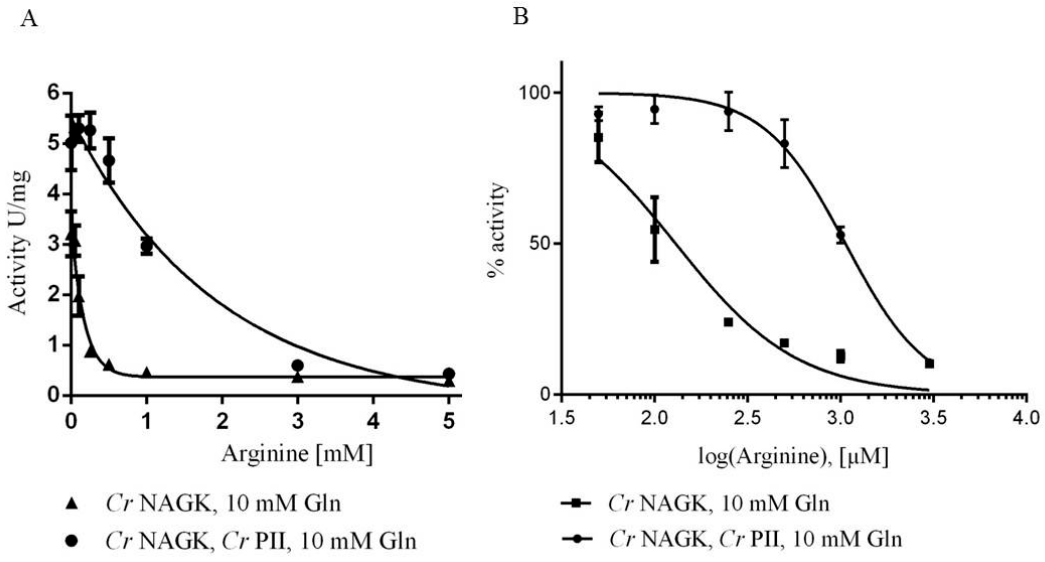

	A) one phase exponential decay equation		B) log(inhibitor) vs. normalized response-variable slope	
	Plateau	Arg IC_{50} [mM]	Hill slope	Arg IC_{50} [mM]
Cr NAGK, 10 mM Gln	0.36	0.12	-1.327	0.13
Cr NAGK, *Cr* PII, 10 mM Gln	-0.24	1.34	-1.994	1.06

Figure 9. Determination of maximum arginine needed to inhibit *Cr* NAGK activity. A) Data fitted to a one phase exponential decay equation. B) Data fitted to a nonlinear regression-log(inhibitor) vs. normalized response (variable slope) equation.

The arginine concentration was further increased up to 5 mM to determine the maximum amount needed to completely inhibit the NAGK activity. Triplicate experiments were performed and the data was fitted as indicated in Fig. 9A, B. The Arg IC_{50} values of free *Cr* NAGK enzyme and *Cr* PII bound form was approx. 120 µM and 1 mM. In the case of *S. elongatus*, the free enzyme had an Arg IC_{50} of 20 µM, which increased 10 fold with the addition of *Se* PII (Beez *et al*, 2009). Interestingly, *A. thaliana* free enzyme had an Arg IC_{50} of 1 mM which increased to about 6 fold with the addition of *At* PII. The non-conserved C-terminus of *S. elongatus* has been found responsible for its increased arginine sensitivity. The IC_{50} values of *Cr* NAGK places it in between the *Se* and *At* NAGK enzymes in terms of arginine sensitivity.

10.2.4 Effect of 2-OG on *Cr* NAGK activity

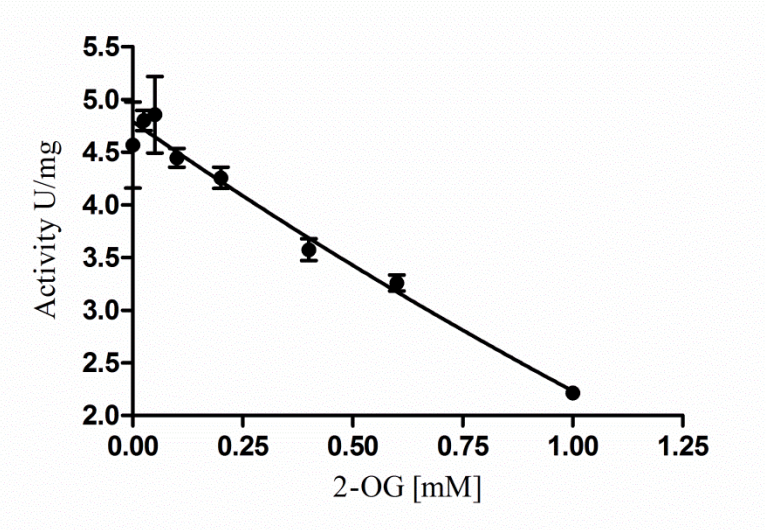

Figure 10. Antagonistic effect of 2-OG on *Cr* NAGK activity in the presence of 400 µM Arg.

The effector molecule 2-OG acts as an antagonist for the complex formation between PII-NAGK in *S. elongatus* and *A. thaliana* (Maheswaran *et al*, 2004; Feria Bourrellier *et al*, 2009). At 400 µM concentration of arginine, increasing amounts of 2-OG from 0.25 mM to 1 mM was applied to the assay system consisting of *Cr* NAGK, *Cr* PII and 10 mM Gln. Up to 1 mM 2-OG was needed to considerably inhibit the *Cr* NAGK activity (Fig. 10). The IC_{50} of 2-OG to inhibit the NAGK activity was 300 µM. The data points from three experimental trials were fitted to a one phase exponential decay equation.

10.2.5 Effect of increasing glutamine on *Cr* NAGK activity

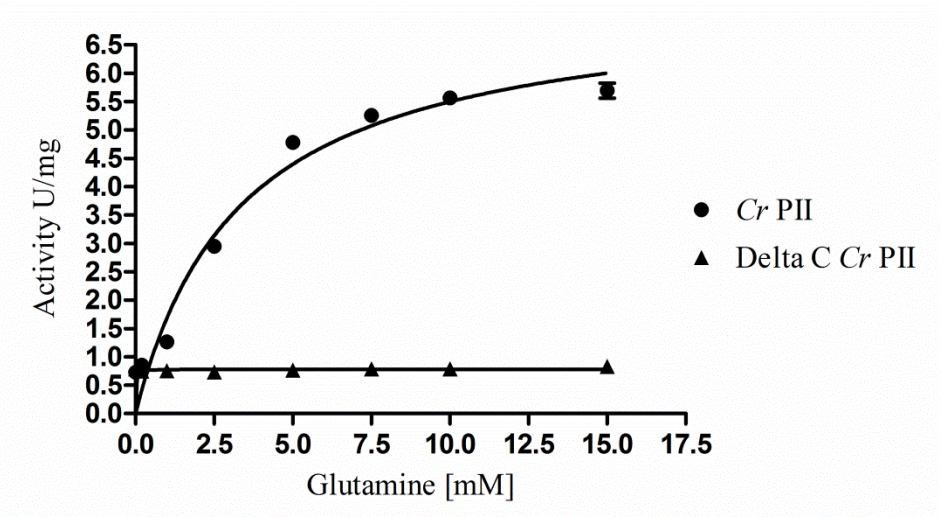

	V_{max} [mM s^{-1}]	K_m [mM]	k_{cat} [s^{-1}]
Cr PII	7.34	3.35±0.55	75.43
Delta C *Cr* PII	0.78	0	n.a

Figure 11. Effect of increasing amounts of glutamine on *Cr* NAGK activity.

Increasing amounts of glutamine was added to examine its effect on *Cr* NAGK activity in the presence of *Cr* PII (Fig. 11). Titration with up to 15 mM glutamine increasingly favoured the complex formation. As a negative control, Delta C *Cr* PII was tested with increasing amounts of glutamine and confirmed no binding. Thus, the C-terminus of *Cr* PII plays an important role in the tight complex formation between *Cr* PII-*Cr* NAGK. The data from three different experiments were fitted to a one site binding hyperbolic equation.

10.3 Surface Plasmon Resonance

To investigate the binding of effector molecules to protein complexes, Surface Plasmon Resonance (SPR) detection experiments were performed by using a BIAcore X biosensor system (GE Healthcare). A buffer containing HBS-Mg [10 mM Hepes, 150 mM NaCl, 1 mM $MgCl_2$, 0.005% Nonidet P-40 (pH 7.5)] was used at a flow rate of 15 µl/min at 25 °C and the experiments were performed as described previously (Maheswaran *et al*, 2004; Fokina *et al*, 2010a, b). His_6-tagged NAGK was immobilized onto a Ni^+-loaded nitrilotriacetate (NTA) sensor chip in a volume of 50 µl at a concentration of 30 nM (hexamer) to receive a signal of 3000 resonance units (RU) and Strep-tagged PII protein was used as an analyte in combination with various effector molecules. 1 µM PII was injected and the binding and dissociation of PII to NAGK was studied and recorded as a response signal difference (ΔRU) of FC2-FC1. Where, FC1 and FC2 are flow cells; FC1 being the reference cell without His_6-NAGK and FC2 was loaded with PII protein. The experiments were performed by loading *Cr* NAGK on the chip in the presence of 1 mM Arg and followed by injection of *Cr* PII.

10.3.1 Effect of glutamine on *Cr* PII-*Cr* NAGK complex formation

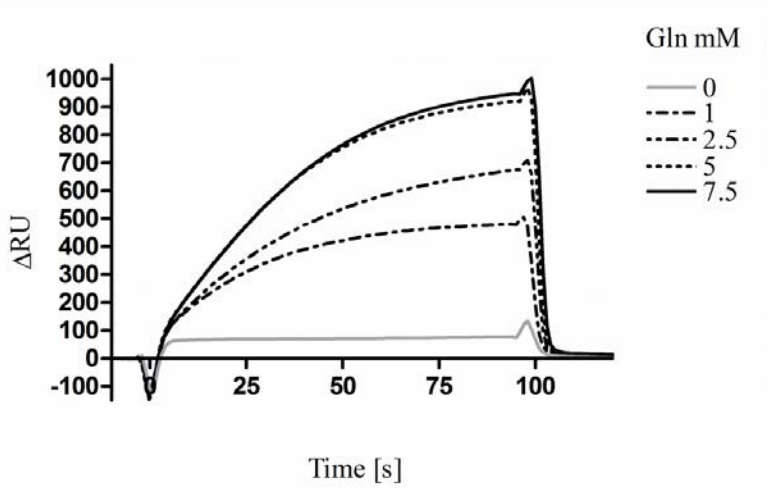

Figure 12. Increasing glutamine and its effect on *Cr* PII-*Cr* NAGK complex formation.

Cr NAGK was loaded with a resonance unit (RU) of ~2700 and increasing amounts of glutamine was injected to assist the complex formation in 50 µl of a buffer containing *Cr* PII, 1 mM ATP and 2 mM $MgCl_2$. In the absence of glutamine there was no complex formation (Fig. 12). Increasing amounts of glutamine, up to 7.5 mM enhanced complex formation between *Cr* PII and *Cr* NAGK. Strikingly, the complex dissociated spontaneously as it encountered a buffer devoid of glutamine. However, in the case of *S. elongatus* the complex dissociation took a considerably longer period and progressed faster with addition of 2-OG or ADP (Fokina *et al*, 2010b).

10.3.2 Effect of increasing 2-OG concentration on *Cr* PII-*Cr* NAGK complex

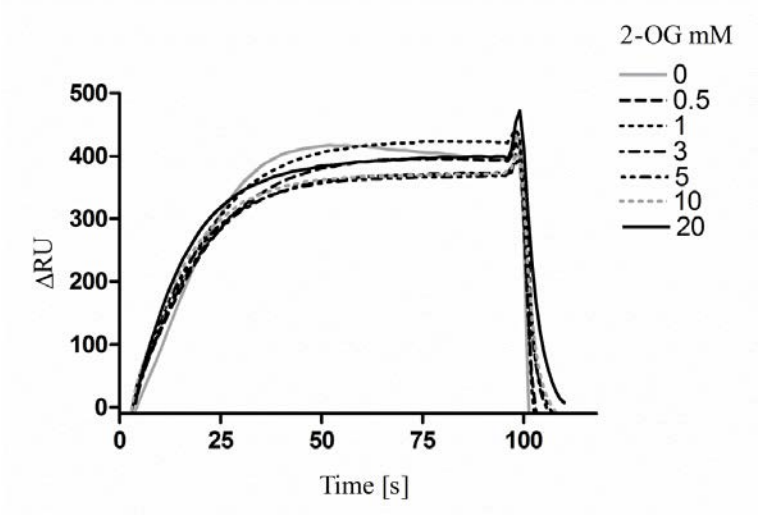

Figure 13. Increasing amounts of 2-OG and its effect on *Cr* PII-*Cr* NAGK complex formation.

Cr NAGK was loaded with a RU of ~2600 and increasing amounts of 2-OG was added to monitor its effect on antagonizing the complex formation along with 50 µl of a buffer containing 1 µM *Cr* PII, 1 mM ATP, 2 mM $MgCl_2$ and 5 mM Gln. The complex formation between PII and NAGK in *S. elongatus* is known to be prevented with the addition of 2-OG, where the T-loops of PII undergo conformational changes that facilitate the dissociation of PII from NAGK (Fokina *et al*, 2010a). However, SPR experiments with *C. reinhardtii* system with increasing amounts of 2-OG did not favour the dissociation of complex even at concentrations as high as 20 mM (Fig. 13). There is a slight reduction in ΔRU values in the presence of 2-OG indicating subtle changes caused by this effector molecule. This indicates tight conformation of *Cr* NAGK and *Cr* PII and inability of 2-OG to cause major conformational changes in the T-loop region of PII proteins.

10.3.3 Effect of glutamine on Delta C *Cr* PII

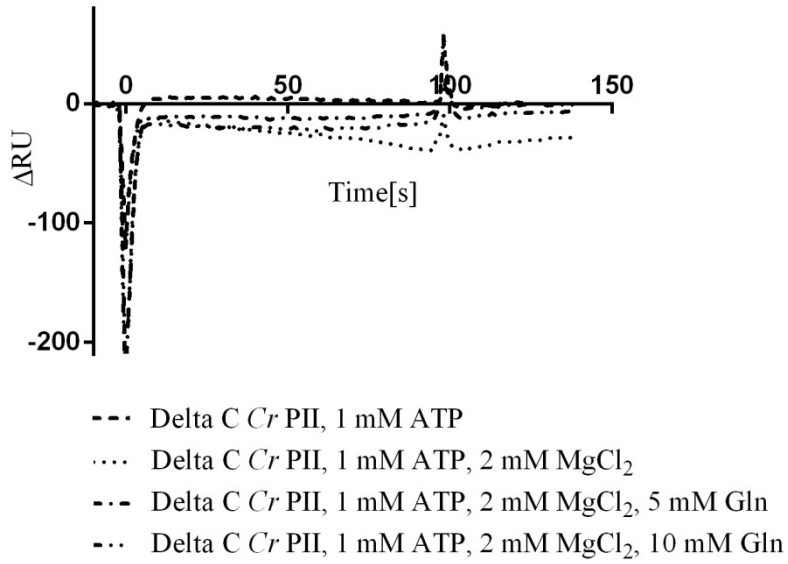

Figure 14. Effect of ATP, $MgCl_2$ and glutamine on Delta C *Cr* PII.

Cr NAGK was loaded with a RU of ~2600 and 50 µl of a buffer containing Delta C *Cr* PII along with various effector molecules as indicated in the above Fig. 14 were added. Delta C *Cr* PII was used as a control to examine the influence of glutamine. Addition of 1 mM ATP in the presence and absence of $MgCl_2$ had no influence on the complex formation. Increasing amounts of glutamine up to 10 mM was used in combination with ATP-Mg and was neither found to have any influence on favouring the complex formation.

10.3.4 Effect of ADP on *Cr* PII

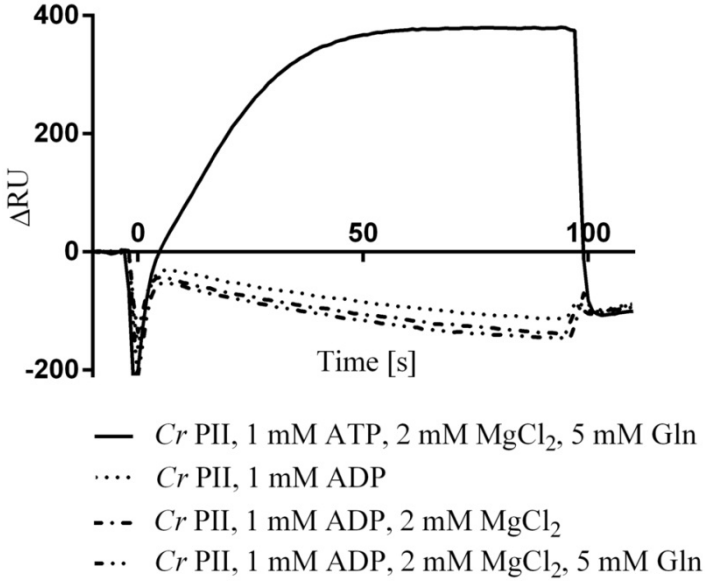

Figure 15. Influence of ADP on *Cr* PII in the presence of glutamine and $MgCl_2$.

Cr NAGK was loaded with a RU of ~2600 and 50 µl of *Cr* PII was injected in the presence of effector molecules (as indicated above) especially ADP, to determine its influence in complex formation (Fig. 15). Addition of ADP alone or in the presence of $MgCl_2$ displayed negative effect on the complex formation. It has been reported previously that the presence of ATP-Mg in the active pocket of PII proteins and not ADP, is crucial for certain interactions (Fokina *et al*, 2010b; Gerhardt *et al*, 2012). Further, the presence of ADP has been reported to display an antagonistic effect on the complex formation between PII and NAGK in *S. elongatus* (Maheswaran *et al*, 2004). In *C. reinhardtii* system, ADP is not capable of replacing ATP to favour complex formation in the presence of glutamine.

10.3.5 Effect of glutamine on WT *Se* PII and *Cr* NAGK

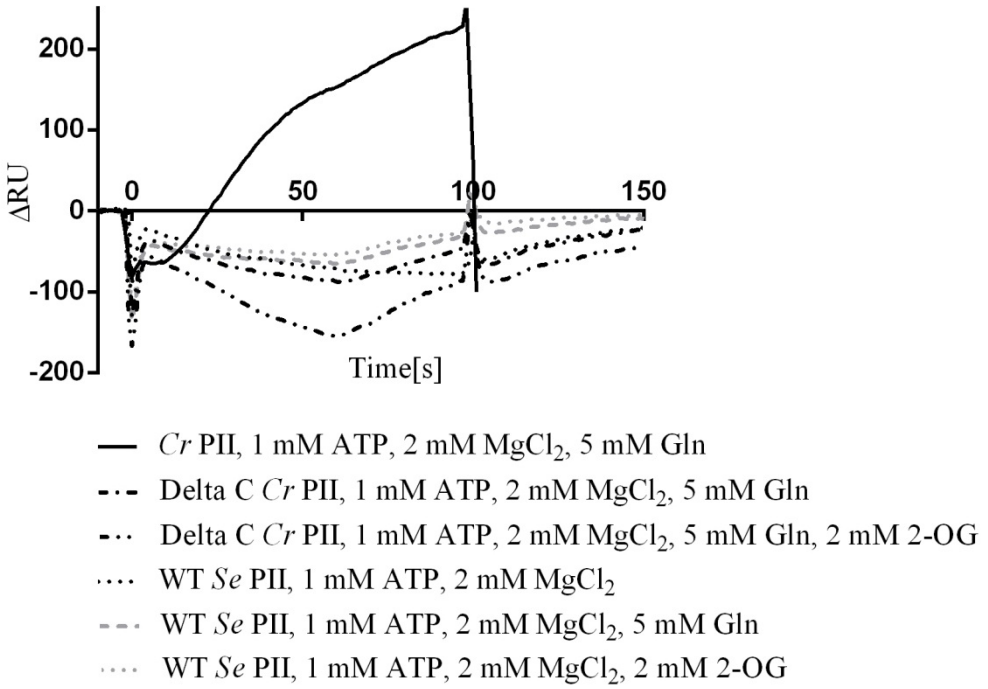

Figure 16. Influence of ATP, $MgCl_2$, 2-OG and glutamine on WT *Se* PII

Cr NAGK was loaded with a RU of ~2700 and 50 µl of *Cr* PII/Delta C *Cr* PII/WT *Se* PII was added in combination with different effector molecules as needed (Fig. 16). *Cr* PII in the presence of ATP-Mg and glutamine was used as a positive control and Delta C *Cr* PII was used as a negative control. The ability of WT *Se* PII to form a complex with *Cr* NAGK in the presence of glutamine was investigated and it was determined that in the presence of ATP-Mg and glutamine the formation of complex was not possible. *S. elongatus* PII protein doesn't respond to glutamine and is not capable of forming a complex with *Cr* NAGK in the presence of glutamine.

10.3.6 Effect of glutamine on WT *Se* NAGK and *Cr* PII

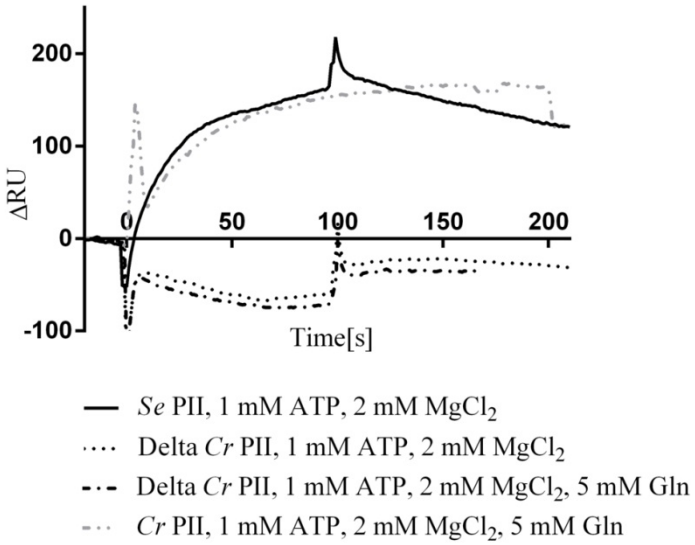

Figure 17. Influence of glutamine on WT *Se* NAGK and *Cr* PII

Se NAGK was loaded with a RU of ~2200 and 50 µl of reaction mix was added consisting of either *Se* PII, Delta C *Cr* PII or *Cr* PII along with effector molecules (Fig. 17). *Se* PII binds to *Se* NAGK in the presence of ATP-Mg and starts to dissociate slowly with the continuous flow of buffer. The ability of *Cr* PII to bind *Se* NAGK was examined with the addition of ATP-Mg in the presence of 5 mM Gln. Interestingly, this resulted in complex formation between *Cr* PII and *Se* NAGK. This experiment confirms that *Cr* PII devoid of its native partner *Cr* NAGK can still form stable complexes with *Se* NAGK in the presence of ATP-Mg and glutamine. Similarly, the ability of PII and NAGK to mutually replace and activate each other from *S. elongatus* and *A. thaliana* has been reported earlier (Beez *et al*, 2009). These results highlight the PII-NAGK functional conservation across the different kingdoms.

10.4 Isothermal Titration Calorimetry

The Isothermal Titration Calorimetry (ITC) experiments were performed on a VP-ITC (MicroCal, LCC) instrument and the buffer consisted of 10 mM potassium phosphate pH 7.5, 100 mM NaCl and 2 mM $MgCl_2$. The titrations were done at 20 °C. For the determination of binding isotherm of 2-OG to *Cr* PII and Delta C *Cr* PII, 33.3 µM (PII trimers) of protein was mixed with 1 mM ATP and titrated against 1 mM or 2 mM 2-OG. The ligand (5 µl) was injected 30-40 times into the 1.4285 ml cell with a stirring speed of 350 rpm. The binding isotherms were calculated from the data and fitted to appropriate equation using the MicroCal ORIGIN software (Northampton, MA).

10.4.1 Binding of 2-OG to *Cr* PII

The effector molecule 2-OG binds to PII proteins by establishing a contact with ATP-Mg. An anti-cooperative manner of 2-OG binding to *S. elongatus* has been already established (Fokina *et al*, 2010a). A preliminary effort to titrate 1 mM 2-OG against *Cr* PII protein resulted in a binding isotherm as depicted below (Fig. 18). When fitted with a one site binding model, the number of sites occupied in the *Cr* PII (trimer concentration) is 1 with a K_d value of 38.90 µM. The 2-OG binding sites are not completely occupied and imply a strong affinity to bind the first site.

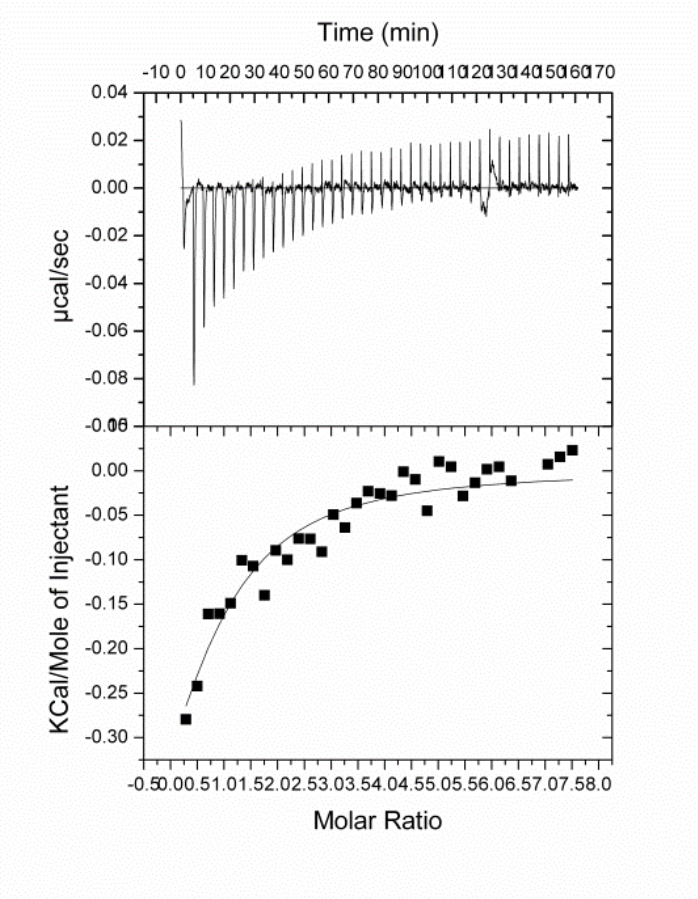

One site binding 1 mM 2-OG	
K_a	2.57 E^4 M^{-1}
K_d	38.90 µM

Figure 18. Binding of 2-OG to *Cr* PII. The upper panel in the figure shows the raw data in the form of heat effect during the titration against ligand. The lower panel shows the binding isotherm and best-fit curve.

10.4.2 Binding of 2-OG to Delta C *Cr* PII

The inability of Delta C *Cr* PII to promote the PII-NAGK complex formation in the presence of glutamine has been described previously (section 10.2.5). Despite its inefficacy, it is important to examine the active and functional status of the Delta C *Cr* PII protein. In order to check the functional state of the protein, a titration of Delta C *Cr* PII (in the presence of ATP-Mg) against 2-OG was carried out. The data obtained fitted well to a one site binding model

(Fig. 19). The number of binding site varies in the presence of 1 or 2 mM 2-OG. At a concentration of 1 mM 2-OG, the number of sites occupied for PII trimer is 1 with a K_d of 90 µM. However, when the concentration of the ligand is increased to 2 mM the number of binding sites is 3 with a similar K_d value of 91.7 µM. The binding of Delta C *Cr* PII to 2-OG is indicative of an active and functional protein which responds by binding to the effector molecules ATP-Mg and 2-OG.

A) B)

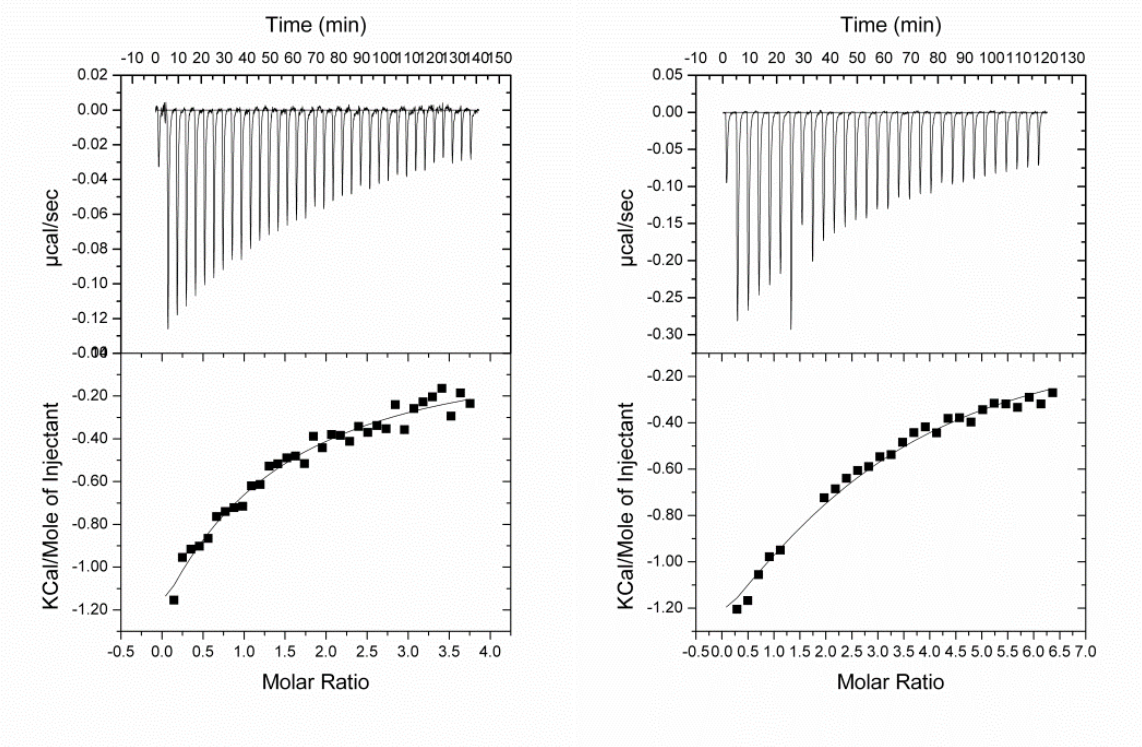

	One site binding	
	1 mM 2-OG	2 mM 2-OG
K_a	1.10 E^4 M^{-1}	1.09 E^4 M^{-1}
K_d	90.00 µM	91.70 µM

Figure 19. Binding of 2-OG to Delta C *Cr* PII. The upper panel in the figure shows the raw data in the form of heat effect during the titration against the ligand. The lower panel shows the binding isotherm and the best-fit curve. A) Binding of 1 mM 2-OG to Delta C *Cr* PII B) Binding of 2 mM 2-OG to Delta C *Cr* PII.

10.4.3 Binding of glutamine to *Cr* PII and Delta C *Cr* PII

Titration of *Cr* PII (in the presence of 1 mM ATP-Mg) against glutamine resulted in K_d values in mM range. The data is not shown as the points were scattered and it was difficult to fit the curve. As a negative control, Delta C *Cr* PII was also titrated against glutamine which resulted in no significant isothermal change.

10.5 Multi-Angle Light Scattering (MALS)

Proteins are composed of complex polypeptides linked together to form arbitrary coils which fold into its characteristic and functional three dimensional structure. These structures are held together due to various forces acting on them such as hydrophobic interactions, Van der Waals forces and intermolecular hydrogen bonding.

The molecular structure of a protein is adapted based on the solution it is subjected and this determines the size of protein. Monitoring the size of a protein is essential to determine the folded state in native conditions. Multiple-Angle Light Scattering (MALS) is a technique that calculates the molar mass of a protein based on the light scattered. They are often used in conjunction with Size Exclusion Chromatography (SEC). Due to complexities in determining the molar mass of proteins with their interaction partners, cross-linking technique was employed to determine the protein-protein interactions. The cross-linked proteins were passed through SEC column and molar mass of the protein was determined using MALS technique. This technique enables the determination of absolute molecular weight, size and conformation of proteins in solution.

Cross-linking method:

The proteins were dialyzed overnight in a buffer containing 10 mM potassium phosphate pH 7.5, 100 mM NaCl, 2 mM $MgCl_2$ and 10% glycerol. The reaction mixture consisted of 500 to 1000 µg of dialyzed proteins, which were mixed together in the presence of 2 mM ATP, 2 mM ADP, 10 mM Gln, 20 µM Arg and 1 mM 2-OG as required. The interacting proteins in a total volume of 1 ml were treated with 50 µl of 2.3% freshly prepared solution of glutaraldehyde for 2 to 5 minutes at 37 ºC. The reaction was stopped with the addition of 100 µl of 1 M Tris pH 8.0.

Light scattering procedure:

A precision column Superdex 200, PC 3.2/30 (GE Healthcare, code no: 17-1089-01) was used for SEC. This column was coupled to a triple-angle light scattering detector from Wyatt Technology corporation: miniDAWN™ TREOS® machine. The experiments were performed at room temperature. To determine a wavelength suitable for the measurement of protein complexes subjected to cross-linking, a protein scan of *Cr* NAGK and *Cr* PII was performed over a range of 200 to 300 nm. The scanning data was analysed and it was determined that at

a wavelength of 238 nm both the proteins had similar absorbance independent of the extinction coefficient. At this wavelength, which corresponds to the close absorption maxima of peptide bonds, the oligomeric constitution of the interacting proteins could be determined effectively.

The cross-linked sample was concentrated and centrifuged to remove any sediment and injected into a 10 µl loop. The running buffer consisted of 10 mM Tris pH 7.8, 300 mM NaCl, 1 mM DTT, 2 mM $MgCl_2$, 20 µM Arg, 0.02% NaN_3 and 2% glycerol. The protein, Bovine serum albumin (BSA) was used to validate the technique. The machine was calibrated and the calibration constant was determined to be $5.4e^{-5}$ and the UV extinction coefficient for proteins was set to $1.45e^{+3}$ at 238 nm. The λ1, λ2 and λ3 were set to 238, 280 and 215 nm respectively. The light scattering data was processed and analysed with the Astra software-5.3.4.20 (Wyatt Corp., Santa Barbara, CA) to determine the oligomeric state and molar mass of proteins. The measured polydispersity of the sample was low indicating that the samples were majorly monodisperse.

10.5.1 Analysis of *Cr* NAGK and *Cr* PII

The oligomerization states of *Cr* NAGK and *Cr* PII (in the presence of 2 mM ATP-Mg) in combination with effector molecules 2 mM ADP, 10 mM Gln and 2 mM 2-OG were determined after cross-linking.

The *Cr* PII protein eluted at approximately 1.6 ml and the average molar mass was estimated to be 48.3 kDa from four different measurements (Fig. 20 and Table 1). The molar mass estimated was accurate in comparison to the expected theoretical value of 51 kDa (corresponding to a trimer). The *Cr* NAGK eluted as two species at approx. 1.25 ml and 1.15 ml, which had molar mass of 212.9 kDa (hexamer) and 403.9 kDa (dodecamer) respectively. The NAGK exists majorly as a hexamer in solution which correlates well with the theoretical value of 201.36 kDa. The polydispersity of the solution was low implicating the presence of highly monodisperse species. Strikingly in solution, *Cr* PII seems to interact with *Cr* NAGK even in the absence of glutamine. This probably could be due to the ability of the cross-linker glutaraldehyde to occupy the glutamine binding site and thereby stabilising the PII proteins to form a complex with NAGK.

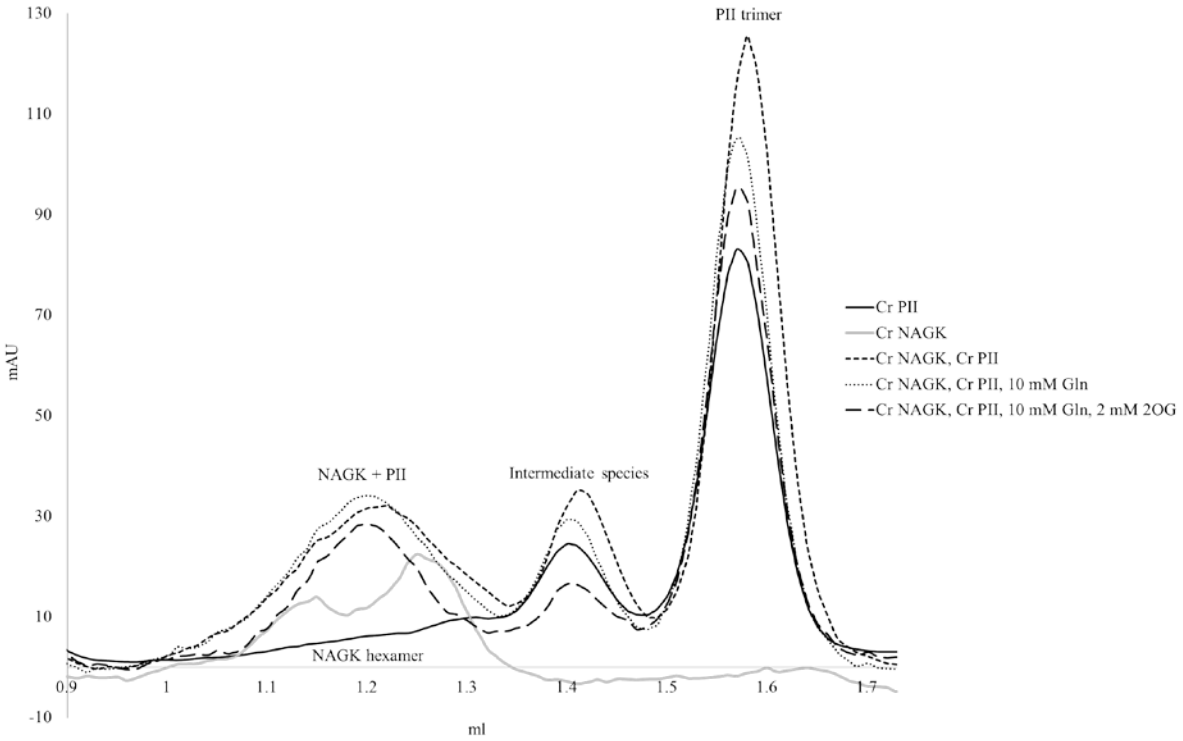

Figure 20. Gel filtration profile for cross-linked *Cr* NAGK and *Cr* PII

Sample [cross-linked]	MW kDa [theoretical]	MW kDa [light scattering] Polydispersity (%)	Interpretation
Cr PII	P3: 51.00	206.8 (9%) 45.42 (4%)	I = 4(P3) P3
Cr NAGK	N6: 201.36	403.9 (4%) 212.9 (3%)	2(N6) N6
Cr NAGK+*Cr* PII	N6: 201.36 P3: 51.00 N6+P3: 252.36 N6+2(P3): 303.36	294.3 (5%) 95.35 (13%) 47.69 (9%)	N6+2(P3) I = 2(P3) P3
Cr NAGK+*Cr* PII, 10 mM Gln		264.3 (3%) 94.60 (10%) 45.86 (8%)	N6+P3 I = 2(P3) P3
Cr NAGK+*Cr* PII, 10 mM Gln, 2 mM 2-OG		258.5 (3%) 166.4 (17%) 46.42 (5%)	N6+P3 I = 3(P3) P3

Table 1. Molar mass determined for *Cr* NAGK and *Cr* PII.
[N6: NAGK hexamer, I: Intermediate species of PII trimer, P3: PII trimer]

10.5.2 Analysis of WT *Se* NAGK and WT *Se* PII

NAGK and PII proteins from WT *S. elongatus* were studied for oligomerization capabilities in the presence of 2 mM ATP (except for conditions with ADP), 2 mM $MgCl_2$ and 2-OG (Fig. 21 and Table 2). NAGK from *S. elongatus* has been already shown to form hexamer and the complex between *S. elongatus* NAGK and PII has been determined (Llácer *et al*, 2007) where NAGK forms a toroid and two PII trimers involve in a tight interaction on either side of the toroid in the crystal structure. The determination of oligomeric state of complex in the solution would be helpful to compare and interpret the data obtained from the crystal structure.

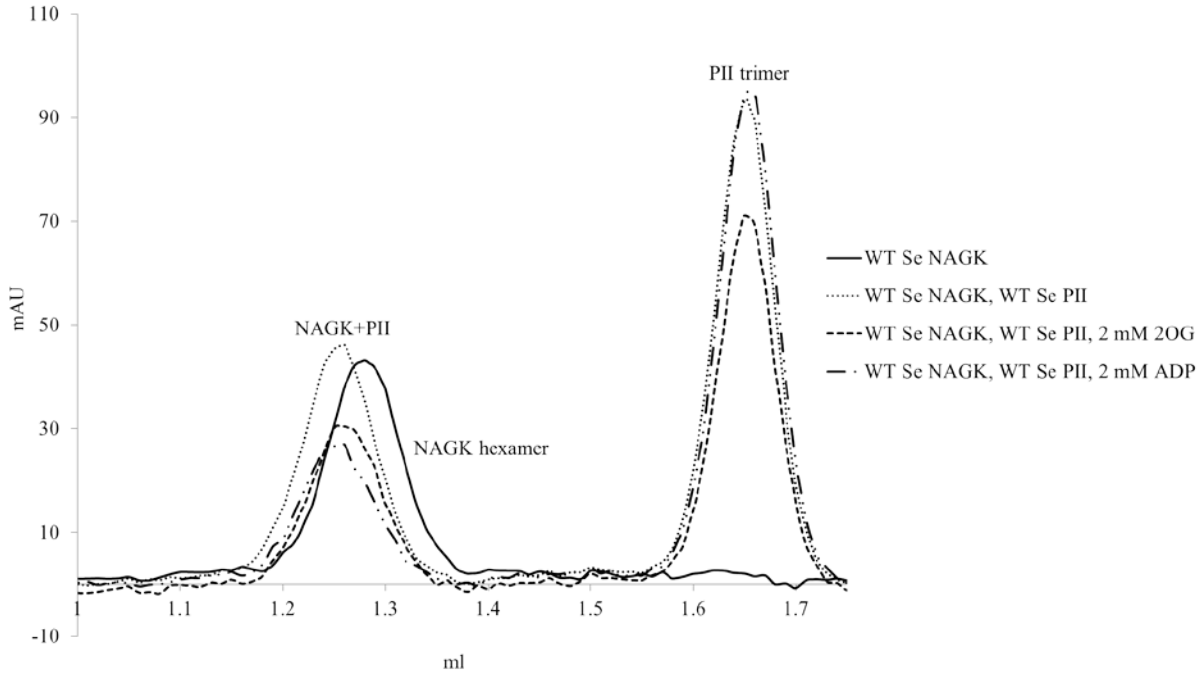

Figure 21. Gel filtration profile for cross-linked WT *Se* NAGK and WT *Se* PII

Sample [cross-linked]	MW kDa [theoretical]	MW kDa [light scattering] Polydispersity (%)	Interpretation
WT *Se* NAGK	N6: 206.7	206.6 (3%)	N6
WT *Se* NAGK+ *Se* PII	N6+P3: 247.4 N6+2(P3): 288.1	267.2 (2%) 54.39 (6%)	N6+(P3+50% P3) P3
WT *Se* NAGK+ *Se* PII, 2 mM 2OG		226.0 (2%) 56.96 (7%)	N6+(50% P3) P3
WT *Se* NAGK+ *Se* PII, 2 mM ADP		228.7 (6%) 48.64 (4%)	N6+(50% P3) P3

Table 2. Molar mass determined for WT *Se* NAGK and WT *Se* PII.
[N6: NAGK hexamer, P3: PII trimer, 50% P3: 50% occupancy of PII trimer]

10.5.3 Complex formation between *At* NAGK and *Cr* PII

A hetero complex of *At* NAGK and *Cr* PII was subjected to cross-linking reaction in the presence and absence of glutamine. *A. thaliana* NAGK forms a hexamer which fits well with the theoretical MW of 200.28 kDa. One trimer of *Cr* PII (average MW: 51 kDa) binds to the *At* NAGK toroid in solution resulting in the molecular weight of the complex to be approx. 259.2 kDa (Fig. 22 and Table 3). The ability of PII from one organism to form a complex with NAGK from another organism has been already studied in *A. thaliana* and *S. elongatus* system (Beez *et al*, 2009). Similarly, the PII from *C. reinhardtii* can form a complex with *A. thaliana* NAGK in solution in the presence of glutamine as determined below.

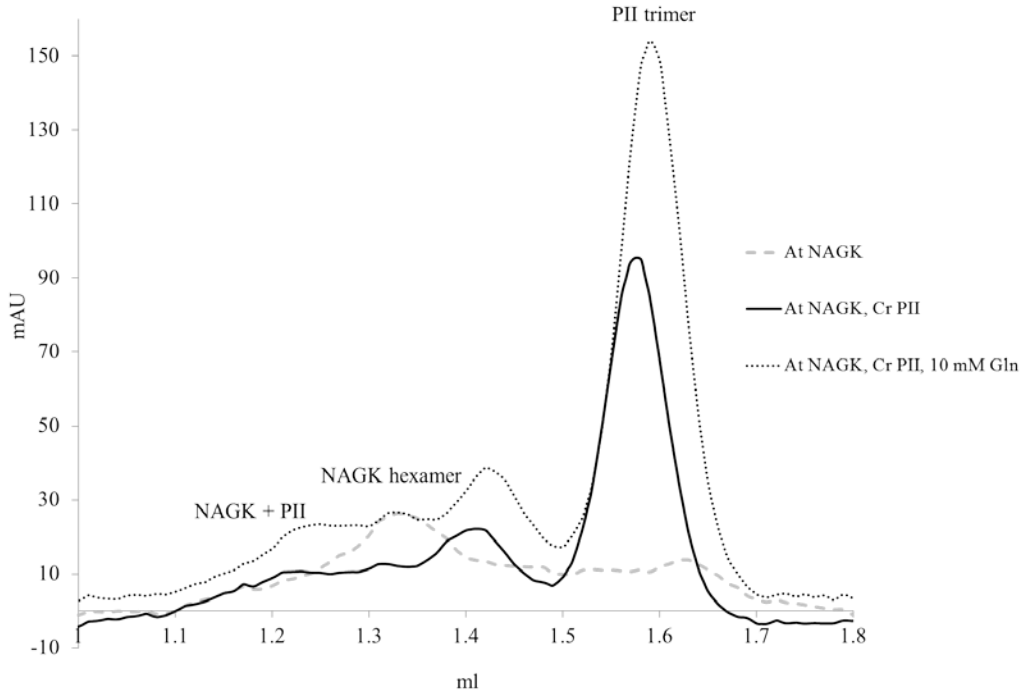

Figure 22. Gel filtration profile for cross-linked *At* NAGK and *Cr* PII

Sample [Cross-linked]	MW kDa [theoretical]	MW kDa [light scattering] Polydispersity (%)	Interpretation
At NAGK	N6: 200.28	193.5 (5%)	N6
At NAGK+*Cr* PII	N6+P3: 251.28 N6+2(P3): 302.28	259.2 (3%) 98.99 (3%) 53.01 (7%)	N6+P3 I = 2(P3) P3
At NAGK+*Cr* PII, 10 mM Gln		253.5 (3%) 97.84 (7%) 50.68 (7%)	N6+P3 I = 2(P3) P3

Table 3. Molar mass determined for *At* NAGK and *Cr* PII.
[N6: NAGK hexamer, I: Intermediate species of PII trimer, P3: PII trimer]

10.5.4 Overlay of PII from *Cr*, Delta C *Cr* and WT *Se*

The gel filtration profiles of PII from *C. reinhardtii*, Delta C *Cr* and WT *Se* are overlaid to compare the elution peak and molar mass of these proteins. *Cr* PII elutes at approx. 1.60 ml, followed by the Delta C *Cr* PII at 1.62 ml and *Se* PII at 1.67 ml (Fig. 23). The calculated MW of these proteins with the light scattering experiment is in agreement with the theoretical values (Table 4). All the PII proteins described below run as a trimer in the SEC column.

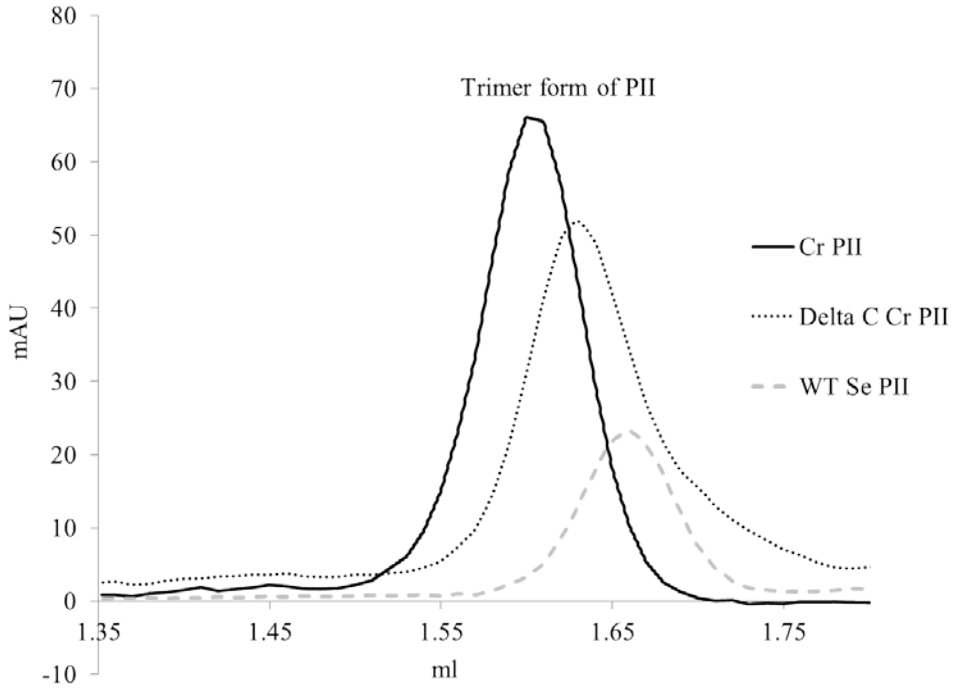

Figure 23. A comparison of gel filtration profile for *Cr* PII, Delta C *Cr* PII and WT *Se* PII

Sample	MW kDa [theoretical]	MW kDa [light scattering] Polydispersity (%)	Interpretation
Cr PII	P3: 51.00	51.90 (4%)	P3
Delta C *Cr* PII	P3: 46.95	49.64 (15%)	P3
WT *Se* PII	P3: 40.77	44.37 (2%)	P3

Table 4. Molar mass determined for PII proteins from *Cr*, Delta C *Cr* and WT *Se*.
[P3: PII trimer]

10.6 Structure determination of proteins

10.6.1 *C. reinhardtii* PII apo form

The *Cr* PII protein at a concentration of 3 mg/ml in a buffer containing 10 mM Tris pH 7.5, 100 mM NaCl, 2 mM ATP, 2 mM $MgCl_2$, 5 mM Gln and 10% glycerol was setup for crystallization with sitting drop method. The protein crystals were formed in a ground solution containing 0.15 M di-ammonium sulfate, 0.1 M Hepes pH 7.0 and 20% *w/v* PEG 4000. The crystals (appeared in 30 days) were picked and flash frozen in liquid nitrogen.

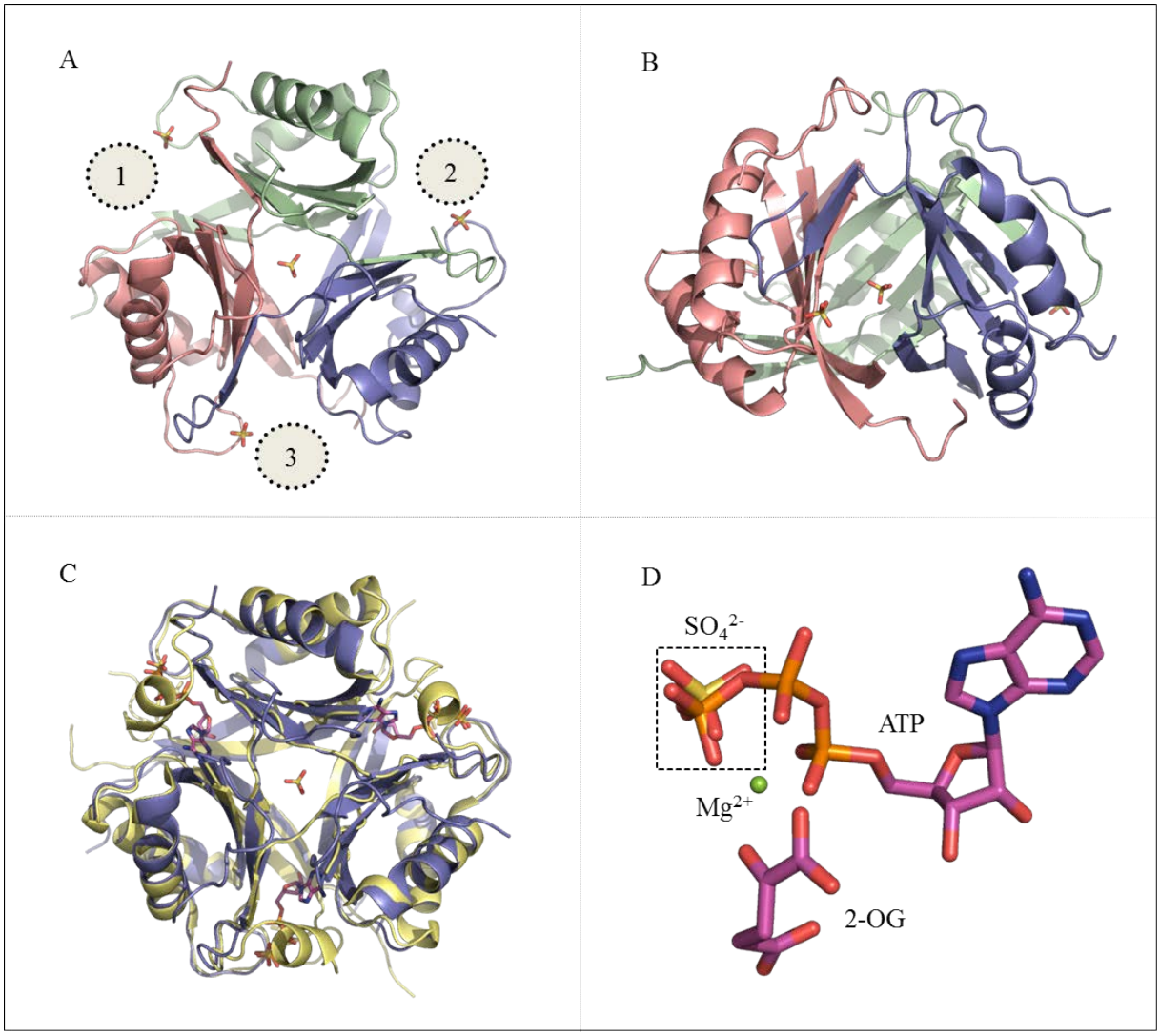

Fig 24: *Cr* PII protein structure in the apo form. A) Top and B) side view of the crystal structure of PII trimer bound to four sulphate molecules. The chains forming a trimer are coloured in salmon, slate and pale green. C) Superimposition of *Cr* PII apo form (slate) over the *S. elongatus* PII protein (yellow) bound to 2-OG (PDB: 2XUL- excess of 2-OG). D) Superimposition of sulfate molecule (yellow) bound to *Cr* PII (apo form) over the ATP-Mg and 2-OG bound form of *S. elongatus* (PDB: 2XUL).

The structure was solved as described in section 10.6.7. The superimposition of *Cr* PII in the apo form bound to four sulfate molecules over the structure of *S. elongatus* PII in complex with 2-OG (PDB: 2XUL-excess of 2-OG) was performed employing the program PyMOL which resulted in a RMSD of 0.729 Å (Fig. 24C). The sulfate molecule, which is apparently derived from the crystallization ground solution, occupies the same position as the gamma phosphate of ATP molecule.

10.6.2 *C. reinhardtii* PII bound to 2-OG

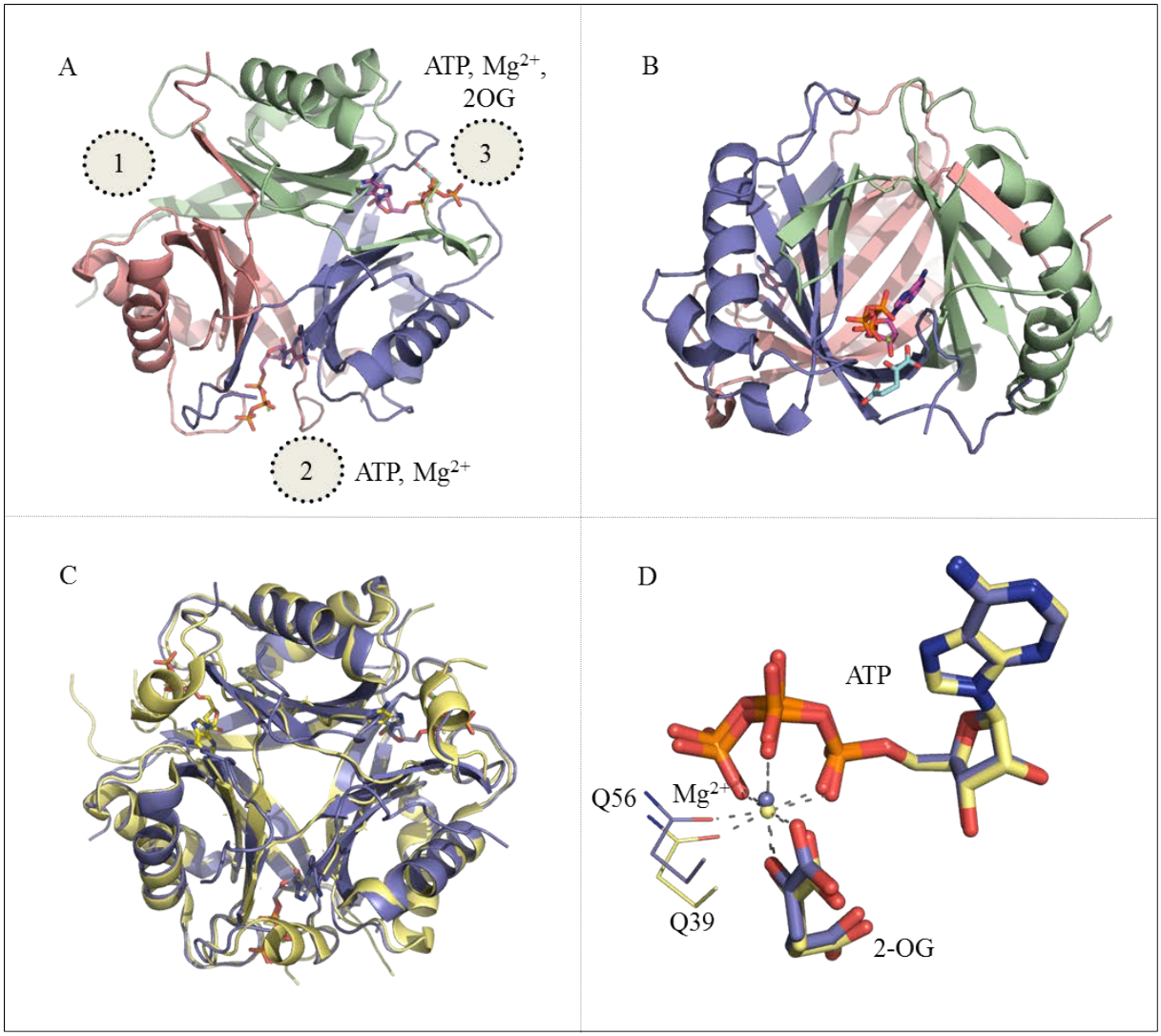

Figure 25. *Cr* PII protein structure in 2-OG bound state. A) Top view of *Cr* PII bound to ATP, Mg^{2+} and 2-OG. The crystal structure of PII trimer is represented with nothing bound in position one, with ATP and Mg^{2+} bound to position two and ATP, Mg^{2+} plus 2-OG occupying position three. B) Side view of the crystal structure representing ATP-Mg^{2+} and 2-OG in the inter subunit cleft. C) Superimposition of *Cr* PII with 2-OG bound form over *S. elongatus* PII with excess of 2-OG (PDB: 2XUL). D) Closer view of ATP-Mg^{2+} and 2-OG in the above superimposed structures. The coordination formed between ATP, Mg^{2+}, 2-OG and Q39/Q56 is represented.

The crystals containing apo-*Cr* PII (same condition) were subjected to a soaking experiment in the presence of 10 mM ATP, 10 mM $MgCl_2$ and 10 mM 2-OG. The crystals were picked up over an interval of 1-8 hrs. The cryo condition consisted of 20% glycerol and crystals were flash frozen in liquid nitrogen. The best data were obtained from crystals soaked for 1 hr.

The crystal structure consisted of a trimer with nothing bound in the 1st site, the 2nd site contained ATP-Mg and the 3rd site was occupied with ATP-Mg along with 2-OG (Fig. 25A). The binding pocket without any ligand could possibly be due to the crystallographic clashes with the symmetry related molecules leading to unfavourable binding of any effector molecule. The crystal structure of *Cr* PII bound to 2-OG was superimposed to 2-OG bound PII from *S. elongatus* (PDB: 2XUL) resulting in a RMSD of 0.665 Å representing a high degree of similarity between the superimposed structures. The binding pocket supports the fact that 2-OG binding is anti-cooperative as shown previously in *S. elongatus*. It has been already determined that the affinity of 2-OG binding to a site is dependent on the occupancy status of the neighbouring site.

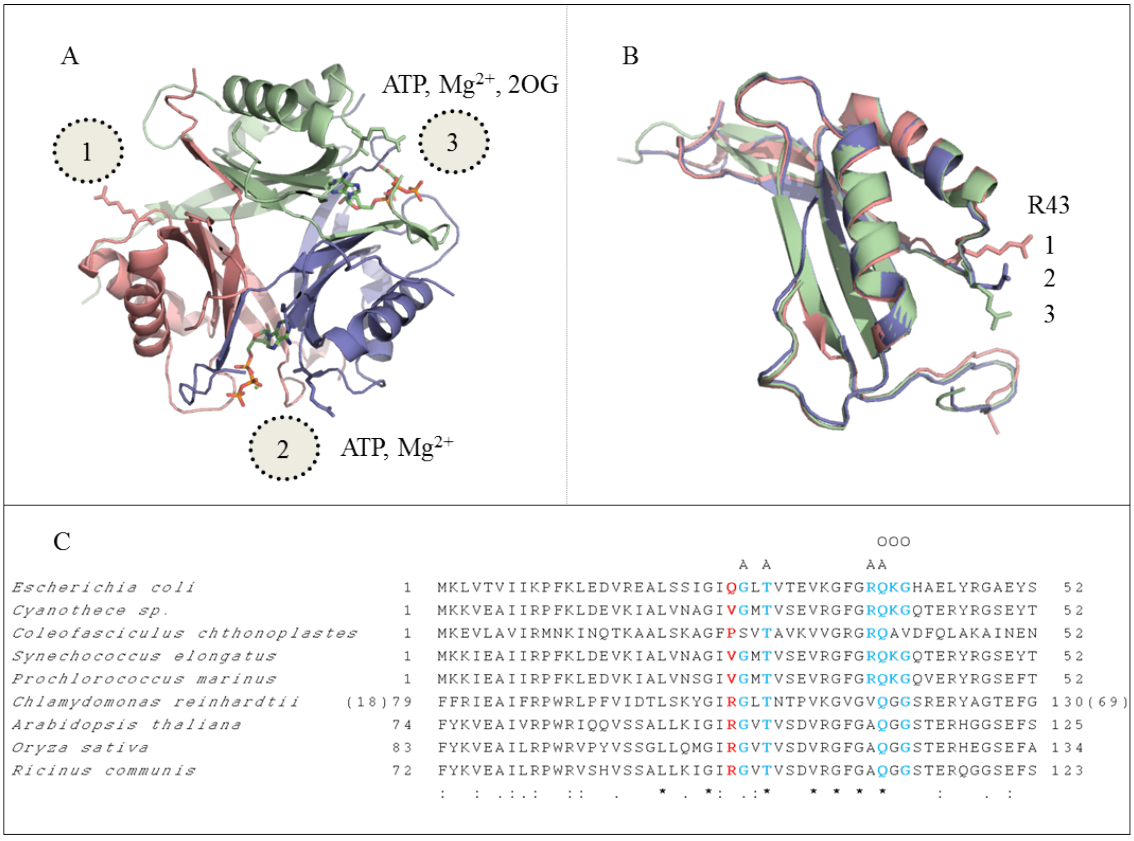

Figure 26. Comparison of three binding sites in *Cr* PII bound to 2-OG crystal structure. A) The R43 residue is highlighted in all three subunits. B) Superimposition of the monomers within the protein structure sheds light on different orientations of R43 (corresponding to R104 in Fig. 26C-highlighted in red) residue. C) Multiple sequence alignment of N-terminal PII sequences from bacteria, cyanobacteria, green algae and plants. The residues highlighted in blue are involved in interaction with ATP (represented with A on top) and 2-OG (represented with O on top).

The superimposition of subunits within the protein structure with different ligand occupancies was performed to determine any conformational changes adopted by these protein monomers. The residue R43 was found to adopt different conformational states as shown in the Fig. 26B. A multiple sequence alignment shows clearly that the residue R43 (highlighted in red- corresponding to R104 in Fig. 26C) is highly conserved only in plants. The highly conserved residues (in bacteria- highlighted in blue) R and K involved in interaction with ATP and 2-OG are not well conserved in green algae and plants. These residues form backbone interactions with the ligands and are preferentially replaced with another aminoacid in higher organisms.

10.6.3 *C. reinhardtii* PII bound to Cadmium

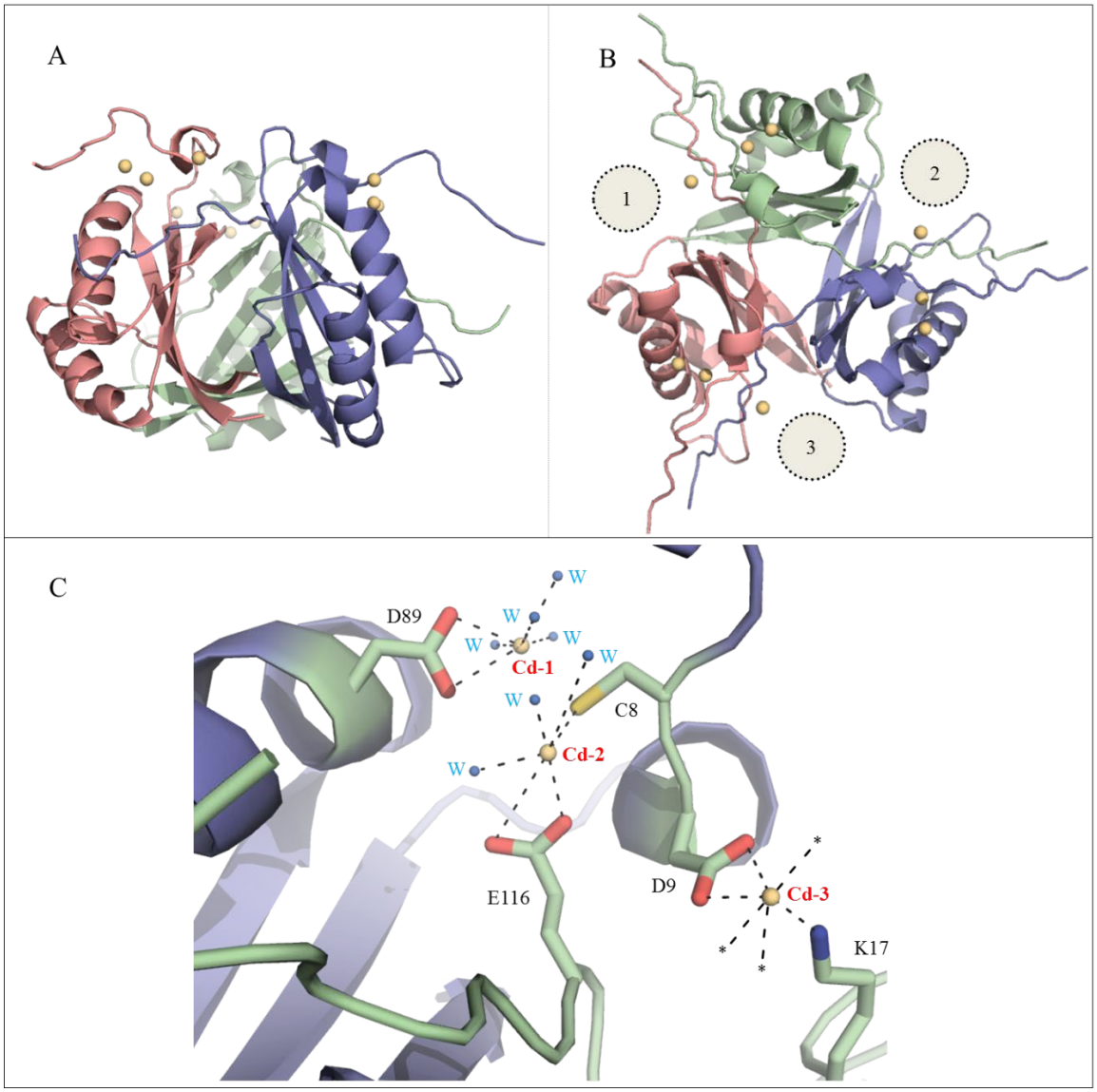

Figure 27. *Cr* PII structure - bound to Cadmium. A) Side view and B) top view of three Cadmium ions bound per monomer unit of *Cr* PII. C) Close view of the polar contacts made by Cd-1, Cd-2 and Cd-3 with neighbouring aminoacids and water molecules (W).
* Polar contacts made by Cd-3 with the symmetry related molecules.

The protein buffer contained 10 mM Tris pH 7.5, 150 mM NaCl, 5 mM $MgCl_2$, 1 mM DTT and 5 mM ADP. The crystals were formed in a condition with the ground solution composed of 0.05 M Cadmium sulfate, 0.1 M Hepes pH 7.5 and 1 M Sodium acetate. The crystals were formed within 7 days and were directly frozen in liquid nitrogen. *Cr* PII crystal structure consisted of three Cadmium ions (Cd-1, Cd-2 and Cd-3) bound per subunit resulting in a total of 9 Cadmium ions per PII trimer (Fig. 27A, B). Cadmium is a toxic component and there has been an extensive study on bio-remediation of Cd from wastes (Xu *et al*, 2008, Du *et al*, 2012, Tao *et al*, 2013, Jamers *et al*, 2009). The relative high number of Cadmium binding sites in *Cr* PII protein raises a possibility to employ *Cr* PII proteins as a cadmium sensor inside the cells.

10.6.4 *C. reinhardtii* PII and *A. thaliana* NAGK complex

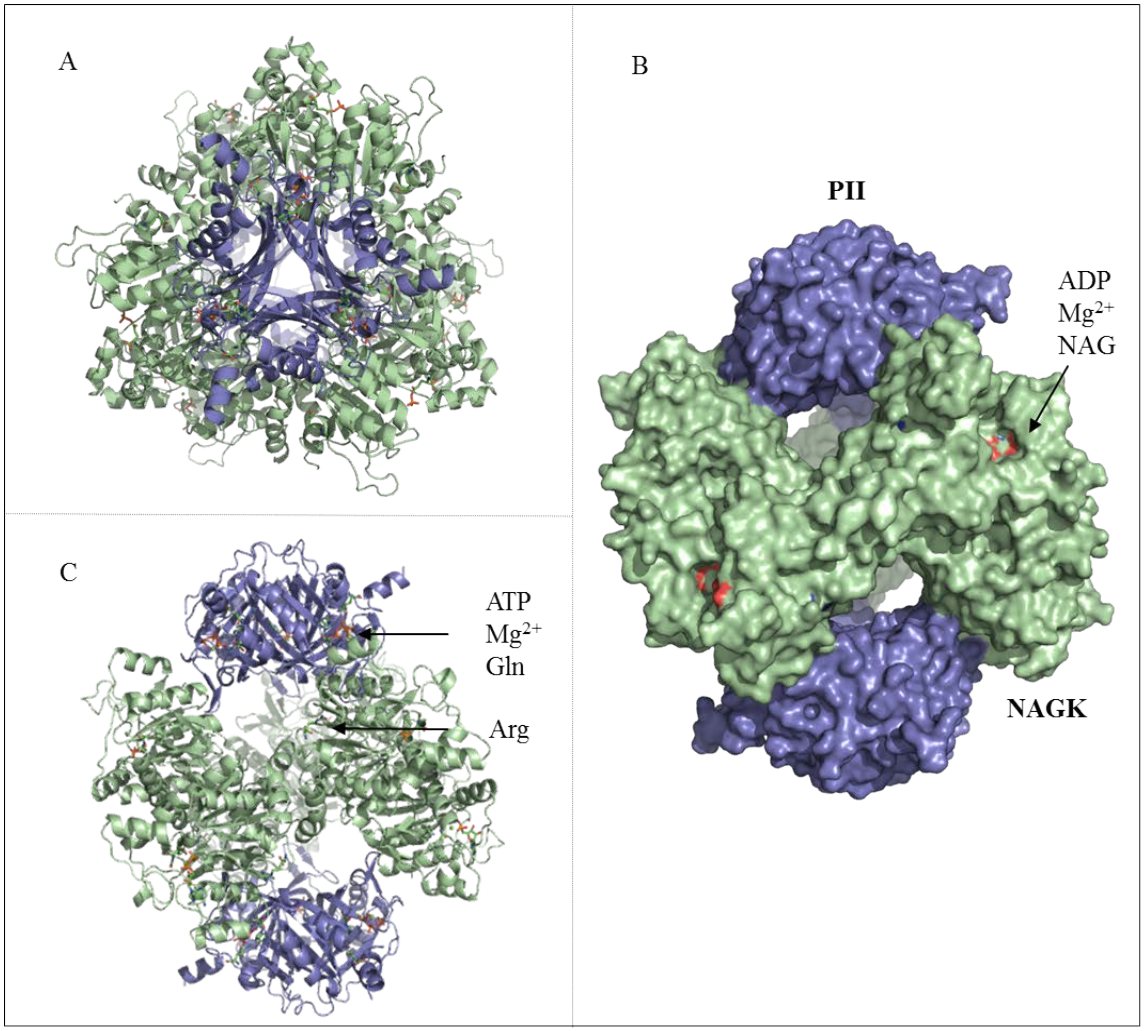

Figure 28. Complex of *Cr* PII and *At* NAGK. A) Top view of the complex representing a *Cr* PII trimer (slate) bound to *At* NAGK (green). B) Surface model of the complex (300 kDa) with *Cr* PII and *At* NAGK highlighting the unique extended C-terminus of *Cr* PII. C) The side view of the complex with the effector molecules ATP-Mg and Gln bound to the *Cr* PII.

The proteins *Cr* PII (2 mg/ml) and *At* NAGK (2 mg/ml) were mixed in the molar ratio of 1:2 in a buffer containing 10 mM Tris pH 7.8, 100 mM NaCl, 40 mM Arg, 10 mM Gln, 2 mM $MgCl_2$, 2 mM ADP, 10 mM NAG and 5% glycerol. The crystals started to form after 7 days in a ground solution containing 0.2 M NaCl, 0.1 M Na/K phosphate pH 6.2 and 50% *v/v* PEG 200. The crystal was flash frozen in liquid nitrogen. The complex structure consists of a hexamer of *At* NAGK forming the shape of a toroid. Two trimers of *Cr* PII are bound on either side of the NAGK toroid structure (Fig. 28B, C) as seen before in the previous structures from *S. elongatus* and *A. thaliana* (Llácer *et al*, 2007; Mizuno *et al*, 2007). No ATP was added during purification and crystallization steps, the presence of ATP in the crystal structure is possibly due to tight binding of ATP derived from PII protein expression in *E. coli* cells.

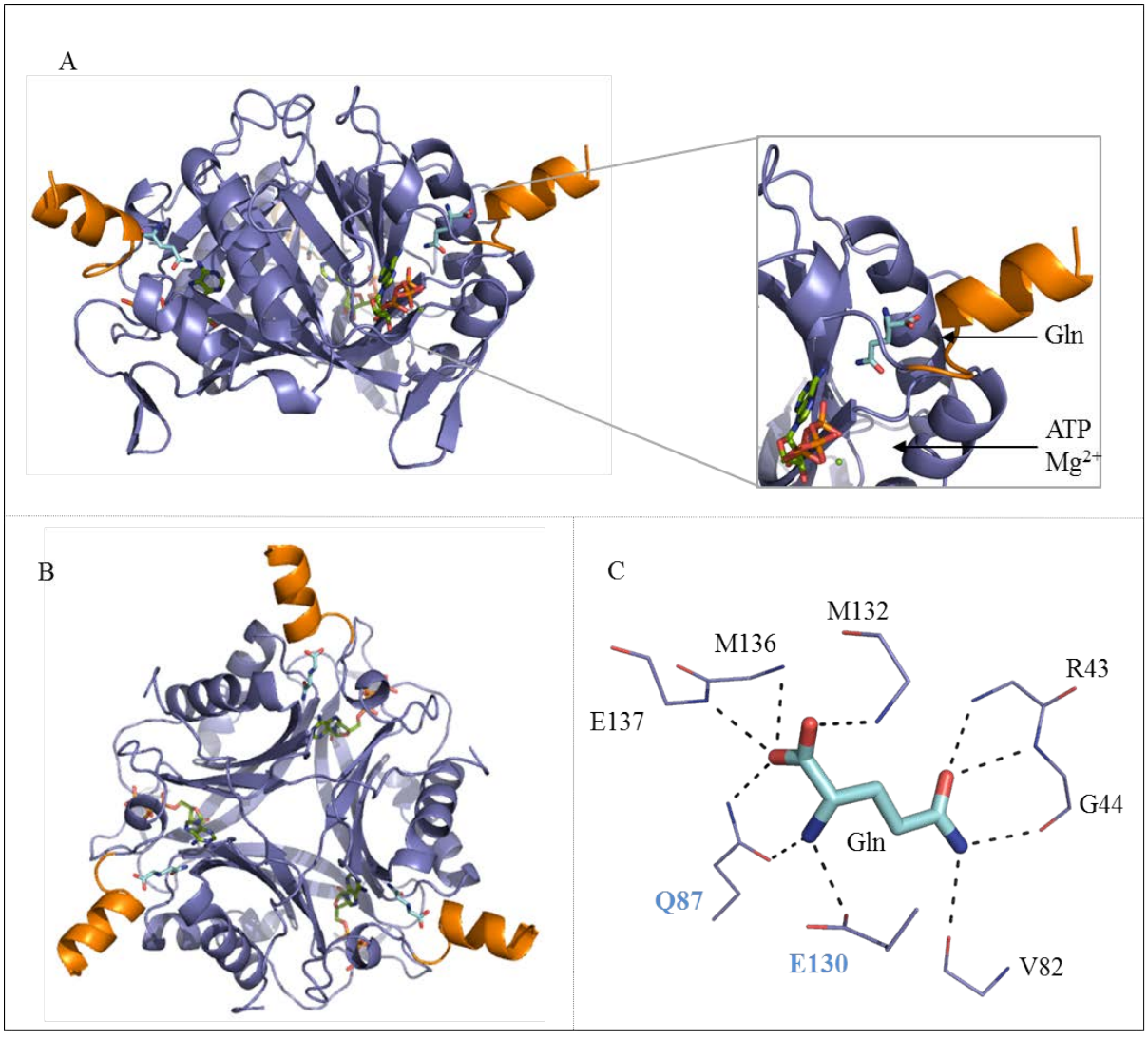

Figure 29. Close view of *Cr* PII in the complex structure. A) Zoomed out view of the binding pocket of glutamine with the C terminus colored in orange. B) Top view of the *Cr* PII trimer in the complex structure. C) Polar contacts formed by glutamine with the neighbouring residues (side chain contacts: blue, main chain contacts: black).

C. reinhardtii has a long C-terminus in comparison to its bacterial counterparts. In the crystal structure, this unique C-terminus faces outwards and acts as a plug to hold the glutamine molecule intact in the binding pocket (Fig. 29A). The glutamine occupies a site close to the ATP binding pocket, however it is located opposite to the 2-OG binding site. Three molecules of glutamine are bound to the *Cr* PII trimer. The glutamine majorly makes a contact with the backbone of the neighbouring residues R43, G44, V82, M132, M136, and E137; and the side chain interactions involve the residues Q87 and E130 (Fig. 29C). The numbering of residues corresponds to the *Cr* PII and *At* NAGK aminoacid sequences without signal peptide.

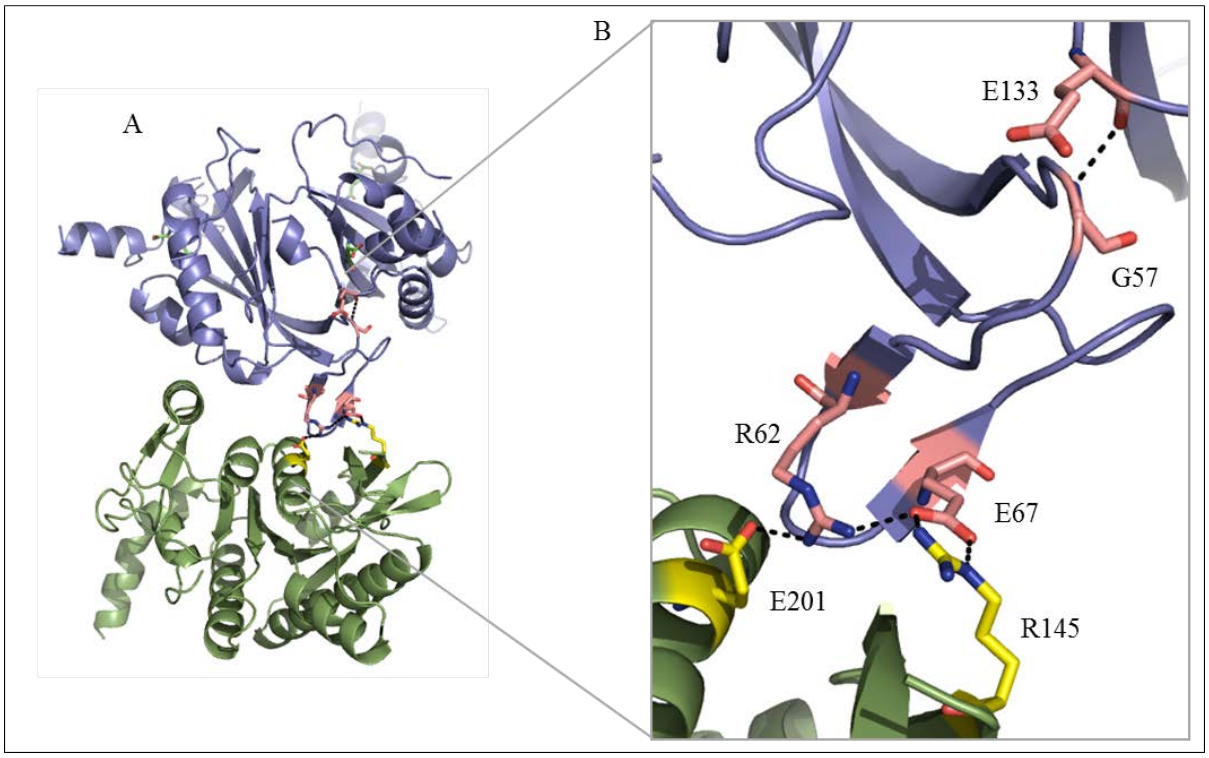

Figure 30. Interaction between *Cr* PII (slate) and *At* NAGK (green). A) *At* NAGK interacts with *Cr* PII by establishing a contact with the help of T-loop. B) A close view of the interaction interface and the residues (forming polar contacts) involved in aiding the kinked T-loop conformation are highlighted.

Due to the binding of glutamine to the C-terminal extension, a polar contact can be formed between the backbones of G57 and E133 (C-terminus) from the adjacent PII monomer (Fig. 30). This bond favours the communication between T-loop and the C-terminus. The polar interaction between the residues R62 and E67 of *Cr* PII with the residues E201 and R145 of *At* NAGK helps the T-loop to adopt a conformation which can insert into the NAGK toroid. Delta C *Cr* PII was unable to bind to NAGK in the presence of ATP-Mg and glutamine, which might be due to the absence of the residue E133 which helps to stabilize the structure of the T-loop that fits into NAGK.

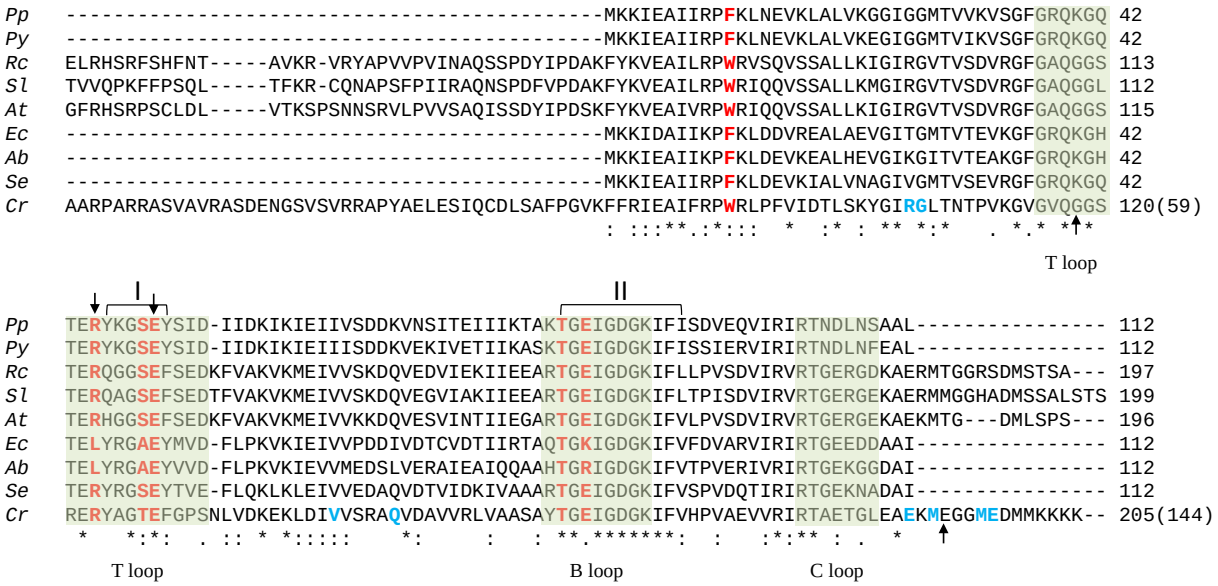

Figure 31. Multiple sequence alignment of PII protein sequences (including signal peptide) from red algae, bacteria and Viridiplantae. The PII signature (I and II) residues known to be involved in interaction with NAGK are highlighted in red. The important residues from *Cr* PII protein that aid the formation of a kinked T-loop [G57 (G118), E133 (E194), R62 (R123), E67 (E128)] that enables to establish a contact with *At* NAGK are indicated with an arrow (residues in bracket correspond to numbering of sequence with the signal peptide). The residues forming a polar contact with the glutamine molecule are represented in blue. [*Pp*: *Porphyra purpurea*, *Py*: *Pyropia yezoensis*, *Rc*: *Ricinus communis*, *Sl*: *Solanum lycopersicum*, *At*: *Arabidopsis thaliana*, *Ec*: *E. coli*, *Ab*: *Azospirillum brasiliensis*, *Se*: *Synechococus elongatus*, *Cr*: *Chlamydomonas reinhardtii*].

In order to understand the conservation of residues involved in the complex formation between *Cr* PII and *At* NAGK, a multiple sequence alignment of PII proteins from red algae, bacteria and plants was performed (Fig. 31). The T loop residue E67 is highly conserved across different organisms and the residue R62 is conserved in cyanobacteria, green plants and red algae but absent in other bacterial PII proteins. The residue G57 is conserved in green plants whereas Rhodophyta, cyanobacteria and other bacteria have a Lysine residue. Intriguingly, the residue E133 which is involved in initiating the complex formation seems to be unique for *Cr* PII.

10.6.5 *C. reinhardtii* PII and *A. thaliana* NAGK complex (2-OG soaking)

Cr PII and *At* NAGK proteins at a concentration of 2 mg/ml were mixed in a stoichiometric molar ratio of 1:2. The buffer consisted of 10 mM Tris pH 7.8, 100 mM NaCl, 40 mM Arg, 10 mM Gln, 2 mM $MgCl_2$, 2 mM ADP, 10 mM NAG and 5% glycerol. Diffraction quality crystals were obtained in a ground solution consisting of 0.1 M MES pH 6.5, 30% *v/v* PEG 400. The crystals were formed in 7 days and were subjected to a soaking experiment. The soaking solution contained the ground solution along with a mixture of NAG, ADP, 2-OG and PEG 400. The crystals diffracted up to 3.3 Angstrom and belonged to the same space group (P

2_1 3-Cubic) as the *Cr* PII-*At* NAGK complex mentioned above. The asymmetric unit consisted of two NAGK monomers and two PII monomers. The three fold symmetric axis of the cubic crystal lattice contained *At* NAGK hexamer sandwiched between two *Cr* PII trimers. The effector molecules ATP-Mg and glutamine bound to PII, ADP-Mg and NAG bound to NAGK were resolved in the binding pocket. B-factor plot comparison of the native and soaked structures revealed higher B factor for one of the PII trimers (soaked structure) showing an elevated flexibility to displace from NAGK toroid (Fig. 32B). This result displays an interesting snapshot of displacement of *Cr* PII trimer from *At* NAGK in the presence of an antagonist 2-OG.

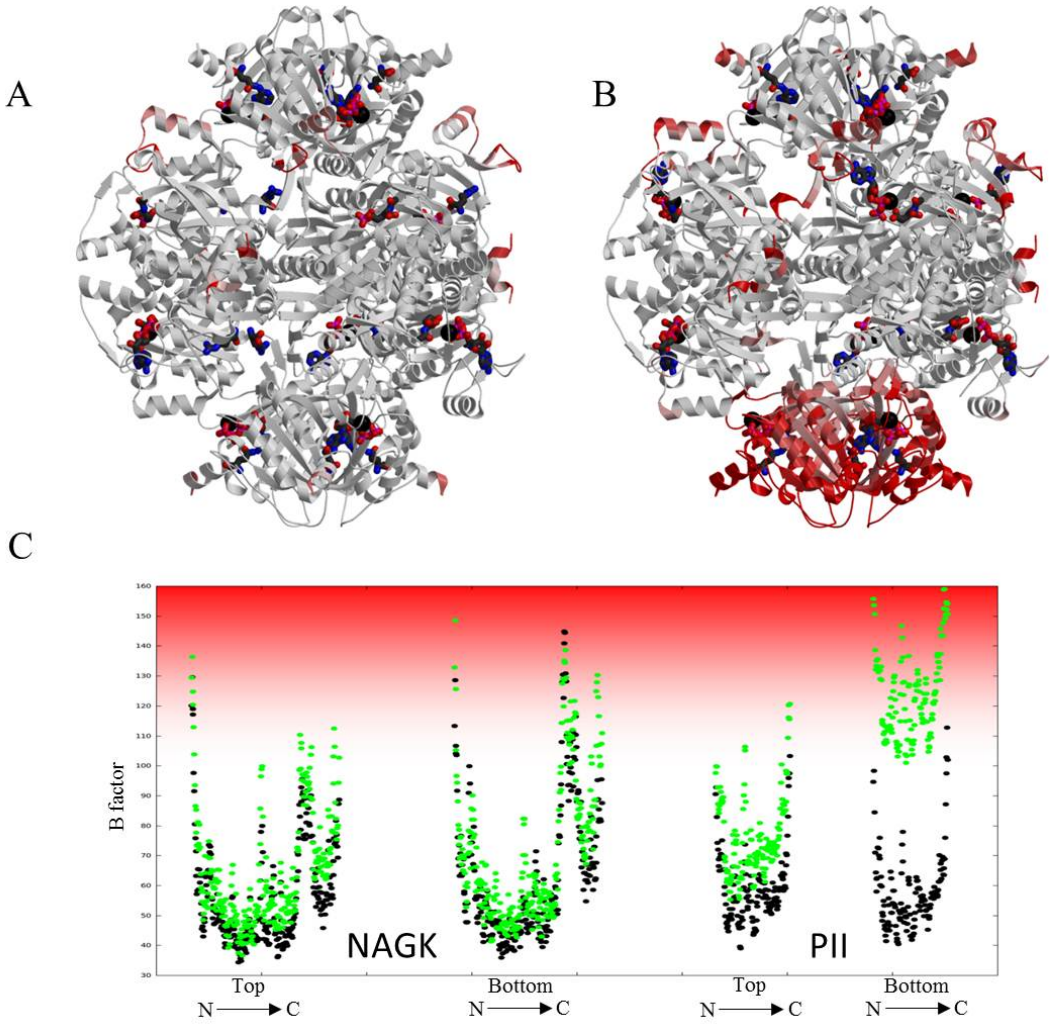

Figure 32. *Cr* PII-*At* NAGK structure subjected to a soaking experiment (NAG, ADP and 2-OG). A) The native complex structure (*Cr* PII-*At* NAGK) obtained is represented in ribbon with the effector molecules in stick B) Structure of the soaked crystal representing the high B factor values (red) for PII trimer which corresponds to the flexible movement of PII from NAGK protein. C) Comparison of the B factor values in the native and soaked crystal. The dots, black (native) and green (soaked) represent the B factor values of residues ranging from N to C-terminus for NAGK and PII. NAGK in the top and bottom of the toroid ring undergo minor changes in the B factor values. The PII trimer (top and bottom) are represented in the right side. An increase in B factor value of the PII trimer (bottom) is evident from the movement of green dots (soaked) away from the black dots (native).

10.6.6 *C. reinhardtii* PII-NAGK complex

The purified proteins *Cr* PII (without strep tag) and *Cr* NAGK at a concentration of 2 mg/ml were mixed together in the ratio of 1:2 in a buffer composed of 20 mM Tris pH 7.5, 150 mM NaCl, 1 mM DTT, 2 mM $MgCl_2$, 15% glycerol, 10 mM NAG, 2 mM ADP, 40 mM Arg and 10 mM Gln. Diffraction quality crystals were obtained within 30 days in a ground solution containing 25% *v/v* ethylene glycol. The crystals were flash frozen and subjected to X-ray diffraction technique.

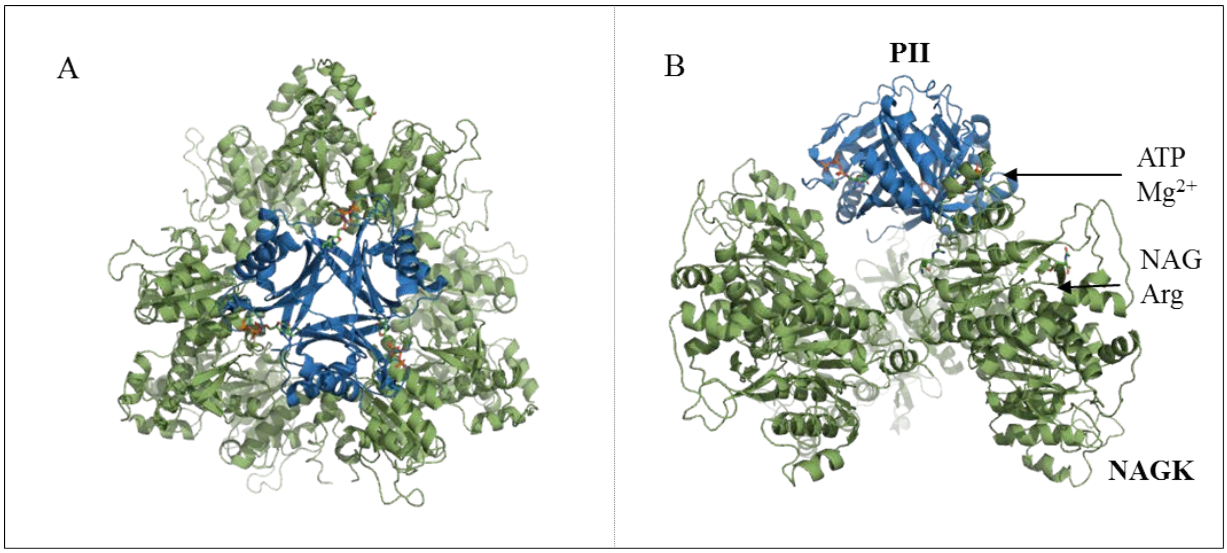

Figure 33. Crystal structure of the *Cr* PII-*Cr* NAGK complex.
A) Top and B) side view of the proteins *Cr* PII (blue) and *Cr* NAGK (green). The ligands ATP-Mg bound to *Cr* PII; and NAG, Arg bound to NAGK are represented as sticks. The complex consists of one PII trimer bound to the NAGK toroid. The previous known complexes of PII-NAGK from *S. elongatus* and *A. thaliana* consist of two PII trimers sandwiching the NAGK toroid from either sides.

The crystal structure was solved at 2.5 Angstrom resolution (P 6_3-Hexagonal) and consists of one *Cr* PII trimer bound to the *Cr* NAGK toroid (Fig. 33). This oligomeric conformation is strikingly different from the already known PII-NAGK complex structures. The structure of PII-NAGK from *S. elongatus* and *A. thaliana* consisted of two PII trimers sandwiching on either side of the NAGK toroid (Llácer *et al*, 2007; Mizuno *et al*, 2007). The opposite side of the NAGK toroid devoid of a PII trimer seems to be destabilized resulting in an extended and flexible NAGK ring form. The crystal structure consisted of ATP-Mg bound to PII and the effector molecules arginine, ADP and NAG bound to NAGK protein. Further, the T-loop of PII proteins was highly disordered in the crystal structure. The structure is in accord to the light scattering data which suggests the presence of one *Cr* PII trimer bound to the *Cr* NAGK toroid in solution.

10.6.7 X-ray crystallographic data

The crystallization trials were set up by using the Honeybee 963 robot from Genomic Solutions by mixing 500 nL of protein solution with 500 nL of reservoir solution in a 96-well sitting drop set up with 50 μL reservoir volume. The crystallization conditions for all crystals mentioned in the text above are included along with the soaking conditions where applicable. In certain cases, the quality of crystal was improved by screening various conditions with the hanging drop set up. All crystals were loop mounted and flash frozen in liquid nitrogen. The diffraction data were collected at the beamline X10SA (PXII) at the Swiss Light Source (Villigen, Switzerland) under cryo conditions at 100 K and the images were recorded on a PILATUS 6M (Dectris) detector (Table 5). Diffraction quality images were processed and scaled employing the XDS program suite (Kabsch, 1993, 2010). All the structures were solved by molecular replacement using the program MOLREP (Vagin and Teplyakov, 1997). Rebuilding and refinement of the structure was performed by using the programs Refmac and Coot (Murshudov *et al*, 1997; Emsley and Cowtan, 2004). The quality of the structure was tested by the program Procheck (Laskowski *et al*, 1993) and the figures were generated using PyMOL (www.pymol.org).

Table 5: Data collection and refinement statistics

	***Cr* PII (Apo)**	***Cr* PII (2-OG soaking)**	***Cr* PII (Cadmium)**
Data collection			
Space group	*P* 1 2_1 1 (Monoclinic)	*P* 1 2_1 (Monoclinic)	P 3 2 1 (Trigonal)
Cell dimensions			
a, *b*, *c* (Å)	41.98, 89.78, 45.94	42.03, 90.01, 46.20	81.22, 81.22, 42.60
α, β, γ (°)	90.00, 97.09, 90.00	90.00, 96.49, 90.00	90.00, 90.00, 120.00
Resolution (Å)	37.79-1.60(1.64-1.59)	32.84-1.49(1.53-1.49)	70.34-1.65(1.69-1.64)
Completeness (%)	100	98.38	94.84
No. of reflections	42096	51850	17902
R_{work}/R_{free}	0.18/0.22	0.17/0.20	0.21/0.26
Mean B value (overall)	18.15	15.53	18.64

	***Cr* PII-*At* NAGK**	***Cr* PII-*At* NAGK (2-OG soaking)**	***Cr* PII-*Cr* NAGK**
Data collection			
Space group	P 2_1 3 (Cubic)	P 2_1 3 (Cubic)	P 6_3 (Hexagonal)
Cell dimensions			
a, *b*, *c* (Å)	171.43, 171.43, 171.43	170.38, 170.38, 170.38	121.51, 121.51, 112.84
α, β, γ (°)	90.00, 90.00, 90.00	90.00, 90.00, 90.00	90.00, 90.00, 120.00
Resolution (Å)	39.33-2.85(2.92-2.85)	39.12-3.3(3.38-3.30)	38.48-2.50(2.56-2.49)
Completeness (%)	99.84	97.90	100.00
No. of reflections	37303	23176	31040
R_{work}/R_{free}	0.21/0.24	0.18/0.23	0.22/0.29
Mean B value (overall)	29.52	79.17	44.91

11. Discussion and outlook

The PII signal transduction proteins are highly conserved in 3D structure in spite of their occurrence in diverse organisms ranging from methanogenic archaea to heterotrophic bacteria and oxygenic phototrophs. They are regarded as the biological CPU due to their intrinsic ability to sense, integrate and respond to targets on binding metabolites. The study of PII proteins from various oxygenic phototrophs motivates to understand the evolutionary adaptation of these proteins. The following research focus was aimed at addressing few missing informational gap between the bacterial and plant PII proteins.

11.1 PII-NAGK complex formation (a two-step model)

Depending on the C/N and energy status of the cell, the PII proteins respond to various effector molecules such as ATP, ADP and 2-OG. Binding of these metabolites stimulates the conformational changes on PII proteins especially in the loop regions. These conformational changes dictate the affinity for their target receptors. One of the well-studied receptors is the second enzyme in the arginine synthesis pathway, NAGK. The crystal structure of PII-NAGK has been solved from *S. elongatus* and *A. thaliana* (Llácer *et al*, 2007; Mizuno *et al*, 2007). Through mutational studies combined with structural information a two-step model for the binding of PII to NAGK has been proposed. The NAGK variant R233A has an impaired ability to bind to *S. elongatus* PII proteins. A screening of PII mutants revealed the variants I86N and I86T to be able to bind to the NAGK R233A mutant. Interestingly, these PII variants showed inability to bind to 2-OG and highlighted the importance of the I86 residue. Solving the structure of the I86N mutant resolved the conformation adopted by the T-loop to be similar to the PII-NAGK bound form. Based on these data a two-step mechanism of binding of PII to NAGK has been proposed. First step involves the formation of an ion-pair between the E85 of PII and R233 of NAGK which results in the bent conformation of T-loop. The second step involves the insertion of this bent loop into the interdomain cavity of NAGK. The first step is initiated through the breaking of ion-pair between the residues R47 (T-loop) and E85 (B-loop) of PII which governs the extended form of the T-loop (Fig. 34), followed by establishing a firm contact between the residues E85 of PII and R233 of NAGK. Further, the crystal structure of PII I86N variant sheds light on the vital ion-pairs R45-E50 and E44-K58 which stabilize the bent conformation of the T-loop. Thus, the conjoint effort between the B and T-loop is essential for the PII interaction with its target receptors.

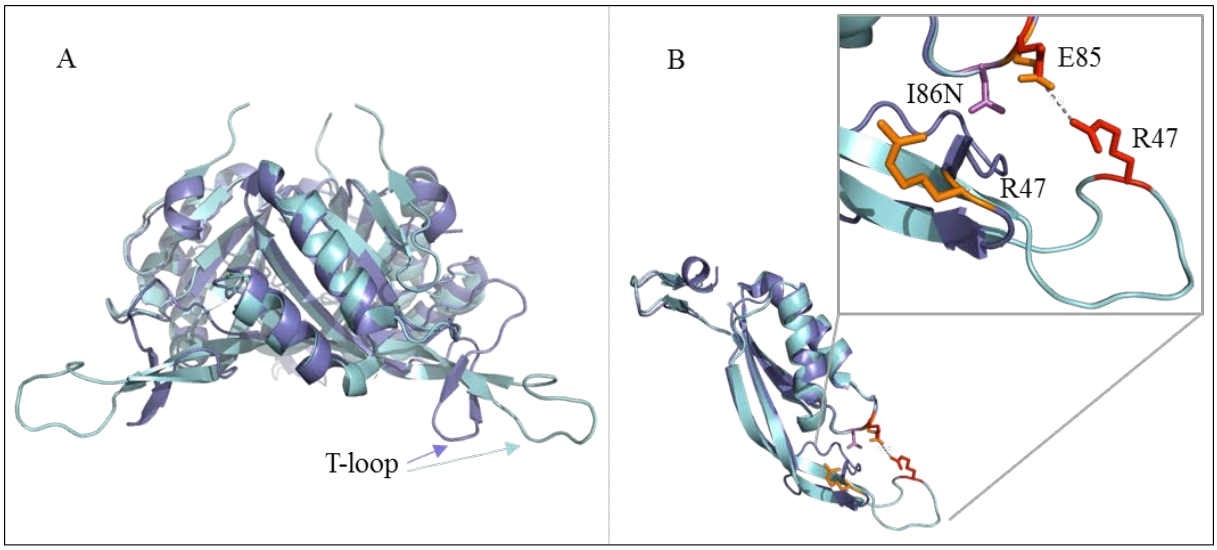

Figure 34. Structure of the PII protein variant I86N. A) Superimposed structure of the free PII (cyan) and the I86N (slate) variant shows the extended and bent conformation of the T-loop. B) Close view of the superimposed monomer highlighting the important residues for the T loop conformation. [1QY7-Cyan; R47 and E85-red, Xu *et al*., 2003], [2XBP-slate, R47 and E85-orange, Fokina *et al*, 2010b].

11.2 Insights into PII mediated 2-OG signalling

Nitrogen depletion condition in cell corresponds to the presence of excess 2-OG. Under these situations, PII proteins as a sensor have been shown to strongly respond to 2-OG in the presence of ATP-Mg (Maier *et al*, 2011; Gerhardt *et al*, 2012; Truan *et al*, 2010; da Rocha *et al*, 2013). The crystal structures of *S. elongatus* PII protein in the presence of excess 2-OG and limited 2-OG reveals the preferential occupation of this effector molecule in the intersubunit cleft. Isothermal titration experiments (ITC) suggested the anti-cooperative binding of the 2-OG molecule to the PII trimer. The binding of 2-OG to one site influences the binding to neighbouring site by leading to an increase in K_d values. Further, a crystal structure of three PII trimers in the asymmetric unit with one trimer containing three ATP, one Mg^{2+} and 2-OG (PII_{OG1}), the second with three ATP, two Mg^{2+} and two 2-OG (PII_{OG2}) and the third site with three molecules of ATP, Mg^{2+} and 2-OG (PII_{OG3}) were obtained. This structure profoundly supported the theory of anti-cooperative binding of 2-OG to PII trimer. The 2-OG binding to PII involves the hexagonal coordination formed by Mg^{2+} between the α, β and γ phosphate of ATP, O2 and O5 of 2-OG and OE1 atom of Q39. The ability of PII to respond to 2-OG in an anti-cooperative manner suggests the highly evolved intersubunit signalling between the PII monomers. The only contrast being the structure from *M. jannaschii*, where the 2-OG molecule binds from the posterior to the tip of T-loop (Yidiz *et al*, 2007). The binding of 2-OG induces the movement of C-terminus towards the ATP binding cleft and forces the T-loop to undergo a flexible and extended conformation

(disordered in crystal structure). The essential residues K58 and Q39 that are important for interaction with 2-OG are found to be highly conserved across organisms. The mutation of residues K58M and R9L in the PII protein resulted in impairment to sense the 2-OG molecule. The SPR experiments support the ability of 2-OG to disrupt the PII-NAGK complex formation. The influence of 2-OG to disrupt the complex formation has also been established in AmtB-GlnK, DraG-GlnZ and PII-PipX (Maier *et al*, 2011; Gerhardt et al., 2012; Laichoubi *et al*, 2012). Thus, the role of PII as a 2-OG sensor is essential to maintain the N balance inside the cell.

11.3 Conservation and evolution of PII functions from cyanobacteria to plastids

The widespread occurrence of the PII superfamily member GlnK and its genetic linkage to the ammonium transporter AmtB lead to the speculation of GlnK as the ancient protein of PII family (Thomas *et al*, 2000; Sant'Anna *et al*, 2009; Pedro-Roig *et al*, 2013). The paralogues of PII namely GlnB and NifI are probably derived from this ancient protein via gene duplication events. These paralogues are involved in control and regulation of nitrogen metabolism through diverse pathways. In addition, a distinct group of PII proteins namely PII-New Group (PII-NG) was found and considered to be involved in the regulation of heavy metal efflux pumps (Sant'Anna *et al*, 2009). Few organisms have been reported to harbour more than two PII paralogues, their function needs to be investigated (Jonsson and Nordlund, 2007). In cyanobacteria and plants the canonical PII protein GlnB, interacts with NAGK to regulate the arginine synthesis pathway. Bioinformatics analysis through construction of phylogenetic tree and cluster based sequence analysis (CLANS: Frickey and Lupas, 2004) have implicated in the coevolution of PII-NAGK from cyanobacteria to plants. CLANS analysis have highlighted that the PII sequence clusters from plant and algae share similarity with cyanobacteria, which in turn are closer to other bacteria. Whereas, the NAGK sequences from cyanobacteria, algae and plants cluster tight together in accordance with the endosymbiotic theory. The NAGK sequences show less divergence in comparison to PII protein sequences revealing their rigorous evolutionary pressure. Due to changes in environmental conditions, organisms have adapted themselves by undergoing stringent manipulations in their metabolic network. This suggests that any change in the NAGK enzyme would have resulted in corresponding alterations in PII protein to keep the N regulation machinery under control.

11.4 Role of glutamine in PII-NAGK complex formation: with a focus on *C. reinhardtii*

Glutamine signalling has been examined in proteobacteria to be mediated through the regulation of GS, UTase/UR system and Ntr regulon (Jiang *et al*, 1997; Forchhammer 2007; Jiang *et al*, 2012). A direct influence of glutamine on the PII proteins has not been reported till date. Surprisingly, in the case of *C. reinhardtii* system, complex formation between PII-NAGK is completely dependent on the presence of ATP-Mg and glutamine. The activity of *Cr* NAGK alone with a K_m of 7.77 mM for NAG drops down significantly to 3.94 mM in the presence of *Cr* PII, ATP-Mg and glutamine, suggesting the activation of *Cr* NAGK. In addition, *Cr* NAGK is highly susceptible to arginine inhibition and *Cr* PII relieves this inhibition only in the presence of glutamine. Enzyme activity assays display a steady increase in the *Cr* PII-NAGK activity with the addition of up to 10 mM Gln. However, the introduction of 2-OG as an antagonist into the system disrupts the enzyme activation process. Importantly, SPR experiments supported the influence of glutamine in complex formation between PII and NAGK. The expulsion of glutamine in the reaction mixture resulted in immediate dissociation of the complex. In contrast to the enzyme activity results, the antagonist 2-OG did not prevent complex formation even at very high concentrations. This might be due to the binding of PII to immobilised NAGK on NTA chip resulting in hindrance to access the binding site. However, the enzyme activity tests allow a greater degree of freedom in solution for the 2-OG accessibility. Furthermore, in the presence of ADP-Mg and glutamine the complex formation was not initiated and hence ADP isn't capable of replacing the function of ATP. A C-terminal truncated version of *Cr* PII (Delta C *Cr* PII) was incapable of binding to *Cr* NAGK even in the presence of ATP, Mg^{2+} and glutamine. This sheds light on the special characteristic feature of the C terminus of *Cr* PII which aids in binding of glutamine. In the SPR experiments, *Se* PII doesn't bind *Cr* NAGK which suggests the unique characteristic of *Cr* NAGK protein to respond only to its native PII protein. No influence of glutamine on WT *Se* PII to initiate complex formation with *Cr* NAGK was found, suggesting the unique feature of *Cr* PII to respond to glutamine. However, it is notable that *Cr* PII can remarkably activate the WT *Se* NAGK in the presence of ATP-Mg and glutamine. This highlights that the glutamine effect is a novel property of *Cr* PII protein. The extraordinary characteristic of *Cr* PII to respond to its non-native NAGK protein sheds light on the possible adaptation of PII proteins through the evolutionary process.

11.5 Novel C-terminus of *C. reinhardtii* and its role

The effect of glutamine to favour the PII-NAGK complex formation process adds another level of complexity to the nitrogen regulation system. This unique feature of glutamine signalling has not been detected earlier in other organisms. The effort to determine similar effect of glutamine on *Se* PII and *At* PII to activate the NAGK failed. This provides insight into the extraordinary feature of the *C. reinhardtii* PII protein. The *Cr* PII protein consists of a unique N and C-terminus and has been found to be localised in the chloroplast. The C-terminus is exclusively longer and terminates with a stretch of positive residues. In order to study this special effect, a 12 aminoacid truncated version of C-terminus, mimicking the bacterial PII protein was constructed. Even in the presence of ATP-Mg and glutamine this construct could not activate the complex formation between PII-NAGK in the enzymatic assays. Furthermore, the truncated *Cr* PII protein was subjected to a titration with 2-OG in an ITC experiment and was found to respond by binding in the presence of ATP-Mg thereby confirming its active state. The influence of C-terminus on the complex formation was further investigated and confirmed employing SPR and ITC experiments. Thus, the presence of glutamine, ATP-Mg along with C-terminus is a prerequisite for the PII-NAGK complex formation in *C. reinhardtii.*

11.6 Binding of effector molecules to *Cr* PII

The PII proteins act as a biological CPU, where the signals from the metabolites ADP, ATP and 2-OG are integrated leading to allosteric and covalent modifications. These modifications result in conformation changes which mediate the varied receptor interactions. The novel trait of PII to bind glutamine and thereby activate the complex formation with NAGK is attributed to the *C. reinhardtii* system. This introduces glutamine as a novel metabolite sensed by the PII signal transduction family (Fig. 35). The special feature of PII mediated glutamine signaling is not associated with *S. elongatus* or *A. thaliana* PII proteins. Up to 15 mM Gln is required to saturate the PII-NAGK activity in the enzyme assays. Binding of glutamine assists in the extended antenna-like framework of the C-terminus which influences the T-loop conformation and thereby its interaction with NAGK. In SPR experiments, the presence of ATP-Mg alone doesn't seem to favour the complex formation. Introduction of ADP neither favours the PII-NAGK complex formation in the presence of glutamine and Mg^{2+}. This suggests the influence and importance of the γ-phosphate of ATP in the complex formation.

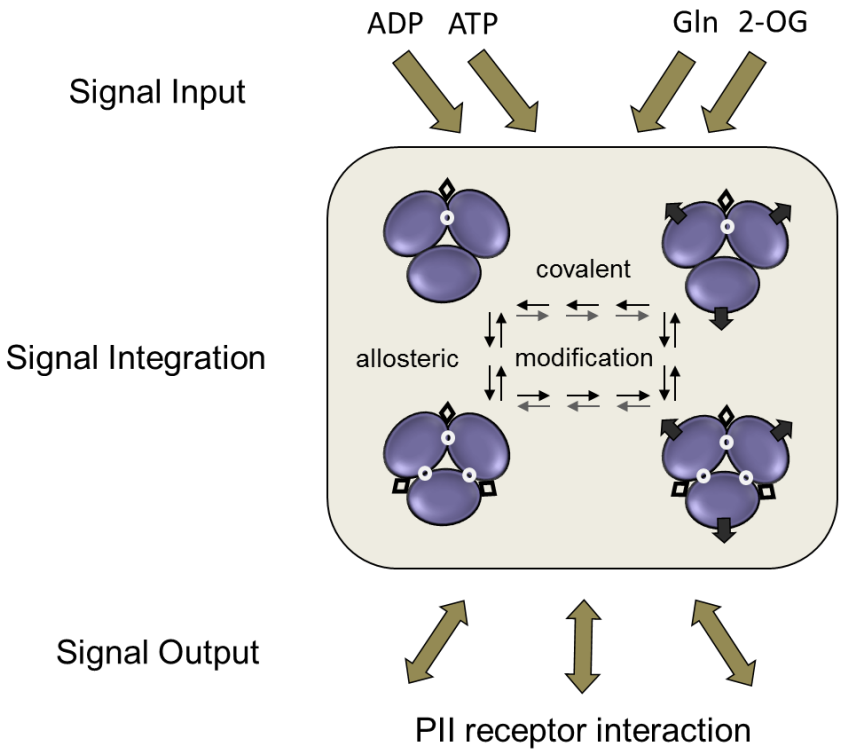

Figure 35. PII proteins act as a biological CPU. Based on the energy status of the cell, the PII proteins have been known to bind the molecules (signal input) ADP, ATP and 2-OG. A new effector molecule glutamine (Gln) has been introduced into the signal input pathway. On sensing these metabolites PII proteins undergo covalent and allosteric modifications (signal integration) which results in the PII-receptor interaction (signal output).

Addition of 2-OG to enzymatic assay inhibits activation of the enzyme activity. However, SPR experiments suggest no influence of 2-OG on complex formation. The fact that 2-OG does not prevent complex formation is also supported with the light scattering analysis. It is possible that 2-OG affects the PII-NAGK complex in a post-binding step, where the T-loop may adopt a different conformation in the presence of 2-OG. With the help of ITC experiments the affinity of 1 mM 2-OG for *Cr* PII was determined to be 39 µM, which is similar to that observed in *S. elongatus* PCC 7942 (Fokina *et al*, 2011). Binding of 2-OG is mediated through ATP-Mg and ADP doesn't seem to support 2-OG binding. However, in *A. thaliana* 2-OG binding was stimulated in the presence of both ATP and ADP (Smith *et al*, 2003).

Further, crystallization of *Cr* PII containing 0.05 M Cadmium sulfate in ground solution resulted in PII protein structures with 9 cadmium ions bound per trimer. Earlier, PII paralogues have been speculated to binding heavy metal efflux pumps, and its noteworthy that *C. reinhardtii* have been used in the waste remediation process to sequester heavy metals (Sant'Anna *et al*, 2009; Wei *et al*, 2011). Hence, it would be worthwhile to analyse the affinity and mechanism of heavy metal binding to *Cr* PII.

11.7 Mechanism of glutamine binding to promote the formation of *Cr* PII and NAGK complexes

The structure of *Cr* PII and *At* NAGK complex revealed the binding site of glutamine near the C-terminus of PII. The PII protein with its unique C-terminus forms an alpha helix that extends outward as an antenna from the PII body and captivates the glutamine in the binding pocket. The movement of the C-terminus closer to the B-loop is favoured by the backbone interaction of G57 (B-loop) and E133 from the C-terminus of neighbouring subunit. This tight conformation mediates the T-loop to undergo a kinked conformation which thereby helps to contact the interdomain crevice of NAGK. The polar network of interaction between the T-loop residues E67 and R62 of *Cr* PII and R145 and E201 of *At* NAGK helps to favour the complex formation. The electrostatic surface potential representation (Fig. 36) gives an insight into the positively charged C-terminus of *Cr* PII protein. These positively charged residues play an essential role by aiding in the suitable conformation of C-terminus (displace away from the PII body) and thereby plugging the glutamine to the binding socket.

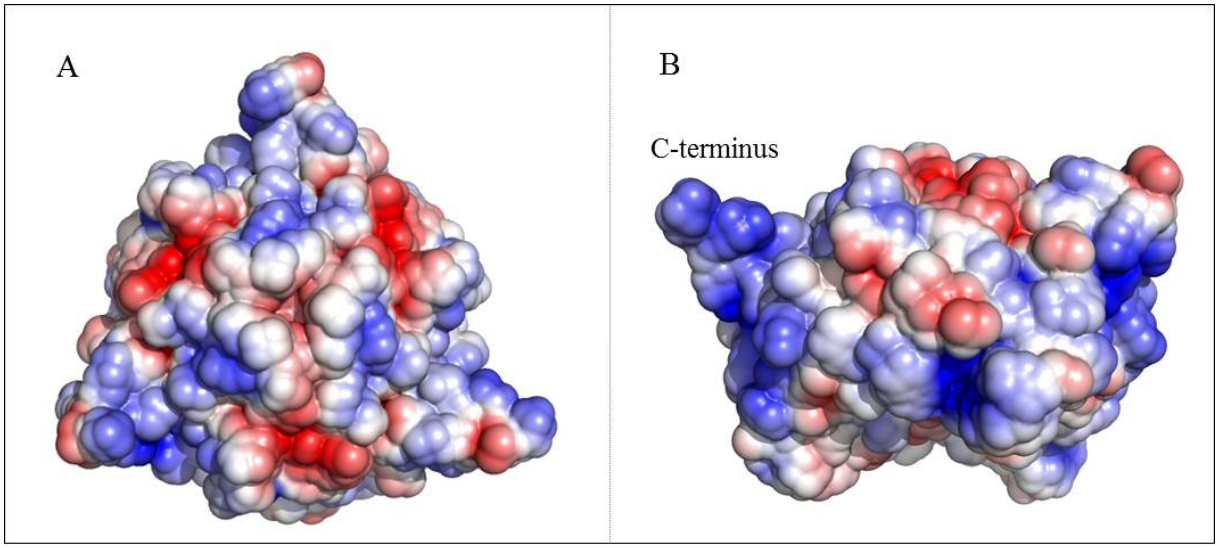

Figure 36. Electrostatic surface potential representation of *Cr* PII in the *Cr* PII-*At* NAGK complex. A) Top view and B) side view of complex highlighting the unique positively charged C terminus of *Cr* PII protein (Positive potentials displayed in blue and negative in red). Figures were generated employing APBS program.

The crystallization of *Cr* (PII-NAGK) resulted in crystal structures with only one PII trimer bound to the NAGK toroid. This is the first reported structure of one PII occupying the complex structure. The interaction of *Cr* (PII-NAGK) seems rather infirm due to the flexible movement of the NAGK toroid ring. Further, the oligomeric state of the *Cr* (PII-NAGK) complex in solution was investigated with light scattering experiments. These results as well supported the existence of one PII trimer bound to the NAGK toroid in solution.

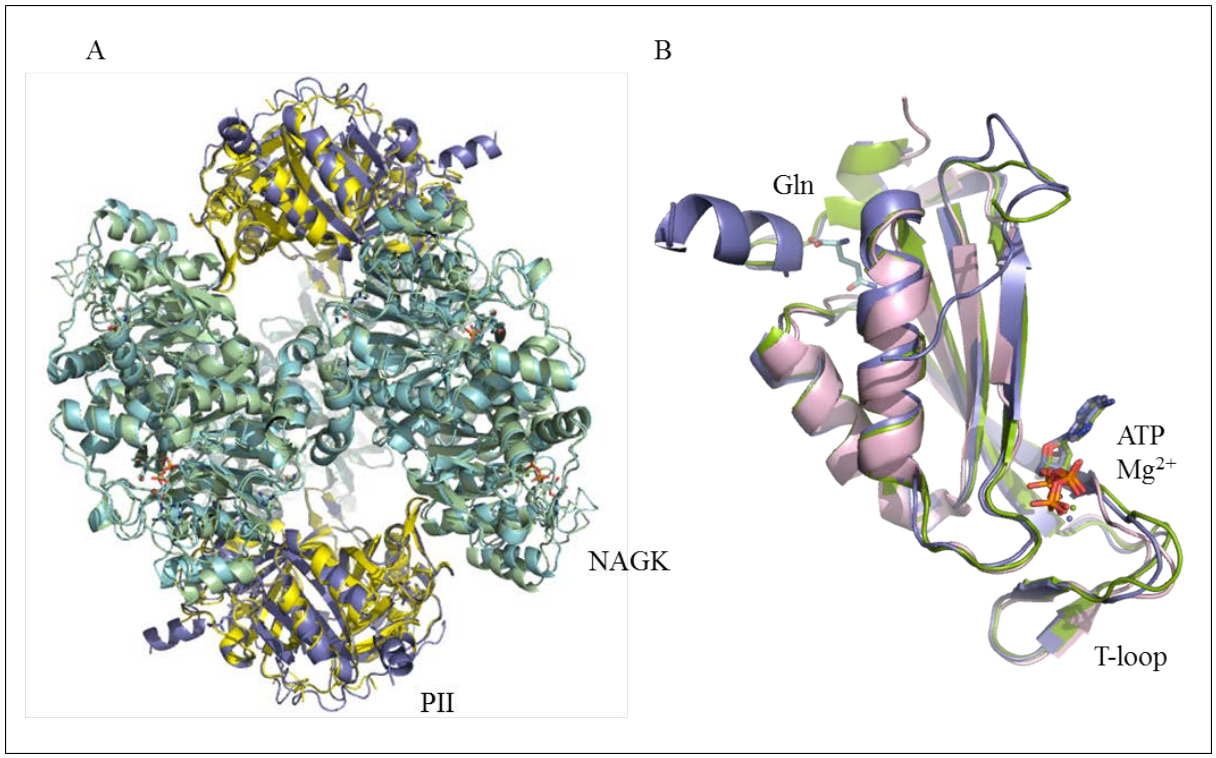

Figure 37. A) Superimposed structures of *Cr* PII (slate)-*At* NAGK (green) complex and *At* PII (yellow)-NAGK (cyan) complex (PDB: 2RD5). B) Superimposed structures of PII monomers from *Cr* PII (slate)-*At* NAGK complex, *A. thaliana* (PII-NAGK)-green (PDB: 2RD5), *S. elongatus* (PII-NAGK)-light pink (PDB: 2JJ4).

The superimposition of native *At* (PII-NAGK) structure with the obtained *Cr* PII-*At* NAGK resulted in NAGK displaying same 3-D structural configuration in both the structures (Fig. 37A). Hence, the crystal structure of *Cr* PII and *At* NAGK together should display a reliable confirmation of the *Cr* PII protein. The superimposition of PII proteins from known PII-NAGK complexes of *A. thaliana* and *S. elongatus* with *Cr* PII from *Cr* PII-*At* NAGK structure is represented in Fig. 37B. The three PII proteins show a high degree of structural conservation and the metabolites ATP-Mg are found to occupy the same position in the binding cavity.

The influence of glutamine on the PII protein needs to be further examined and explored in other organisms. It is possible to envision *Cr* PII as a potential candidate for a glutamine biosensor. This study has allowed the understanding of the role of glutamine in the PII-NAGK complex formation process in *C. reinhardtii*. Further, the unique evolutionary feature of PII mediated glutamine signalling for the regulation of N metabolism is evident. This signalling has not been found in *S. elongatus* and *A. thaliana* PII proteins and it's tempting to speculate that green algae have specially acquired this specific quality which was probably lost in higher plants. Further studies need to be performed to bridge the informational gap between the evolution of PII proteins from cyanobacteria to plants.

12. References

Adler SP, Purich D, Stadtman ER (1975). Cascade control of *Escherichia coli* glutamine synthetase. Properties of the PII regulatory protein and the uridylyltransferase-uridylyl-removing enzyme. *J Biol Chem*: 250(16), 6264-72.

Anderson JW and Done J (1978). Light-dependent assimilation of nitrite by isolated chloroplasts. *Plant Physiol*: 61, 692-97.

Arcondéguy T, Jack R, Merrick M (2001). P(II) signal transduction proteins, pivotal players in microbial nitrogen control. *Microbiol Mol Biol Rev*: 65(1), 80-105.

Atkinson MR, Blauwkamp TA, Bondarenko V, Studitsky V, Ninfa AJ (2002). Activation of the *glnA*, *glnK*, and *nac* promoters as *Escherichia coli* undergoes the transition from nitrogen excess growth to nitrogen starvation. *J Bacteriol*: 184, 5358-63.

Atkinson MR, Kamberov ES, Weiss RL, Ninfa AJ (1994). Reversible uridylylation of the *Escherichia coli* PII signal transduction protein regulates its ability to stimulate the dephosphorylation of the transcription factor nitrogen regulator I (NRI or NtrC). *J Biol Chem*: 269(45), 28288-93.

Ball S (1998). Regulation of starch biosynthesis. The molecular biology of chloroplasts and mitochondria in *Chlamydomonas*. eds Rochaix JD, Goldschmidt-Clermont M, Merchant S (Kluwer, Dordrecht, The Netherlands): 549-67.

Baud S, Feria Bourrellier AB, Azzopardi M, Berger A, Dechorgnat J, Daniel-Vedele F, Lepiniec L, Miquel M, Rochat C, Hodges M, Ferrario-Méry S (2010). PII is induced by WRINKLED1 and fine-tunes fatty acid composition in seeds of *Arabidopsis thaliana*. *The Plant Journal*: 64, 291-303.

Beez S, Fokina O, Herrmann C, Forchhammer K (2009). N-acetyl-L-glutamate kinase (NAGK) from oxygenic phototrophs: P(II) signal transduction across domains of life reveals novel insights in NAGK control. *J Mol Biol*: 389(4), 748-58.

Blankenship RE (2002). Molecular Mechanisms of Photosynthesis. Blackwell Science, Oxford.

Blankenship RE (2010). Early Evolution of Photosynthesis. *Plant Physiol*: 154(2), 434-38.

Björn LO and Govindjee G (2009). The evolution of photosynthesis and chloroplasts. *Curr Sci*, 96, 1466-74.

Brunswick P and Cresswell CF (1988). Nitrite uptake into intact pea chloroplast. II. Influence of electron transport regulators, uncouplers, ATPase and anion uptake inhibitors and protein binding reagents. *Plant Physiol*: 86, 384-89.

Bueno R, Pahel G, Magasanik B (1985). Role of glnB and glnD gene products in regulation of the glnALG operon of *Escherichia coli*. *J Bacteriol*: 164(2), 816-22.

Burillo S, Luque I, Fuentes I, Contreras A (2004). Interactions between the nitrogen signal transduction protein PII and N-acetyl glutamate kinase in organisms that perform oxygenic photosynthesis. *J Bacteriol*: 186(11), 3346-54.

Chen Q and Silflow CD (1996). Isolation and characterization of glutamine synthetase genes in *Chlamydomonas reinhardtii*. *Plant Physiol*: 112(3), 987-96.

Chen YM, Ferrar TS, Lohmeier-Vogel EM, Morrice N, Mizuno Y, Berenger B, Ng KK, Muench DG, Moorhead GB (2006). The PII signal transduction protein of *Arabidopsis thaliana* forms an arginine-regulated complex with plastid N-acetyl glutamate kinase. *J Biol Chem*: 281, 5726-33.

Colegrave N (2002). Sex releases the speed limit on evolution. *Nature*: 420(6916), 664-66.

Collins S and Bell G (2004). Phenotypic consequences of 1,000 generations of selection at elevated CO2 in a green alga. *Nature*: 431(7008), 566-69.

Conroy MJ, Durand A, Lupo D, Li XD, Bullough PA, Winkler FK, Merrick M (2007). The crystal structure of the *Escherichia coli* AmtB-GlnK complex reveals how GlnK regulates the ammonia channel. *Proc Natl Acad Sci*: 104(4), 1213-8.

Coutts G, Thomas G, Blakey D, Merrick M (2002). Membrane sequestration of the signal transduction protein GlnK by the ammonium transporter AmtB. *EMBO J*: 21, 536-45.

da Rocha RA, Weschenfelder TA, de Castilhos F, de Souza EM, Huergo LF, Mitchell DA (2013). Mathematical model of the binding of allosteric effectors to the *Escherichia coli* PII signal transduction protein GlnB. *Biochemistry*: 52(15), 2683-93.

De Visser JAGM, Hoekstra RF, Van Den Ende H (1996). The effect of sex and deleterious mutations on fitness in *Chlamydomonas*. *Proc R Soc Lond B*: 263, 193-200.

Du Y, Zhu L, Shan G (2012). Removal of Cd^{2+} from contaminated water by nano-sized aragonite mollusk shell and the competition of coexisting metal ions. *J Colloid Interface Sci*: 367(1), 378-82.

Durand A and Merrick M (2006). In vitro analysis of the *Escherichia coli* AmtB-GlnK complex reveals a stoichiometric interaction and sensitivity to ATP and 2-oxoglutarate. *J Biol Chem*: 281, 29558-67.

Eisenberg D, Gill HS, Pfluegl GM, Rotstein SH (2000). Structure-function relationships of glutamine synthetases. *Biochim Biophys Acta*: 1477(1-2), 122-45.

Emanuelsson O, Nielsen H, von Heijne G (1999). ChloroP, a neural network-based method for predicting chloroplast transit peptides and their cleavage sites. *Protein Sci*: 8, 978-84.

Emsley P and Cowtan K (2004). Coot: Model-building tools for molecular graphics. *Acta Cryst D*: 60, 2126-32.

Ermilova E and Forchhammer K (2013). PII signaling proteins of cyanobacteria and green algae. New features of conserved proteins. *Russ J Plant Physiol*: 60 (4), 483-90.

Ermilova E, Lapina T, Zalutskaya Z, Minaeva E, Fokina O, Forchhammer K (2013). PII Signal Transduction Protein in *Chlamydomonas reinhardtii*: Localization and Expression Pattern. *Protist*: 164(1), 49-59.

Espinosa J, Forchhammer K, Burillo S, Contreras A (2006). Interaction network in cyanobacterial nitrogen regulation: PipX, a protein that interacts in a 2-oxoglutarate dependent manner with PII and NtcA. *Mol Microbiol*: 61(2), 457-69.

Espinosa JK, Forchhammer K, Contreras A (2007). Role of the *Synechococcus* PCC 7942 nitrogen regulator protein PipX in NtcA-controlled processes. *Microbiology*: 153, 711-18.

Feria Bourrellier AB, Ferrario-Méry S, Vidal J, Hodges M (2009). Metabolite regulation of the interaction between *Arabidopsis thaliana* PII and N-acetyl-l-glutamate kinase. *Biochem Biophys Res Commun*: 387(4), 700-4.

Feria Bourrellier AB, Valot B, Guillot A, Ambard-Bretteville F, Vidal J, Hodges M (2010). Chloroplast acetyl-CoA carboxylase activity is 2-oxoglutarate regulated by interaction of PII with the biotin carboxyl carrier subunit. *Proc Natl Acad Sci*: 107, 502-7.

Fernandez E and Galvan A (2008). Nitrate Assimilation in *Chlamydomonas Eukaryotic Cell*: 7(4), 555-59.

Ferrario-Méry S, Meyer C, Hodges M (2008). Chloroplast nitrite uptake is enhanced in *Arabidopsis* PII mutants. *FEBS Lett*: 582(7), 1061-6.

Florencio FJ and Vega JM (1983). Utilization of nitrate, nitrite and ammonium by *Chlamydomonas reinhardii*. *Planta*: 158, 288-93.

Fokina O, Chellamuthu VR, Forchhammer K, Zeth K (2010a). Mechanism of 2-oxoglutarate signaling by the *Synechococcus elongatus* PII signal transduction protein. *Proc Natl Acad Sci*: 107(46), 19760-65.

Fokina O, Chellamuthu VR, Zeth K, Forchhammer K (2010b). A novel signal transduction protein P(II) variant from *Synechococcus elongatus* PCC 7942 indicates a two-step process for NAGK-P(II) complex formation. *J Mol Biol*: 399(3), 410-21.

Fokina O, Herrmann C, Forchhammer K (2011). Signal-transduction protein P(II) from *Synechococcus elongatus* PCC 7942 senses low adenylate energy charge in vitro. *Biochem J*: 440(1), 147-56.

Forchhammer K (2007). Glutamine signaling in bacteria. *Front. Biosci*: 12, 358-70.

Forchhammer K (2008). P(II) signal transducers: novel functional and structural insights. *Trends Microbiol*: 16(2), 65-72.

Forchhammer K (2010). The Network of P_{II} Signalling Protein Interactions in Unicellular Cyanobacteria. *Adv Exp Med Biol*: 675, 71-90.

Forchhammer K and Tandeau de Marsac N (1994). The PII protein in the cyanobacterium *Synechococcus* sp. strain PCC 7942 is modified by serine phosphorylation and signals the cellular N-status. *J Bacteriol*: 176(1), 84-91.

Forchhammer K and Tandeau de Marsac N (1995). Phosphorylation of the PII protein (glnB gene product) in the cyanobacterium *Synechococcus* sp. strain PCC 7942: analysis of in vitro kinase activity. *J Bacteriol*: 177(20), 5812-7.

Frickey T and Lupas A (2004). CLANS: a Java application for visualizing protein families based on pairwise similarity. *Bioinformatics*: 20, 3702-4.

Ghoshroy S, Binder M, Tartar A, Robertson DL (2010). Molecular evolution of glutamine synthetase II: Phylogenetic evidence of a non-endosymbiotic gene transfer event early in plant evolution. *BMC Evol Biol*: 10, 198. doi: 10.1186/1471-2148-10-198.

Gibson DG, Young L, Chuang RY, Venter JC, Iii CAH, Smith HO (2009). Enzymatic assembly of DNA molecules up to several hundred kilobases. *Nat Methods*: 6, 12-16.

Goodman HJ and Woods DR (1993). Cloning and nucleotide sequence of the *Butyrivibrio fibrisolvens* gene encoding a type III glutamine synthetase. *J Gen Microbiol*: 139, 1487-93.

Gerhardt EC, Araujo LM, Ribeiro RR, Chubatsu LS, Scarduelli M, Rodrigues TE, Monteiro RA, Pedrosa FO, Souza EM, Huergo LF (2012). Influence of the ADP/ATP ratio, 2-oxoglutarate and divalent ions on *Azospirillum brasilense* PII protein signaling. *Microbiology*: 158, 1656-63.

Grossman AR, Harris EE, Hauser C, Lefebvre PA, Martinez D, Rokhsar D, Shrager J, Silflow CD, Stern D, Vallon O, *et al* (2003). *Chlamydomonas reinhardtii* at the crossroads of genomics. *Eukaryot Cell*: 2(6), 1137-50.

Gruswitz F, O'Connell J III, Stroud RM (2007). Inhibitory complex of the transmembrane ammonia channel, AmtB, and the cytosolic regulatory protein, GlnK, at 1.96 A. *Proc Natl Acad Sci*: 104(1), 42-7.

Harris EH (2009). The *Chlamydomonas* sourcebook: Introduction to *Chlamydomonas* and its laboratory use, 2nd ed., vol. 1, Elsevier, Amsterdam, The Netherlands.

Hayes JM (1996). The earliest memories of life on Earth. *Nature*: 384(6604), 21-2.

Heinrich A, Maheswaran M, Ruppert U, Forchhammer K (2004). The *Synechococcus elongatus* PII signal transduction protein controls arginine synthesis by complex formation with N-acetyl-L-glutamate kinase. *Mol Microbiol*: 52(5), 1303-14.

Hemschemeier A, Fouchard S, Cournac L, Peltier G, Happe T (2008). Hydrogen production by *Chlamydomonas reinhardtii*: an elaborate interplay of electron sources and sinks. *Planta*: 227(2), 397-407.

Hill RT, Parker JR, Goodman HJK, Jones DT, Woods DR (1989). Molecular analysis of a novel glutamine synthetase of anaerobe *Bacteroides fragilis*. *J Gen Microbiol*: 135, 3271-79.

Hsieh MH, Lam HM, van de Loo FJ, Coruzzi G (1998). A PII-like protein in *Arabidopsis*: putative role in nitrogen sensing. *Proc Natl Acad Sci*: 95(23), 13965-70.

Huergo LF, Pedrosa FO, Muller-Santos M, Chubatsu LS, Monteiro RA, Merrick M, Souza EM (2012). PII signal transduction proteins: pivotal players in post-translational control of nitrogenase activity. *Microbiology*: 158(1), 176-90.

Irmler A and Forchhammer K (2001). A PP2C-type phosphatase dephosphorylates the PII signaling protein in the cyanobacterium *Synechocystis* PCC 6803. *Proc Natl Acad Sci*: 98, 12978-83.

Jaggi R, Ybarlucea W, Cheah E, Carr PD, Edwards KJ, Ollis DL, Vasudevan SG (1996). The role of the T-loop of the signal transducing protein PII from *Escherichia coli*. *FEBS Lett*: 391, 223-8.

Jamers A, Lenjou M, Deraedt P, van Bockstaele D, Blust R, de Coen W (2009). Flow cytometric analysis of the cadmium-exposed green algae *Chlamydomonas reinhardtii* (Chlorophyceae). *Eur J Phcol*: 44, 541-50.

Javelle A and Merrick M (2005). Complex formation between AmtB and GlnK: an ancestral role in prokaryotic nitrogen control. *Biochem Soc Trans*: 33(1), 170-72.

Javelle AE, Severi E, Thornton J, Merrick M (2004). Ammonium sensing in *Escherichia coli*. Role of the ammonium transporter AmtB and AmtB-GlnK complex formation. *J Biol Chem*: 279, 8530-8.

Jiang P and Ninfa AJ (2009). alpha-Ketoglutarate controls the ability of the *Escherichia coli* PII signal transduction protein to regulate the activities of NRII (NtrB) but does not control the binding of PII to NRII. *Biochemistry*: 48, 11514-21.

Jiang P, Peliska JA, Ninfa AJ (1998a). Enzymological characterization of the signal-transducing uridylyltransferase/uridylyl-removing enzyme (EC2.7.7.59) of *Escherichia coli* and its interaction with the PII protein. *Biochemistry*: 37, 12782-94.

Jiang P, Peliska JA, Ninfa AJ (1998b). Reconstitution of the signal transduction bicyclic cascade responsible for the regulation of Ntr gene transcription in *Escherichia coli*. *Biochemistry*: 37, 12795-801.

Jiang P, Peliska JA, Ninfa AJ (1998c). The regulation of *Escherichia coli* I glutamine synthetase revisited: role of 2-ketoglutarate in the regulation of glutamine synthetase adenylylation state. *Biochemistry*: 37, 12802-10.

Jiang P and Ninfa, AJ (1999). Regulation of autophosphorylation of *Escherichia coli* nitrogen regulator II by the PII signal transduction protein. *J Bacteriol*: 181, 1906-11.

Jiang P, Ventura AC, Ninfa AJ (2012). Characterization of the reconstituted UTase/UR-PII-NRII-NRI bicyclic signal transduction system that controls the transcription of nitrogen-regulated (Ntr) genes in *Escherichia coli*. *Biochemistry*: 51(45), 9045-57.

Jiang P, Zucker P, Atkinson MR, Kamberov ES, Tirasophon W, Chandran P, Schefke BR, Ninfa AJ (1997). Structure/function analysis of the PII signal transduction protein of *Escherichia coli*: genetic separation of interactions with protein receptors. *J Bacteriol*: 179, 4343-53.

Johnson X and Alric J (2013). Central Carbon Metabolism and Electron Transport in *Chlamydomonas reinhardtii*: Metabolic Constraints for Carbon Partitioning between Oil and Starch. *Eukaryotic Cell*: 12(6), 776-93.

Jonsson A and Nordlund S (2007). In vitro studies of the uridylylation of the three PII protein paralogs from *Rhodospirillum rubrum*: the transferase activity of *R. rubrum* GlnD is regulated by alpha-ketoglutarate and divalent cations but not by glutamine. *J Bacteriol*: 189(9), 3471-8.

Joyard J, Ferro M, Masselon C, Seigneurin-Berny D, Salvi D, Garin J, Rolland N (2010). Chloroplast proteomics highlights the subcellular compartmentation of lipid metabolism. *Prog Lipid Res*: 49(2), 128-58.

Kabsch W (1993). Automatic processing of rotation diffraction data from crystals of initially unknown symmetry and cell constants. *J Appl Cryst*: 26, 795-800.

Kabsch W (2010). XDS. *Acta Cryst D*: 66, 125-32.

Kloft N and Forchhammer K (2005). Signal transduction protein P-II phosphatase PphA is required for light-dependent control of nitrate utilization in *Synechocystis* sp. strain PCC 6803. *J Bacteriol*: 187, 6683-90.

Krajewski WW, Collins R, Holmberg-Schiavone L, Jones TA, Karlberg T, Mowbray SL (2008). Crystal structures of mammalian glutamine synthetases illustrate substrate-induced conformational changes and provide opportunities for drug and herbicide design. *J Mol Biol*: 375(1), 317-28.

Laichoubi KB, Espinosa J, Castells MA, Contreras A (2012). Mutational analysis of the cyanobacterial nitrogen regulator PipX. *PLoS One*: 7(4), e35845, doi: 10.1371/journal.pone.0035845.

Laskowski RA, Macarthur MW, Moss DS, Thornton JM (1993). Procheck-a program to check the stereochemical quality of protein structures. *J Appl Cryst*: 26, 283-91.

Lee HM, Flores E, Herrero A, Houmard J, Tandeau de Marsac N (1998). A role for the signal transduction protein PII in the control of nitrate/nitrite uptake in a cyanobacterium. *FEBS Lett*: 427(2), 291-5.

Leigh JA and Dodsworth JA (2007). Nitrogen regulation in bacteria and archaea. *Annu Rev Microbiol*: 61, 349-77.

León R, Couso I, Fernández E (2007). Metabolic engineering of ketocarotenoids biosynthesis in the unicelullar microalga *Chlamydomonas reinhardtii*. *J Biotechnol*: 130(2), 143-52.

Litz C, Helfmann S, Gerhardt S, Andrade SL (2011). Structure of GlnK1, a signalling protein from *Archaeoglobus fulgidus*. *Acta Cryst F*: 67 (2), 178-181.

Llácer JL, Contreras A, Forchhammer K, Marco-Marin C, Gil-Ortiz F, Maldonado R, Fita I, Rubio V (2007). The crystal structure of the complex of PII and acetylglutamate kinase reveals how PII controls the storage of nitrogen as arginine. *Proc Natl Acad Sci*: 104(45), 17644-49.

Llácer JL, Espinosa J, Castells MA, Contreras A, Forchhammer K, Rubio V (2010). Structural basis for the regulation of NtcA-dependent transcription by proteins PipX and PII. *Proc Natl Acad Sci*: 107(35), 15397-402.

Llácer JL, Fita I, Rubio V (2008). Arginine and nitrogen storage. *Curr Opin Struct Biol*: 18 (6), 673-81.

Luque I, Flores E, Herrero, A (1994). Molecular mechanism for the operation of nitrogen control in cyanobacteria. *EMBO J*: 13, 2862-9.

Maheswaran M, Urbanke C, Forchhammer K (2004). Complex formation and catalytic activation by the PII signaling protein of N-acetyl-L-glutamate kinase from *Synechococcus elongatus* strain PCC 7942. *J Biol Chem*: 279, 55202-10.

Maier S, Schleberger P, Lü W, Wacker T, Pflüger T, Litz C, Andrade SLA (2011). Mechanism of disruption of the Amt-GlnK complex by PII-mediated sensing of 2-oxoglutarate. *PLoS ONE*: 6(10), e26327. doi:10.1371/journal.pone.0026327.

McFadden GI (2001). Primary and secondary endosymbiosis and the origin of plastids. *J Phycology*: 37(6), 951-9.

Mittag M, Kiaulehn S, Johnson CH (2005). The Circadian Clock in *Chlamydomonas reinhardtii*. What Is It For? What Is It Similar To? *Plant Physiol*: 137(2), 399-409.

Melcher K, Ng LM, Zhou XE, Soon FF, Xu Y, Suino-Powell KM, Park SY, Weiner JJ, Fujii H, Chinnusamy V *et al* (2009). A gate-latch-lock mechanism for hormone signalling by abscisic acid receptors. *Nature*: 462(7273), 602-8.

Merchant SS, Prochnik SE, Vallon O, Harris EH, Karpowicz SJ, Witman GB, Terry A, Salamov A, Fritz-Laylin LK, Maréchal-Drouard L *et al* (2007). The *Chlamydomonas* Genome Reveals the Evolution of Key Animal and Plant Functions. *Science*: 318(5848), 245-50.

Merrick MJ and Edwards RA (1995). Nitrogen Control in Bacteria. *Microbiol Rev*: 59, 604-22.

Mizuno Y, Berenger B, Moorhead GB, Ng KK (2007). Crystal structure of *Arabidopsis* PII reveals novel structural elements unique to plants. *Biochemistry*: 46(6), 1477-83.

Mojzsis SJ, Arrhenius G, McKeegan KD, Harrison TM, Nutman AP, Friend CR (1996). Evidence for life on Earth before 3,800 million years ago. *Nature*: 384(6604), 55-9.

Murshudov GN, Vagin AA, Dodson EJ (1997). Refinement of macromolecular structures by the maximum-likelihood method. *Acta Cryst D*: 53, 240-55.

Ninfa AJ and Atkinson MR (2000). PII signal transduction proteins. *Trends Microbiol*: 8(4), 172-9.

Ninfa AJ and Jiang P (2005). PII signal transduction proteins: sensors of alpha-ketoglutarate that regulate nitrogen metabolism. *Curr Opin Microbiol*: 8(2), 168-73.

Ninfa AJ and Magasanik B (1986). Covalent modification of the glnG product, NRI, by the glnL product, NRII, regulates the transcription of the *glnALG* operon in *Escherichia coli*. *Proc Natl Acad Sci*: 83, 5909-13.

Nowack EC, Melkonian M, Glockner G (2008). Chromatophore genome sequence of *Paulinella* sheds light on acquisition of photosynthesis by eukaryotes. *Curr Biol*: 18, 410-18.

Osanai T, Kanesaki Y, Nakano T, Takahashi H, Asayama M, Shirai M, Kanehisa M, Suzuki I, Murata N, Tanaka K (2005a). Positive regulation of sugar catabolic pathways in the cyanobacterium *Synechocystis sp*. PCC 6803 by the group 2 sigma factor sigE. *J Biol Chem*: 280(35), 30653-9.

Osanai T, Sato S, Tabata S, Tanaka K (2005b). Identification of PamA as a PII-binding membrane protein important in nitrogen-related and sugar-catabolic gene expression in *Synechocystis sp*. PCC 6803. *J Biol Chem*: 280(41), 34684-90.

Osanai T and Tanaka K (2007). Keeping in touch with PII: PII-interacting proteins in unicellular cyanobacteria. *Plant Cell Physiol*: 48(7), 908-14.

Palinska KA, Laloui W, Bedu S, Loiseaux-de Goer S, Castets AM, Rippka R and Tandeau de Marsac N (2002). The signal transducer P(II) and bicarbonate acquisition in *Prochlorococcus marinus* PCC 9511, a marine cyanobacterium naturally deficient in nitrate and nitrite assimilation. *Microbiology*: 148, 2405-12.

Pedro-Roig L, Lange C, Bonete MJ, Soppa J, Furlow JM (2013). Nitrogen regulation of protein-protein interactions and transcript levels of GlnK PII regulator and AmtB ammonium transporter homologs in Archaea. DOI: 10.1002/mbo3.120.

Pinto TS, Malcata FX, Arrabaça JD, Silva JM, Spreitzer RJ, Esquível MG (2013). Rubisco mutants of *Chlamydomonas reinhardtii* enhance photosynthetic hydrogen production. *Appl Microbiol Biotechnol*: 97(12), 5635-43.

Plaxton WC. The organization and regulation of plant glycolysis (1996). *Annu Rev Plant Physiol Plant Mol Biol*: 47, 185-214.

Radchenko M and Merrick M (2011). The role of effector molecules in signal transduction by PII proteins. *Biochem Soc Trans*: 39(1), 189-94.

Rajendran C, Gerhardt EC, Bjelic S, Gasperina A, Scarduelli M, Pedrosa FO, Chubatsu LS, Merrick M, Souza EM, Winkler FK, Huergo LF, Li XD (2011). Crystal structure of the GlnZ-DraG complex reveals a different form of PII-target interaction. *Proc Natl Acad Sci*: 108(47), 18972-6.

Raymond J (2008). Coloring in the tree of life. *Trends Microbiol*: 16, 41-43.

Rexach J, Fernandez E, Galvan A (2000). The *Chlamydomonas reinhardtii* Nar1 gene encodes a chloroplast membrane protein involved in nitrite transport. *Plant Cell*: 12, 1441-53.

Ruppert U, Irmler A, Kloft N, Forchhammer K (2002). The novel protein phosphatase PphA from *Synechocystis* PCC 6803 controls dephosphorylation of the signalling protein P-II. *Mol Microbiol*: 44, 855-64.

Rye R and Holland HD (1998). Paleosols and the evolution of atmospheric oxygen: a critical review. *Am J Sci*: 298(8), 621-72.

Sant'Anna FH, Trentini DB, de Souto Weber S, Cecagno R, da Silva SC, Schrank IS (2009). The PII superfamily revised: a novel group and evolutionary insights. *J Mol Evol*: 68(4), 322-36.

Schimper AFW (1883). Über die Entwicklung der Chlorophyllkörner und Farbkörper. *Bot. Zeitung*: 41, 105-14, 121-31, 137-46, 153-62.

Schlicker C, Fokina O, Kloft N, Grune T, Becker S, Sheldrick GM, Forchhammer K (2008). Structural analysis of the PP2C phosphatase tPphA from *Thermosynechococcus elongatus*: a flexible flap subdomain controls access to the catalytic site. *J Mol Biol*: 376(2), 570-81.

Shapiro BM (1969). The glutamine synthetase deadenylylating enzyme system from *Escherichia coli.* Resolution into two components, specific nucleotide stimulation, and cofactor requirements. *Biochemistry*: 8, 659-70.

Smith CS, Weljie AM , Moorhead GB (2003). Molecular properties of the putative nitrogen sensor PII from *Arabidopsis thaliana. Plant J*: 33, 353-60.

Stadtman E (2001). The story of glutamine synthetase regulation. *J Biol Chem*: 276, 44357-64.

Stryer L, Berg JM, Tymoczko JL (2007). *Biochemistry* (6th ed.), San Francisco: W.H. Freeman, 679-706.

Sugiyama K, Hayakawa T, Kudo T, Ito T, Yamaya T (2004). Interaction of N-acetylglutamate kinase with a PII-like protein in rice. *Plant Cell Physiol*: 45, 1768-78.

Su J and Forchhammer K (2012). The Role of Arg13 in Protein Phosphatase M tPphA from *Thermosynechococcus elongatus*. *Enzyme Res*: 272706. doi:10.1155/2012/272706.

Su J and Forchhammer K (2013). Determinants for substrate specificity of the bacterial PP2C protein phosphatase tPphA from *Thermosynechococcus elongatus*. *FEBS J*: 280(2), 694-707.

Su J, Schlicker C, Forchhammer K (2011). A third metal is required for catalytic activity of the signal-transducing protein phosphatase M tPphA. *J Biol Chem*: 286(15), 13481-88.

Tao HC, Peng ZW, Li PS, Yu TA, Su J (2013). Optimizing cadmium and mercury specificity of CadR-based *E. coli* biosensors by redesign of CadR. *Biotechnol Lett*: 35(8), 1253-8.

Thomas G, Coutts G, Merrick M (2000). The glnKamtB operon. A conserved gene pair in prokaryotes. *Trends Genet*: 16(1), 11-14.

Truan D, Huergo LF, Chubatsu LS, Merrick M, Li XD, Winkler FK (2010). A new P(II) protein structure identifies the 2-oxoglutarate binding site. *J Mol Biol*: 400(3), 531-39.

Vagin A and Teplyakov A (1997). MOLREP: An automated program for molecular replacement. *J Appl Cryst*: 30, 1022-25.

Vega-Palas MA, Flores E, Herrero A (1992). NtcA, a global nitrogen regulator from the cyanobacterium *Synechococcus* that belongs to the Crp family of bacterial regulators. *Mol Microbiol*: 6(13), 1853-9.

Vílchez C**,** Garbayo I, Markvicheva E, Galván F, León R (2001). Studies on the suitability of alginate-entrapped *Chlamydomonas reinhardtii* cells for sustaining nitrate consumption processes. *Biores Tech*: 78(1), 55-61.

Wei TF, Ramasubramanian TS, Pu F, Golden JW (1993). *Anabaena* sp. strain PCC 7120 *bifA* gene encoding a sequence-specific DNA-binding protein cloned by in vivo transcriptional interference selection. *J Bacteriol*: 175, 4025-35.

Wei YY, Zheng Q, Liu ZP, Yang ZM (2011). Regulation of tolerance of *Chlamydomonas reinhardtii* to heavy metal toxicity by hemeoxygenase-1 and carbonmonoxide. *Plant Cell Physiol*: 52(9), 1665-75.

Weiss DS, Batut J, Klose KE, Keener J, Kustu S (1991). The phosphorylated form of the enhancer-binding protein NTRC has an ATPase activity that is essential for activation of transcription. Cell: 67(1), 155-67.

Weiss V and Magasanik B (1988). Phosphorylation of nitrogen regulator I (NRI) of *Escherichia coli*. *Proc Natl Acad Sci*: 85(23), 8919-23.

William M, Roettger M, Kloesges T, Thiergart T, Woehle C, Gould S, Dagan T (2012). Modern endosymbiotic theory: Getting lateral gene transfer into the equation. *J Endocyt Cell Res*: 23, 1-5.

Wolfe DM, Zhang Y, Roberts GP (2007). Specificity and regulation of interaction between the PII and AmtB1 proteins in *Rhodospirillum rubrum*. *J Bacteriol*: 189, 6861-9.

Work VH, Radakovits R, Jinkerson RE, Meuser JE, Elliott LG, Vinyard DJ, Laurens LML, Dismukes GC, Posewitz MC (2010). Increased Lipid Accumulation in the *Chlamydomonas reinhardtii* sta7-10 Starchless Isoamylase Mutant and Increased Carbohydrate Synthesis in Complemented Strains**.** *Eukaryot Cell*: 9(8), 1251-61.

Xu Y, Carr PD, Clancy P, Garcia-Dominguez M, Forchhammer K, Florencio F, Vasudevan SG, Tandeau de Marsac N, Ollis DL (2003). The structures of the PII proteins from the cyanobacteria *Synechococcus* sp. PCC 7942 and *Synechocystis* sp. PCC 6803. *Acta Cryst D*: 59, 2183-90.

Xu Y, Carr PD, Huber T, Vasudevan SG, Ollis DL (2001). The structure of the PII-ATP complex. *Eur J Biochem*: 268, 2028-37.

Xu Y, Cheah E, Carr PD, van Heeswijk WC, Westerhoff HV, Vasudevan SG, Ollis DL (1998). GlnK, a PII-homologue: structure reveals ATP binding site and indicates how the T-loops may be involved in molecular recognition. *J Mol Biol*: 282, 49-65.

Xu Y, Feng L, Jeffrey PD, Shi Y, Morel FM (2008). Structure and metal exchange in the cadmium carbonic anhydrase of marine diatoms. *Nature*: 452(7183), 56-61.

Yildiz O, Kalthoff C, Raunser S, Kühlbrandt W (2007). Structure of GlnK1 with bound effectors indicates regulatory mechanism for ammonia uptake. *EMBO J*: 26(2), 589-99.

Zeth K, Fokina O, Forchhammer K (2012). An engineered PII protein variant that senses a novel ligand: atomic resolution structure of the complex with citrate. *Acta Cryst D*: 68, 901-8.

Zhang Y, Pu H, Wang Q, Cheng S, Zhao W, Zhang Y, Zhao J (2007). PII is important in regulation of nitrogen metabolism but not required for heterocyst formation in the Cyanobacterium *Anabaena* sp. PCC 7120. *J Biol Chem*: 282(46), 33641-8.

13. Abbreviations

Ab	*Azospirillum brasiliensis*
ABC	ATP-binding cassette
ACCase	acetyl-CoA carboxylase
ADP	adenosine diphosphate
AmtB	ammonium transporter
Arg	arginine
ATase	adenylyltransferase
At	*Arabidopsis thaliana*
***At* NAGK**	NAGK from *Arabidopsis thaliana*
***At* PII**	PII from *Arabidopsis thaliana*
ATP	adenosine triphosphate
Å	angstrom
B factor	temperature factor
C	carbon
°C	degree Celsius
Cd	cadmium
Cl^-	chloride ion
CLANS	cluster analysis of sequences
CoA	coenzyme A
CPU	central processing unit
Cr	*Chlamydomonas reinhardtii*
***Cr* NAGK**	NAGK from *Chlamydomonas reinhardtii*
Crp	cAMP receptor protein
***Cr* PII**	PII from *Chlamydomonas reinhardtii*
DraG	dinitrogenase reductase-activating glycohydrolase
DTT	dithiothreitol
DNA	deoxyribonucleic acid
Ec/E. coli	*Escherichia coli*
FC1	flow cell 1
FC2	flow cell 2
Fd	ferredoxin
FdxH	[2Fe-2S]-type ferredoxin
Fig.	figure
FNR	ferredoxin $NADP^+$ reductase
Gln	glutamine
Glu	glutamate
GOGAT	glutamine-2-oxoglutarate-amido transferase
GS	glutamine synthetase
GSI	glutamine synthetase type I
GSII	glutamine synthetase type II
GSIII	glutamine synthetase type III
G3P	glyceraldehyde-3-phosphate
HEPES	4-(2-hydroxyethyl)-1-piperazineethanesulfonic acid
IC_{50}	half maximal inhibitory concentration
ITC	isothermal titration calorimetry
K_{cat}	turnover number
K_d	dissociation constant
K_m	michaelis constant
kDa	kilo-Dalton
MES	2-(*N*-morpholino)ethanesulfonic acid
Mg	magnesium
MscS	mechanosensitive ion channel

N	nitrogen
NADPH	nicotinamide adenine dinucleotide phosphate
NAG	*N*-acetyl-L-glutamate
NAG-P	*N*-acetyl-L-glutamyl 5-phosphate
NAGK	*N*-acetyl-L-glutamate kinase
NH_4^+	ammonium
NiR	nitrite reductase
NO_2^-	nitrite
NO_3^-	nitrate
NR	nitrate reductase
NRI	nitrogen regulator I
NRII	nitrogen regulator II
NTA	nitrilotriacetic acid
PamA	PII associated membrane protein A
PEG	polyethylene glycol
Pi	inorganic phosphate
PipX	PII interaction protein X
Pp	*Porphyra purpurea*
PP2C	protein phosphatase 2C
PSI	photosystem I
PSII	photosystem II
Py	*Pyropia yezoensis*
Rc	*Ricinus communis*
RNA	ribonucleic acid
RU	resonance units
Se	*Synechococus elongatus*
SEC	size exclusion chromatography
***Se* NAGK**	NAGK from *Synechococcus elongatus*
***Se* PII**	PII from *Synechococcus elongatus*
SigE	sigma factor E
Sl	*Solanum lycopersicum*
SPR	surface plasmon resonance
TCA	tricarboxylic acid
U	unit
UTase/UR	uridylyltransferase/uridylyl-removing enzyme
V_{max}	maximum reaction velocity
W	water molecule
WT	wild type
2-OG	2-oxoglutarate
3D	3-dimensional
3-PGA	3-phosphoglycerate

14. Acknowledgements

I feel privileged to work with Prof. Karl Forchhammer who had offered this interesting project which lead to wonderful findings. His helpful guidance as an excellent mentor and inquisitive discussions has helped me to gain more knowledge and experience. My sincere thanks to Prof. Andrei Lupas for considering my research interest and accepting as a PhD student which introduced me to the MPI network. I am thankful to him for offering timely guidance and support during critical times. Further, I am grateful for the excellent lab setup offered at the University and MPI, Tuebingen without which this work wouldn't have been possible.

My special thanks to Olexandra Fokina, Marcus Hartmann, Prof. Kornelius Zeth, Jan Lüddecke and Vikram Alva for their fruitful discussions on research perspectives and help extended in this project. My sincere gratitude to Reinhard Albrecht and Christina Hermann for the timeless technical assistance offered during various stages of this project.

The whole department at the MPI and the Interfakultäres Institut für Mikrobiologie und Infektionsmedizin has been greatly helpful throughout this endeavor. I would like to extend my humble gratitude to all department members for helping me directly/indirectly and letting me explore the various techniques. My close colleagues at both the institutes deserve my heartfelt thanks for providing a very friendly atmosphere at work and outside, which I would cherish forever.

The entire PhD duration was generously supported by the funding agencies Max Planck Society and Deutsche Forschungsgemeinschaft (DFG).

I am extremely indebted to my mother Muthulakshmi and father Chellamuthu, my beloved husband Shyam Sundar Dhanabalan, sister Kavitha, family members and friends for their continuous support throughout my studies and especially during hard times. Their encouragement and faith on me across the oceans has motivated me throughout this learning process.

I would like to dedicate this thesis to all my teachers and mentors, whom I consider as the source of inspiration for my studies and appreciate their motivation which helped me to climb up this ladder.